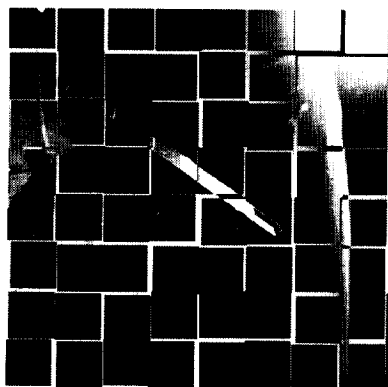


NASA Conference Publication 3162
Part 2



LDEF Materials Workshop '91



Proceedings of a workshop held at
H. J. E. Reid Conference Center
NASA Langley Research Center
November 19-22, 1991

(NASA-CP-3162-PT-2) LDEF MATERIALS
WORKSHOP 1991, PART 2 (NASA)
291 p.

N93-10573
--THRU--
N93-10592
Unclass

01/27 0120860



NASA Conference Publication 3162
Part 2

LDEF Materials Workshop '91

Compiled by

Bland A. Stein and Philip R. Young

Langley Research Center

Hampton, Virginia

Proceedings of a workshop sponsored by
Langley Research Center and held at
H. J. E. Reid Conference Center
NASA Langley Research Center
November 19-22, 1991



National Aeronautics and
Space Administration

Office of Management

Scientific and Technical
Information Program

1992

COVER ILLUSTRATION

LDEF retrieval—the dawn of new and comprehensive understanding of space environmental effects on materials. Through analysis and modeling of materials exposed on LDEF, the enigmas of the combined effects of space environment parameters on spacecraft materials behavior in low-Earth orbit are being replaced by an emerging comprehension.

FOREWORD

The National Aeronautics and Space Administration Long Duration Exposure Facility (LDEF) was launched into low-Earth Orbit (LEO) from the payload bay of the Space Shuttle Orbiter Challenger in April 1984. It was retrieved from orbit by the Columbia in January 1990. The 57 LDEF experiments covered the disciplines of materials, coatings, and thermal systems; power and propulsion; space science; and electronics and optics. LDEF was designed to provide a large number of economical opportunities for science and technology experiments that require modest electrical power and data processing while in space and which benefit from post-flight laboratory investigations of the retrieved experiment hardware on Earth. Most of the materials experiments were completely passive; their data are being obtained in post-flight laboratory tests and analyses.

The 5.8-year flight of LDEF greatly enhanced the potential value of most LDEF materials, compared to that of the original 1-year flight plan. NASA recognized this potential by forming the LDEF Space Environmental Effects on Materials Special Investigation Group (MSIG) in early 1989. MSIG was chartered to investigate the effects of the long LEO exposure on structure and experiment materials which were not originally planned to be test specimens, and to integrate the results of this investigation with data generated by the Principal Investigators of the LDEF experiments into an LDEF Materials Data Base.

As a follow-on to the Materials Sessions at the First LDEF Post-Retrieval Symposium (in Kissimmee, Florida, June 1991), this workshop was envisioned as a series of technical sessions on LDEF materials themes, followed by theme panel meetings. The themes included Materials, Environmental Parameters, and Data Bases; LDEF Contamination; Thermal Control Coatings, Protective Coatings, and Surface Treatments; Polymers and Films; Polymer Matrix Composites; Metals, Ceramics, and Optical Materials; and Lubricants, Adhesives, Seals, Fasteners, Solar Cells, and Batteries. Each half-day technical session contained invited overview papers, with ample time for specific discussion after each paper and for general discussion on the technical session theme at the end of each session.

These technical sessions were followed by concurrent half-day meetings of each panel to produce theme reports and summary charts. These meetings addressed the following general questions plus a few specific questions developed by the panel chairmen concerning the panel theme discipline.

- How have initial LDEF results affected
 - potential space applications of this class of materials or understanding of environmental parameters?
 - materials development or environmental parameter definition needs?
 - ground simulation testing needs?
 - space environmental effects analytical modeling needs?


- What are the LDEF data-basing requirements for this discipline?
- What are the general needs for future flight experiments?

LDEF materials data has been eagerly awaited by the Space Environmental Effects on the Materials Technical Community for the better part of a decade. The most optimistic expectations of that community have been fulfilled. The remarkable attitude stability of LDEF during its entire flight permits evaluation of many well-defined combinations of space environment parameters on specimens of identical and/or similar materials located on experiment trays and on the spacecraft structure at various positions on the sides and ends of the satellite. As this workshop indicated, the LDEF data are, in general, remarkably consistent. Even at this interim point in the LDEF materials analyses, it is apparent that LDEF will provide a "benchmark" for materials design data bases for satellites in low-Earth orbit. Some materials were identified to be encouragingly resistant to LEO SEE for 5.8 years; other "space qualified" materials displayed significant environmental degradation. Molecular contamination was widespread; LDEF offers an unprecedented opportunity to provide a unified perspective of unmanned LEO spacecraft contamination mechanisms. New material development requirements for long-term LEO missions have been identified, and current ground simulation testing methods/data for new, durable materials concepts can be validated with LDEF results.

This is the report resulting from LDEF Materials Workshop 1991. It contains most of the papers presented at the technical sessions plus the panel theme reports. The approximately 200 persons who attended the Workshop were quite pleased with the information presented and with the technical interactions. The Workshop Chairmen wish to express thanks to the coordinator, Dr. Arlene Levine, to the staff at the NASA Langley H. J. E. Reid Activities Center, and to the session chairman recorders and authors who aided us in the planning of LDEF Materials Workshop 1991. We also wish to thank those who presented the papers and conducted the theme panel activities. We hope that this document satisfies the documentation requirements of the Workshop participants and other recipients.

The LDEF mission was a noteworthy success. It remains for us, the international space environmental effects technical community, to complete the analyses of the data, to generate new models for space environmental parameter interactions with materials from this data, and to devise more accurate ground simulation tests for space environmental effects on materials using the LDEF data for validation.

Certain materials are identified in this publication in order to specify procedures adequately. In no case does such identification imply recommendation or endorsement by the government, nor does it imply that the materials are the only or best ones available for the purpose.



Bland A. Stein and Philip R. Young
NASA Langley Research Center

CONTENTS

Foreword iii

Part 1*

LDEF Materials: An Overview of the Interim Findings 1
Bland A. Stein

LDEF Materials, Environmental Parameters, and Data Bases

Co-Chairmen: Bruce Banks and Mike Meshishnek
Recorder: Roger Bourassa

LDEF Atomic Oxygen Fluence Update 59
Roger J. Bourassa and J. R. Gillis

LDEF Yaw and Pitch Angle Estimates 71
Bruce A. Banks and Linda Gebauer

LDEF Contamination

Co-Chairmen: Wayne Stuckey and Steve Koontz
Recorder: Russell Crutcher

**Materials SIG Quantification and Characterization of Surface
Contaminants** 95
Russ Crutcher

Z306 Molecular Contamination Ad Hoc Committee Results 115
Johnny L. Golden

Long Duration Exposure Facility (LDEF) Contamination Modeling 141
Tim Gordon and Ray Rantanen

Surface Contamination on LDEF Exposed Materials 159
C. S. Hemminger

Sources and Transport on Silicone NVR 175
Gale A. Harvey

*Part 1 is presented under separate cover.

Thermal Control Coatings, Protective Coatings, and Surface Treatments

Co-Chairmen: Ann Whitaker and Wayne Slemp
Recorder: Johnny Golden

Thermal Control Surfaces on the MSFC LDEF Experiments	187
Donald R. Wilkes, Ann Whitaker, James M. Zwiener, Roger C. Linton David Shular, Palmer Peters, and John Gregory	
Anodized Aluminum on LDEF: A Current Status of Measurements on Chromic Acid Anodized Aluminum	211
Johnny L. Golden	
Performance of Thermal Control Tape In the Protection of Composite Materials	223
Rachel R. Kamenetzky and Ann F. Whitaker	
Fluorescence of Thermal Control Coatings on S0069 and A0114	233
James M. Zwiener, Richard J. Mell, Palmer N. Peters, Donald R. Wilkes, Edgar R. Miller, and John C. Gregory	
Long Duration Exposure Facility M0003-5 Thermal Control Coatings on DoD Flight Experiment	245
Charles J. Hurley and William Lehn	
Element Material Exposure Experiment by EFFU	283
Yoshihiro Hashimoto, Masaaki Ito, and Masahiro Ishii	
Skylab DO24 Thermal Control Coatings and Polymeric Films Experiment	293
William L. Lehn and Charles J. Hurley	

Polymers and Films (Including Ag/FEP)

Co-Chairmen: Phil Young and David Brinza
Recorder: Gary Pippin

Effects of the LDEF Environment on the Ag/FEP Thermal Blankets	311
Francois Levadou and Gary Pippin	
Recession of FEP Specimens from Trays D11 and B7	345
H. G. Pippin	
Characterization of Selected LDEF—Exposed Polymer Films and Resins	357
Philip R. Young and Wayne S. Slemp	
Effects of Orbital Exposure on Halar during the LDEF Mission	391
William E. Brower, Jr., Harish Holla, and Robert A. Bauer	

Long Duration Exposure Facility M0003-5 Recent Results on Polymeric Films	417
Charles J. Hurley and Michele Jones	
LDEF Materials Workshop '91 Agenda	449
Attendee List	455

Part 2

Metals, Ceramics, and Optical Materials

Co-Chairmen: Roger Linton and John Gregory
Recorder: Gail Bohnhoff-Hlavacek

Selected Results for Metals from LDEF Experiment A0171	467
Ann F. Whitaker	
Some Results of the Oxidation Investigation of Copper and Silver Samples Flown on LDEF	479
A. de Rooij	
Changes in Oxidation State of Chromium during LDEF Exposure	491
Johnny L. Golden	
Effect of Space Exposure on Pyroelectric Infrared Detectors	501
James B. Robertson	
Long Duration Exposure Facility (LDEF) Optical Systems SIG Summary and Database	507
Gail Bohnhoff-Hlavacek	

Polymer Matrix Composites

Co-Chairmen: Gary Steckel and Rod Tennyson
Recorder: Pete George

Polymer Matrix Composites on LDEF Experiments M0003-9 and 10	515
Gary L. Steckel, Thomas Cookson, and Christopher Blair	
Space Environmental Effects on LDEF Low Earth Orbit Exposed Graphite Reinforced Polymer Matrix Composites	543
Pete George	
Additional Results on Space Environmental Effects on Polymer Matrix Composites—Experiment AO180	571
R. C. Tennyson	
Proposed Test Program and Data Base for LDEF Polymer Matrix Composites	593
R. C. Tennyson, P. George, G. Steckel, and D. G. Zimcik	

**Lubricants, Adhesives, Seals, Fasteners, Solar Cells,
and Batteries**

Co-Chairmen: James Mason and Joel Edelman
Recorder: Harry Dursch

Identification and Evaluation of Lubricants, Adhesives, and Seals Used on LDEF	603
Bruce Keough	
Results from the Testing and Analysis of LDEF Batteries	619
Steve Spear, Harry Dursch, and Chris Johnson	
Effects of Long-Term Exposure on LDEF Fastener Assemblies	633
Steve Spear and Harry Dursch	
Results from Testing and Analysis of Solar Cells Flown on LDEF	649
Harry Dursch	
System Related Testing and Analysis of FRECOPA	661
Christian Durin	

Panel Discussion Summary

Theme Panel Discussion Topics	679
Bland A. Stein and Philip R. Young	
LDEF Materials, Environmental Parameters, and Data Bases	681
Bruce Banks, Mike Meshishnek and Roger Bourassa	
LDEF Contamination	689
Wayne Stuckey, Steve Koontz, and Russell Crutcher	
Thermal Control Coatings, Protective Coatings, and Surface Treatments	699
Ann Whitaker, Wayne Slemp, and Johnny Golden	
Polymers and Films (Including Ag/FEP)	707
Philip R. Young, David Brinza, and Gary Pippin	
Metals, Ceramics, and Optical Materials	719
Roger Linton, John Gregory, and Gail Bohnhoff-Hlavacek	
Polymer Matrix Composites	727
Gary Steckel, Rod Tennyson, and Pete George	
Lubricants, Adhesives, Seals, Fasteners, Solar Cells, and Batteries	737
James Mason, Joel Edelman, and Harry Dursch	
LDEF Materials Workshop 1991	747

LDEF Materials Workshop '91 Agenda	749
Attendee List	755



PART 2

Metals, Ceramics, and Optical Materials

Co-Chairmen: Roger Linton and John Gregory
Recorder: Gail Bohnhoff-Hlavacek

SELECTED RESULTS FOR METALS FROM LDEF EXPERIMENT A0171

Ann F. Whitaker
NASA Marshall Space Flight Center
Marshall Space Flight Center, AL 35812

INTRODUCTION

Metal specimens in disk type and ribbon configurations of interest to various programs at the Marshall Space Flight Center were exposed to the LEO environment for 5.8 years on LDEF Experiment A0171. Most of the metals flown were well heat sunk in the LDEF experiment tray which experienced benign temperatures, but a few metals were thermally isolated allowing them to experience greater thermal extremes. All metal specimens whose preflight weights were known showed a weight change as a result of exposure. Optical property and mass changes are attributed principally to atomic oxygen exposures. Silver and copper were grossly affected whereas tantalum, molybdenum and several preoxidized alloys were the least affected.

Metals contained in this experiment are shown in Table I. Results including mass, surface morphology and optical property changes from selected evaluations of these metals are presented.

RESULTS

Mass Change

Oxidation of metals from thermal atomic oxygen has been shown to be thermally activated, and results from various short term flight exposures of silver to orbital atomic oxygen show a temperature dependence of oxidation. Responses of metals flown on A0171 are consistent with these previous findings. Metals which were well heat sunk to the experiment structure are presumed to have been exposed to a benign thermal environment since the LDEF structure temperature never exceeded 100°F. Several silver ribbon samples were thermally isolated so their upper temperatures were expected to far exceed 100°F. At this time these temperature extremes have not been calculated nor estimated. Most of the exposed metals increased in weight. Preoxidized Ni-Cr-Al and Tophet 30 alloys experienced a slight decrease in weight whereas preoxidized Hos-875 had a slight increase. Reactivity numbers for several metals along with their atomic oxygen accommodation numbers are shown in Table II. The reactivity values were generated based on the assumption that the highest oxide state was formed during exposure. These values may require modification if future work indicates that a different oxide other than the highest state is found. Accommodation numbers shown are defined as the ratio of atomic oxygen atoms reacted to incident atomic oxygen.

Some explanations for the data in Table II can be given in view of the facts that oxidation of

metals follows logarithmic and parabolic laws and is highly sensitive to pressure and temperature conditions. Short time exposures at high temperatures should yield high reactivity and accommodation values. The low accommodation and reactivity numbers for several metals from A0171 shown in Table II are consistent with long term exposures under low temperature conditions. The order of magnitude difference in the reactivity between the silver samples attests to the sensitivity of the atomic oxygen reaction to temperature, stress and microstructural differences. The cold rolled silver ribbon contained a stress loop and was thermally isolated from its ambient temperature base so it was expected to thermal cycle through temperatures more extreme than experienced by the disk type samples. The complex dependencies of fluence and temperature prevent the extrapolation of short term effects to long term effects.

Surface Morphology

The disk configured metals were not highly polished so some features which are more distinctive via of the scanning electron microscope (SEM) photographs are somewhat masked by flaws of the machined surfaces. Some differences are noted for the copper exposed and unexposed regions (Figures 1a and 1b). The exposed area shows a fine structure and the unexposed area shows some corrosion which has accumulated on the surface since the samples have returned from flight. The silver oxide formed on the silver samples during exposure produced considerably different surface morphologies for the coarsely machined, fine grained disk samples (Figures 2a and 2b) and the cold rolled ribbon sample (Figure 3). The exposed disk configured silver appears to form peak type oxide scale structures reminiscent of that characteristically observed on exposed polymer structures - a phenomena which has not previously been observed in silver. Elongated silver oxide scales present on the ribbon samples are similar to those formed during short term atomic oxygen exposures on Shuttle flights. Figure 4 is an SEM of molten aluminum sprayed from a debris impact on the mounting hardware onto a copper sample.

Optical Properties

Considerable decreases in solar reflectivity resulted for LDEF exposed silver and copper as shown in Figures 5 and 6, respectively, where their exposed and unexposed regions are compared. More subtle reflectivity changes are present in the lesser reactive materials as noted in Figures 7, 8 and 9. The LDEF exposure of the Ni-Cr-Al alloy resulted in a decrease in reflectance below 2000 nm with this degradation increasing through the visible and ultraviolet spectrum. The reflectance curves for unpolished molybdenum are typical. Its exposure resulted in a slight increase in reflectance above 1700 nm and a more pronounced decrease below 1700 nm. A small decrease in reflectance below 750 nm and a small broadband increase above 750 nm were observed for the tantalum specimen.

SUMMARY

Macroscopic oxidation effects were observed for LDEF exposed silver and copper. Morphology changes induced in exposed silver were peculiar to the type of silver. Quantitative oxidation effects were observed in other metals not previously reported. Atomic oxygen accommodation and reactivity values generated for various metals are characteristic of long exposures at low temperatures.

Additional studies are required to yield explanations for the observed phenomena in these metals. Measurements and calculations related to the metals evaluations on this experiment are only partially complete.

REFERENCES

1. Whitaker, A.F.: RF Oxygen Plasma Effects on Polymeric Materials. A Dissertation Prepared for the Degree of Doctor of Philosophy, March 1989.
2. Whitaker, A.F.; Little, S.A.; Harwell, R.J.; Griner, D.B.; DeHaye, R.F.; and Fromhold, A.T., Jr.: Orbital Atomic Oxygen Effects on Thermal Control and Optical Materials - STS-8 Results. AIAA-85-0416, Jan. 1985.
3. Whitaker, A.F.; Burka, J.A.; Coston, J.E.; Dalins, I.; Little, S.A.; and DeHaye, R.F.: Protective Coatings for Atomic Oxygen Susceptible Spacecraft Materials - STS-41G Results. AIAA-85-7017-CP, Nov. 1985.

TABLE I. METALS ON LDEF EXPERIMENT A0171

<u>METAL</u>	<u>CONFIGURATION</u>	<u>NO. OF SAMPLES</u>
COPPER	1" DIA DISK (1/2 EXP)	(2)
TITANIUM Ti-75A	1" DIA DISK (1/2 EXP)	(1)
MOLYBDENUM	1" DIA DISK (1/2 EXP)	(1)
MAGNESIUM AZ31B	1" DIA DISK (1/2 EXP)	(1)
Ni-14Cr-14al-2Zr ALLOY		
- PREOXIDIZED	1" DIA DISK (1/2 EXP)	(1)
- AS RECEIVED	1" DIA DISK (1/2 EXP)	(1)
SILVER	1" DIA DISK (1/2 EXP)	(2)
NIOBIUM	1" DIA DISK (1/2 EXP)	(1)
TOPHET-30		
- PREOXIDIZED	1" DIA DISK (1/2 EXP)	(1)
- AS RECEIVED	1" DIA DISK (1/2 EXP)	(1)
HOS-875		
- PREOXIDIZED	1" DIA DISK (1/2 EXP)	(1)
- AS RECEIVED	1" DIA DISK (1/2 EXP)	(1)
TUNGSTEN	1" DIA DISK (1/2 EXP)	(1)
ALUMINUM 2219	1" DIA DISK (1/2 EXP)	(1)
TANTALUM	1" DIA DISK (1/2 EXP)	(1)
SILVER FILMS ON VARIOUS SUBSTRATES	1" DIA DISK FULLY EXPOSED	(18)
ALUMINUM FILMS ON VARIOUS SUBSTRATES	1" DIA DISK FULLY EXPOSED	(17)
SILVER-COLD ROLLED RIBBON	1/2" x 1"	(4)
SILVER-COLD ROLLED RIBBON IN STRESS LOOP	1/2" x 2-1/2"	(1)
COPPER IN FLAT CONDUCTOR CABLE	1/4" x 5"	(MULTISTRANDED)
SILVER-ON SOLAR CELLS, INTERCONNECTS AND BACK METALLIZATIONS	----	VARIOUS CONFIGURATIONS AND MULTIPLE SAMPLES
COPPER-WELD INNERCONNECTS	----	PARALLEL GAPS

**TABLE II. ATOMIC OXYGEN EFFECTS ON SEVERAL METALS
FROM EXPERIMENT A0171**

<u>METAL</u>	<u>ATOMIC OXYGEN* ACCOMMODATION</u>	<u>ATOMIC OXYGEN REACTIVITY (CM³/ATOM)</u>
SILVER (MULTI CRYSTALLINE DISK)	1/10 ³	3.6 x 10 ⁻²⁶
SILVER (COLD ROLLED RIBBON IN STRESS LOOP - THERMALLY ISOLATED)	8/10 ³	2.8 x 10 ⁻²⁵
COPPER	2/10 ⁴	2.0 x 10 ⁻²⁶
MOLYBDENUM	3/10 ⁴	1.44 x 10 ⁻²⁷
TITANIUM (75A)	9/2 x 10 ⁵	3.9 x 10 ⁻²⁷

* AO ACCOMMODATION IS THE RATIO OF ATOMIC OXYGEN ATOMS ACCOMMODATED TO INCIDENT ATOMIC OXYGEN ATOMS.

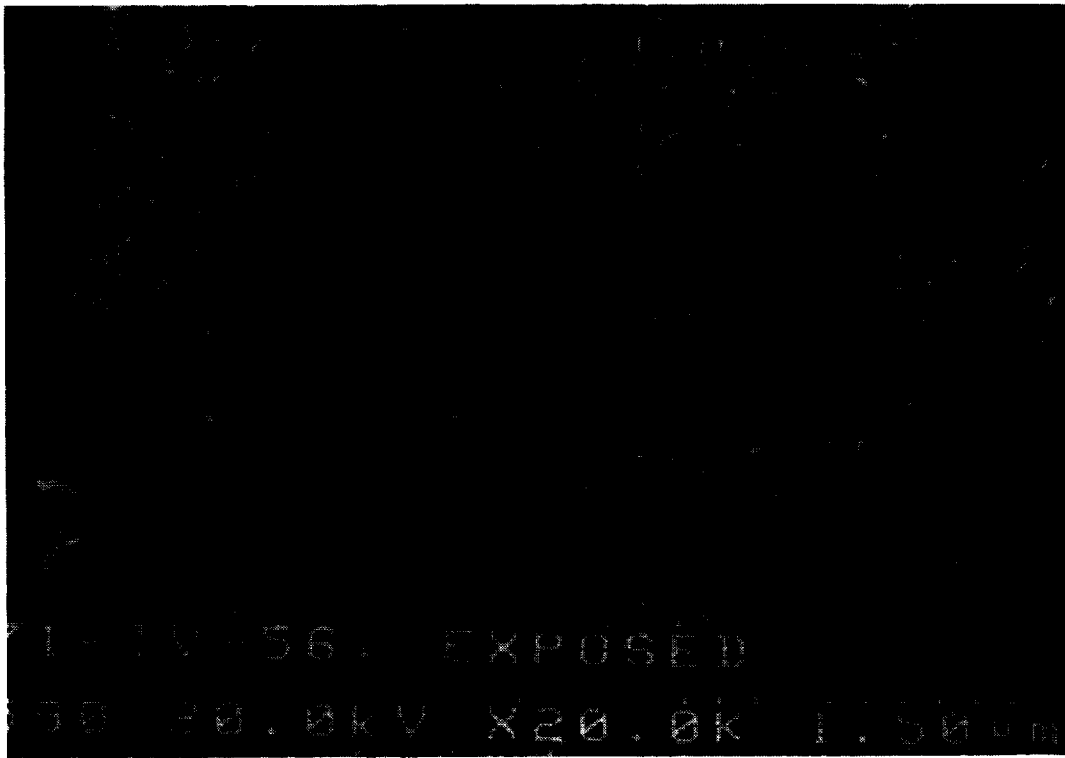


Figure 1a. Exposed Copper Surface Showing Fine Oxide Structures.

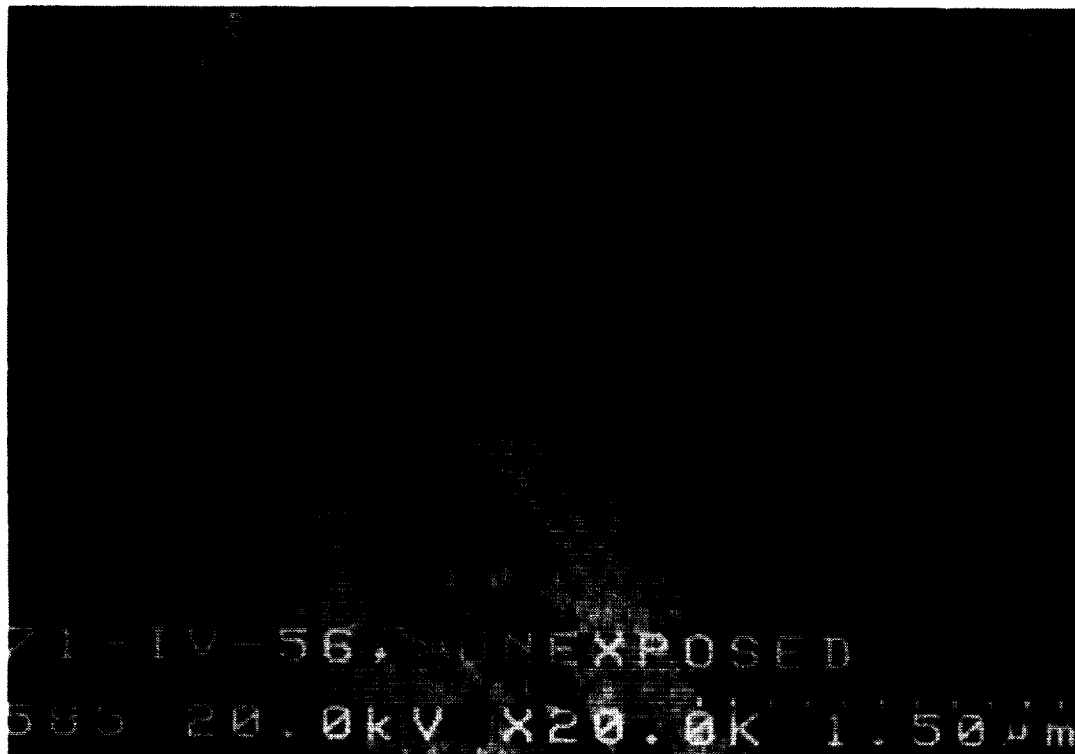


Figure 1b. Unexposed Copper Surface Showing Some Accumulated Corrosion.

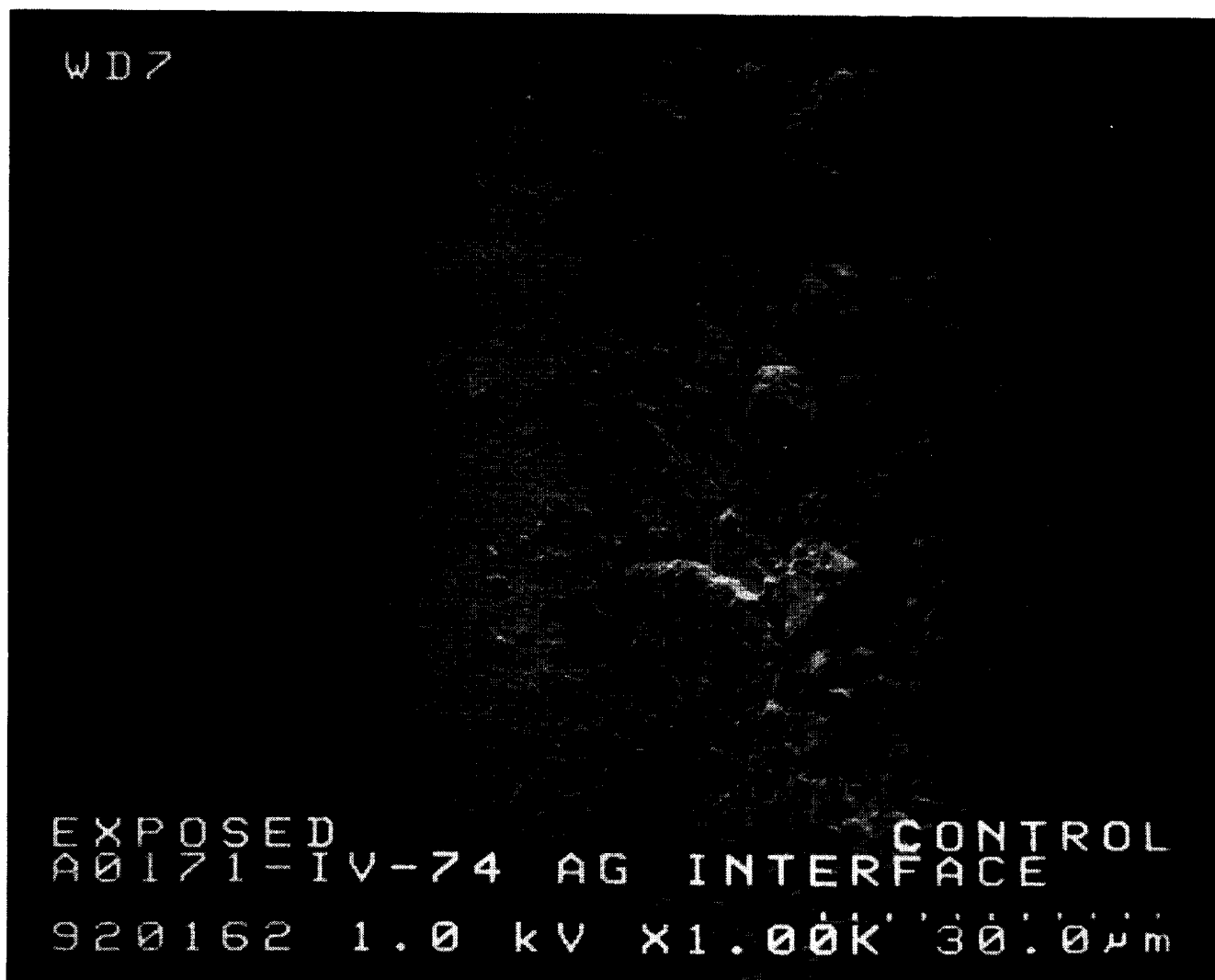


Figure 2a. Scanning Electron Microscope (SEM) View of Silver Exposed (Left), Interface (Center), and Unexposed (Right) Surfaces of Coarsely Machined, Fine Grain Disk Sample.

ORIGINAL PAGE
BLACK AND WHITE PHOTOGRAPH

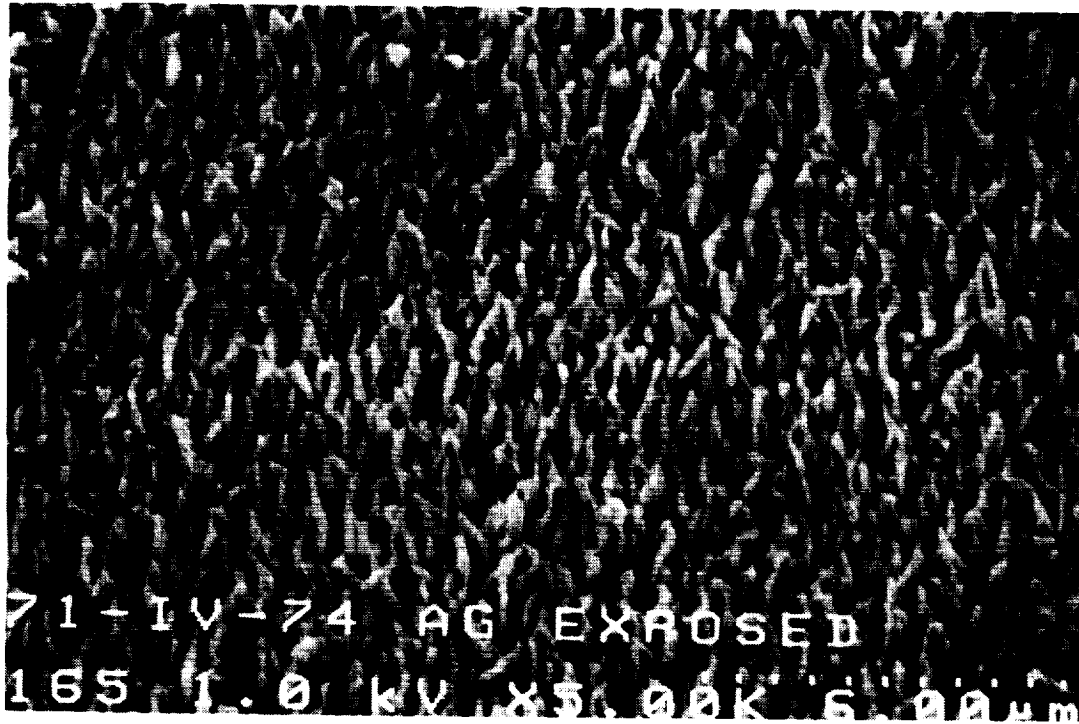


Figure 2b. Exposed Area of Silver from SEM Photograph of Disk Sample.

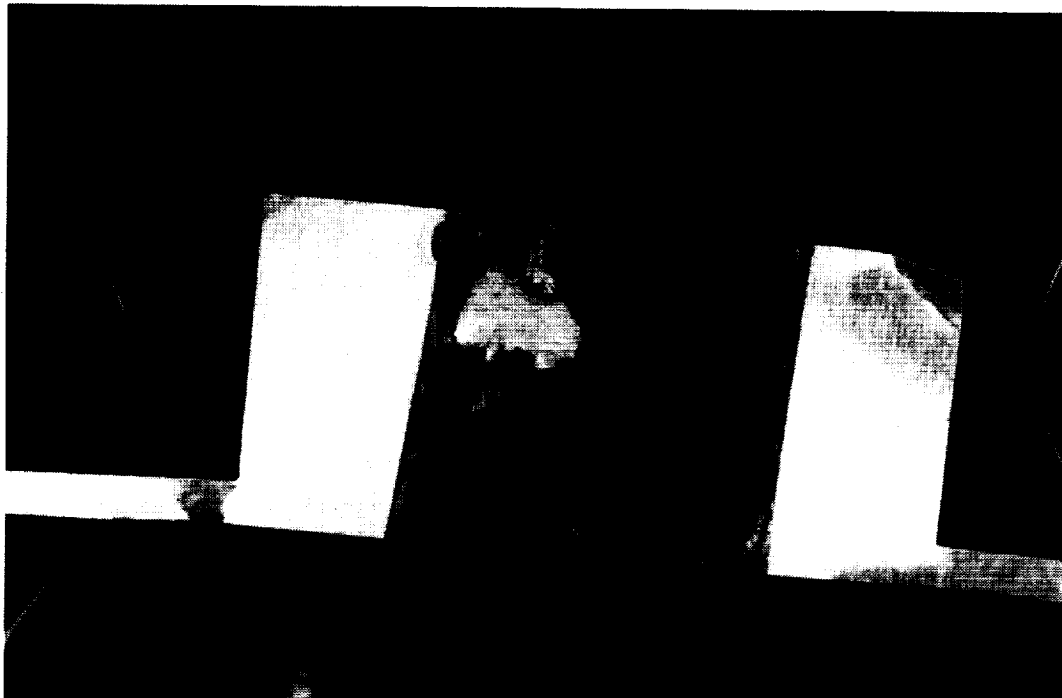


Figure 3. Cold Rolled Silver Ribbon Showing Exposed Area (Dark Scale) and Protected Area.



Figure 4. Scanning Electron Microscope View of Sample Coated With Aluminum Produced From Debris Impact.

SEM IMAGE
BLACK AND WHITE PHOTOGRAPH

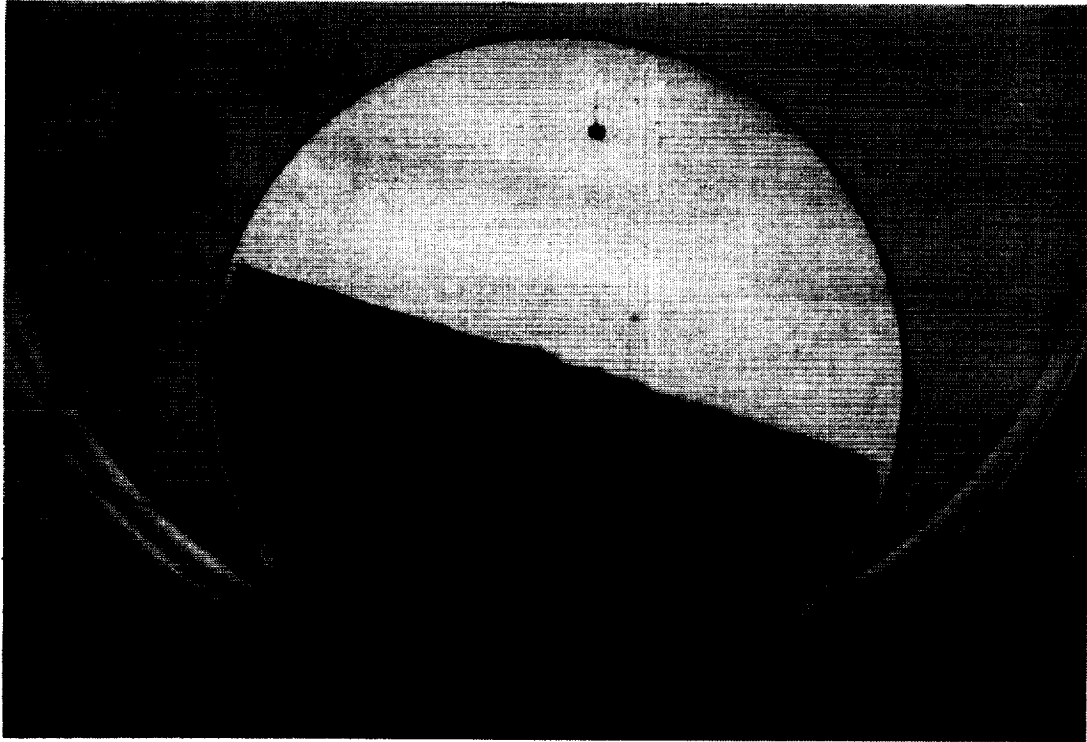


Figure 5. Dark Region of Silver Disk Indicates Area of Decreased Reflectivity.

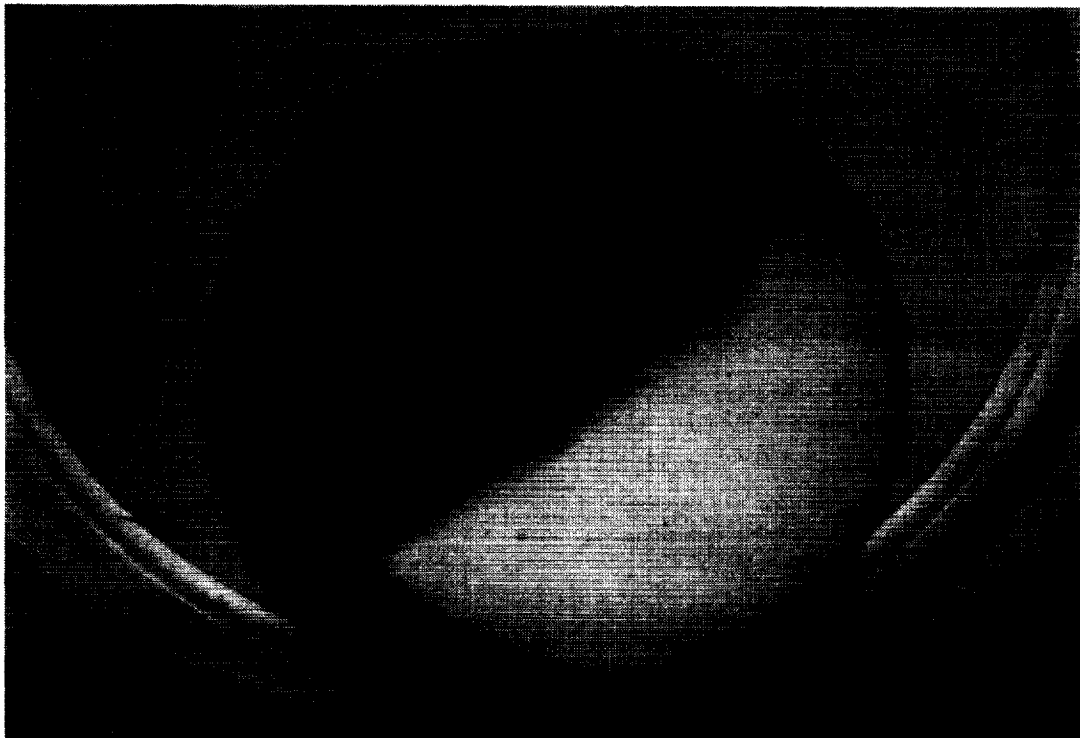


Figure 6. Dark Region of Copper Indicates Area of Decreased Reflectivity.

LDEF Experiment AO171

Sample: AO171-IV-50 Ni Cr Al Alloy

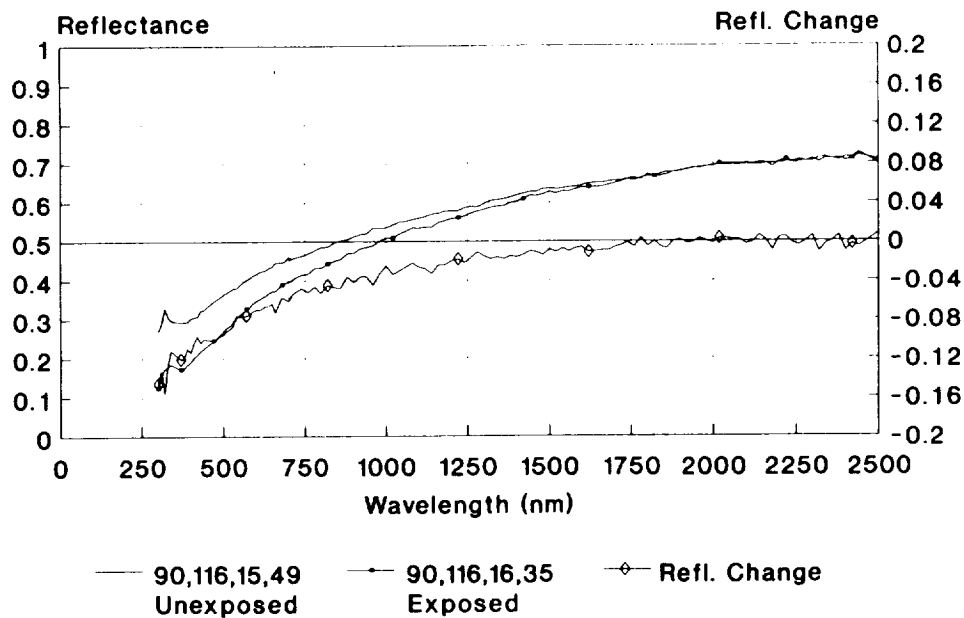


Figure 7. Solar Reflectivity Data for Ni-Cr-Al Alloy.

LDEF Experiment AO171

Sample: AO171-IV-53 Molybdenum

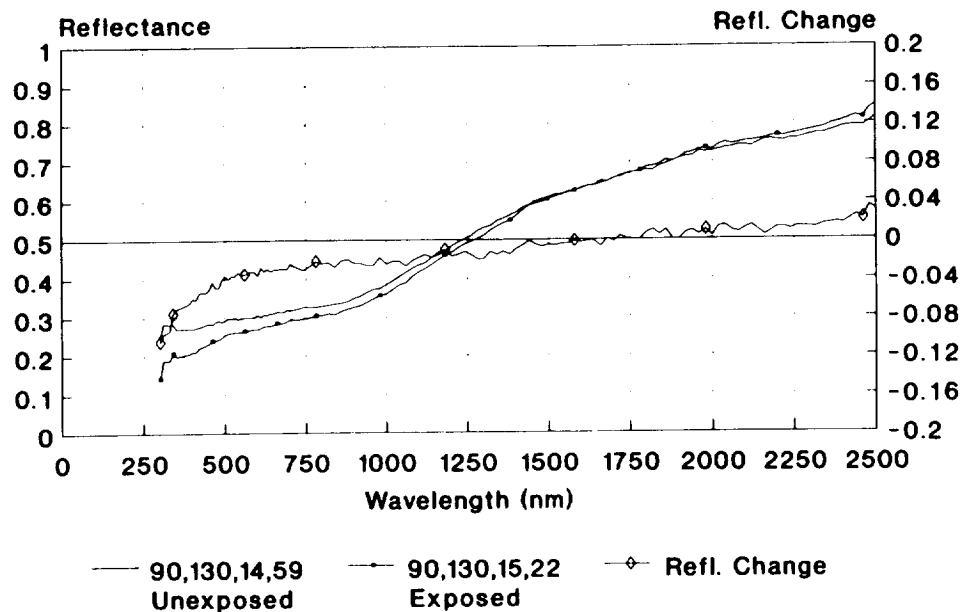


Figure 8. Solar Reflectivity Data for Molybdenum.

LDEF Experiment AO171

Sample: AO171-IV-73 Tantalum

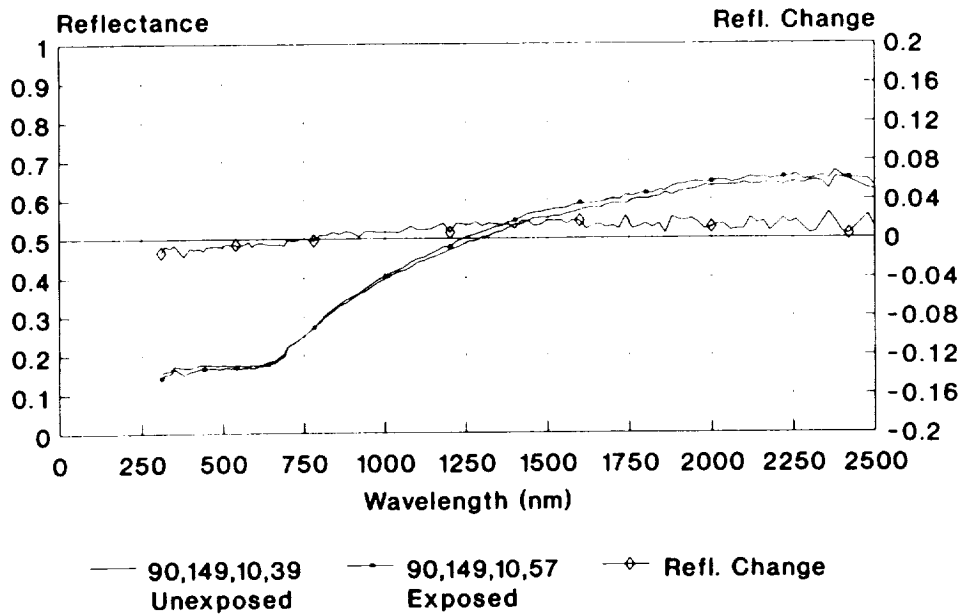


Figure 9. Solar Reflectivity Data for Tantalum.

SOME RESULTS OF THE OXIDATION INVESTIGATION OF COPPER AND SILVER SAMPLES FLOWN ON LDEF

A. de Rooij
ESA/ESTEC
Noordwijk, The Netherlands

INTRODUCTION

The LDEF mission provides a unique opportunity to study the long term effects of the space environment on materials. The LDEF has been deployed in orbit on 7 April 1984 by the shuttle Challenger in an almost circular orbit with a mean altitude of 477 km and an inclination of 28.5°. It was retrieved from its decayed orbit of 335 km by the shuttle Columbia on 12 January 1990 after almost 6 years in space.

The LDEF is a 12-sided, 4.267 m diameter and 9.144 m long structure. The experiments, placed on trays, are attached to the twelve sides and the two ends of the spacecraft. The LDEF was passively stabilized with one end of the spacecraft always pointing towards the earth centre and one of the sides (row 9) always facing the flight direction.

The materials investigated in this paper originate from the Ultra-Heavy Cosmic Ray Experiment (UHCRE). The main objective of this experiment is a detailed study of the charge spectra of ultraheavy cosmic-ray nuclei from zinc to uranium and beyond using solid-state track detectors. Besides the aluminium alloy used for the experiment, UHCRE comprises several other materials. The results of space exposure for two of them, the copper grounding strips and the thermal covers (FEP Teflon/Ag/Inconel) painted black on the inner side (Chemglaze Z306), will be presented here.

The three samples of thermal covers were taken from tray 10 (E10) and were examined using the SEM. Line profiling was performed to investigate the distribution of oxygen and fluor over the sample. Size measurements were performed on the silver as well on the FEP (coated with gold for conductivity reasons) using the scanning electron microscope. The five grounding strips originating from trays 1, 2, 6, 7 and 10 were examined. Originally these copper strips were used as grounding strips on the experiment trays. The strips came from different trays and as such had different atomic oxygen levels. A part of the strips, fixed under the experiment trays, was not exposed to atomic oxygen. The copper strips were examined using a Cambridge S360 scanning electron microscope equipped with a Link X-ray analyser, an LaB₆ electron gun, a windowless detector and a four-element solid state back-scatter detector. The thickness of the oxide layer was determined using the TFOS (Thin Film On Substrates) programme supplied with the LINK X-ray analyser (ref 1). Auger-XPS profiling was performed using a VG SCIENTIFIC ESCALAB MKII Spectrometer fitted with an LEG200 electron gun and an AG21 Ar⁺ ion gun.

RESULTS and DISCUSSION

Three pieces of thermal blanket were examined originating from different locations and each showing a penetration by presumably a micro-meteoroid. Those locations were selected having different penetration hole sizes. The samples were cut out and the top FEP layer was mechanically separated from the underlying metal layers. The layout of the UHCRE thermal blanket is illustrated in figure 1.

The first noticeable observation on the silver layer that can already be done by the naked eye is the presence of black concentric rings around the hole in the silver layer. All three samples exhibit these attributes to the extent that the bigger the hole in the silver layer the more pronounced the presence of these concentric rings. Closer observation always reveals the same pattern. Around the hole a dark region is found, surrounded by a light ring. Further away the dark rings are recognised. These rings are found in clusters of three to four rings. An example of these clusters of rings is given in figure 2. This exposure is achieved using the electron backscatter technique in the atomic number contrast mode. In this mode the brightness of the features on the photo is related to the atomic number: the higher the atomic number, the brighter the feature. Silver-oxide would appear dark and silver would appear as white, because the average atomic number of silver-oxide is lower than of silver itself.

These types of rings are often seen on outer surfaces that are bombarded with hyper-velocity particles and originate from the impact shock wave and vapourised matter from the target and source material. However, in the case of the thermal blanket the silver layer is not the outer layer, but is found under the FEP top layer.

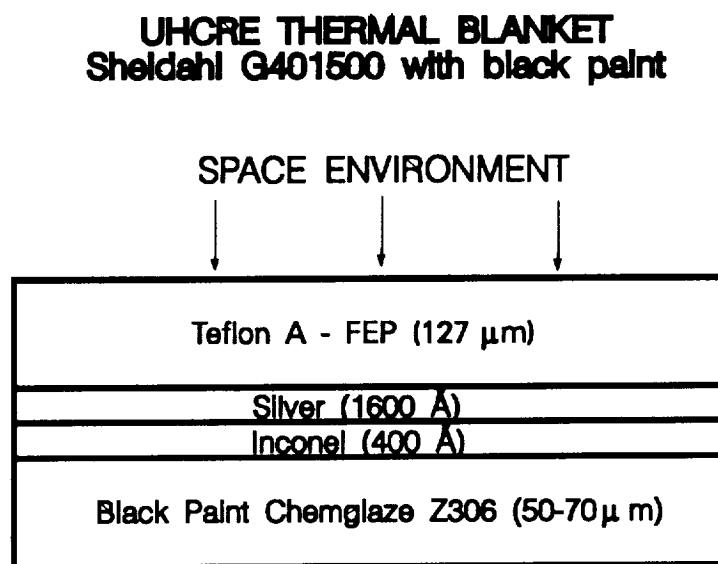


Figure 1. Layout of UHCRE thermal blanket



Figure 2. SEM backscatter image of oxidised rings found on the silver layer under the FEP top layer of the UHCRE thermal blanket. Magn. X20

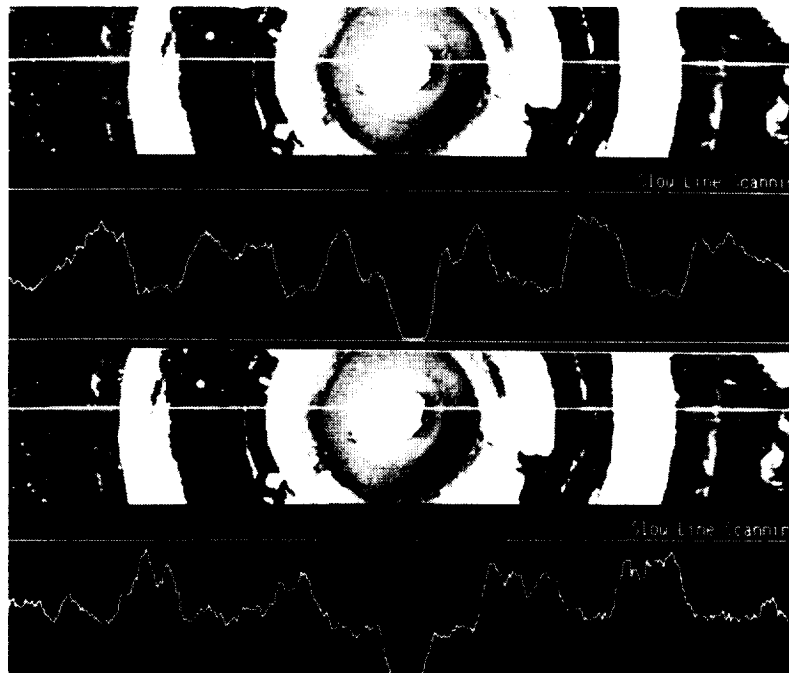


Figure 3. Oxygen linescan (top) and Fluor linescan across the rings.

Obviously these dark rings are oxidised silver. Oxidised silver frequently occurs when silver is exposed to atomic oxygen found in low earth orbit. X-ray analysis indeed confirms the presence of silver-oxide in these black regions. The X-ray spectrum of the light rings shows the presence of fluor, which was absent on the dark rings. Indeed, a linescan across the sample, on oxygen and fluor, reveals an alternating pattern of oxygen and fluor with oxygen in the dark areas and fluor in the light areas. Carbon is found everywhere on these rings. A linescan across one of the samples is found in figure 3.

The circular patterns on the silver layer result from the ejection of fluor/carbon atoms caused by the impact produced shock waves and local vaporizing of the FEP. Due to this impact the silver layer locally debonded from the FEP. Through the hole in the FEP, the silver was oxidised by the atomic oxygen. On the circular locations, where a thin fluor/carbon layer was formed by the vaporizing of the FEP and the shock wave, no attack of the silver was possible. Usually these thin layers are not very protective, but the incoming atomic oxygen has only its highest energy at the centre of the hole. Further away from the centre, the silver is attacked by reflected atomic oxygen that has a much lower energy and these oxygen atoms are unable to remove the protective fluor/carbon layers.

The sizes of the impact holes were measured in the FEP layer as well as in the silver/inconel layer and at the rear side of the silver/inconel where the black paint is present. The hole size increases with the journey of the micro-meteoroid through the sample. The smallest hole size is found at the FEP side. At the exposed FEP side the surface shows clearly signs of atomic oxygen attack. A substantial increase in hole dimensions is measured going from the FEP to the silver/inconel layer.

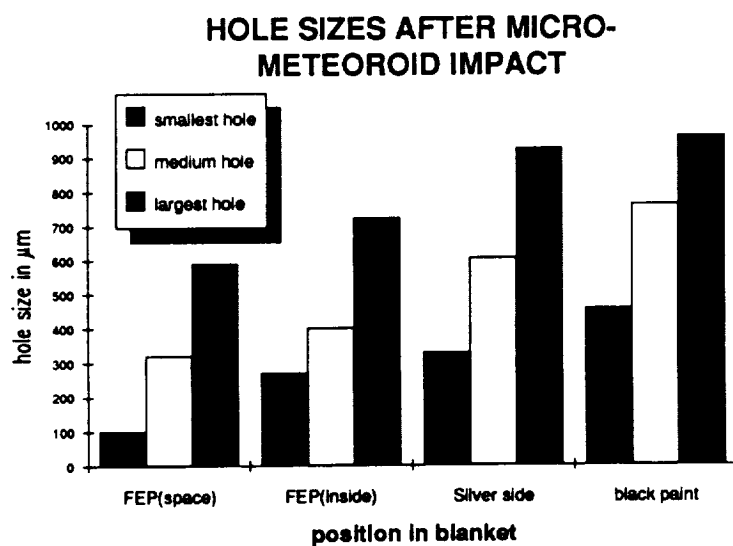


Figure 4a. Holes sizes measured in UHCRE Thermal blanket after micro-meteoroid impact

The sizes of the impact holes of the three examined samples are given in figure 4a. The first position is the space side of the FEP. The second position is the under side of the FEP that was in contact with the silver layer. The third position is the entrance hole in the silver layer, while the fourth position is the rear side of the blanket, i.e. the black paint Chemglaze Z306. A specific row of holes is illustrated in figs. 4b– e.

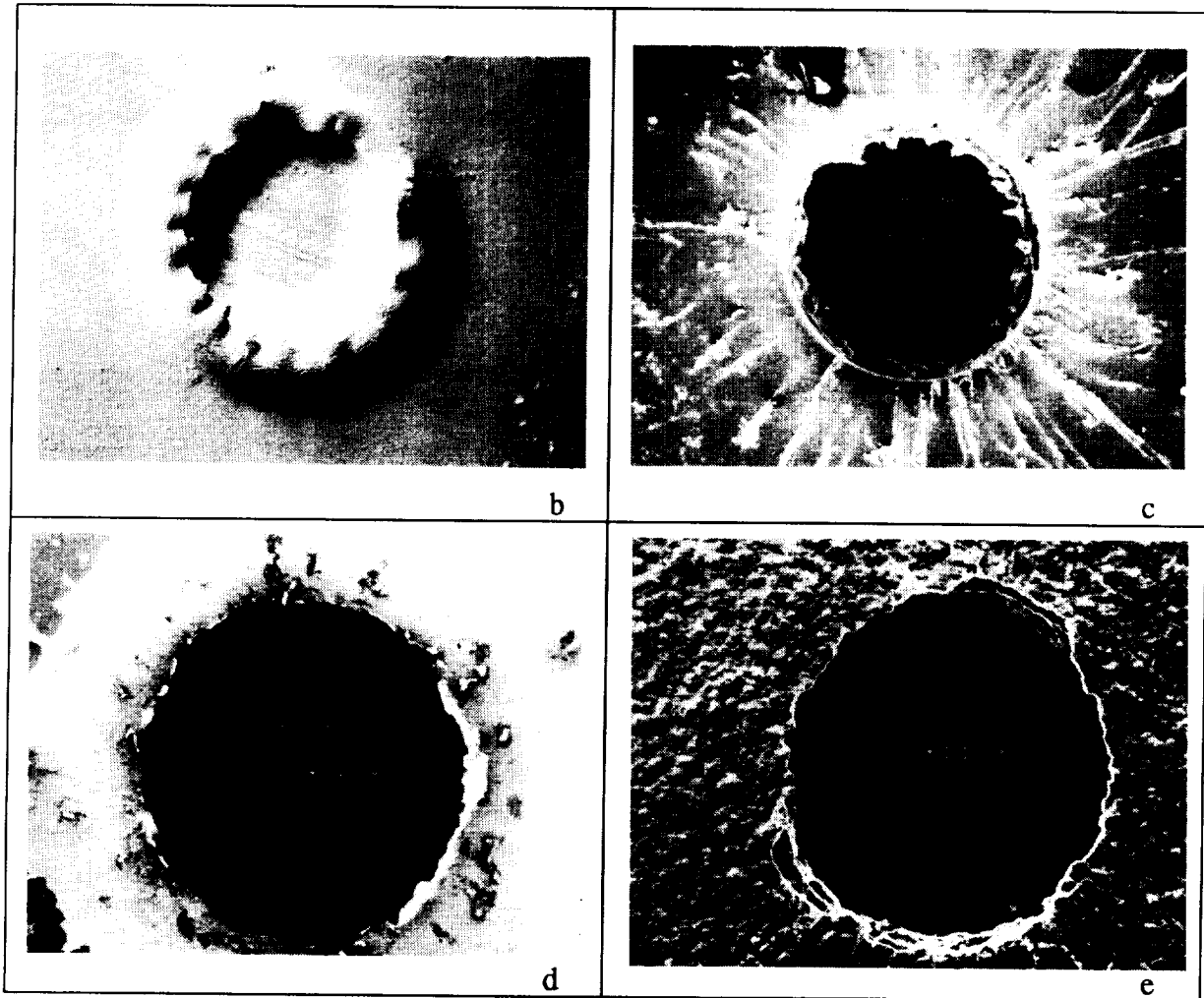


Figure 4b. SEM view on the space exposed side of the FEP layer showing the smallest hole with deformed edges and atomic oxygen erosion (size 590 μm).

Figure 4c. SEM view on the silver contacted side of the FEP layer showing an already larger hole than seen in figure 5a and radial marks of re-solidified FEP (size 710-735 μm).

Figure 4d. SEM view on the layer of silver/inconel. The hole size is approximately 1.5 times as large as found in figure 5b (size 909-940 μm).

Figure 4e. SEM view on the black paint on the rear side of the thermal blanket (size 917-1010 μm).

Five copper grounding strips were examined. These five strips came from different experimental trays. The atomic oxygen fluences experienced by the grounding strips are related to the position of the experimental tray, and for the five grounding strips the fluences following reference 2 are given as:

Table I. Atomic Oxygen Fluence Experienced By The Examined Copper Grounding Strips

Strip nr.	Fluence at/cm ²
D01	1.22 .10 ¹⁷
E02	1.37 .10 ⁰⁹
C06	4.93 .10 ¹⁹
D07	3.16 .10 ²¹
E10	7.78 .10 ²¹

The fluence values given in table I are maximum values because the grounding strips are generally not in plane with the experimental tray. Only close to the fixation point have the grounding strips seen these fluences.

The visual result of the exposure to atomic oxygen on copper is a discolouration of the surface to levels corresponding to the oxygen fluences. The oxide type on copper is usually Cu₂O and has a ruby red appearance. From these colours the oxide thickness can be estimated. Several authors have found a relationship between the oxide thickness and the colour of the oxide layer (see reference 3).

Before measuring the thickness of the tarnish film, the type of oxide film is established. The chemical shift effect in X-ray photoelectron spectroscopy (XPS) provides us with the information about the chemical structure and the oxidation state of the surface compound. The XPS spectra from Cu₂O (Cu¹⁺) and CuO (Cu²⁺) exhibit different binding energies while also the Cu²⁺ spectrum shows 'shake-up' satellite peaks, as illustrated in figure 5.

The identification of CuO on the oxidised samples is performed by positions of the Cu(2p_{3/2})-XPS spectrum, by Cu(L₃M_{4,5}M_{4,5})-Auger spectra and the O(1s) line positions. These three spectra enable us to distinguish between Cu, Cu₂O, CuO and Cu(OH)₂. Especially the difference between CuO and Cu(OH)₂, both Cu²⁺, can be determined with high confidence in the O(1s)-XPS energy region.

It was noted that during the Auger-XPS depth profiling measurements the CuO powder was reduced to Cu₂O. The reduction of CuO to Cu₂O has been reported in literature under intense beam fluxes (see reference 4). Several measurements on the CuO powder were performed to gain insight into this phenomenon. These experiments demonstrate that the reduction of CuO to Cu₂O was caused by the ion etching necessary for depth profiling and not by the electron beam. Ion etching changes the sample composition by selective removal of atoms in the topmost one or two atom layers and by cascade mixing over a depth of about 1-20 nm depending on the sample and sputtering conditions.

The Auger-XPS spectra are measured at the surface of the sample E10 and after repeated etching with the Argon ion gun. At the surface the presence of a thin CuO layer is determined. After two sputtering events the CuO signal disappears and a Cu₂O signal is measured. As discussed, the measurement of a Cu₂O signal after a CuO signal does not necessarily mean that Cu₂O is really present. A part of the oxide layer of sample E10 was removed using a new scalpel blade while the specimen was positioned on the Auger specimen table. Immediately after the partial removal of the oxide layer the sample was returned into the airlock to avoid any re-oxidation. Auger-XPS spectrum of this area shows the presence of Cu₂O instead of CuO. This sequence of oxide layers is consistent with observations on copper oxidised in air at low temperature as depicted in figure 6.

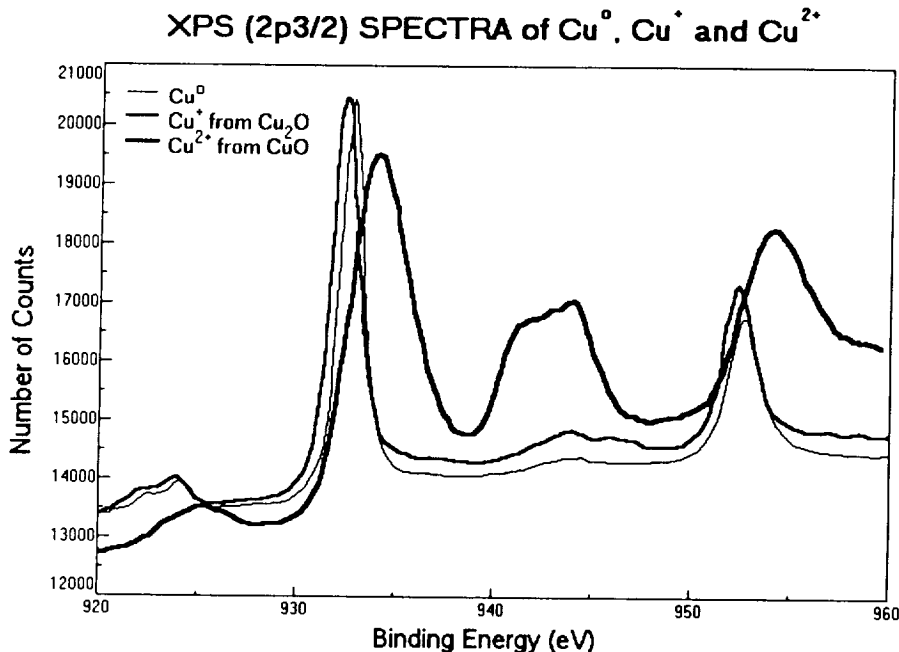


Figure 5. Copper 2p spectra of Cu⁰, Cu⁺ and Cu²⁺ showing the chemical shifts due to the oxidation state. The 2p spectrum of Cu²⁺ shows the two strong 'shake up' satellites.

At low oxygen pressures, the only oxide found on copper is Cu_2O as illustrated in figure 7. It is reasonable to assume that this is also true for copper exposed under low earth orbit conditions. The presence of a CuO layer on top of the Cu_2O layer as found on the LDEF samples should then be questioned. It can be argued that this CuO layer is formed on ground during the time of storage after retrieval of LDEF.

Although fundamentally significant for understanding the corrosion mechanism of copper under low earth orbit conditions, the presence of a very thin CuO layer on top of a Cu_2O layer is of minor importance for oxide thickness determinations.

Several authors have applied spectrophotometric techniques to the determination of the thickness of oxide films on copper. Several tables exist that give the relation between the observed colour of the oxide and the oxide thickness. The colour of the oxide layer on sample E10 is red brown. This colour leads to a thickness estimation between 400 and 500 Å.

X-ray analysis of surface layers measures partly the layer and partly the underlying base metal if the thickness of the layer is smaller than the X-ray generation depth. The X-ray generation depth depends on the material properties (atomic mass, density), X-ray line measured and the acceleration voltage. Using the TFOS programme supplied with the Link AN10000 X-ray analyser the thickness of the oxide layer on sample E10, assuming a Cu_2O layer, is calculated as 505 Å. For this calculation to be accurate a specimen with a known oxide thickness has to be used. A non exposed part of the copper strips is used as a standard. Under ambient conditions copper oxidises very slowly and it tends to be an almost constant value after several days. This constant value is approximately 50-60 Å. A value of 60 Å is taken as reference for the X-ray calculations.

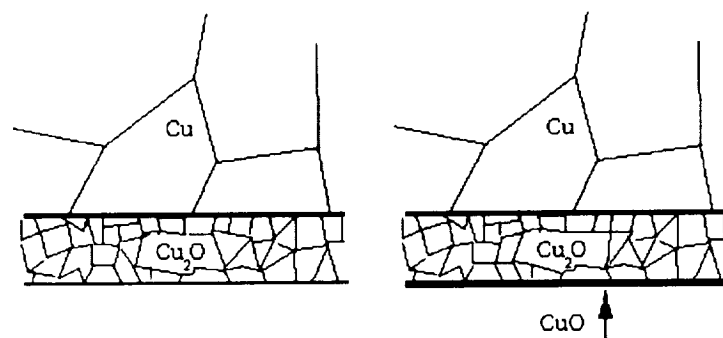


Figure 6. *Left: pure copper oxidised at low pressure or in air above 1025 °C. Right: pure copper oxidised in air below 1025 °C. (from ref. 5)*

The third method of oxide thickness determination is the depth profile during Auger-XPS measurements. This method depends on knowledge of the sputtering rates of the materials under ion bombardment. A clean copper sample was ion etched under the same depth profiling conditions as the LDEF samples. After 38000 seconds

of etching a step of 5 μm was measured on the copper surface yielding a sputtering rate of 1.3 $\text{\AA}/\text{s}$ for copper. Taking into account the different molecular mass and density of Cu_2O as opposed to copper, the sputtering rate of Cu_2O is estimated lower than the one for copper. A value of 1 $\text{\AA}/\text{s}$ is taken for Cu_2O . Depth profiles of four LDEF samples are given in figure 7. Using the calculated sputter rate the copper profile and the oxygen profile of sample E10 reveal an oxide layer thickness between 500 and 600 \AA .

The colour as seen by the naked eye does not enable us to deduce the oxide thickness with confidence. The results of the X-ray and Auger-XPS measurements are combined and displayed in table II. The validity of the values given in table II has to be judged against the accuracies of the method employed. Both methods (X-ray and Auger depth profiling) depend on the knowledge of the type of oxide layer. Studies show that copper oxidised at low temperature exhibits a Cu_2O layer with a large non-stoichiometry (reference 6). The X-ray method of depth calculation depends on an accurate knowledge of the X-ray generation depth, which depends among others on the electron escape depth. The X-ray generation depth in the surface layer relies on the density, the mean atomic mass and the mean atomic number of this layer. Also very elaborate methods for the calculation of the thickness of layers on substrates, such as the PAP model from reference 7, require a realistic description of the depth distribution function.

Accurate depth profile measurements using Auger-XPS depend on obtaining a flat bottomed crater during ion sputtering of the calibration sample. The accuracy measured using a Talystep on the copper calibration sample is $\pm 20\%$. This measurement was not possible on the oxide layer and correction procedures in the calculation of the sputtering yield were used. The expected accuracy on the thickness determination is not better than $\pm 30\%$.

Table II. Individual And Average Results In \AA On Thickness Determination

Strip nr.	X-ray on thin films	Auger-XPS profiling	Colour of surface	Average
E02	167	150		158
C06	299	350		325
D07	491	500		495
E10	505	525	400-500	515

The average result from table II is graphically displayed in figure 8, where the thickness is plotted against the atomic oxygen fluence at the end of mission for each sample investigated. A logarithmic function can be fitted to the data points. Direct logarithmic or inverse logarithmic relationships are usually found for the oxidation of copper oxidised at low temperature and small film thicknesses.

DEPTH PROFILE of LDEF EXPOSED CU SAMPLES

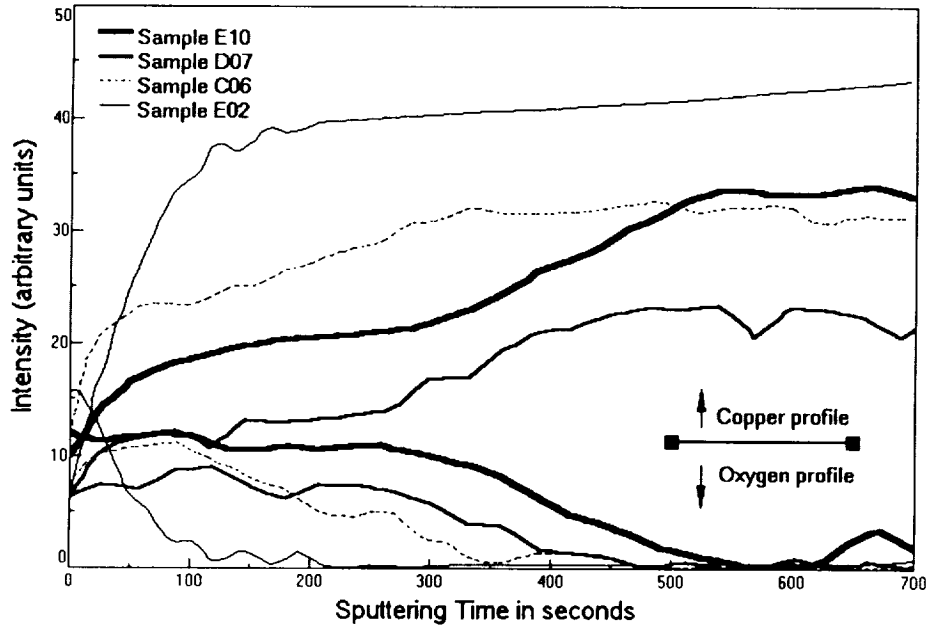


Figure 7. Depth profile of Copper and Oxygen from the Cu samples exposed on LDEF. The four upward curves are the Cu profiles and the four downward curves are the oxygen profiles.

OXIDE THICKNESS vs ATOMIC OXYGEN FLUENCE

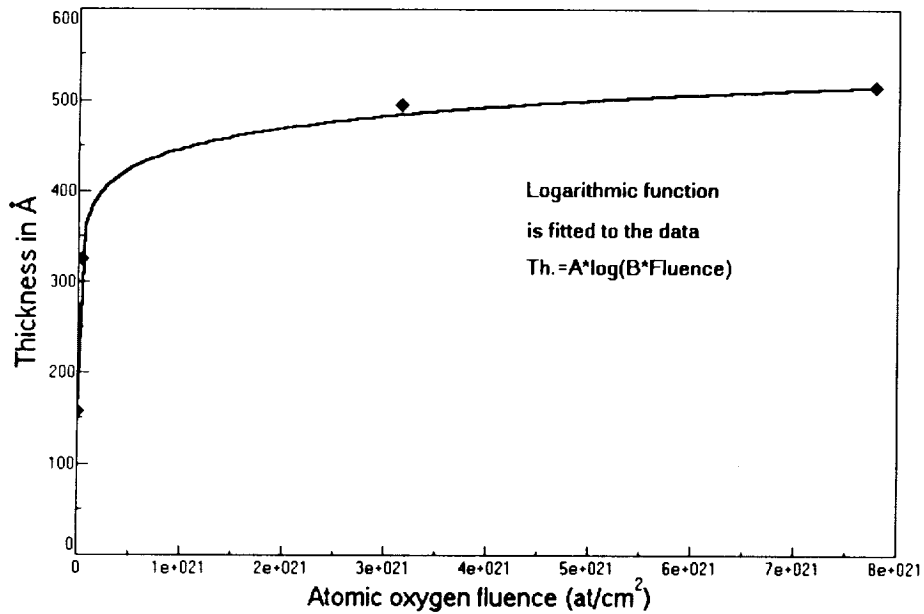


Figure 8. Thickness of oxide film measured on copper after exposure in low earth orbit.

DEPTH PROFILE of SAMPLE D01

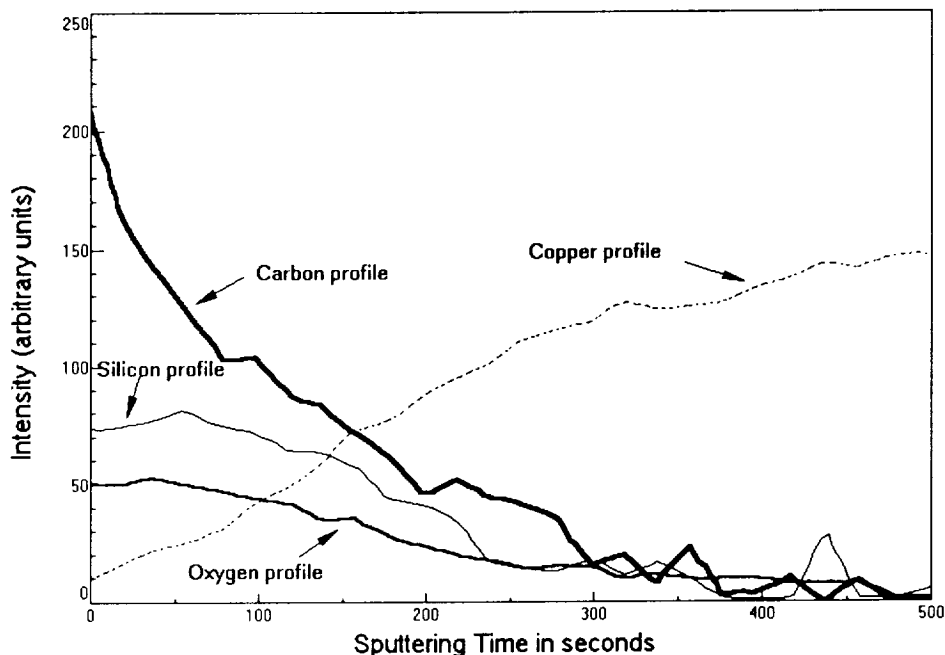


Figure 9. Depth profile of Carbon, Copper, Silicon and Oxygen from sample D01. The Carbon, the Silicon and the Oxygen decay in the same manner.

The thickness of the oxide layer of four of the five samples could be measured. X-ray measurements on the sample from tray 1 (D01) revealed the presence of high amounts of carbon and silicon. The depth profiles of the elements present in the surface layer are shown in figure 9.

The copper signal starts off much lower than the oxygen signal as opposed to the signal seen in figure 8. The carbon, the silicon and the oxygen signals decay in the same manner reaching zero intensity at the same sputtering time. When the intensities of these three signals are negligibly small the copper signal approaches its maximum. This indicates the presence of a silicon oxide instead of a copper oxide. The silicon oxide contains significant amounts of carbon, so probably the silicon oxide originated from a silicone contaminant. This contamination occurred very early in the mission because no significant traces of a copper oxide layer are found.

CONCLUSION

The silver samples, being part of the UHCRE thermal blanket, were oxidised through holes in the outer Teflon A-FEP layer. The micro-meteoroids that caused these holes evaporate the FEP locally. The shock wave, induced by the impact, redistributes the evaporated FEP over the underlying silver in a circular pattern with high and low density regions of fluor/carbon. The areas of low density are subsequently oxidised by reflected atomic oxygen.

Copper is oxidised by atomic oxygen to thicknesses that exceed the ones found for standard atmosphere oxidation. The oxide was found to be adherent to the surface and consisted of Cu_2O and can be removed mechanically by rubbing. The top layer of CuO was probably formed during ground storage after retrieval of LDEF.

More accurate thickness determinations are needed to calculate the growth of the oxide layer under atomic oxygen bombardment. Controlled samples and probably optical techniques should be used to achieve this.

ACKNOWLEDGEMENT

The author wishes to acknowledge Mr. Vincent Schorer of the Components Division, ESTEC, for performing the Auger-XPS measurements and Mr. François Levadou of the Materials Division, ESTEC for supplying the samples.

REFERENCES

1. TFOS (Thin Film on a Substrate), SR2-500-TFS-0484, LINK Analytical Ltd, 1984, based on Yakowitz and Newbury (proceedings of the Ninth Annual Scanning Electron Microscopy Symp, 1976, p 151).
2. R.J. Bourassa, Boeing Defense and Space Group, LDEF Materials Workshop, Nov. 1991, NASA-LaRC, Hampton, VA, USA.
3. O. Kubaschewski and B.E. Hopkins. *Oxidation of Metals and Alloys*, 2nd edition, Butterworths, London, 1962, p 188.
4. D. Briggs and M.P. Seah, *Practical Surface Analysis by Auger and X-ray Photoelectron Spectroscopy*, John Wiley & Sons, New York, 1983, p 409
A.W. Czanderna, *Methods of Surface Analysis, Vol. 1*, Elsevier, Amsterdam, 1975, p 140.
5. H.H. Uhlig, *The Corrosion Handbook*, John Wiley & Sons, New York, 1948, p 622.
6. M. Lenglet, J.M. Machefert, J.M. Claude, B. Lefez, J. Lopitiaux and A.D'Huysser, *Study of the Large Non-stoichiometry of Copper(I) Oxide on Oxidized Copper ($T < 573\text{K}$, $p\text{O}_2 = 0.21\text{ atm}$)*, Surface and Interface Analysis, Vol 16, 289-292 (1990).
7. J.L. Pouchou and F. Pichoir, *Surface Film X-ray Microanalysis*, Scanning Vol 12, 212-224 (1990).

**CHANGES IN OXIDATION STATE OF CHROMIUM
DURING LDEF EXPOSURE****Johnny L. Golden****Boeing Defense & Space Group
Seattle, WA 98124-2499****Phone: 206/773-2055, FAX: 206/773-4946****INTRODUCTION**

The solar collector used for the McDonnell-Douglas Cascade Variable Heat Pipe, Experiment A0076 (Michael Grote - Principal Investigator) was finished with black chromium plating as a thermal control coating. The coating is metallic for low emittance, and is finely microcrystalline to a dimension which yields its high absorptivity. An underplate of nickel was applied to the aluminum absorber plate in order to achieve optimal absorptance characteristics from the black chromium plate surface.

Experiment A0076 was located at tray position F9, receiving a projected 8.7×10^{21} atomic oxygen atoms/sq.cm and 11,200 ESH solar radiation. During retrieval, it was observed that the aluminized kapton thermal blankets covering most of the tray had been severely eroded by atomic oxygen, and that a "flap" of aluminum foil was overlaying a roughly triangular shaped portion of the absorber panel (see figure 1). The aluminum foil "flap" was lost sometime between LDEF retrieval and deintegration. At deintegration, the black chromium was observed to have discolored where it had been covered by the foil "flap" (see figure 2). The following is a summary of the investigation into the cause of the discoloration.

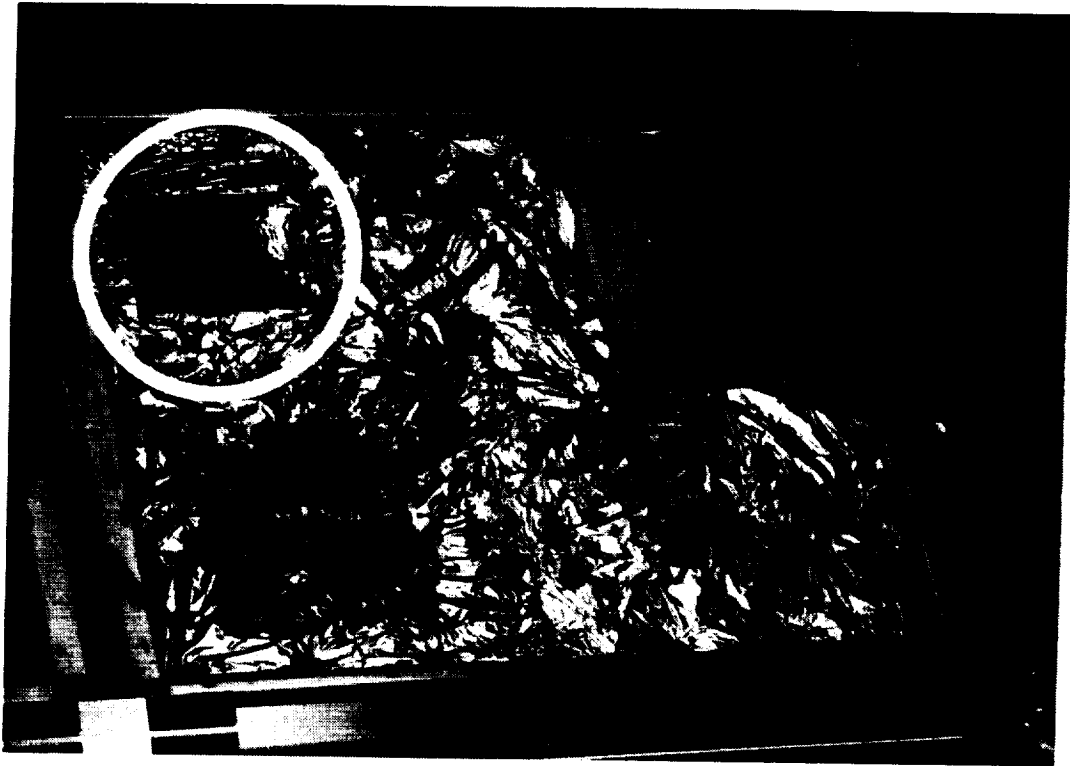


Figure 1. On-Orbit Photograph of Experiment A0076.

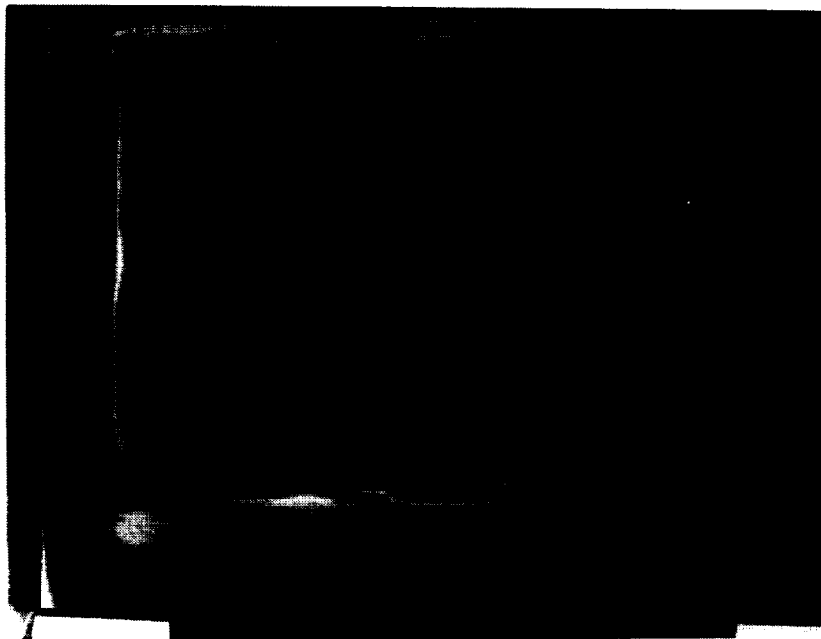


Figure 2. Close-Up on Solar Collector Panel After Deintegration.

Optical properties of the black chromium surface were measured and results are shown in figures 3 and 4. Measurements made at unexposed areas of the absorber panel indicate that these areas still meet or exceed the coating specification performance criteria ($\alpha > 0.90$, $\epsilon < 0.10$). Surfaces exposed to atomic oxygen and UV radiation for the full LDEF mission now have a blue tint. The optical properties of the blue area were minimally affected with a slight reduction in absorptance and no change in emittance. However, the surface which was covered with the aluminum flap for an unknown portion of the mission had degraded significantly in absorptance and slightly in emittance, resulting in a tan-color appearance.

The original hypothesis for this discoloration effect was based on contamination, in which the kapton film decomposition products from its atomic oxygen erosion would be deposited onto the black chromium surface. IR spectroscopy of specimens taken from the discolored area did not yield any measurable absorptions by organic contamination, however.

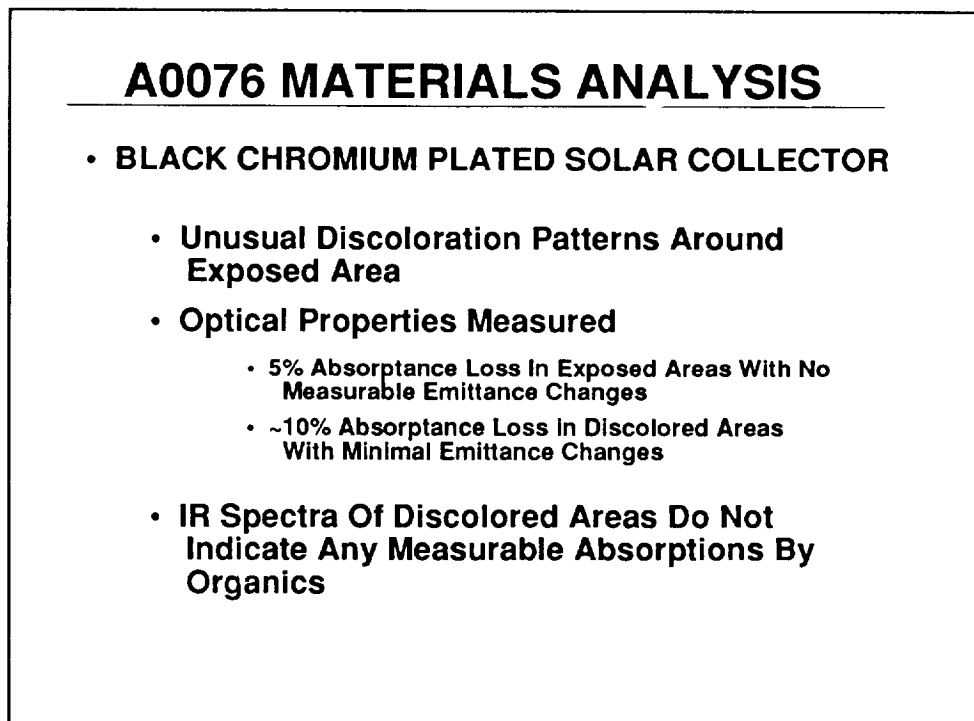
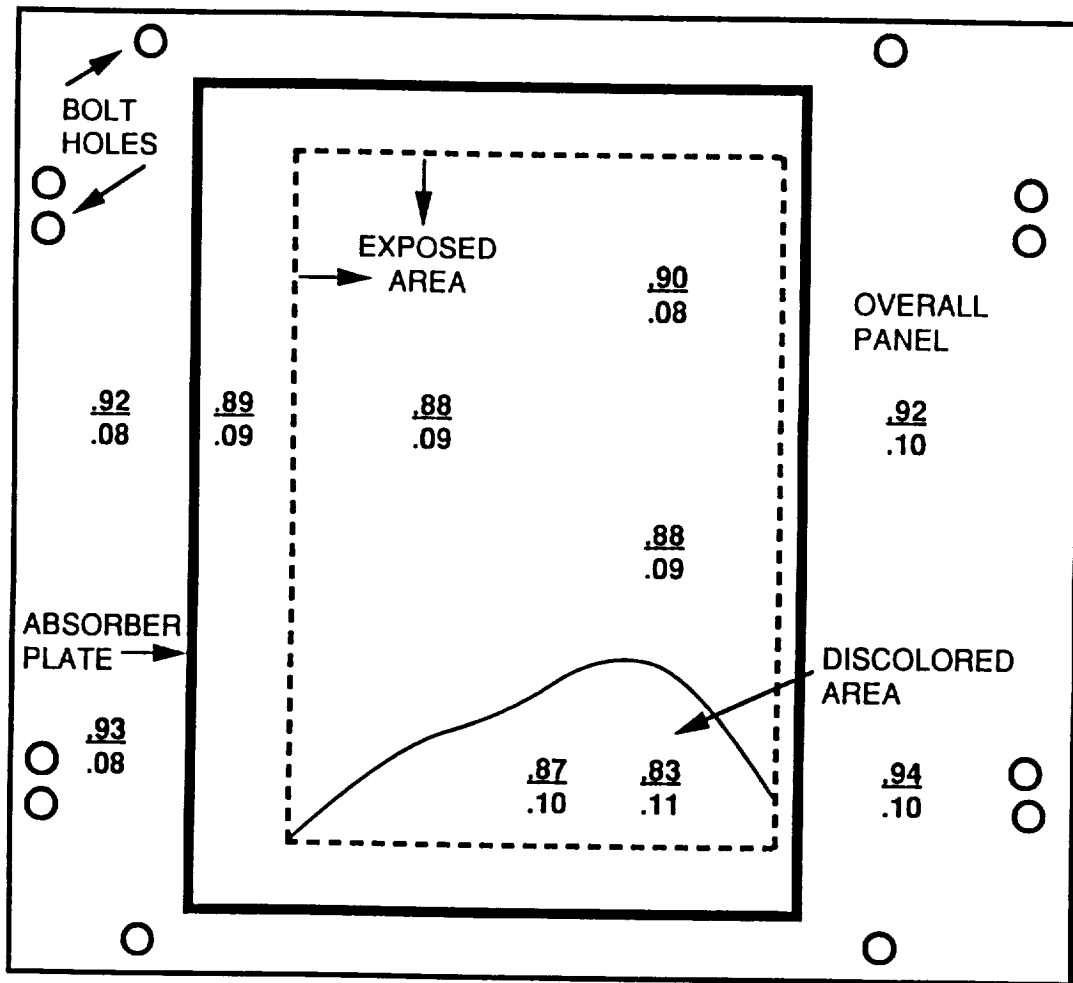


Figure 3.

McDonnell Douglas (LDEF F9 / A0076) Solar Collector
 Black Chrome Oxide Plated 7075 Aluminum



Readings are absorptance
emittance

Figure 4.

X-ray mapping was conducted for specimens taken from the discolored area. Silicon contamination was observed, but this contamination was limited to the extreme corners of the exposed absorber panel area. Silicone contamination was also observed on other structural parts from the interior of the A0076 experiment (fig. 5).

EDX was performed, an example of which is shown in figure 6. The penetration depth of the EDX analysis permits detection of the nickel underplate through the thin chromium layer. No discernable differences between nominal and discolored areas were detected.

SEM of the unexposed, exposed, and exposed and discolored areas of the black chromium are shown in figure 7, at 10,000X magnification. These views indicate fewer and more rounded crystallites in the discolored areas, but the same can be said for the exposed area which did not change significantly in optical properties.

Auger emission spectroscopy profiles were made of the three different areas; these are shown in figures 8, 9, and 10. Differences between the spectra are slight, and the elemental profiles are broad, making interpretation difficult. It appears that the chromium layer has thickened and the oxygen to chromium ratio has increased for the discolored (tan) area, as one compares spectra to those for the blue and then black areas.

A0076 MATERIALS ANALYSIS

- **BLACK CHROMIUM PLATED SOLAR COLLECTOR (Continued)**
 - **X-Ray Mapping Indicates Silicon Contamination Localized To Extreme Corners**
 - **EDX Detects Nickel Underplating**
 - **SEM Indicates Fewer And Rounded Crystallites In The Discolored Area**
 - **Surface Spectroscopy Measurements Indicate A Thickening Of The Surface Oxide In The Discolored Area**

31 May 91
BOA 50/JLG

Figure 5.

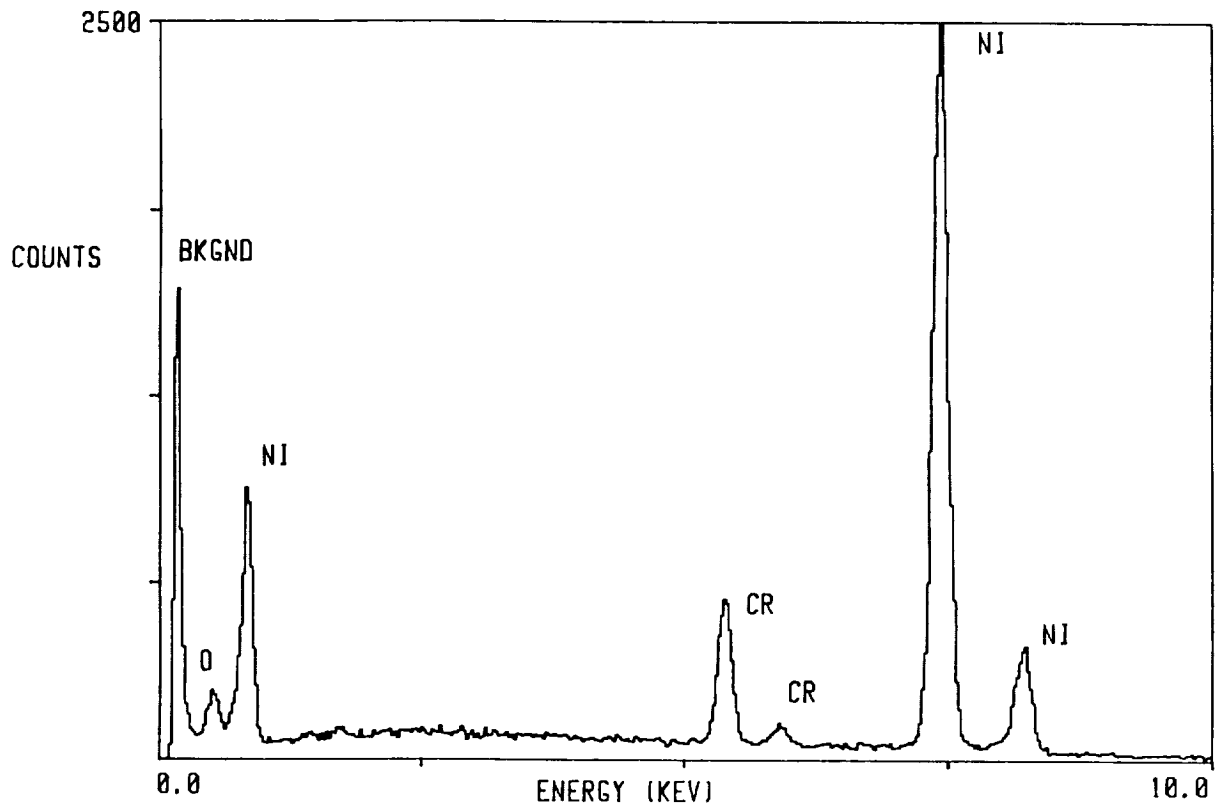
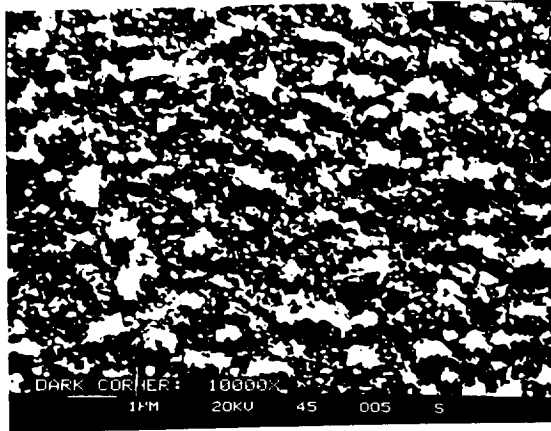
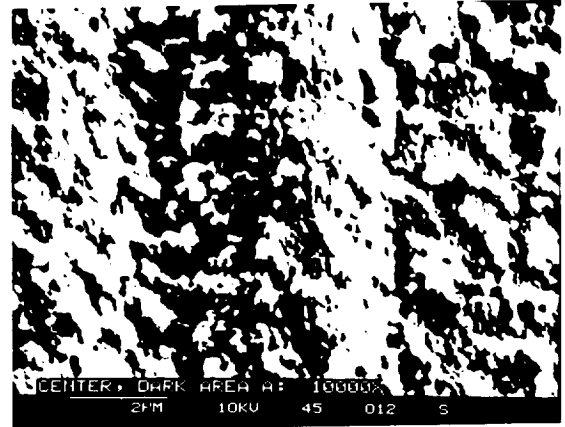


Figure 6. EDX of Discolored Area on Solar Collector Panel.



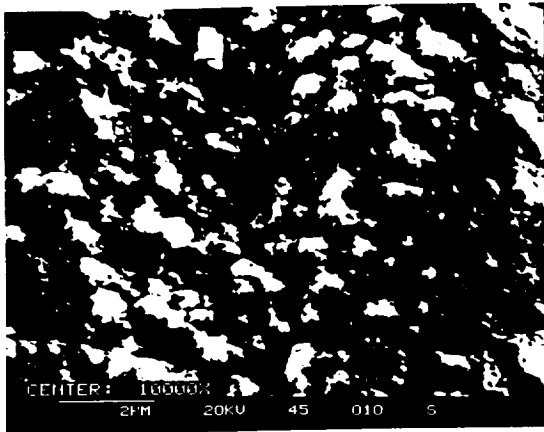
UNEXPOSED

B

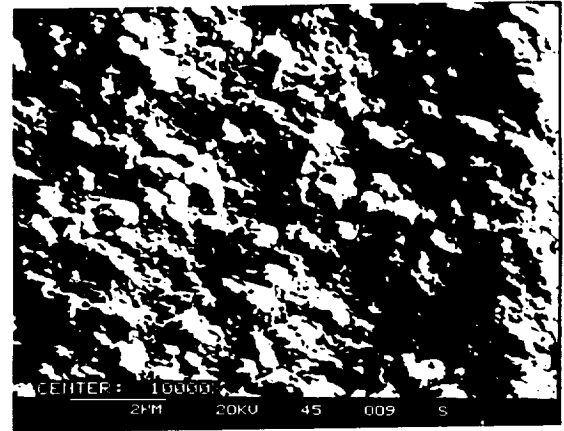


EXPOSED AND DISCOLORED

A



EXPOSED



EXPOSED AND DISCOLORED

Figure 7. SEM of Black Chromium Surfaces.

(Original photographs unavailable).

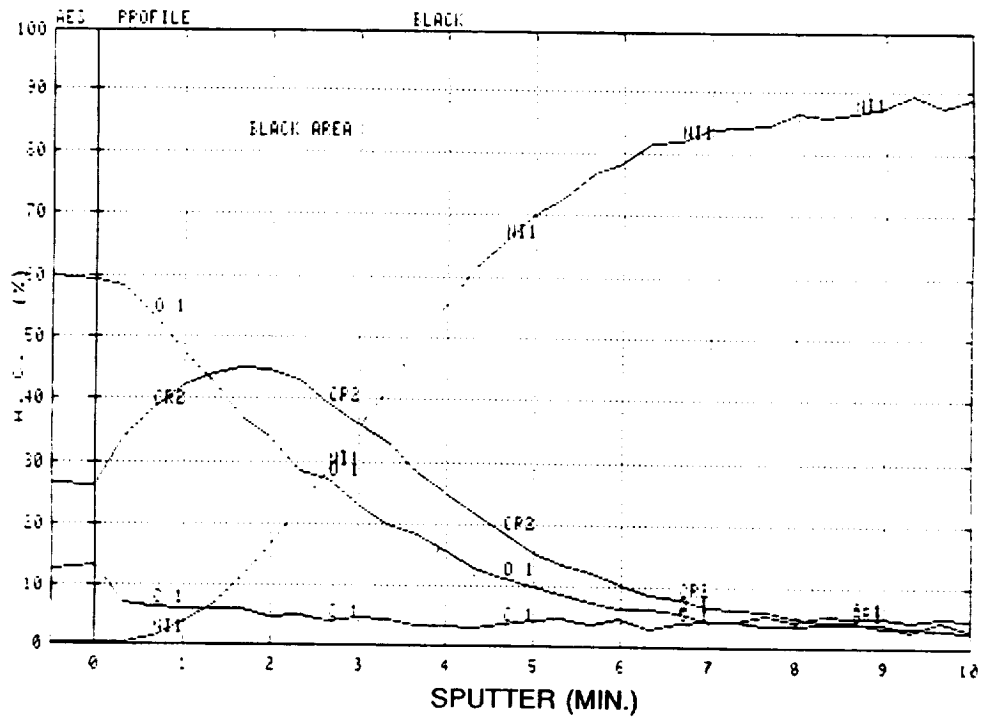


Figure 8. Auger Emission Spectroscopy Profile of Unexposed (Black) Area.

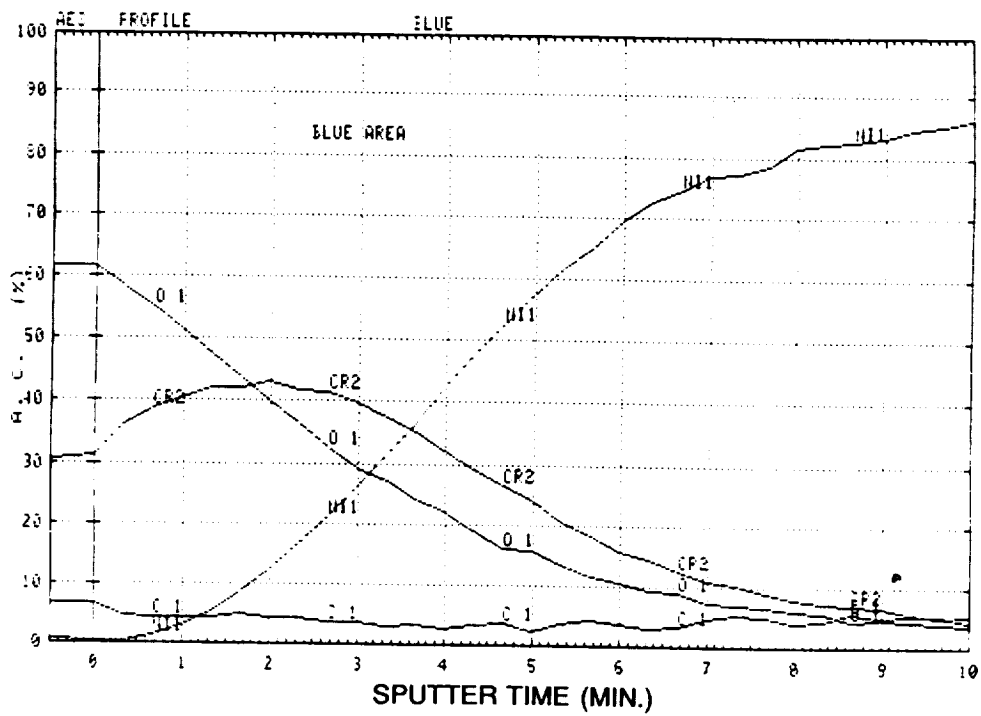


Figure 9. Auger Emission Spectroscopy Profile of Exposed (Blue) Area.

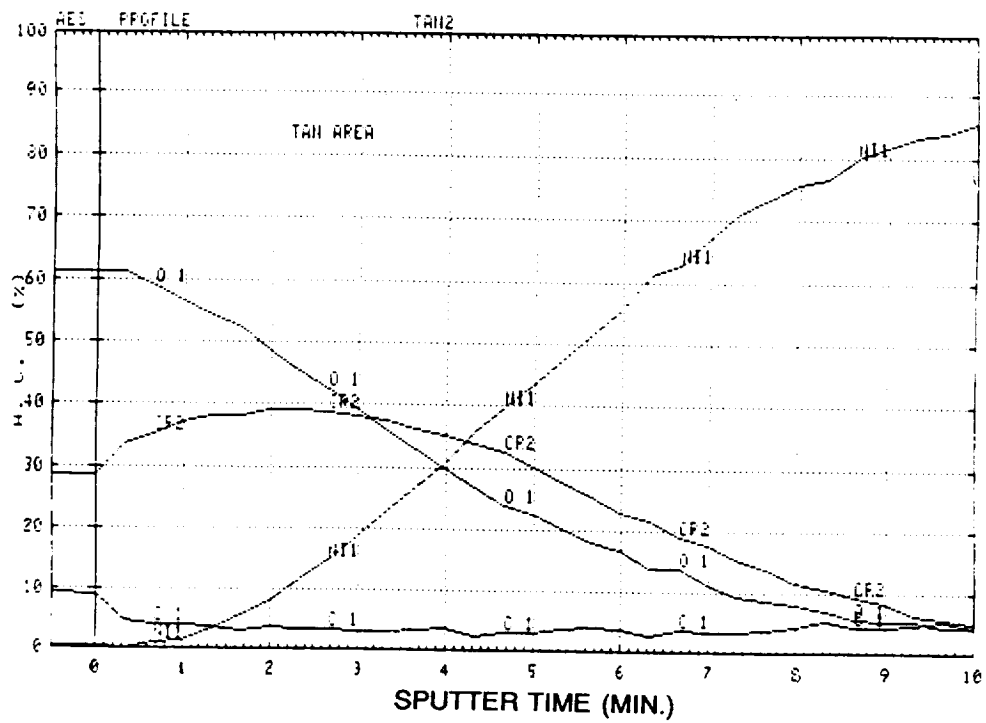


Figure 10. Auger Emission Spectroscopy Profile of Exposed & Discolored (Tan) Area.

These results are not conclusive. But based on the Auger results the following hypothesis is proposed. The discoloration was induced by a thermal effect, caused by the close proximity of the aluminum foil flap to the black chromium coating. The aluminum foil flap, with a low thermal mass and high absorptance to emittance ratio, became very hot, accelerating the atomic oxygen driven oxidation of the chromium. This hypothesis is currently in test using ESCA profiling to determine the chromium oxidation states as a function of depth (fig. 11).

A0076 MATERIALS ANALYSIS

HYPOTHESIS

- **Discoloration Was Caused By A Heating Effect. Residual Aluminum Foil (Low Thermal Mass, High a/e) From Degraded Thermal Blankets Super-Heated Areas Where It Contacted The Black Chromium Coating. Oxidation Of The Chromium Was Accelerated Due To Increased Temperature.**

Figure 11.

EFFECT OF SPACE EXPOSURE ON PYROELECTRIC INFRARED DETECTORS

James B. ROBERTSON
 NASA Langley Research Center
 Hampton, VA

INTRODUCTION

Pyroelectric detectors are one of the many different types of infrared radiation detectors. Pyroelectric detectors are of interest for long-term space use because they do not require cooling during operation. Also, they can detect at very long wavelengths and they have a relatively flat spectral response. A disadvantage is that the radiation must be chopped in order to be detected by a pyroelectric detector.

The objective of the experiment was to determine the effects of launch and space exposure on the performance of commercially available pyroelectric detectors.

The approach was to measure performance parameters of the detectors before and after flight on the Long-Duration Exposure Facility (LDEF) and determine the loss of detector performance. The experiment was passive; no data was taken during flight.

Experiment

A total of twenty pyroelectric detectors were flown on the LDEF and another nine were stored in unsealed containers on the ground as control samples. The detectors were chosen from what was commercially available in 1978. The detectors were mounted on tray E-5 of the LDEF, which was a slightly-trailing-side location. The tray was covered with a perforated aluminum plate for thermal control. The plate blocked 50% of incident radiation. Four of the twenty flight detectors were covered with a solid aluminum plate which shielded them from most of the space radiation but left them exposed to space vacuum.

The detectors used in the experiment represented three different pyroelectric materials, three different window materials and three different manufacturers (figure 1). The detector materials included lithium-tantalate (LT), strontium-barium-niobate (SBN) and triglycine-sulfate (TGS). The window materials included zinc-sulfide (ZnS), thalium-bromide-iodide (TlBrI), and polished germanium (Ge). Five of the flight detectors had no material in their windows. A list of the detectors with their material types, windows and location during flight is given in table 1.

The primary figure of merit for infrared detectors is the detectivity, D^* . D^* is calculated from the measured values of signal and noise voltage using the following equation:

$$D^* = \frac{S/N \sqrt{\Delta f}}{H \sqrt{A_d}} \quad (\text{cm } \sqrt{\text{Hz}} / \text{W})$$

where:

S = signal (volts)
 N = noise (volts)
 Δf = bandwidth (Hz)
 H = radiant energy flux (watts/cm²)

A_d = detector area (cm²)

Signal and noise measurements were made using a 500 K blackbody, a light chopper, a preamplifier and a wave analyzer and were made at chopping frequencies of 5, 10, 20 and 50 Hz.

Eleven LT detectors were flown. Five of these detectors had windows made of ZnS, one had a window of TlBrI and five had no window material, which exposed the pyroelectric material of these detectors directly to the space environment.

Five SBN detectors were flown. All SBN detectors had windows of polished germanium.

Four TGS detectors were flown. Three of the TGS detectors had windows of TlBrI, and one had a window of polished germanium. The cases of all of the TGS detectors were hermetically sealed.

The LDEF was put into orbit in April 1984 and was brought back to earth in January, 1990. Performance parameters of the flight detectors were measured after their return and compared to their pre-flight values. The same measurements were made on the control detectors. Results for flight detectors were compared to results for controls to separate the effects due to aging from the effects of space exposure.

POST-FLIGHT RESULTS

Visual Observations

There was a brown discoloration on the outer surfaces of the detectors similar to the "tobacco stain" that was found on much of the LDEF.

A much more noticeable effect was the existence of cloudy-white regions on the surface of the detector windows which were made of thallium-bromide-iodide (figure 2). This effect was seen only in the TlBrI of the exposed detectors and will be discussed in the Results section.

Detectivity

The results of the post-flight detectivity measurements are summarized in table 1. The table lists the detectors according to detector material, window material and location of the detector during the experiment (i.e. control sample, exposed flight sample or flight sample covered by the aluminum plate). Changes in noise measurement less than +/- 25% are not considered statistically significant.

LT Detectors

Among the LT detectors there were three "failures", i.e. no signal or erratic, unrepeatable signal. The erratic output signal suggests mechanical failure rather than radiation damage to pyroelectric material. The failure rate among the flight LT detectors (2 out of 9) was comparable to that for the control LT detectors (1 out of 4).

Differences between the pre-flight and post-flight detectivities were within the error bounds of the measurement with one exception. The exception was a LT detector with a TlBrI window whose post-flight signal was 38% less than its pre-flight signal. This loss is attributed to a decrease in transmissivity of the window material which is discussed in a later paragraph.

This decrease in signal combined with a 57% increase in noise produced a 61% decrease in D^* .

SBN Detectors

All of the SBN detectors survived the storage and flight. Differences between post-flight and pre-flight detectivities were within the error bounds of the measurement.

TGS Detectors

The detectors made of TGS did not fare well, either during flight or storage. Three of the four TGS flight detectors had zero signal response after flight. The fourth flight detector maintained its signal strength but had a 40% increase in noise. All of the TGS control detectors (4 out of 4) suffered complete loss of signal during storage on the ground. The failure of the TGS detectors during flight cannot be ascribed to space exposure since all of the control detectors failed during the same period of time.

Detector Windows

Some of the detector housings had infrared-transmitting materials in their windows; some had no material in their windows. Three different window materials were used: germanium (Ge), thallium bromide iodide (TlBrI) and zinc sulfide (ZnS). There was no visible damage in the germanium or zinc sulfide windows. Also, there was no significant loss in signal strength of the flight detectors having these window materials as compared to control detectors of the same type.

The TlBrI windows which were exposed during flight sustained noticeable damage. The damage was in the form of non-uniform white areas on the front surface of the windows (figure 2). This effect was not present in the TlBrI windows of the covered flight detector or in the control detectors. Similar damage was noted in two other LDEF experiments which exposed TlBrI during flight (experiment A0134, W. Slemp and experiment A0056, J. Seely et al.)

Transmission measurements were made on two of the damaged TlBrI windows and on a TlBrI window from one of the control detectors. The windows were removed from the detector cases in order to make the measurements. A 500 K blackbody was used as the radiation source, and the radiation flux was measured with a broad-band IR detector. The transmissivity was taken to be the ratio of detector signal with the window in the beam to the detector signal with no window in the beam. The exit aperture of the blackbody was smaller than the TlBrI windows allowing transmission measurements through several different areas of the same window. Transmission through the damaged TlBrI windows was compared to transmission through the control window. Loss of transmission through the damaged windows ranged from 17% to 50% depending upon the window and the location on each window; greater transmission loss corresponded to regions of greater visible damage.

Only one detector containing a TlBrI window was operable after flight. This detector was made of lithium-tantalate. All of the other TlBrI-windowed detectors were made of TGS. The decrease in signal strength from this detector after flight was 38%. This is consistent with the amount of IR transmission loss in the TlBrI windows.

Electron Spectroscopy for Chemical Analysis (ESCA) was performed on the same windows on which transmission measurements were made. Measurements were made at several locations on each window surface. The depth of this analysis

was approximately 5 nanometers. The analysis showed the presence of silicon, in the form of silicates, on the surface of the exposed windows. The Si concentration was higher in the regions of lesser damage and lower in regions of greater damage. Another significant result of the analysis was the change in the ratio of thalium to bromine, Tl:Br, in the surface of the exposed windows. In the control window, the Tl:Br ratio is approximately 1:1. In the low-damage areas of the exposed windows the Tl:Br ratio was 4.6:1, and in the high-damage areas the Tl:Br ratio was >26:1 (see table 2).

CONCLUSIONS

Detectivity

This experiment has shown that pyroelectric detectors made of lithium-tantalate or strontium-barium-niobate are suitable for long-term space use. The LT and SBN detectors survived six years of storage plus almost six years of exposure to space with little or no loss of performance.

Based on the results from detectors from one manufacturer, the detectors made of TGS, however, cannot be recommended because of their apparent short shelf life. Seven of the eight TGS detectors failed to respond after storage and/or flight. The exact cause of their failure has not yet been determined.

Window Material

The damage to the TlBrI windows was an interesting result. The damage was not uniform and was limited to the detector windows which had direct exposure to space. The presence of silicon in the form of silicates on the window surfaces is similar to reports from many LDEF experiments. The reason for the non-uniformity of the silicon concentration is not known. However, the inverse relationship between the silicon concentration and the amount of Br loss from the surface suggests that the silicate acted as a shield which lessened the loss of Br and I.

This experiment shows that the choice of window and lens material are of major importance. When used in space, a detector will be part of a system and will be located behind a lens or window of some sort. Damage to the lens or windows will most likely play a larger role in loss of system performance than will damage to the detector material.

Table 1
Changes in Detector Parameters

Detector Type (No. of Samples)	Window Material	Location During Flight	% Change Signal (avg)	% Change Noise (avg)	% Change D* (avg)
LT (1)	none	control	+ 2.5	- 9	+ 5.8
LT (1)	none	control	- 100		
LT (1)	none	covered	+ 1.0	- 10	+ 5
LT (1)	none	exposed	erratic		
LT (3)	none	exposed	- 5.3	+ 1	- 10
LT (2)	ZnS	control	- 4.0	+ 23	- 23
LT (1)	ZnS	covered	- 3.5	+ 4	- 5.5
LT (1)	ZnS	exposed	erratic		
LT (3)	ZnS	exposed	- 6.7	+ 24	- 25
LT (1)	TlBrI	exposed	- 38	+ 57	- 61
SBN (1)	Ge	control	+ 0.5	+ 1	0
SBN (1)	Ge	covered	- 1.4	+ 1	+ 2
SBN (4)	Ge	exposed	- 2.0	- 22	+ 28
TGS (4)	TlBrI	control	- 100		
TGS (1)	TlBrI	covered	- 100		
TGS (2)	TlBrI	exposed	- 100		
TGS (1)	Ge	exposed	0	+ 40	- 30

Table 2.
ESCA Analysis of TlBrI Windows

Sample	Si conc. (atomic %)	Tl:Br ratio
control	0	1:1
exposed low damage	17%	4.6:1
exposed high damage	6%	> 26:1

Examples of Pyroelectric Detectors

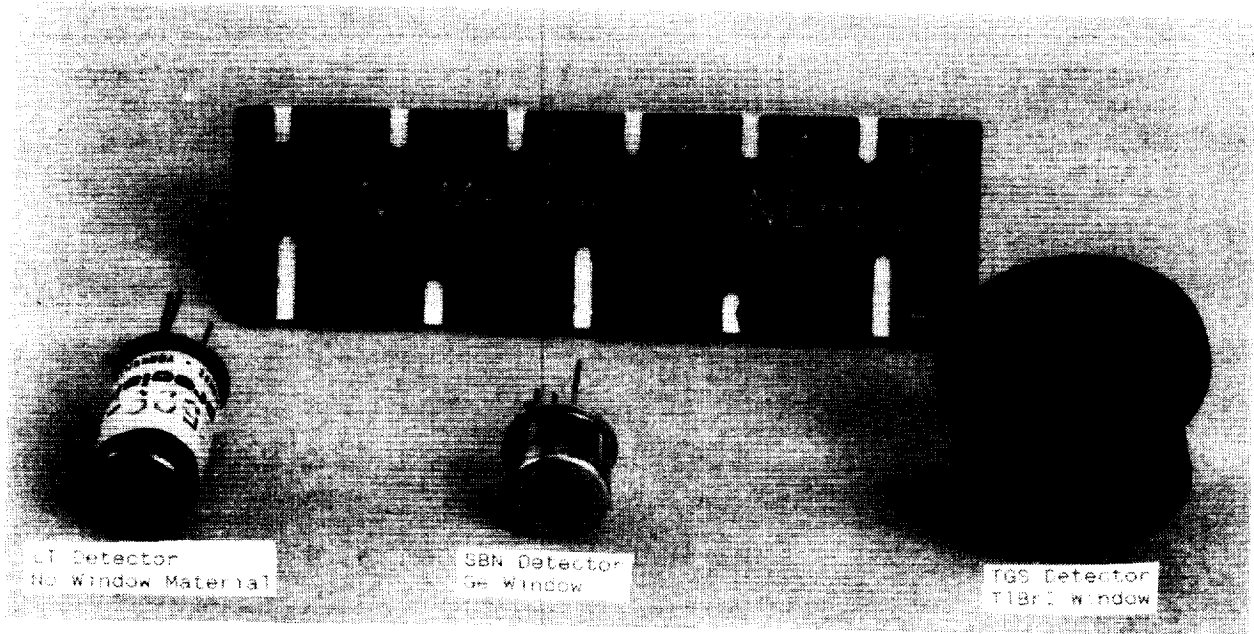


Figure 1

TlBrI Windows Showing Damage in Exposed Samples

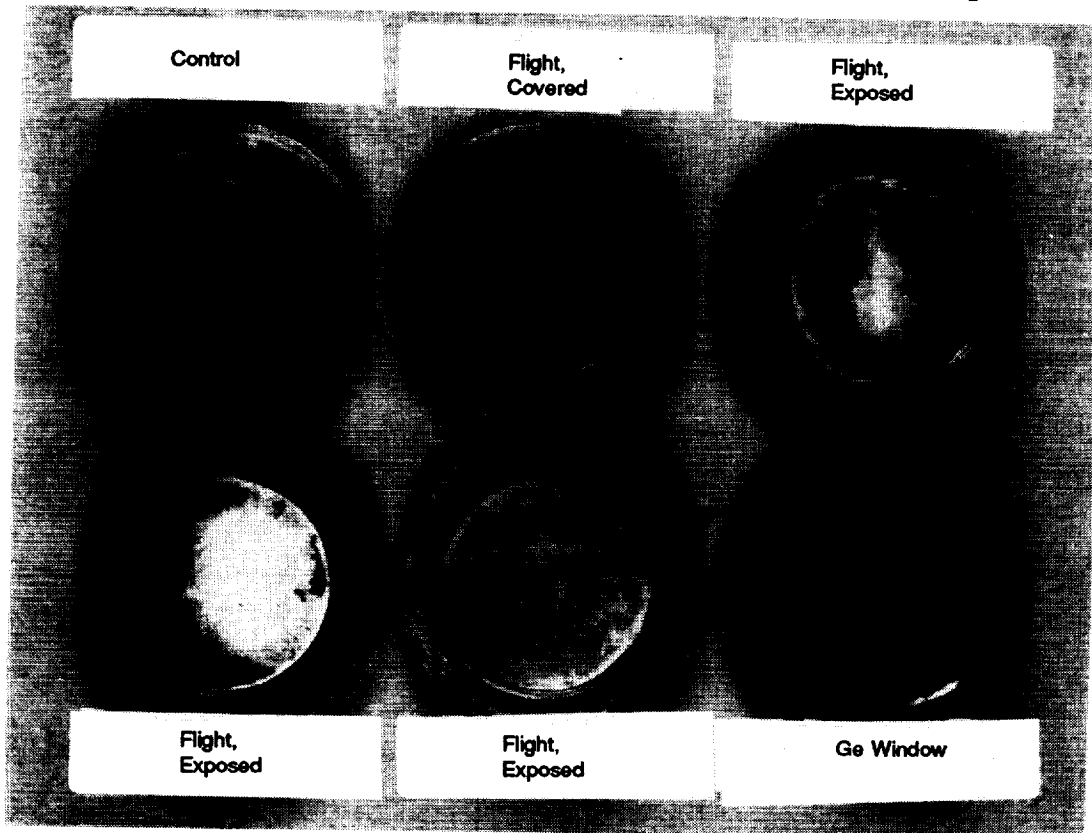


Figure 2

LONG DURATION EXPOSURE FACILITY (LDEF)
OPTICAL SYSTEMS SIG SUMMARY AND DATABASE

Gail Bohnhoff-Hlavacek
Boeing Defense & Space Group
P.O. Box 3999 M/S 8H-01
Seattle, WA 98124

INTRODUCTION

The main objectives of the LDEF Optical Systems Special Investigative Group (SIG) discipline are to develop a database of experimental findings on LDEF optical systems and elements hardware, and provide an optical system overview. Unlike the Electrical and Mechanical disciplines, the Optics effort relies primarily on the testing of hardware at the various principal investigator's laboratories, since minimal testing of optical hardware was done at Boeing. This is because all space-exposed optics hardware are part of other individual experiments.

At this time, all optical systems and elements testing by experiment investigator teams is not complete, and in some cases has hardly begun. Most experiment results to date, document observations and measurements that "show what happened". Still to come from many principal investigators is a critical analysis to explain "why it happened" and future design implications.

This paper summarizes the original optical system related concerns, the lessons learned at a preliminary stage in the Optical Systems Investigations and describes the design of the Optical Experiments Database. Finally, this paper describes how to acquire and use the database to review the LDEF results in detail.

OPTICAL SYSTEMS RELATED CONCERNS

From a system's point of view, the degradation of an individual optical element can easily affect the overall system performance. For instance, surface degradation of a space-exposed transparent optical element, may cause an increase in diffuse scatter with a resulting loss of light transmission. In terms of the optical system, this could significantly degrade the final image resolution. The following outline identifies some of the original optical systems-related concerns:

Degradation of transparent elements (darkening, contamination, impacts)

- reduce the throughput of available light for radiometric, photometric, and imaging systems
- degrade image resolution

Degradation of optical coatings (erosion, discoloration, delamination, pitting, contamination)

- holes in coating may alter wavelength dependent transmission and reflection properties of the coating
- degraded or damaged coating may encourage initiation of other types of damage
- re-deposition of contaminants (including damaged coating material) on other system optics may cause loss of resolution, reduced throughput or altered wavelength dependence

Degradation of diffuse paints or diffuse metal coatings in optical systems (erosion, discoloration)

- baffling efficiency may decrease due to increase in specular reflection, or may increase due to an increase in roughness of baffle surface topography
- re-deposition on other materials
- contamination of system optics (loss of resolution, reduced throughput, altered wavelength dependence)

Degradation of fiber optics (radiation darkening, impacts, contamination)

- reduced transmission
- complete loss of signal
- increase in system bit error rate (digital)

- decrease in signal-to-noise ratio (analog)
- Detector changes
- responsivity
 - detectivity
 - rise time (system bandwidth)

LDEF OPTICAL MATERIALS "LESSONS LEARNED". SUMMARY

The LDEF optical hardware samples can be divided into seven groups for summarizing the general "lessons learned" up to the time of this report. Those groups are uncoated optical materials, coated optical materials, solar cells, fiber optics, detectors, reflectometers and radiometers, and optical sources. The results summaries are described in the following paragraphs.

Uncoated Optical Materials

Five LDEF experiments containing uncoated optical materials were reviewed. In general, hard uncoated optical materials were found to be quite resistant to the space environment. Even micrometeoroid/debris (M/D) impacts tended to have only localized damage without significant degradation of the optical performance. The impact sites appeared as craters surrounded by an expanded area of damage caused by melting, cratering, spallation or small fracture patterns.^{1 2} On samples exhibiting contamination, the spectral transmission could vary from no detectable change to catastrophic loss in transmission.^{3 4} This emphasizes the need for contamination prevention throughout any future mission duration. Exposed soft uncoated optical materials like thallium bromide (KRS-5 and KRS-6) experienced gross physical degradation of the substrate material as a result of excess space exposure, especially the effects of atomic oxygen bombardment.⁵

Coated Optical Materials

Several important observations were described on the LDEF experiments coated optical materials after their exposure to low earth orbit environments. Specifically, copper and silver coated optics showed oxidation due to atomic oxygen bombardment.⁶ Thermal cycling or thermal excursions were implicated in the delamination of dielectric and metallic coated optics.⁷ Contamination was shown to degrade transmission in many coated optical materials; however when the contaminant was cleaned, transmission results often returned to pre-flight measurements.⁸ Some evidence of environmental degradation in the fluoride compound protective or antireflection coatings (e.g. MgF₂, CaF₂) was noted.⁹ As with the uncoated optical materials, the micrometeoroid and debris (M/D) impacts showed localized impact damage effects, but their actual damage potential was often dependent on the impact density on the coated optical material.¹⁰

Note that some causes of anomalies on the LDEF coated optical materials have not yet been determined. Further, other non-environmental sources of material degradation (e.g. sample shelf life, sample handling, manufacturing defects) must be reassessed prior to making final conclusions about the extent of low Earth orbit (LEO) space exposure on LDEF coated optical materials.

Solar Cells

Solar cell components flew on three LDEF experiments reviewed. In general, solar cell experiments revealed a variety of effects from the space exposure including: micrometeoroid impacts (from small nicks in cover glass to penetration of the cell), broken interconnects, silver oxidation or loss, scattered contamination, and a loss of fluorine in the antireflection coatings.^{11 12 13} Some power degradation was also noted which was dependent on the severity of the M/D impacts.¹⁴ A great deal of information is still forthcoming from the principal investigators on optical properties of the surfaces of the cells, electrical characteristics, semiconductor properties, and radiation damage assessment.

Fiber Optics

Three experiments flew fiber optics, and a fourth experiment evaluated fiber optic connectors. Overall, fiber optics performed well in the low earth orbit space environments during the LDEF mission, with little or no degradation to the optical performance.^{15 16 17} Environmental effects were generally confined to the protective sheathing, suggesting fiber optic systems can be successfully used in low earth orbit. However, if struck with a direct hit by a micrometeoroid impact or debris that reaches the optical fibers, as was observed on only one link during the 2115 days in orbit, then catastrophic damage can result.¹⁸ Further studies into contamination protection schemes and temperature effects on optical performance were also suggested.¹⁹

For instance, post-flight experiments performed on space exposed fibers in the S0109 experiment showed an increase in transmission loss with decreasing temperature, becoming much steeper near the lower end of their temperature range. This was observed in most (but not all) fiber cables in experiment S0109. The largest change was seen in the C-6 sample, which had an attenuation increase about 3.5 dB at the low temperature extreme. The principal investigator for this experiment, describes this behavior as due to the specific cable structure (rather than the fiber), and would preclude its use in a severe space environment.²⁰

Contamination was recorded on internal and external surfaces on two experiments.^{21 22} Experiment results suggest only a slight degradation to nominal optical performance due to contaminants. Since contaminating films or particles over the optically important core would contribute to degradation in optical performance, recommendations were made to mate or cover connectors in a manner that protects the core from contamination.

Finally, experimenters discussed the expectation that using today's improved radiation hard fiber optic cable would enable space missions to experience longer runs and higher doses of radiation. The data from these LDEF experiments, provides for improved radiation exposure data and performance predictions for future use of fiber optics in space.^{23 24}

Detectors

Four LDEF experiments contained detectors to test their resistance to space environmental exposure. Most detectors were not degraded by the space exposure. One notable exception was the tryglycine sulfide pyroelectric detector which had a 100% detectivity failure rate on both the control and flight samples.²⁵ This was in contrast to the lithium tantalate and strontium-barium-niobate pyroelectric detectors which suffered no measureable loss of performance.²⁶ The other detectors on the LDEF included HgCdTe detectors, InGaAs photodiodes, large area silicon photodiodes and PIN diodes. These detectors had good performance and no apparent degradation effects.^{27 28 29 30}

In addition to the sensor elements, one LDEF experiment underlined the importance of the choice of lens or window for the detector. Since the detector is located behind the window, a damaged window can contribute significantly to the degradation of the entire detector system optical performance. For instance on this experiment, the thallium bromide windows (KRS-5) failed, while the germanium windows did not.³¹

Reflectometers and Radiometers

Certain LDEF experiments described the performance of radiometers and reflectometers for the measurement of solar and thermal properties. In general, all of the measuring instruments met their performance criteria, and provided valuable data on incident radiation.^{32 33 34}

Optical Sources

Several kinds of optical sources flew on LDEF including solid and gas lasers, flashlamps, standard lamps, and light-emitting-diodes (LED's). Of the laser optical sources, the semiconductor laser diodes and light-emitting-diodes (LED's) were not degraded by the space environment.^{35 36} However, no lasing action could be obtained from the gas lasers, which was thought to be due to changes as a result of gas diffusion through the glass envelope.³⁷

The deuterium ultraviolet (UV) lamp and tungsten filament quartz envelope lamp, which were part of a reflectometer subsystem, showed nominal power and computer-control post-flight functional test results. However, the deuterium lamp irradiance appeared slightly unstable (flickering of the light arc); while the tungsten lamp irradiated normally.³⁸ Other optical sources are still under investigation.

OPTICAL EXPERIMENTS DATABASE

One of the main objectives of the LDEF Systems SIG Optics discipline is to develop a database that identifies the optical hardware flown, summarize experimental results and conclusions, and provide future design considerations. Compiling this information into an easily accessible database format, and making it available to the space community, is a major task accomplished by the System SIG Optics effort.

After a trade study of Boeing standard software packages, Filemaker Pro was chosen as the Optical Experiments Database software application program. Filemaker Pro is a database manager for the Macintosh computer produced by Claris Corp.³⁹ It is a flat, text-retrievable database that provides access to the data via an intuitive user interface without tedious programming. Though this software is available only for the Macintosh computer at this time, copies of the database can be saved to a format that is readable on a personal computer as well. "Relational" databases were examined for this application, but found to have many features and capabilities unnecessary for this application.

Within the Filemaker Pro application, the LDEF Optical Systems information is placed in a file called "LDEF_data". Within that file, each individual LDEF experiments has its own "record". Each record contains specific information using "field name" headings, from which one can view or print reports from the provided layout. The database was designed to 1) be user friendly, 2) ensure data traceability, 3) acknowledge authors, 4) be upgradeable, and 5) have access privileges that allow full viewing but not editing.

The database will be available to the space community for review by contacting the LDEF Project office for information. Along with a disc copy of the database, you will receive an LDEF User's Manual which will detail the following steps:

1. Computer start-up and database password access
2. Working with information
 - a. finding information
 - b. browsing records
 - c. moving from record to record
 - d. sorting information
3. Previewing and Printing
4. Exchanging Information
5. Help function
6. Quitting Filemaker Pro

CONCLUSIONS

The Optical Systems SIG have provided to NASA an Optical Systems Overview and an LDEF Optical Experiments Database, which were summarized in this paper. Further details of this investigation can be found in the LDEF Systems Special Investigation Group Final Report, Boeing Defense and Space Group, NASA contract NAS1-19247 Task 1, January 1992. The support of NASA Langley Research Center through the LDEF Project Office is gratefully acknowledged in this effort.

-
- ¹Vallimont, John and Keith Havey, "Effects of Long Term Exposure on Optical Substrates and Coatings", *LDEF- 69 Months in Space*, First LDEF Post-Retrieval Conference, NASA CP 3134, 1992.
 - ²Hawkins, Gary, John Seeley and Roger Hunneman, "Exposure to Space Radiation of High Performance Infrared Multilayer Filters and Materials Technology", *LDEF-69 Months in Space*, LDEF Post-Retrieval Conference, NASA CP-3134, 1992.
 - ³Harvey, Gale "Effects of Long Duration Exposure on Optical Systems Components", NASA Langley Research Center, *LDEF-69 Months in Space*, First LDEF Post Retrieval Conference, NASA CP 3134, 1992.
 - ⁴Hickey, John "Passive Exposure of Earth Radiation Budget Experiment Components", Eppley Laboratory, *LDEF-69 Months in Space*, First LDEF Post-Retrieval Conference, NASA CP 3134, 1992.
 - ⁵Hawkins, Gary, John Seeley and Roger Hunneman, *ibid.*
 - ⁶Whitaker, Ann and Leighton Young, "An Overview of the First Results on the Solar Array Passive LDEF Experiment", *LDEF-69 Months in Space*, First Post-Retrieval LDEF Symposium, NASA CP-3134, 1992.
 - ⁷Gvetnay, Sandra, M0003 Preliminary Results, First LDEF Post-Retrieval Conference Poster Session photomicrographs, Kissimee, Florida, June 1991.
 - ⁸Vallimont, John and Keith Havey, *ibid.*
 - ⁹Trumble, Terry M. "Experiment M0003-4 Advanced Solar Cell and Coverglass Analysis", *LDEF-69 Months in Space*, First LDEF Post-Retrieval Symposium, NASA CP-3134, June 1992.
 - ¹⁰Gvetnay, Sandra, *ibid.*
 - ¹¹Trumble, Terry M. , *ibid.*
 - ¹²Whitaker, Ann, *ibid.*
 - ¹³Brinker, David J., John Hickey and David Scheiman, "Advanced Photovoltaic Experiment S0014", *LDEF-69 Months in Space*, First LDEF Post-Retrieval Conference, NASA CP-3134, 1992.
 - ¹⁴Brinker, David J., John Hickey and David Scheiman, *ibid.*
 - ¹⁵Johnston, A. R., L. A. Bergman and R. Hartmayer, "LDEF Fiber Optic Exposure Experiments S0109", *LDEF-69 Months in Space*, LDEF First Post-Retrieval Conference, NASA CP-3134, 1992.
 - ¹⁶Taylor, E.W., J. N. Berry, et.al., "Preliminary Analysis on WL Experiment 701 Space Environmental Effects on Operating Fiber Optic Systems", First LDEF Post-Retrieval Symposium, NASA CP-3134, 1992.
 - ¹⁷Mulkey, Owen, "Final Report on the LDEF M0003-8 Fiber Optics Experiment", *LDEF-69 Months in Space*, First LDEF Post-Retrieval Symposium Proceedings, NASA CP-3134, 1992.
 - ¹⁸Taylor, E.W., J.N. Berry, et.al., *ibid.*
 - ¹⁹Johnston, A.R., L.A.Bergman and R. Hartmayer, *ibid.*
 - ²⁰Johnston, A.R., L.A.Bergman and R. Hartmayer, *ibid.*
 - ²¹Taylor, E.W., J.N. Berry, et.al., *ibid.*
 - ²²Johnston, A.R., L.A.Bergman and R. Hartmayer, *ibid.*
 - ²³Taylor, E.W., J.N. Berry, et.al., *ibid.*
 - ²⁴Johnston, A.R., L.A.Bergman and R. Hartmayer, *ibid.*
 - ²⁵Robertson, James B., "Effect of Space Exposure on Pyroelectric Infrared Detectors", NASA Langley Research Center, *LDEF-69 Months in Space*, First LDEF Post-Retrieval Symposium Proceedings, NASA CP-3134, 1992.
 - ²⁶Robertson, James B., *ibid.*
 - ²⁷Mulkey, Owen, *ibid.*

-
- ²⁸Robertson, James B., *ibid.*
- ²⁹Blue, Donald M., "LDEF Active Optical System Component Experiment", *LDEF-69 Months in Space*, First LDEF Post-Retrieval Symposium, NASA CP-3134, 1992.
- ³⁰Hodgson, Randall and James Holsen, "Post-Flight Characterization of Optical System Samples, Thermal Control Samples and Detectors from LDEF Experiment M0003", *LDEF-69 Months in Space*, First LDEF Post-Retrieval Conference, NASA CP-3134, 1992.
- ³¹Robertson, James B., *ibid.*
- ³²Wilkes, Donald R., "Thermal Control Surfaces Experiment Initial Flight Data Analysis Final Report", NASA subcontract NAS8-36289-SC03, AZ Technology, June 1991.
- ³³Brinkley, David J., John Hickey and David Scheiman, "Advanced Photo-Voltaic Experiment", *LDEF-69 Months in Space*, LDEF First Post-Retrieval Conference, NASA CP-3134, 1992.
- ³⁴Hickey, John R. *ibid.*
- ³⁵Blue, Donald M., *ibid.*
- ³⁶Mulkey, Owen, *ibid.*
- ³⁷Blue, Donald M., *ibid.*
- ³⁸Wilkes, Donald R., *ibid.*
- ³⁹Clarix Customer Relations, Clarix Corp., 5201 Patrick Henry Drive, Santa Clara, CA, 950052-8168, 1-800-735-7393.

Polymer Matrix Composites

Co-Chairmen: Gary Steckel and Rod Tennyson
Recorder: Pete George



POLYMER MATRIX COMPOSITES ON LDEF EXPERIMENTS M0003-9 and 10*

Gary L. Steckel

The Aerospace Corporation
El Segundo, CA 90245

Phone: 310/336-7116, Fax: 310/336-7055

Thomas Cookson

General Dynamics Space Systems Division
San Diego, CA 92138

Phone: 619/547-5081, Fax: 619/974-4000

Christopher Blair

Lockheed Missiles & Space Company
Sunnyvale, CA 94089-3504

Phone: 408/743-0007, Fax: 408/742-7743

ABSTRACT

Over 250 polymer matrix composites were exposed to the natural space environment on LDEF experiments M0003-9 and 10. The experiments included a wide variety of epoxy, thermoplastic, polyimide, and bismalimide matrix composites reinforced with graphite, glass or organic fibers. This paper is a review of the significant observations and test results obtained to date. Estimated recession depths from atomic oxygen exposure are reported and the resulting surface morphologies are discussed. The effects of the LDEF exposure on the flexural strength and modulus, short beam shear strength, and coefficient of thermal expansion of several classes of bare and coated composites are reviewed. Lap shear data are presented for composite-to-composite and composite-to-aluminum alloy samples that were prepared using different bonding techniques and subsequently flown on LDEF.

*Funding for the work performed by The Aerospace Corporation was processed through Air Force Space Systems Division Contract F04701-88-C-0089 under an interagency agreement with Air Force Wright Laboratory. The Lockheed Missiles & Space Company work was supported by Independent Development funds. General Dynamics Space Systems Division performed their work under an Independent Research and Development program.

INTRODUCTION

Polymer matrix composites were included in several sub-experiments of LDEF Experiment M0003, "Space Environmental Effects on Spacecraft Materials". The sub-experiments that incorporated polymer matrix composites included M0003-8, -9, -10, and -16. The polymer matrix composites (PMCs) flown on subexperiment M0003-8, a Boeing Defense and Space Group experiment, are discussed elsewhere in this conference publication (ref. 1). J. Mallon of The Aerospace Corporation is the principal investigator for M0003-16. This sub-experiment included a small number of samples relative to the other experiments and was not discussed at the workshop. However, the composites in M0003-16 had polymer matrices of polyarylacetalene and polyphenylquinoxiline that are much different from the polymer matrices included in any other LDEF experiments. Thus, the results of this experiment will undoubtedly be of great interest once they are published. The PMCs included in the remaining subexperiments, M0003-9 & 10, are discussed in this paper. M0003-9 is a Lockheed Missiles & Space Company experiment with B. Petrie serving as the principal investigator. This subexperiment included several graphite/epoxy systems. Subexperiment M0003-10, The Advanced Composites Experiment, is a joint effort between government and industry with Air Force Wright Laboratory, Flight Dynamics Laboratory, and The Aerospace Corporation, Mechanics and Materials Technology Center, serving as experimenters. General Dynamics Space Systems Division (GDSSD), Lockheed Missiles & Space Company (LMSC), Boeing Defense and Space Group, McDonnell Douglas Space Systems Company (MDSSC), and United Technologies Research Center (UTRC) also participated in this subexperiment. The experiment includes several classes of graphite fiber-reinforced polymer matrix composites. Experiment M0003-10 will be reviewed in detail, while only a brief review highlighting the experimental results will be given for the PMCs included in experiment M0003-9.

EXPERIMENT DESCRIPTION

Experiment M0003-10 consists of approximately 500 flight samples, including around 300 metal matrix composites and 200 PMCs. The metal matrix composites include graphite fiber-reinforced aluminum and magnesium and silicon carbide reinforced aluminum. The PMCs include graphite/epoxy, graphite/polysulfone, and graphite/polyimide composites. The majority of the PMCs were uncoated, but several samples were flown with various thermal control or protective coatings. The metal matrix composites were supplied by Aerospace and the organic matrix composites were supplied by GDSSD, LMSC, Boeing, and MDSSC. In addition, a

number of graphite fiber-reinforced glass matrix composites were provided by United Technologies Research Center (UTRC). Each material supplier is responsible for performing postexposure tests and analyses on their flight articles and ground control samples. Since the scope of the workshop session was limited to polymer matrix composites, no further discussion of the metal or glass matrix composites will be included in this paper. The results for these composites are discussed elsewhere (refs. 2-4).

The experiment occupied approximately one-sixth of a 6 in.-deep peripheral tray on both the leading and trailing edges of LDEF. The trays were located on LDEF Bay D, Row 4 on the trailing edge and Bay D, Row 8 on the leading edge. The samples were mounted on both sides of cassettes with one side (Deck A) exposed to the space environment and the other side (Deck B) facing inward. The environments for the samples mounted on the leading and trailing A decks were similar except those on the leading edge were also exposed to a relatively high fluence of atomic oxygen (6.6×10^{21} atoms/cm², ref. 5). Although the samples on the B decks were not exposed to the radiation environment, the experiment design was such that they experienced thermal excursions similar to those of the exposure samples. The sample cassettes were decoupled from LDEF in order to maximize the thermal excursions. For most materials, at least one sample was located on each deck and additional samples were maintained in a laboratory environment.

Although this was essentially a passive experiment, one or more samples of each class of composites was instrumented with thermistors and strain gages to monitor the thermal excursions on the leading and trailing edges and the resulting dimensional changes. The data acquisition system was set up to record temperatures and strains during the duration of an orbit once every 107 hours (approximately 78 orbits). Data were collected approximately every three minutes during the selected orbits. The data were recorded on magnetic tape until the tape was fully loaded, approximately fourteen months into the flight. No data were recorded during the unplanned final 4.5 years of the flight. The strain data are still being interpreted and will not be presented in this paper. The thermistor data indicated that the maximum and minimum temperatures for the uncoated graphite/epoxy composites were approximately +80°C and -45°C, respectively. The temperature data will be discussed in more detail below.

Most of the composite samples were 3.5 by 0.5 in. (8.9 by 1.3 cm) strips. There were also a limited number of 1 in. (2.5 cm) diameter mirror samples, a few 2.4 by 0.5 in. (6.1 by 1.3 cm) strips and several graphite/aluminum, graphite/magnesium and silicon carbide/aluminum wires. The organic matrix composites in the experiment are listed in table I. Because of the cooperative effort, a very broad test matrix of graphite/epoxy composites

having several different fiber-matrix combinations and lay ups were flown. Most of the graphite/epoxy composites were uncoated. With the exception of a T300/polyethersulfone composite, all of the graphite/thermoplastic composites had the P-1700 polysulfone matrix. Most of these composites had thermal control coatings. The remainder of the organic matrix composites had high-temperature polyimide or bismalimide matrices.

Each organization submitted a matrix of materials appropriate for studying specific phenomenon or for obtaining data on a certain composite system or set of systems. For example, the primary objective of the McDonnell Douglas experiment was to determine the effectiveness of various protective coatings for preventing property degradations in graphite/epoxy, graphite/polyimide and graphite/thermoplastic composites. Thus for each composite system, they flew uncoated control samples and those having up to three different coatings. Lockheed was interested in determining the effects of composite lay up and matrix cure temperature on the degree of thermal cycling induced microcracking. They submitted a test matrix consisting of unidirectional and cross-plyed graphite/epoxy composites having three different fiber-matrix combinations in order to achieve these objectives. Thus, the different organizations submitted separate, independent experiments, but are working together to maximize the data output of the overall experiment.

Most of the composites in the experiment were developed for space structural applications. Thus, the primary properties of interest include the flexural or tensile properties, the coefficient of thermal expansion, solar emittance and absorptance, specific heat, thermal conductivity and physical properties such as fiber volume, void content and density. Post-exposure measurements vary for the different classes of composites, but include most of the above properties as well as surface analyses, macrophotography and microstructural analyses. The remainder of the paper will include discussions of the results obtained by The Aerospace Corporation on the PMCs in M0003-10, by GDSSD on their samples in M0003-10, and by LMSC on their samples from M0003-9 & 10. The results obtained by Boeing for their samples on M0003-10 are given by P. George (ref. 1). MDSSC is very early in the evaluation of their samples so no results will be presented for their portion of M0003-10.

AEROSPACE RESULTS FOR M0003-10

The analyses performed on the PMCs at The Aerospace Corporation include preflight and post-flight photography of the cassettes and individual samples, an evaluation of the active temperature and strain data, preflight and post-flight mass measurements and scanning electron microscopy (SEM) on some of

the uncoated composites that were mounted on the leading edge.

Several observations were made from a visual inspection and by comparing preflight and post-flight photographs of the sample cassette assemblies (fig. 1). First, it was noted that all of the composites survived in excellent physical condition. Surface roughening due to atomic oxygen erosion for uncoated PMCs mounted on the exposed leading edge was the only significant visible damage. However, the erosion depth appeared to be shallow relative to the overall thickness of the affected composites. Contamination was evident on both the leading and trailing edges. For example, a large contaminated area is apparent on seven samples in the lower left corner of the leading edge cassette in the post-flight photograph of figure 1. This contamination was from another experiment or from the LDEF structure. However, there were also rainbow outgassing stains on trailing edge samples adjacent to elastomeric samples, which were from a different subexperiment of M0003 but were mounted on the Advanced Composites Experiment cassette. The most dramatic change was a yellowing or browning of many of the thermal control coatings. This was only observed for the exposed samples on the trailing edge (fig. 1). The exposed leading edge paints and those on the Deck B samples remained white. The yellowed samples were MDSSC samples having a ZnO silicone coating and the brown samples included GDSSD samples with ZnO and TiO₂ coatings and MDSSC samples with a leafing aluminum coating.

The PMC systems that were instrumented were as follows:

STRAIN GAGE ON LEADING AND TRAILING EDGES

GY70/X-30 (0/45/90/135)_{2S}
T300/934 (0)
AS/3501-6 (0)
CELION 6000/PMR-15 (0)
GR/LARC 160
T300/V378A (0/45/90/135)_{2S}
T300 FABRIC/P-1700
W-722 FABRIC/P-1700
T300/POLYSULFONE
T300/POLYETHERSULFONE

THERMISTOR ON LEADING AND TRAILING EDGES

T300/934 (0)

Plots of the maximum and minimum temperatures that were recorded on the leading and trailing edges for each of the selected orbits over the first fourteen months of the flight are shown in figure 2. The maximum and minimum temperatures on the leading edge tended to be somewhat lower than for the trailing edge. The variation in the temperature extremes as a function of orbital time was much greater, particularly for the maximum temperature,

on the leading edge. For example, the maximum temperature on the leading edge for a given orbit varied from -40°C at 65 days to 83°C at 270 days, while the lowest and highest recorded maximum temperatures on the trailing edge were -7°C and 76°C , respectively. However, the difference between the maximum and minimum temperatures for a given orbit was usually greater on the trailing edge. Thus, thermal cycling conditions were somewhat more severe on the trailing edge than on the leading edge.

The mass measurements were made after the samples had equilibrated in a constant temperature, constant humidity laboratory. Thus, moisture variations were eliminated and the only significant mass changes were those that could be attributed to atomic oxygen erosion on the exposed leading edge. The erosion depth was calculated from the known composite density and exposure area and the measured mass loss. Since the fibers and matrix have different erosion rates and densities, this technique of determining the erosion depth is an approximation. The actual erosion depths are probably somewhat higher because the samples had resin-rich surfaces and the epoxy, which has a lower density than the graphite fibers, erodes at a higher rate than the fibers. The most interesting results were for the General Dynamics composites. They flew several graphite/epoxy composites having several different fiber-matrix combinations and a wide range of fiber contents. The calculated erosion depths for these composites were inversely proportional to the fiber content (fig. 3). All of the composites provided by General Dynamics were fabricated following similar procedures. In particular, the same bleeder cloth was used so that the composites had similar surface conditions. Composites prepared by other experiment participants having significantly different surface conditions (either more matrix rich or less matrix rich) did not fall on the erosion depth versus fiber content curve established by the General Dynamics composites. Thus, it would appear that the fiber content and surface conditions are more important variables than the graphite fiber type or epoxy matrix type in determining the susceptibility of graphite/epoxy to atomic oxygen erosion. Perhaps the most important observation was that the erosion depths of the uncoated organic matrix composites were much less than for monolithic polymers. The estimated erosion depth for most of the graphite/epoxy composites was less than 0.007 cm, much less than the predicted erosion of 0.012 cm for monolithic epoxies (ref. 6) for the LDEF atomic oxygen fluence of approximately 6.6×10^{21} atoms/cm² for Row 8 (ref. 5).

The data from figure 3 are replotted in figure 4 along with the results for a graphite/polysulfone composite and for a graphite/bismalimide composite. Both of these composites were also prepared by GDSSD using the same bleeder cloth as for the graphite/epoxy composites. Note that the graphite/polysulfone

falls on the same curve as the graphite/epoxies, but the graphite/bismalimide has a much higher erosion depth for its fiber content than the other composites. In fact, the T300/V378A graphite/bismalimide composite had the highest erosion rate of all the PMCs in experiment M0003-10. This result does not necessarily indicate that bismalimide matrix composites as a class are more susceptible to atomic oxygen erosion. A graphite/bismalimide composite flown on Experiment A0175 (ref. 7) did not show excessive erosion relative to other composites included in the experiment.

Figure 5 shows SEM micrographs of the original, as fabricated surfaces of a P75S/934 graphite/epoxy composite and the T300/V378A graphite/bismalimide composite. Both composites were supplied by GDSSD and both have a 16 ply (0/45/90/135)_{2S} lay up. The woven appearance on the composites is a replication of the bleeder cloth in the resin on the composite surface. Note the bottom of the micrographs where the surface resin has chipped away revealing the outer 0° ply of graphite fibers. The 0° direction in these micrographs extends in the vertical direction. A low magnification view of the eroded leading edge samples of these composites are shown in fig. 6. The woven pattern persists on the surface even though several mils of material have been eroded away. The fact that the original surface features are maintained indicates that the erosion is uniform on a macroscopic scale. There are, however, differences in the erosion features for the two composites. Deep erosion grooves were formed on the graphite/bismalimide composite, but did not form on the graphite/epoxy composite. These grooves extend most prominently from left to right, corresponding with the direction from which the oxygen atoms approached the surface. (The velocity vector was 38° left of normal to the surfaces in the micrographs.) At a higher magnification (fig.7), major differences in the erosion features for the two composites are observed. The "Christmas tree" or cone-like erosion fragments on the graphite/epoxy sample are typical of many of the uncoated PMCs in the experiment. The rows of erosion fragments on these samples run parallel to the fiber direction with the apex of the cones or "Christmas trees" pointing in the direction of the LDEF velocity vector. The graphite/bismalimide composite formed deep erosion grooves between what appears in figure 7b to be relatively flat regions. When viewed from a different angle (fig. 8a), however, it is evident that the erosion fragments in these flat regions were finer with more of an acicular appearance and random arrangement as compared to the P75S/934 composite. The acicular erosion features, but without the deep erosion grooves, were also observed for three other composites, such as the Celion 6000/PMR-15 graphite/polyimide composite shown in figure 8b. This composite also has a "spider web" or "hair net" ash-like material on the surface. All of the uncoated PMCs in Experiment M0003-10 had erosion features showing the coarse, "Christmas tree"

structure or the fine, needle structure as indicated in table II. An attempt was made to correlate the type of erosion features with the graphite fiber type, matrix type, or lay up. The only correlation that could be made was that all of the composites that had the coarse "Christmas tree" features had high-modulus GY70 (70×10^6 psi modulus) or P75S (75×10^6 psi modulus) fibers while the composites with the fine, needle structure had low-modulus T300 or Celion 6000 fibers (both having a $30-35 \times 10^6$ psi modulus). This correlation is not presented as proof that the fiber type controls the appearance of the atomic oxygen erosion features. In fact, the correlation is somewhat surprising since the GY70 fiber, which is processed from a polyacrylonitrile precursor, and the P75S fiber, which is processed from a mesophase pitch precursor, have much different structures. It is hoped that these observations will encourage further investigations into the origins of the different types of atomic oxygen erosion features found on the LDEF PMCs.

GDSSD RESULTS FOR M0003-10

As indicated in table I, GDSSD provided GY70/X-30, GY70/CE-339, P75S/CE-339, P75S/934 and GY70/934 graphite/epoxy, W-722/P-1700 graphite/glass/polyethersulfone and T300/V378A graphite/bismalimide composites. The GY70/X-30 was flown bare and with a Sn-In eutectic alloy moisture barrier coating and the W-722/P-1700 was flown bare and with thermal control coatings. All of the other composites were flown with no coating. All of the GDSSD composites had a (0/45/90/135)_{2S} lay up except for those having the W-722 woven graphite/glass fabric as a reinforcement. The coated W-722/P-1700 composites included lap shear samples that had been spot welded together. All of the other GDSSD composites were 3.5 in. by 0.5 in. strips.

GDSSD performed flexural tests to determine the flexural strength and modulus and short beam shear tests for the strip samples and lap shear strength measurements for the spot welded samples. A bar graph showing the ultimate flexural strength results for each sample for the P75S/934 composite is shown in figure 9. All of the samples had similar strength values except for those that were subjected to atomic oxygen erosion on the leading edge. In order to show the true loss in load carrying ability, the strength and modulus calculations for the leading edge samples were based upon the original area of the samples. There was no apparent loss in strength relative to the laboratory controls for the samples mounted on the interior of the cassettes or those mounted on the outer trailing edge. There was also no loss in strength relative to the average preflight value, indicated by the INITIAL value marked on the ordinate. The results for this composite are typical of the flexural strength,

flexural modulus, and short beam shear strength data for all of the uncoated GDSSD composites. That is, there was no reduction in mechanical properties except that due to atomic oxygen erosion on the leading edge. In order to quantify the property loss on the leading edge, the average property value for the leading edge samples was divided by the average value for all of the remaining samples (laboratory controls, all deck B samples, and trailing edge deck A samples). This gave a normalized strength for the leading edge for all of the GDSSD uncoated composites as presented in figure 10. The five graphite/epoxy composites all had normalized leading edge strength values that were at least 70% of the original value, about as expected considering that the outer 0° ply was mostly or completely eroded away. The T300/V378A graphite/bismalimide composite strength on the leading edge was only 40% of the original strength. The mass loss for this material was somewhat greater than for the other composites, but not to the extent that one would expect such a large loss of strength.

The flexural modulus results for the leading edge are shown in figure 11. The T300/V378A composite also showed the largest modulus reduction, along with the P75S/934 composite at approximately 65% of the original modulus. But the reduction in the modulus was not nearly as great as for the strength. All of the composites showed only a 10% reduction in the short beam shear strength as indicated in figure 12. This is not surprising since short beam shear strength is not as sensitive to surface degradation as are flexural properties.

The lap shear strength results for the spot welded W-722/P-1700 composites with the ZnO coating are shown in figure 13. There was an insufficient number of samples to allow any comparisons between the different exposure conditions. However, it is apparent that there was no reduction in strength as all but one sample had a higher strength than the average value measured prior to the flight. Similar results were obtained for W-722/P-1700 composites with the TiO₂ coating.

LMSC RESULTS FOR M0003-9 AND 10

All of the composites flown by LMSC had epoxy matrices. Most of the LMSC composites were reinforced with graphite fibers, but one set of samples was reinforced with DuPont's Kevlar 49 aramid fibers and two sets of composites were reinforced with E-Glass fibers. A listing of the LMSC composites is given in table III and includes the prepreg supplier for each system. The Lockheed experiment included a wide variety of epoxy matrix composites. The epoxy matrices had a wide range of cure temperatures and glass transition temperatures and the fibers ranged from the

relatively low-modulus E-Glass to the high-modulus P75 and GY70 graphite fibers. The HMS/3501, GY70/X904B, and E-Glass/X904B composites were flown on subexperiment 10 and all the rest of the LMSC composites were on subexperiment 9. The subexperiment 9 composite strips were 3.5 in. long by 0.75 in. wide, which is the same length but 0.25 in. wider than the subexperiment 10 strips. In addition to strips, the LMSC experiment also included double lap shear samples of HMF 330/934 graphite fabric reinforced epoxy bonded to 2024 aluminum with Hysol 9628 epoxy film adhesive.

Subexperiment 9 was located on Bay D, Row 3 on the trailing edge of LDEF and Bay D, Row 9 on the leading edge. Most of the samples were mounted facing outward so that they were exposed to the full space environment, but a few of the samples were covered so that they were protected from radiation and atomic oxygen.

The LMSC analyses and property measurements include macrophotography, mass loss measurements, SEM surface morphology of eroded surfaces and impact damage, microphotography of microcrack formation, ESCA contamination analysis, short beam shear strength, flexural strength and modulus, double lap shear strength, and coefficient of thermal expansion (CTE) measurements. This paper includes the mechanical property and CTE results.

The results of the flexural testing are given in table IV. None of the composites show any clear variation in strength or modulus between the exposure samples and the laboratory controls. For the leading edge samples which experienced a loss of material from atomic oxygen, LMSC based their strength and modulus calculations on the final thickness of the composites. Thus, their results show that the strength and modulus of the composites were unaffected by the mass loss. However, for a real structure, one would need to determine the effect of the mass loss on the load carrying capability and stiffness. GDSSD based their calculations on the initial thickness, which partially accounts for the fact that they measured a reduction in strength and modulus while LMSC did not. In addition to the different approaches in defining the sample thickness, the composite lay ups were also significantly different between the GDSSD and LMSC samples. All of the GDSSD composites had a 0° ply at the surface, whereas all of the LMSC samples had a 45° ply at the outer surface. In a flexural test, the loss of a 0° ply from the surface will have a much more pronounced effect on the strength than the loss of a 45° ply. Thus, mass losses from atomic oxygen would be expected to affect the flexural properties of the GDSSD composites to a greater extent than for the LMSC composites. In assessing the effect of atomic oxygen erosion on the strength and modulus of composites, the composite lay up is an important consideration.

Short beam shear strength measurements were made on ten different unidirectional composites as shown in table V. The short beam shear strength ranged from a low value of less than 4 Ksi for a Kevlar 49/X904B composite to a high of nearly 13 Ksi for T50/F263 composites. The LDEF exposure had no apparent effect on the short beam shear strength for any of the epoxy matrix composites. Here again, the LMSC strength calculations were based upon the final area which accounts for the fact that they did not report a strength reduction for the leading edge, whereas GDSSD reported a small strength reduction based upon the initial area.

Table VI shows the shear strength results for the HMF 330/934//Hysol 9628 Adhesive//2024 Aluminum double lap shear samples. Four samples were tested for each flight condition along with eight control samples. There was no apparent reduction in shear strength for the leading edge exposure or for the flight controls as compared to the laboratory control samples. The trailing edge exposure resulted in approximately a 25% reduction in lap shear strength.

CTE measurements were made using a quartz dilatometer on four unidirectional graphite/epoxy composites as indicated in table VII. Within the accuracy of the technique, there were no significant changes in the CTE for any of the composites.

SUMMARY

The findings to date for LDEF Experiments M0003-9 and 10 on polymer matrix composites may be summarized as follows.

The Aerospace Corporation Results

1. Atomic oxygen erosion depths are in the range from 0.0015 to 0.0035 in. (0.0038 to 0.0089 cm) based upon mass loss measurements.
2. Atomic oxygen erosion depth is an inverse function of fiber content for graphite/polymer composites.
3. Two types of atomic oxygen erosion morphologies were observed for graphite/polymer composites. Preliminary observations suggest that the erosion features may be a function of the fiber modulus or structure.

General Dynamics Space Systems Division Results

1. Atomic oxygen erosion on the leading edge of LDEF resulted in a 20-30% reduction in the strength and modulus for uncoated graphite/epoxy composites. An uncoated graphite/bismalimide

composite, T300/V378A had a 60% reduction in strength.

2. Atomic oxygen erosion on the leading edge resulted in a 10% reduction in short beam shear strength for uncoated graphite/epoxy and T300/V378A composites.
3. There were no significant changes in the flexural strength or modulus or short beam shear strength for any uncoated composites on the trailing edge of LDEF or for flight control samples.
4. There were no significant changes in the flexural strength or modulus or short beam shear strength for any composites having thermal control or Sn-In coatings. These coatings, provided protection from atomic oxygen.
5. The lap shear strength of spot welded W-722/P-1700 composites having ZnO or TiO₂ coatings was unaffected by exposure on the leading or trailing edges of LDEF.

Lockheed Missiles And Space Company Results

1. The extended LDEF exposure had no effect on the flexural strength or modulus or the short beam shear strength of any of the LMSC epoxy matrix composites.
2. The lap shear strength for an HMF330/934 composite bonded to 2024 aluminum with Hysol 9628 epoxy film adhesive was reduced by approximately 25% by exposure on the trailing edge of LDEF as compared to laboratory control samples. There was no effect on the shear strength for samples exposed on the leading edge or for flight control samples.
3. The LDEF exposure did not have a significant effect on the coefficient of thermal expansion of unidirectional GY70/CE-339, T50/F263, T50/934, or T50/X904B graphite/epoxy composites.

REFERENCES

1. George, P.: Space Environmental Effects on LDEF Low-Earth Exposed Graphite-Reinforced Polymer-Matrix Composites. LDEF Materials Workshop '91, NASA CP-3162, 1992.
2. Steckel, G. L. and Le, T. D.: M0003-10: LDEF Advanced Composites Experiment. First LDEF Post-Retrieval Symposium, NASA CP-3134, 1992, pp. 1041-1053.
3. Tredway, W. K. and Prewo, K. M.: Analysis of the Effect of Space Environmental Exposure on Carbon Fiber Reinforced Glass. United Technologies Research Center Report R91-112542-4, May, 1991.
4. Steckel, G. L. and Le, T. D.: Composites Survive Space Exposure. Advanced Materials and Processes, vol. 139, no.8, August, 1991. pp. 35-38.
5. Bourassa, R. J.; Gillis, J. R.; and Rousslang, K. W.: Atomic Oxygen and Ultraviolet Radiation Mission Total Exposures For LDEF Experiments. First LDEF Post-Retrieval Symposium, NASA CP-3134, 1992, pp. 643-661.
6. Banks, B. A.: Atomic Oxygen Interaction with Materials on LDEF. LDEF Materials Data Analysis Workshop, NASA CP 10046, July 1990, pp. 191-216.
7. Vyhnal, R.: Evaluation of Long-Duration-Exposure to the Natural Space Environment on Graphite-Polyimide and Graphite-Epoxy Mechanical Properties. LDEF Materials Workshop '91, NASA CP-3162, 1992.

TABLE I.- LIST OF ORGANIC MATRIX COMPOSITES

MATERIAL DESCRIPTION FIBER/MATRIX/COATING	LAY UP	SUPPLIER	NUMBER OF SAMPLES					
			LEADING		TRAILING		CONTROL	
			A	B	A	B	A	B
<u>GRAPHITE/EPOXY STRIPS</u>								
GY70/X-30/NONE, Sn-In	(0/45/90/135) ^{2S}	GDSSD	4	4	3	3	5	
GY70/X904B	(0) ¹⁶ , (0/90 ₂ /0) ^{2S}	LMSC	3	3	3	3	0	
GY70/934	(0/45/90/135) ^{2S}	GDSSD	2	3	2	2	7	
GY70/CE-339	(0/45/90/135) ^{2S}	GDSSD	2	3	3	3	6	
P75S/CE-339	(0/45/90/135) ^{2S}	GDSSD	2	3	2	2	8	
P75S/934	(0/45/90/135) ^{2S}	GDSSD	2	2	2	2	8	
T300/5208/NONE, ZnO, Al FLAKE		MDSSC	1	2	2	3	0	
T300 TAPE/934	(0) ¹⁶	BOEING	3	3	3	3	4	
AS/3501-6	(0) ¹⁶	BOEING	3	3	3	3	3	
HMS/3501-5A	(0) ¹⁶ , (0/90 ₂ /0) ^{2S}	LMSC	2	2	0	0	0	
E-GLASS FABRIC/X904B	(0) ¹⁶ , (0) ¹⁶	LMSC	1	1	1	1	0	
<u>GRAPHITE/THERMOPLASTIC STRIPS</u>								
T300 FABRIC/P-1700 PS	(0/90) ⁸	BOEING	3	3	3	3	4	
T300/P-1700 PS/NONE,								
TiO ₂ , ZnO, LEAFING Al		MDSSC	4	0	0	0	0	
T300/PES/NONE, TiO ₂ ,								
ZnO, LEAFING Al		MDSSC	1	0	5	2	0	
W-722 FABRIC/P-1700 PS/NONE,								
TiO ₂ , ZnO	(0/90) ⁸	GDSSD	15	11	15	11	12	
<u>GRAPHITE/POLYIMIDE STRIPS</u>								
GRAPHITE/LARC 160	(0) ¹⁶	BOEING	2	3	2	3	5	
CELION 6000/PMR-15	(0) ¹⁶	BOEING	3	1	2	3	4	
CELION 6000/PI/NONE, ZnO		MDSSC	1	0	1	0	0	
T300/V378A (BISMALIMIDE)	(0/45/90/135) ^{2S}	GDSSD	3	3	3	3	4	

W-722 is a graphite/glass fabric.

The control samples listed were stored at The Aerospace Corporation. For those composites for which no control samples are listed, the controls were stored at the supplier's facility and were not included in The Aerospace Corporation records.

TABLE II.-ATOMIC OXYGEN EROSION FEATURES FOR POLYMER MATRIX COMPOSITE

<u>OBSERVED EROSION FEATURES</u> COMPOSITE SYSTEM	COMPOSITE SUPPLIER
<u>COARSE, CHRISTMAS TREE STRUCTURE</u>	
GY70/X904B	LMSC
GY70/X-30	GDSSD
GY70/CE-339	GDSSD
GY70/934	GDSSD
P75S/934	GDSSD
P75S/CE-339	GDSSD
<u>FINE, NEEDLE STRUCTURE</u>	
T300/934	BOEING
T300/V378A*	GDSSD
T300 FABRIC/P-1700	BOEING
CELION 6000/PMR-15**	BOEING
GR/LARC 160**	BOEING
T300/POLYSULFONE**	MDSSC
<u>TRANSITIONAL STRUCTURE</u>	
T300/POLYETHERSULFONE	MDSSC

- * Deep Erosion Grooves
 ** Spider Web Pattern On Surface

TABLE III.- LIST OF LMSC COMPOSITES IN EXPERIMENTS M0003-9 & 10

<u>MATERIAL DESCRIPTION</u> FIBER/MATRIX	LAY UP ORIENTATION	PREPREG SUPPLIER
GY70/CE-339	(0) ₁₆ & (45/-45 ₂ /45) _{4T}	FERRO
T50/F263	(0) ₁₆ & (45/-45 ₂ /45) _{4T}	HEXCELL
T50/934	(0) ₁₆ & (45/-45 ₂ /45) _{4T}	FIBERITE
T50/X904B	(0) ₁₆ & (45/-45 ₂ /45) _{4T}	FIBERITE
T50/E788	(0) ₁₆ & (45/-45 ₂ /45) _{4T}	HEXCELL
P75/934		FIBERITE
P75/F593		HEXCELL
HMS/3501	(0) ₁₆ & (45/-45 ₂ /45) _{4T}	NARMCO
CELION 6000/E788	(0) ₁₆ & (45/-45 ₂ /45) _{4T}	HEXCELL
HMF 176/934 FABRIC	(0) ₁₆ & (±45) _{4S}	FIBERITE
GY70/X904B	(0) ₁₆ & (45/-45 ₂ /45) _{4T}	FERRO
KEVLAR 49/X904B FABRIC	(0) ₁₆ & (±45) _{4S}	FIBERITE
E-GLASS/CE-339	(0) ₁₆	FERRO
E-GLASS/X904B	(0) ₁₆	FERRO

TABLE IV.-FLEXURAL TEST DATA FOR LMSC COMPOSITES

<u>MATERIAL DESCRIPTION</u> SAMPLE LOCATION	FLEXURAL STRENGTH (KSI)	FLEXURAL MODULUS (MSI)
<u>GY70/CE-339 (45/-45₂/45)_{4T}</u>		
LEADING EDGE	35.2	2.14
TRAILING EDGE	37.9	2.55
LAB CONTROL	38.2	2.48
<u>GY70/X904B (45/-45₂/45)_{4T}</u>		
LEADING EDGE	-----DAMAGED SAMPLE-----	
TRAILING EDGE	21.1	1.50
FLIGHT CONTROL (LEADING)	22.1	1.80
FLIGHT CONTROL (TRAILING)	22.4	1.60
LAB CONTROL	23.6	2.00
<u>T50/F263 (350^{OP} CURE) (45/-45₂/45)_{4T}</u>		
LEADING EDGE	49.4	3.49
TRAILING EDGE	47.0	3.14
LAB CONTROL	47.7	3.26
<u>T50/F263 (300^{OP} CURE) (45/-45₂/45)_{4T}</u>		
LEADING EDGE	55.9	3.61
TRAILING EDGE	51.4	3.39
LAB CONTROL	54.4	3.56
<u>T50/934 (45/-45₂/45)_{4T}</u>		
LEADING EDGE	48.7	2.71
TRAILING EDGE	52.1	3.01
LAB CONTROL	48.3	2.90
<u>T50/X904B (45/-45₂/45)_{4T}</u>		
LEADING EDGE	46.3	2.29
TRAILING EDGE	40.0	1.97
LAB CONTROL	47.1	2.31
<u>HMF 176/934 FABRIC (+/-45)_{4S}</u>		
LEADING EDGE	66.8	3.16
TRAILING EDGE	67.6	3.14
LAB CONTROL	67.0	3.23
<u>KEVLAR 49/X904B FABRIC (+/-45)_{4S}</u>		
LEADING EDGE	28.4	1.10
TRAILING EDGE	24.4	0.93
LAB CONTROL	26.9	1.16

TABLE V.-SHORT BEAM SHEAR DATA FOR LMSC COMPOSITES

<u>MATERIAL DESCRIPTION</u> SAMPLE LOCATION	SHORT BEAMS SHEAR STRENGTH (KSI)
<u>GY70/CE-339 (0)₁₆</u>	
LEADING EDGE	8.6
TRAILING EDGE	8.1
LAB CONTROL	7.6
<u>GY70/X904B (0)₁₆</u>	
LEADING EDGE	8.2
TRAILING EDGE	8.5
FLIGHT CONTROL (LEADING)	8.6
FLIGHT CONTROL (TRAILING)	8.5
LAB CONTROL	8.4
<u>T50/F263 (0)₁₆</u>	
LEADING EDGE	12.7
TRAILING EDGE	12.6
LAB CONTROL	12.6
<u>T50/934 (0)₁₆</u>	
LEADING EDGE	11.8
TRAILING EDGE	12.1
LAB CONTROL	10.0
<u>T50/X904B (0)₁₆</u>	
LEADING EDGE	10.6
TRAILING EDGE	10.8
LAB CONTROL	7.7
<u>HMF 176/934 FABRIC (0)₁₆</u>	
LEADING EDGE	10.9
TRAILING EDGE	12.1
LAB CONTROL	10.7
<u>KEVLAR 49/X904B FABRIC (0)₁₆</u>	
LEADING EDGE	3.6
TRAILING EDGE	3.8
LAB CONTROL	3.7
<u>HMS/3501 (0)₁₆</u>	
LEADING EDGE	7.1
FLIGHT CONTROL (LEADING)	7.6
CONTROL	6.7
<u>E-GLASS/CE-339 (0)₁₆</u>	
LEADING EDGE	7.4
TRAILING EDGE	7.4
CONTROL	7.1
<u>E-GLASS/X904-B (0)₁₆</u>	
LEADING EDGE	8.7
TRAILING EDGE	9.0
FLIGHT CONTROL (LEADING)	8.9
FLIGHT CONTROL (TRAILING)	9.0
CONTROL	8.3

TABLE VI.-LMSC DOUBLE LAP SHEAR STRENGTH DATA

HMF 330/934 BONDED TO 2024 ALUMINUM WITH HYSOL 9628 EPOXY FILM
ADHESIVE

SAMPLE LOCATION	DOUBLE LAP SHEAR STRENGTH (PSI) SAMPLE	AVERAGE
CONTROL	4020	
CONTROL	3910	
CONTROL	4210	
CONTROL	4260	
CONTROL	4060	4080±110
CONTROL	4090	
CONTROL	4040	
CONTROL	4040	
LEADING EDGE	4290	
LEADING EDGE	3780	
LEADING EDGE	3270	3850±440
LEADING EDGE	4040	
FLIGHT CONTROL (LEADING)	3960	
FLIGHT CONTROL (LEADING)	4250	
FLIGHT CONTROL (LEADING)	4190	4110±140
FLIGHT CONTROL (LEADING)	4020	
TRAILING EDGE	3240	
TRAILING EDGE	2910	
TRAILING EDGE	3280	2910±500
TRAILING EDGE	2190	
FLIGHT CONTROL (TRAILING)	4130	
FLIGHT CONTROL (TRAILING)	4230	
FLIGHT CONTROL (TRAILING)	4170	4160±60
FLIGHT CONTROL (TRAILING)	4100	

TABLE VII.-COEFFICIENT OF THERMAL EXPANSION DATA FOR LMSC COMPOSITE

<u>MATERIAL DESCRIPTION</u> SAMPLE LOCATION	THERMAL EXPANSION (PPM/°C)
<u>GY70/CE-339 (0)₁₆</u>	
LEADING EDGE	-0.93
TRAILING EDGE	-0.98
CONTROL	-0.93
<u>T50/F263 (0)₁₆</u>	
LEADING EDGE	-0.30
TRAILING EDGE	-0.51
CONTROL	-0.50
<u>T50/934 (0)₁₆</u>	
LEADING EDGE	-0.59
TRAILING EDGE	-0.63
CONTROL	-0.23
<u>T50/X904B (0)₁₆</u>	
LEADING EDGE	-0.47
TRAILING EDGE	0.10
CONTROL	-0.27

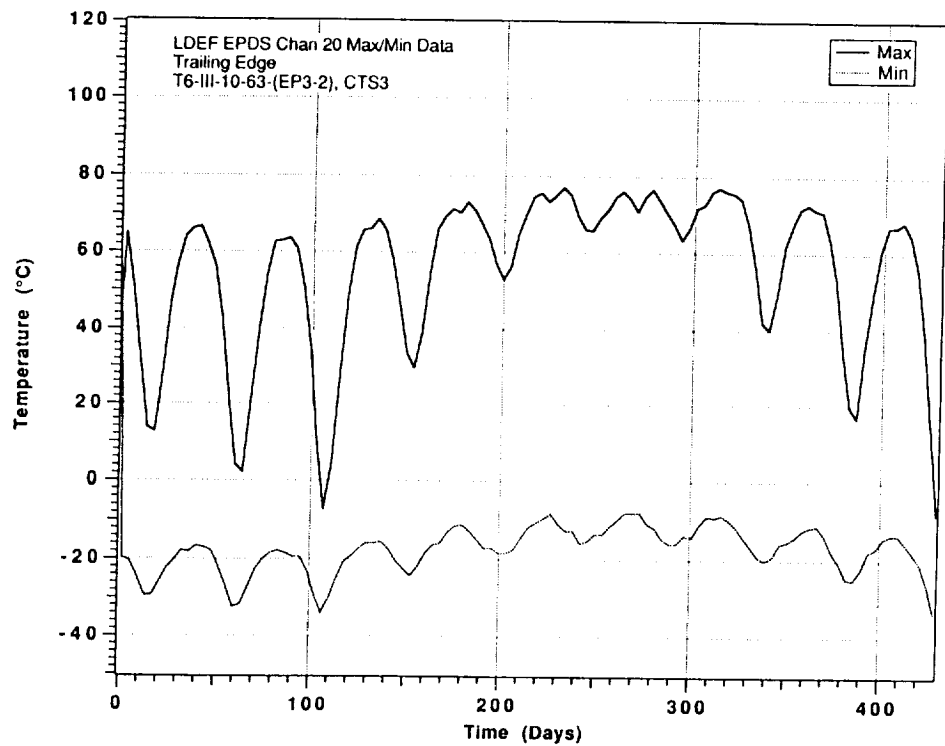
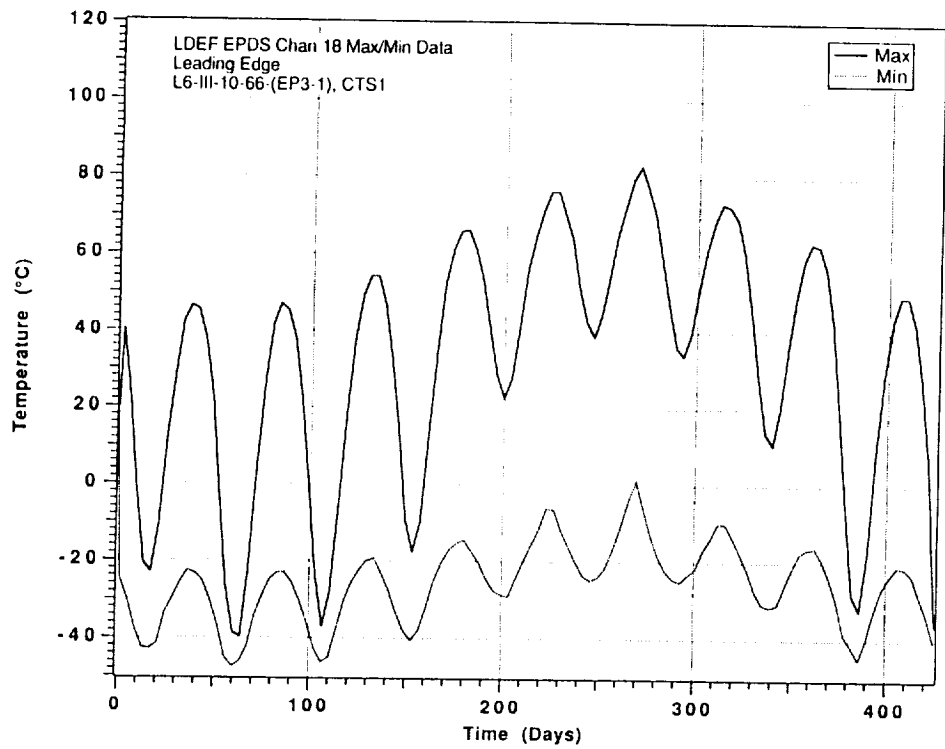
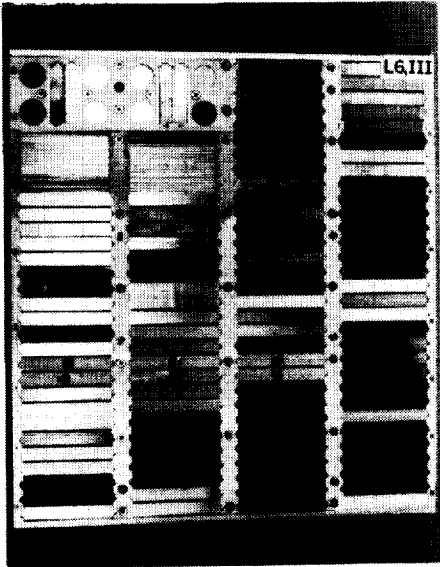


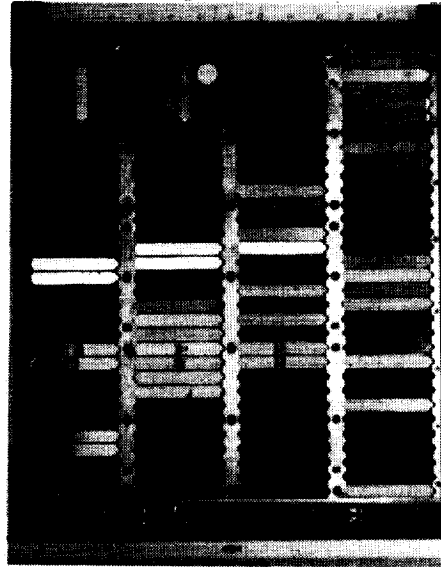
Figure 1. Maximum and Minimum Temperature Recorded for Each Orbit for T300/934 Graphite/Epoxy Samples Mounted on the Leading and Trailing Edges of LDEF.

LEADING EDGE EXPOSED

PREFLIGHT

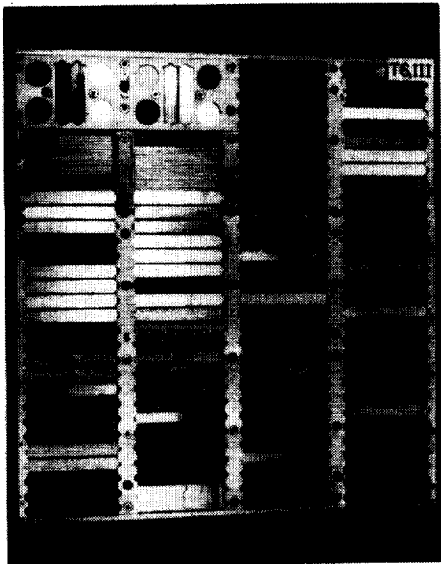


POSTFLIGHT



TRAILING EDGE EXPOSED

PREFLIGHT



POSTFLIGHT

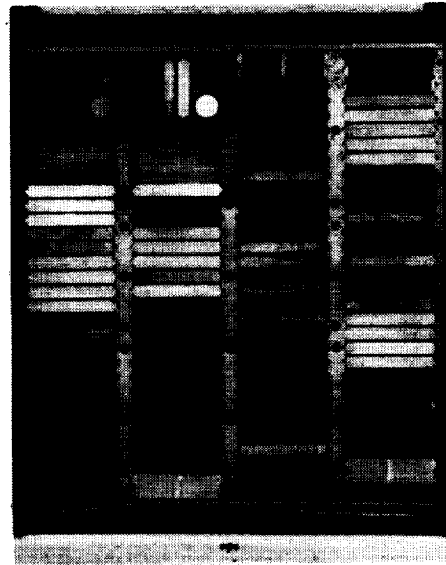


Figure 2. Preflight and Post-Flight Photographs of Exposed Side of Leading Edge and Trailing Edge Sample Cassettes.

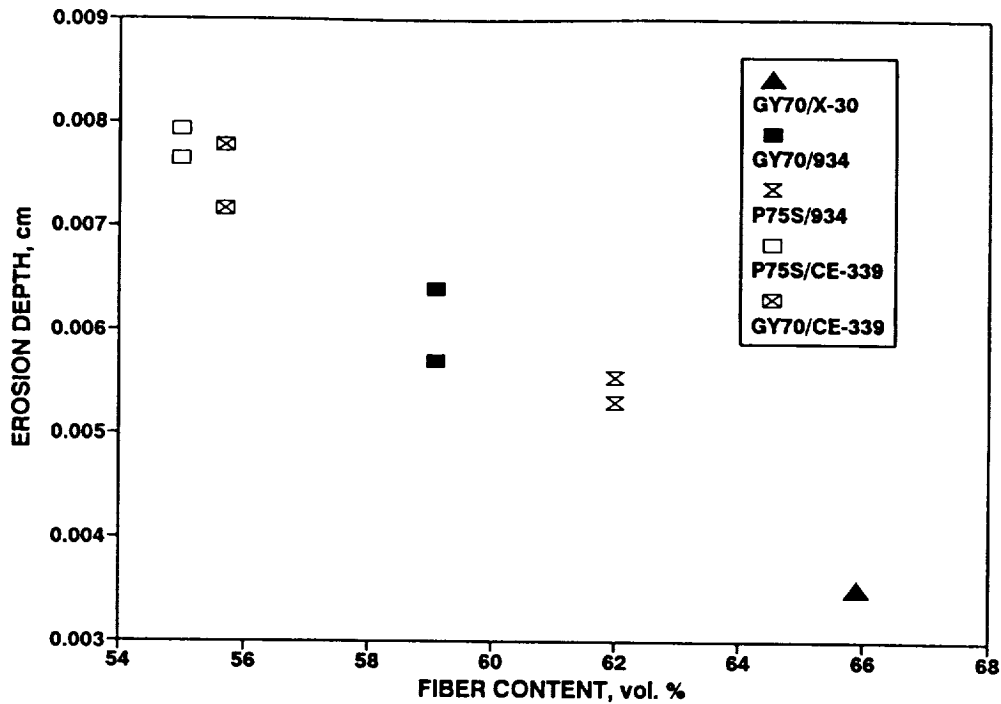


Figure 3. Estimated Atomic Oxygen Erosion Depth Versus Fiber Content for Several GDSSD Graphite/Epoxy Composite Systems.

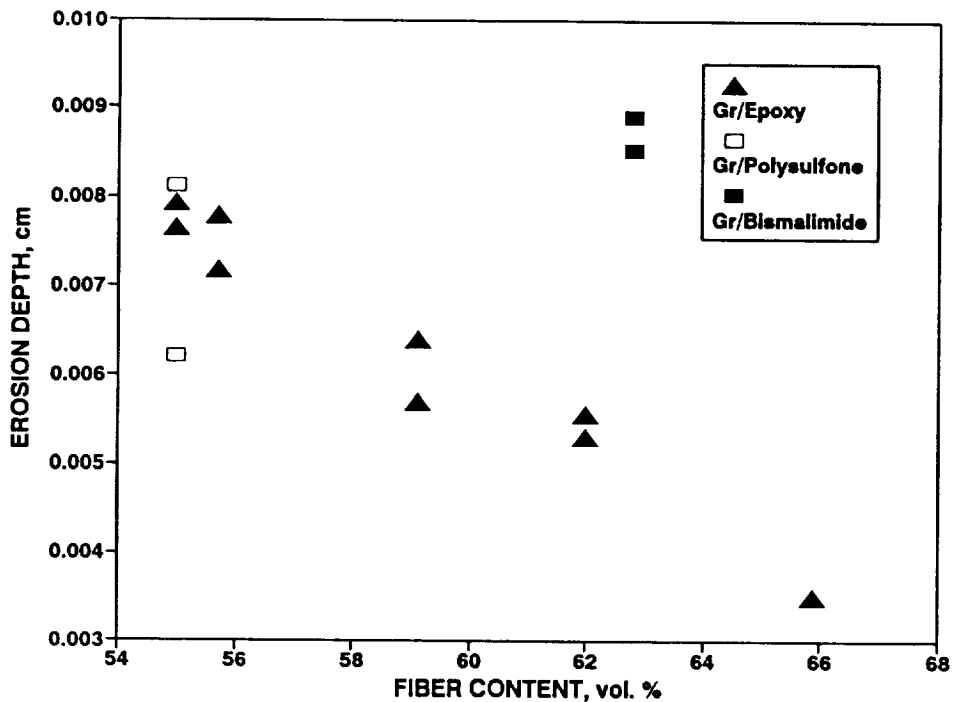
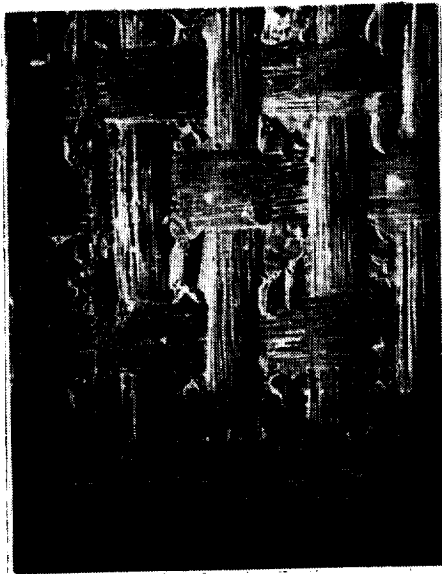
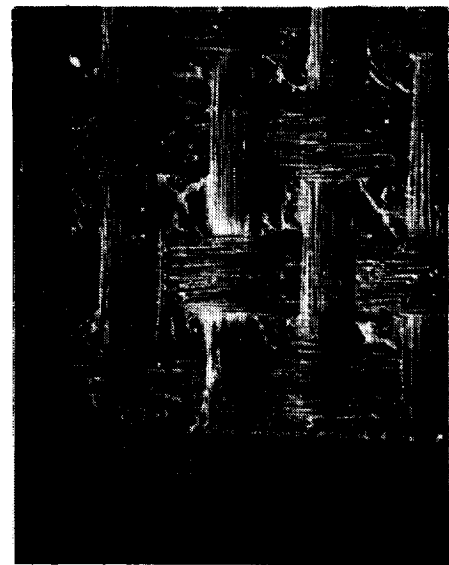


Figure 4. Estimated Atomic Oxygen Erosion Depth Versus Fiber Content for Several GDSSD Graphite/Epoxy, Graphite/Polysulfone, and Graphite/Bismalimide Composite Systems.

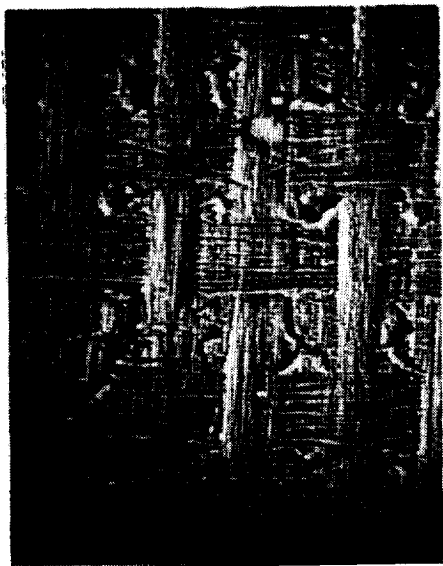


(a)

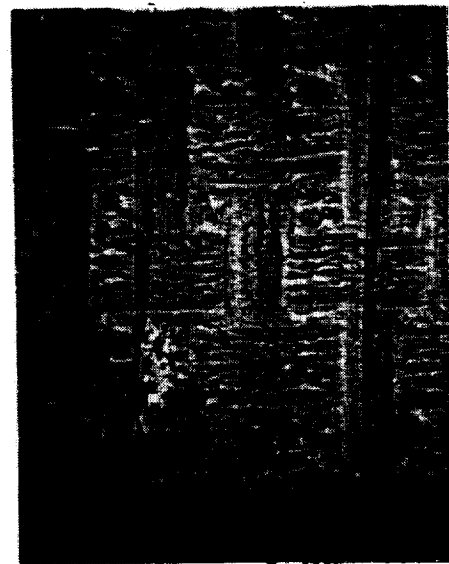


(b)

Figure 5. Scanning Electron Micrographs of Initial Surfaces of (a) P75S/934 Graphite/Epoxy Composite and (b) T300/V378A Graphite/Bismalimide Composite.

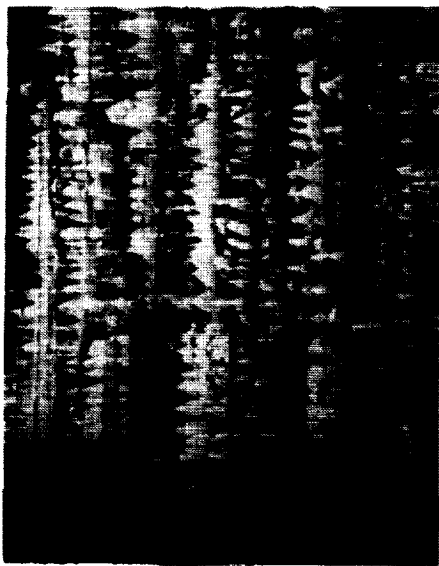


(a)

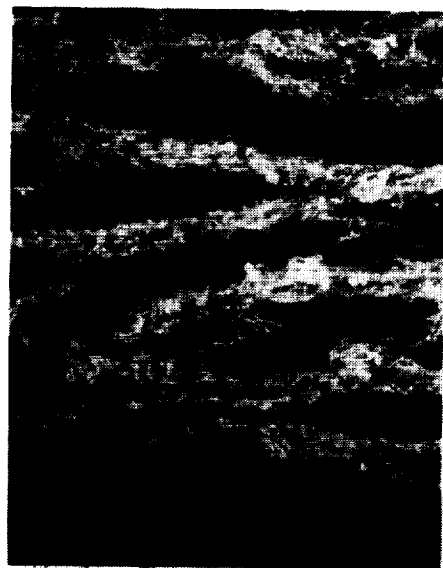


(b)

Figure 6. Low-Magnification Scanning Electron Micrographs of Eroded Surfaces of (a) P75S/934 Graphite/Epoxy Composite and (b) T300/V378A Graphite/Bismalimide Composite.

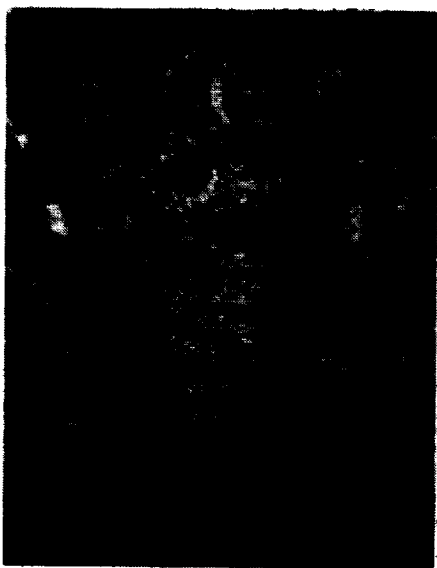


(a)

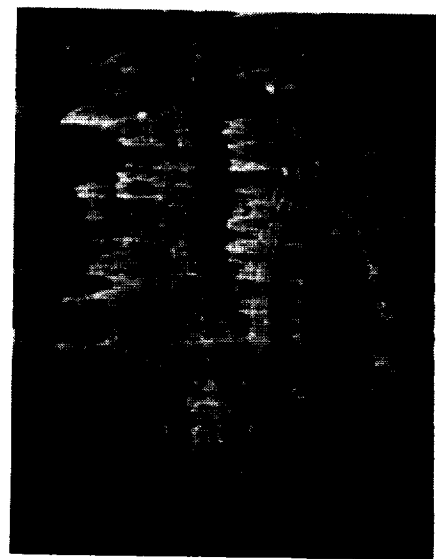


(b)

Figure 7. High-Magnification Scanning Electron Micrographs of Eroded Surfaces of (a) P75S/934 Graphite/Epoxy Composite and (b) T300/V378A Graphite/Bismalimide Composite.



(a)



(b)

Figure 8. High-Magnification Scanning Electron Micrographs of Eroded Surfaces of (a) T300/V378A Graphite/Bismalimide Composite at a Different Angle From Figure 7a and (b) Celion 6000/PMR-15 Graphite/Polyimide Composite.

ULTIMATE STRENGTH(KSI)

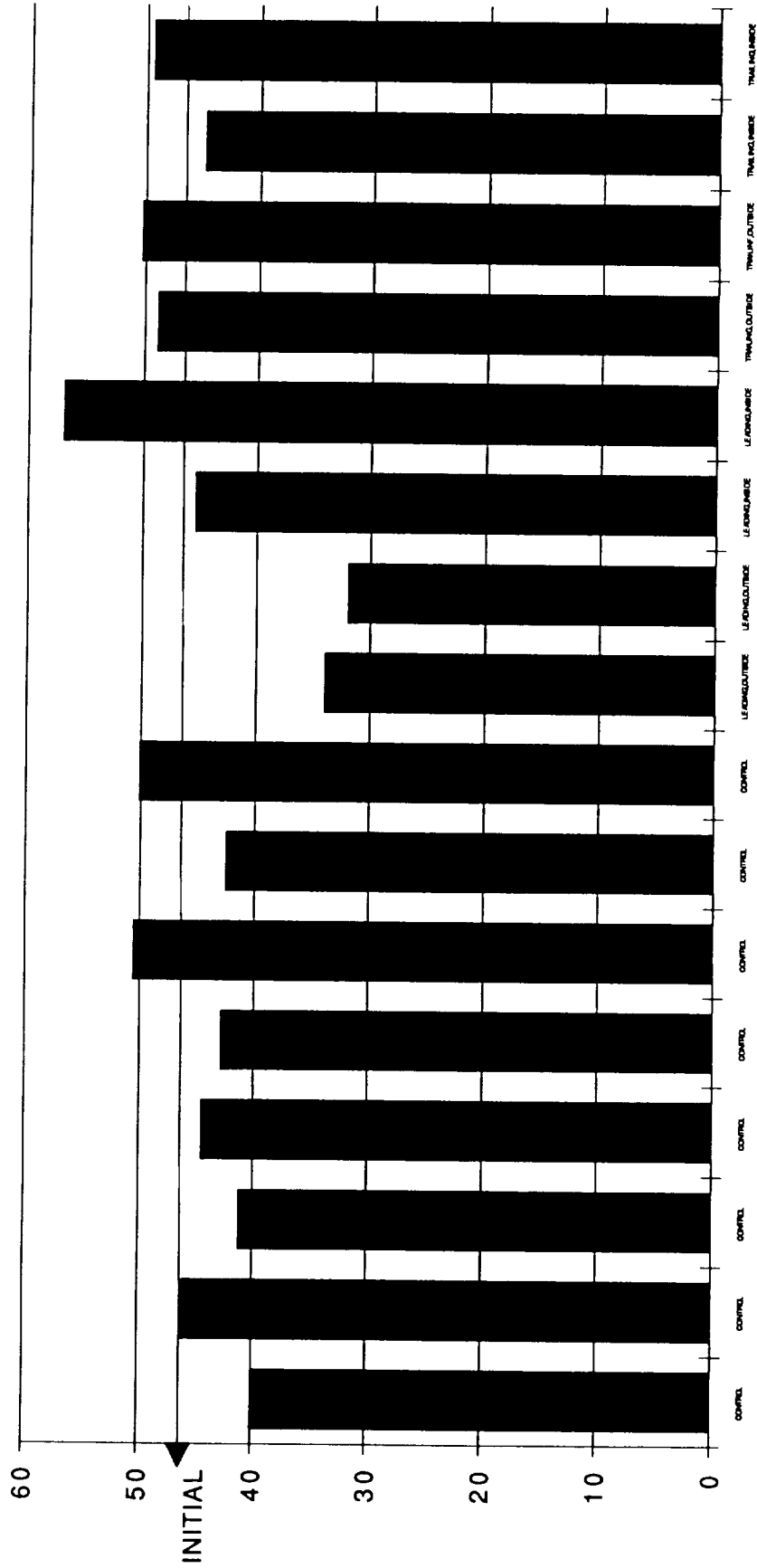


Figure 9. Bar Graph Showing Flexural Strength Data For All Samples for GDSSD P75S/934 Graphite/Epoxy Composite.

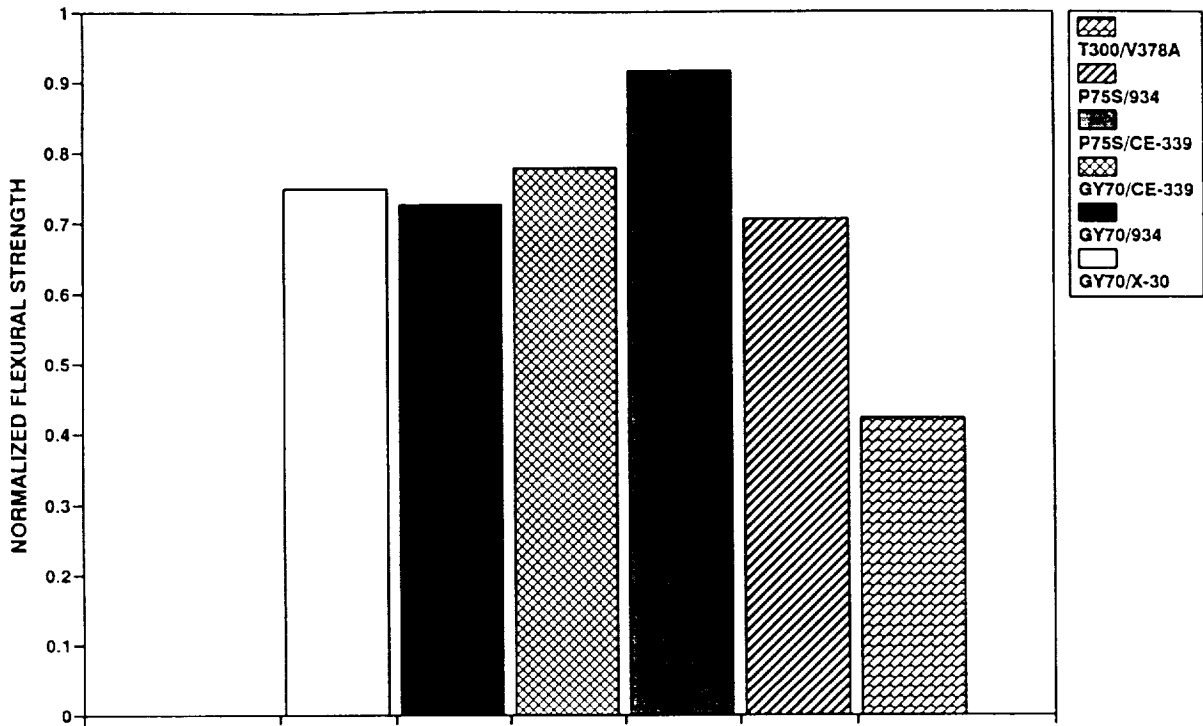


Figure 10. Bar Graph Showing Reduction in Flexural Strength for Uncoated GDSSD Composites on the Leading Edge of LDEF.

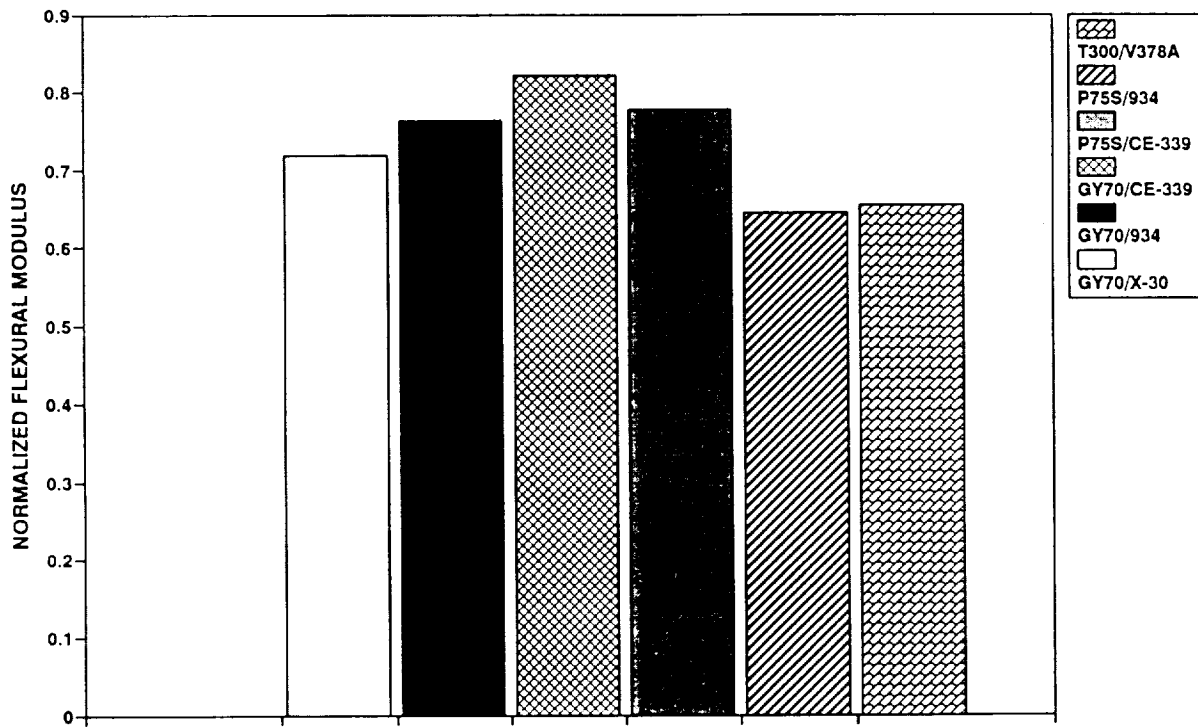


Figure 11. Bar Graph Showing Reduction in Flexural Modulus for Uncoated GDSSD Composites on the Leading Edge of LDEF.

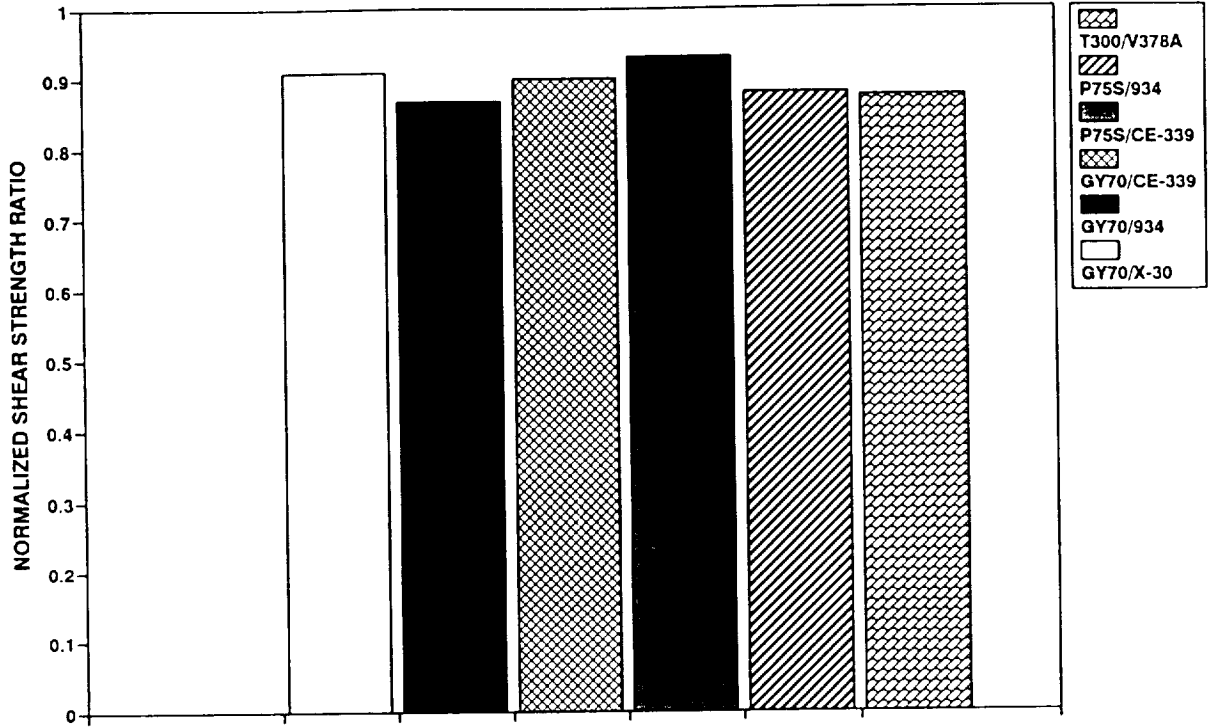


Figure 12. Bar Graph Showing Reduction in Short Beam Shear Strength for Uncoated GDSSD Composites on the Leading Edge of LDEF.

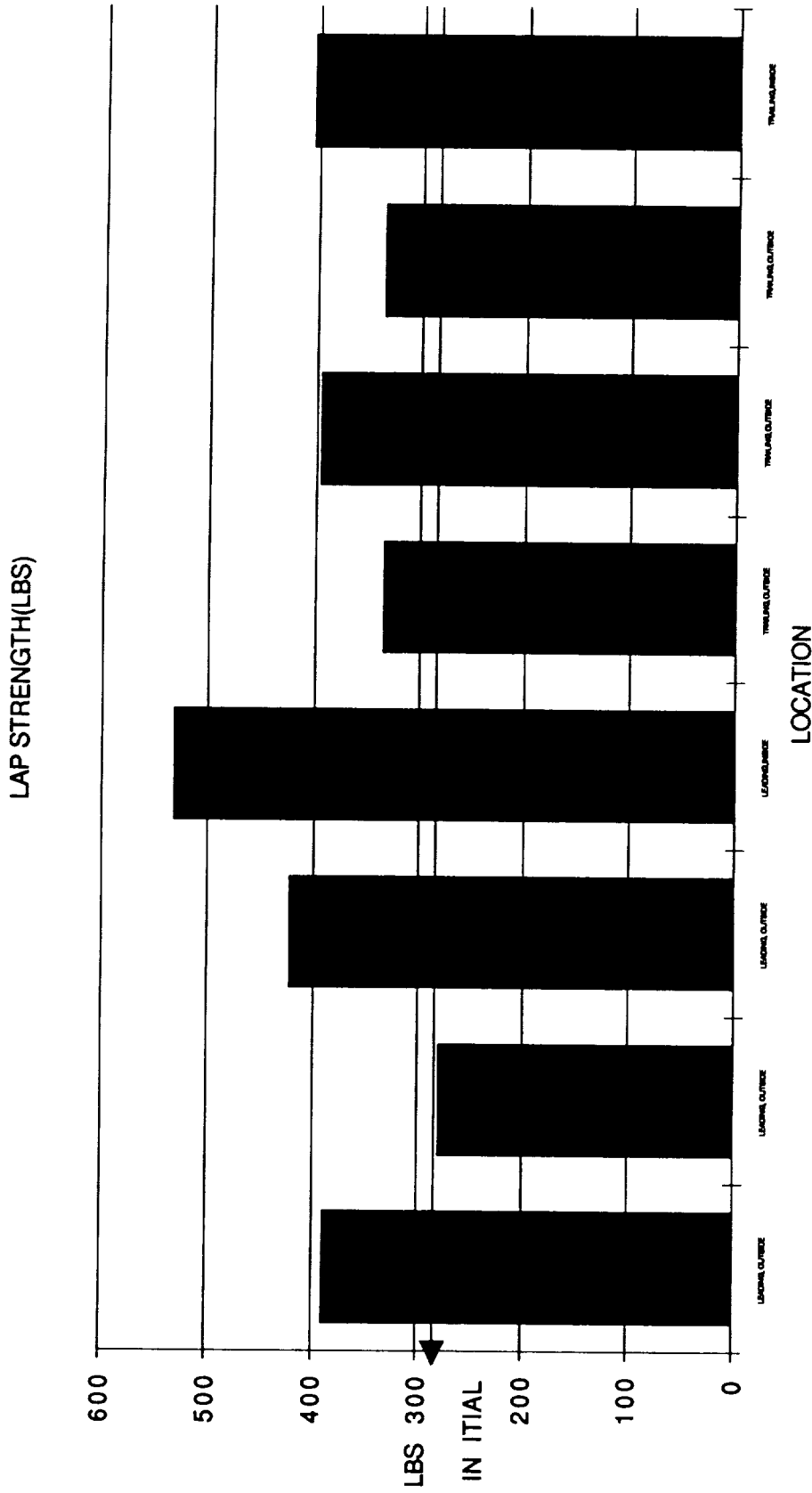


Figure 13. Bar Graph Showing Lap Shear Strength Data For All Samples for GDSSD Spot Welded W722/P-1700 Composites with a ZnO Coating.

SPACE ENVIRONMENTAL EFFECTS ON LDEF LOW EARTH ORBIT EXPOSED GRAPHITE REINFORCED POLYMER MATRIX COMPOSITES

Pete George
Boeing Defense & Space Group
Seattle, Wa

INTRODUCTION

The Long Duration Exposure Facility (LDEF) was deployed on April 7, 1984 in low earth orbit (LEO) at an altitude of 482 kilometers. On board experiments experienced the harsh LEO environment including atomic oxygen (AO), ultraviolet radiation (UV), and thermal cycling. During the 5.8 year mission the LDEF orbit decayed to 340 kilometers where significantly higher AO concentrations exist. LDEF was retrieved on January 12, 1990 from this orbit.

One experiment on board LDEF was M0003, "Space Effects on Spacecraft Materials". As a subset of M0003 nearly 500 samples of polymer, metal and glass matrix composites were flown as the "Advanced Composites Experiment" M0003-10. The Advanced Composites Experiment is a joint effort between government and industry with the Aerospace Corporation serving as the experiment integrator. A portion of the graphite reinforced polymer matrix composites were furnished by the Boeing Defense & Space Group, Seattle, Washington.

This paper presents test results and discussions for the Boeing portion of M0003-10. Experiment and specimen location on the LDEF are presented along with a quantitative summary of the pertinent exposure conditions. Matrix materials selected for the test were epoxy, polysulfone and polyimide. These composite materials were selected due to their suitability for high performance structural capability in space craft applications. Graphite reinforced polymer matrix composites offer high strength to weight ratios along with excellent dimensional stability.

The Boeing space exposed and corresponding ground control composite specimens have been subjected to post flight mechanical, chemical, and physical testing in order to determine any changes in critical properties and performance characteristics. Among the more significant findings are the erosive effect of atomic oxygen on leading edge exposed specimens and microcracking in non-unidirectionally reinforced flight specimens .

The M0003-10 Advanced Composites Experiment was located at both the leading and trailing edges of the LDEF as shown in Figure 1. The leading edge specimens were at position D8 on the satellite which was 38 degrees from the direction of motion (ram direction). The trailing edge specimens were located at position D4, 158 degrees from the ram direction.

The specimens of experiment M0003-10 were intentionally positioned at both leading and trailing edges in order to provide varied exposure conditions. At the mission altitudes the atomic oxygen was swept by the LDEF leading edge surface. The trailing edge specimens received practically no atomic oxygen exposure.

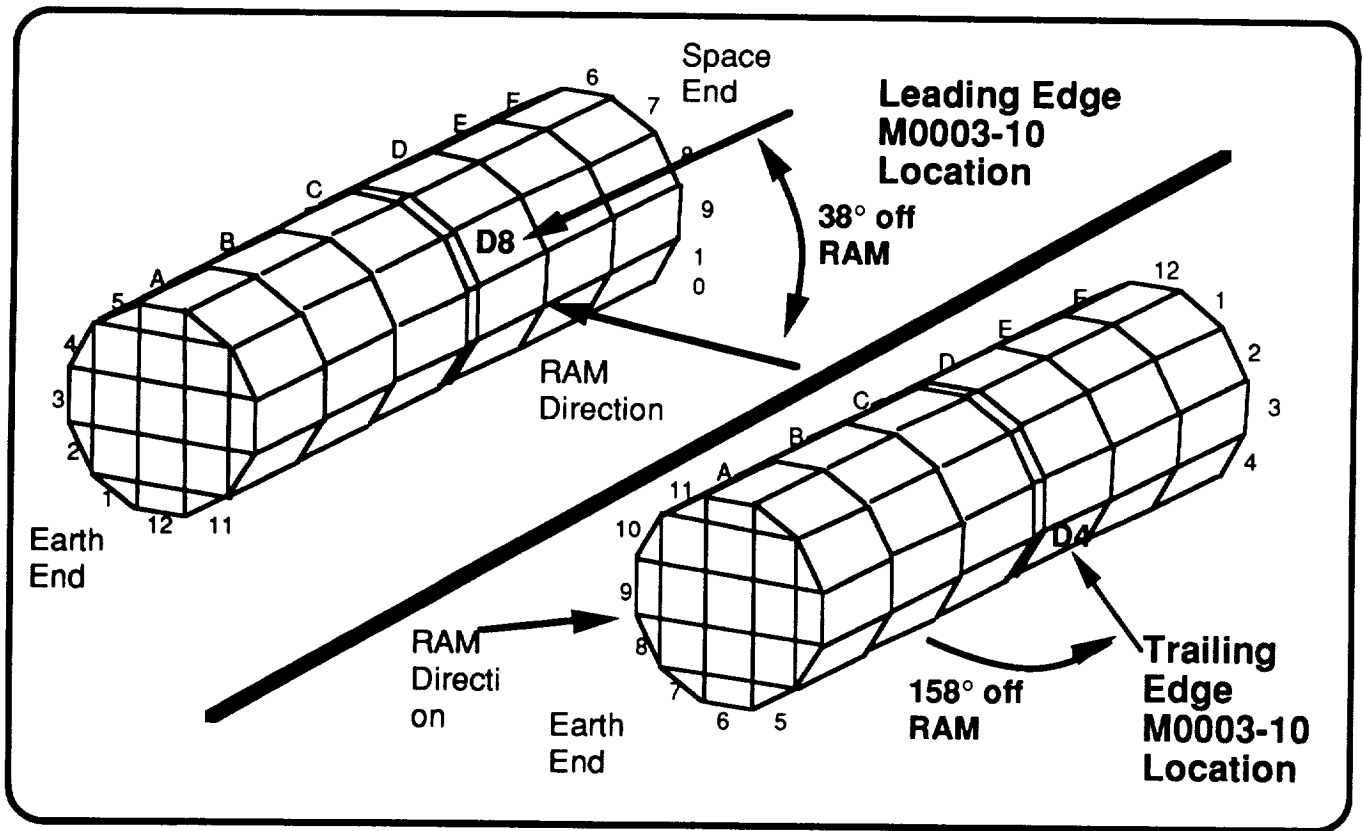


Figure 1. Location of M0003-8 experiment on LDEF

Graphite fiber reinforced polymer matrix composites were located at both the leading and trailing edge positions as shown in Figure 2. Complete sets of the five material types listed in Figure 2 were flown in both direct space exposure positions on the "A-deck" as well as in shielded positions on the "B-deck" at the leading and trailing edges. Also, a complete set of specimens were kept at controlled temperature and humidity conditions at the Aerospace Corporation. These specimens were shielded from exposure to ambient light and were used as ground controls.

Specimen configuration was 3.5 inches long by 0.5 inches wide with the 0 degree direction parallel to the length. Thickness of the specimens varied between matrix types due to differences in number of plies and ply thickness. Matrix resins and reinforcements along with ply stacking sequences for the specimens are listed in Figure 2. The original documentation does not list the specific type of reinforcement for the LARC 160 polyimide. However it is known that the fibers are of the low modulus (33 Msi) range as are all of the reinforcing fibers for these specimens.

The epoxy specimens represented the state of the art for epoxy systems at the time of experiment integration. The polysulfone specimens were selected due to their excellent outgassing properties as well as their potential for on orbit manufacture and repair. The polyimides represent the upper end of temperature capability for polymer matrix composites

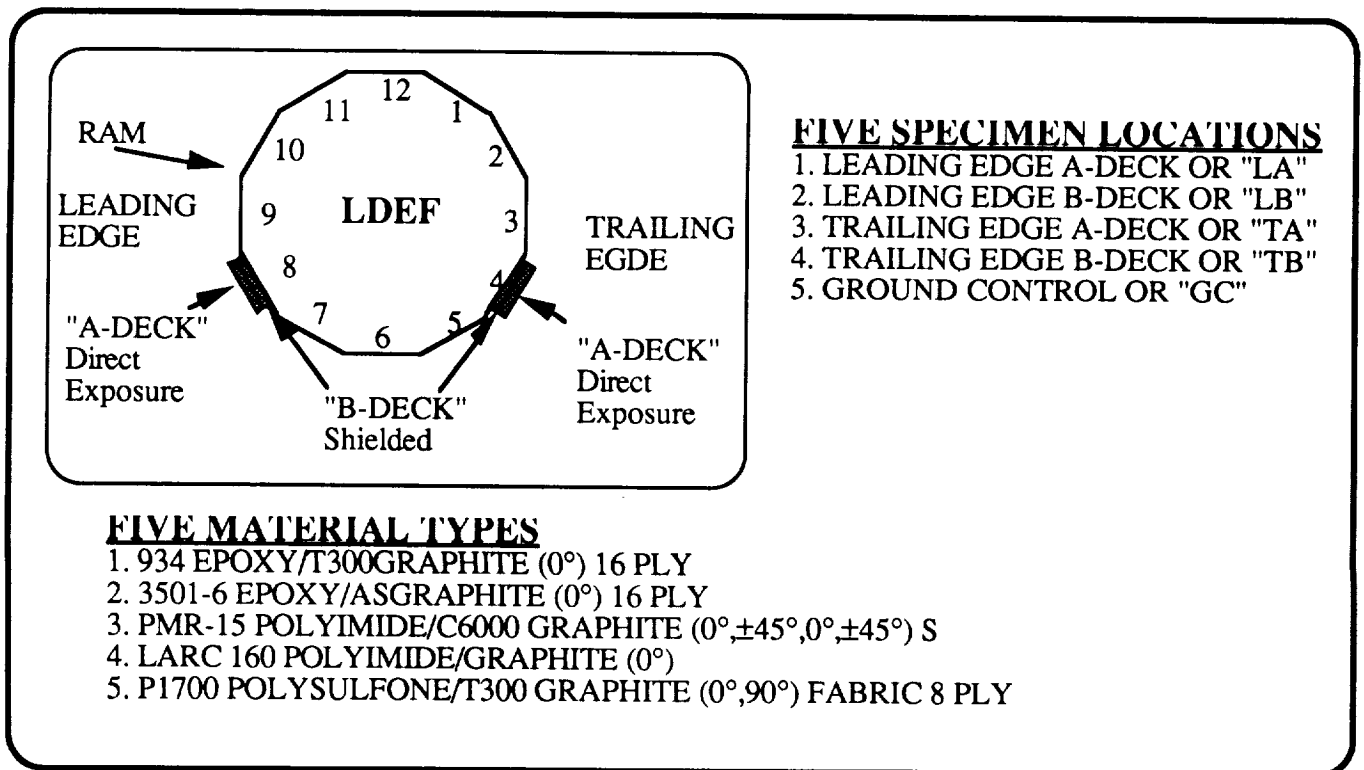


Figure 2. Material types and locations

Table 1 lists the exposure conditions for the flight test specimens at the leading and trailing edge A-deck positions as well as for the shielded B-deck positions. The leading edge A-deck specimens were exposed to relatively high fluxes of atmospheric constituents, primarily highly reactive atomic oxygen at the altitudes involved with the LDEF mission. Solar, including ultraviolet, and particulate radiation were similar for leading and trailing edge A-deck specimens. B-deck specimens did not receive any AO or UV exposure.

Thermistor data collected by the Aerospace Corporation from leading and trailing edge instrumented A-deck specimens indicates significant thermal cycling of the composites during the flight.¹ B-deck thermistor data was not available. However, the thermal coupling of the specimens was designed such that temperature excursions for the A and B deck were to be similar. Microcrack data presented later in this paper suggests that the B-deck specimens may have experienced milder temperature excursions and/or milder thermal shock conditions.

Table 1. ATOMIC OXYGEN, SOLAR EXPOSURE AND THERMAL CYCLING

	LEADING EDGE "A-DECK" ,ROW 8	TRAILING EDGE "A-DECK" ,ROW 4	LEADING & TRAILING EDGE "B"DECK
ATOMIC OXYGEN EXPOSURE (Impacts / cm ²)	6.93 x 10 ²¹	9.32 x10 ⁴	0
INCIDENT SOLAR & EARTH REFLECTED RADIATION (Equivalent solar hours)	9,300	10,500	0
THERMAL CYCLING (In Flight Measurement)	-53°F to 183°F 32,422 CYCLES	-27°F to 170°F 32,422 CYCLES	Unknown, B-deck expected to be less than A deck, leading expected to be less than trailing

Two to four specimens of each material were flown at each position (and ground control). One each was dedicated to chemical and physical testing. The remaining specimens were tested for mechanical properties. The tests performed are listed in Figure 3 along with the potential uses of the resulting data.

The specimens were configured as 3.5 inch by 0.5 inch strips for flexure testing. Although flexure testing is not the preferred method of the designer, it allows good relative performance measurements. The data collected is useful for determining mechanical performance degradations between exposure and ground control specimens.

Chemical testing by infrared (IR) spectroscopy can reveal the changes in organic functional group chemistry. Energy dispersive X-ray spectroscopy (EDX) is a sensitive technique for measuring the elemental composition of surfaces. These test results may help to determine the underlying degradation mechanism of atomic oxygen on polymer matrix composites.

Physical tests include glass transition temperatures as measured by thermomechanical analysis (TMA), surface recession by mass loss and microcracking by cross sectional microscopy, total mass loss (TML) and volatile condensable materials (VCM) by outgassing tests, and coefficients of thermal expansion by dilatometry. These test results are valuable for determining dimensional stability and outgassing characteristics.

MECHANICAL: FLEXURE MODULUS AND STRENGTH

- ROUGH DESIGN KNOCKDOWN ESTIMATES FOR UNCOATED COMPOSITES IN LEO APPLICATIONS
- VERIFICATION OF LEO SIMULATION AND MODELING
- RESISTANCE TO LEO EFFECTS OF COMPOSITES WITH DAMAGED PROTECTIVE COATINGS

CHEMICAL: IR SPECTROSCOPY AND EDX

- UNDERLYING MECHANISM FOR DEGRADATION OF PERFORMANCE PROPERTIES DUE TO LEO EXPOSURE

PHYSICAL: GLASS TRANSITION , SURFACE RECESSION, MICROCRACKING,TML & VCM, AND CTE

- KNOCKDOWN IN USE TEMPERATURE CAPABILITY DUE TO RESIN DEGRADATION
- STRUCTURAL PERFORMANCE REDUCTION DUE TO LEO EXPOSURE
- RESIDUAL OUTGASSING PROPERTIES
- THERMAL EXPANSION PROPERTIES

FIGURE 3. PROPERTIES MEASURED - POTENTIAL USES OF DATA

Figures 4 through 8 show the flexure test results for the space exposed, shielded and ground control specimens. Three point flexure testing was performed per ASTM D790 using an Instron model TT-D equipped with a deflectometer. A cross head speed of 0.1"/minute and a 21T span to depth ratio were used. All testing was performed at room temperature.

The 934 epoxy/T300 graphite specimens did not show any significant loss in flexure properties between the different positions on LDEF and the ground control. These results are based on the post flight cross-sectional areas. The loss of material for the leading edge exposed specimens results in a performance reduction for a given specimen. As these specimens were unidirectionally (0°) reinforced, the load that would have been carried by the eroded material on the leading edge exposed specimens was carried by the remaining 0° material. For these specimens the only mechanical performance loss was due to material loss on the leading edge exposed specimens. Ply orientation plays a significant role in flexure properties behavior when AO erosion is involved.

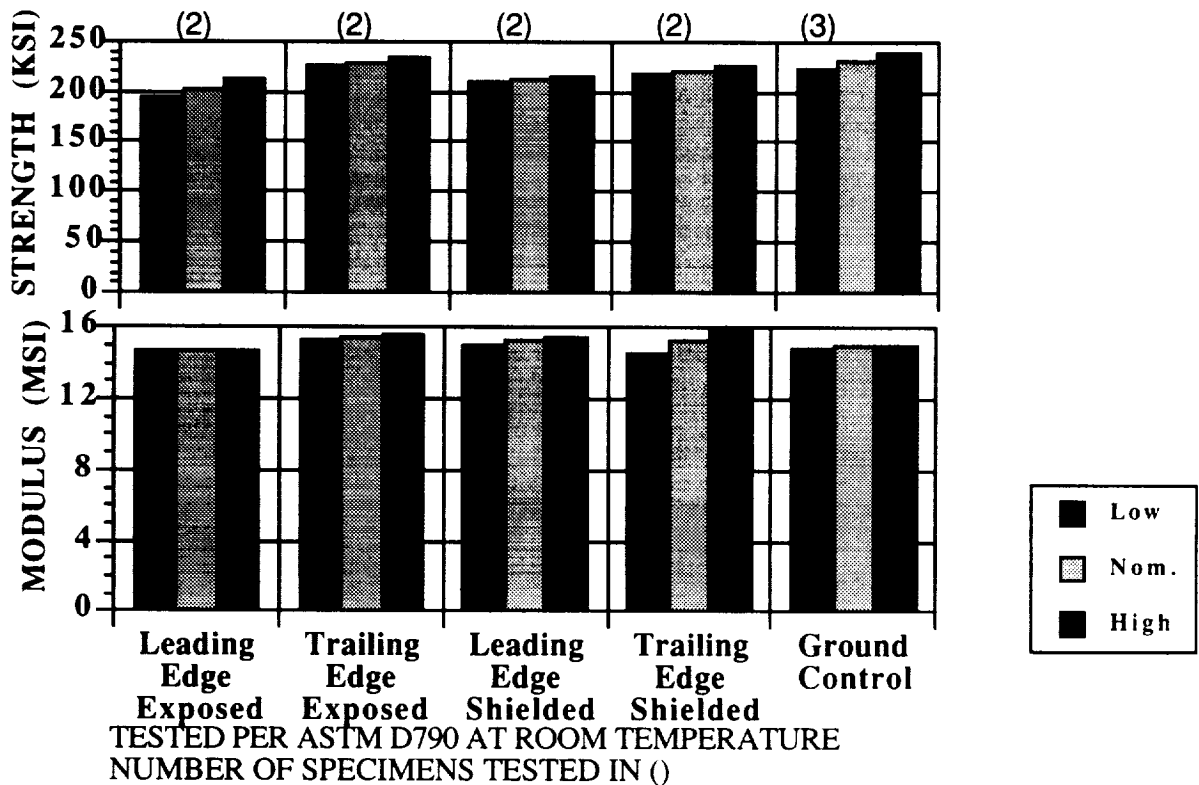


Figure 4. Flexure strength and modulus of 934/T300 specimens, (0°) 16 plies

The 3501-6 epoxy/AS graphite flexure test results show very little change in modulus values among the different exposure conditions and the ground control. The strength values show some variation from position to position, most likely due to the inherent scatter with polymer matrix composite strength measurements and the small sample size. Once again the 0° orientation of the reinforcement allows the underlying plies to pick up the load from the eroded surface ply on the leading edge exposed specimens. This is a similar situation to the 934/T300 results where mechanical performance reductions are due to erosion of material on the leading edge specimens.

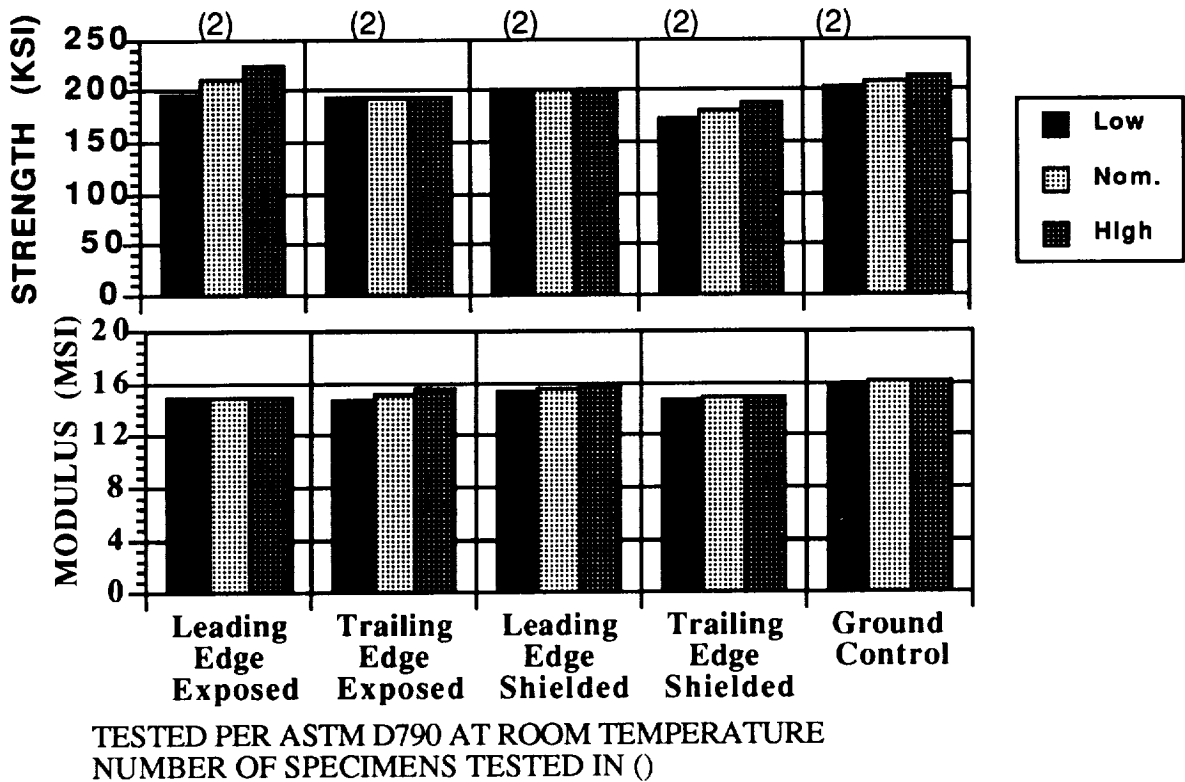


Figure 5. Strength and modulus of 3501-6/AS specimens, (0°) 16 plies

The P1700 polysulfone/T300 graphite specimens were reinforced with a 0°,90° woven fabric. Here also as with the unidirectionally reinforced specimens there is continuous reinforcement in the load direction in each ply. No significant changes in either flexure modulus or strength were found.

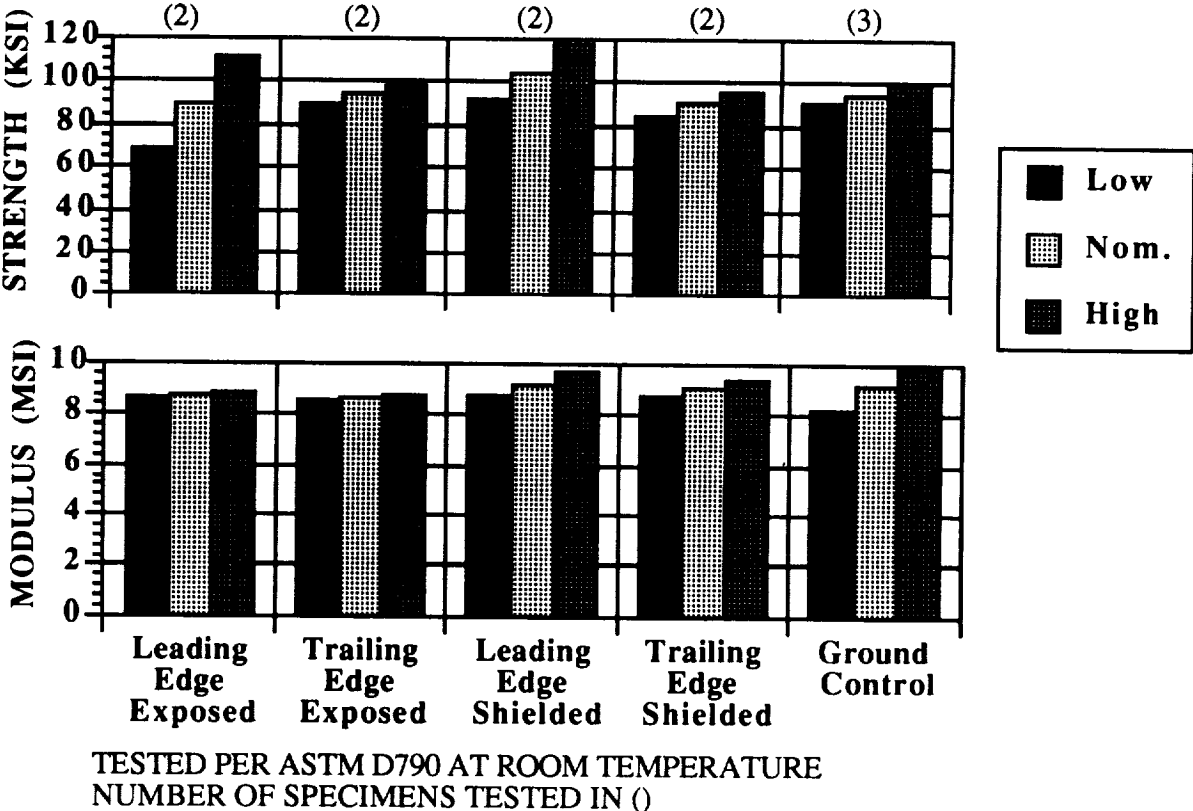


Figure 6. Flexure strength and modulus for P1700/T300 specimens, (0°,90°) fabric 8 plies.

The PMR-15 polyimide/ C6000 graphite specimens were reinforced with an angle ply stacking sequence of $(0^\circ, \pm 45^\circ, 0^\circ, \pm 45^\circ)_s$. As can be seen from the data in Figure 7 the strength and modulus values drop off significantly for the leading edge exposed specimens. This is due to the almost complete loss of the 0° ply on the exposed surface of the specimen due to AO erosion. Unlike the unidirectionally reinforced specimens, the ply underneath is at $+45^\circ$ and has a lower stiffness and strength in the load direction. This behavior has been seen in other leading edge LDEF specimens with multidirectional reinforcement.²

The non AO exposed specimen data show no significant change in flexure properties compared with the ground control data.

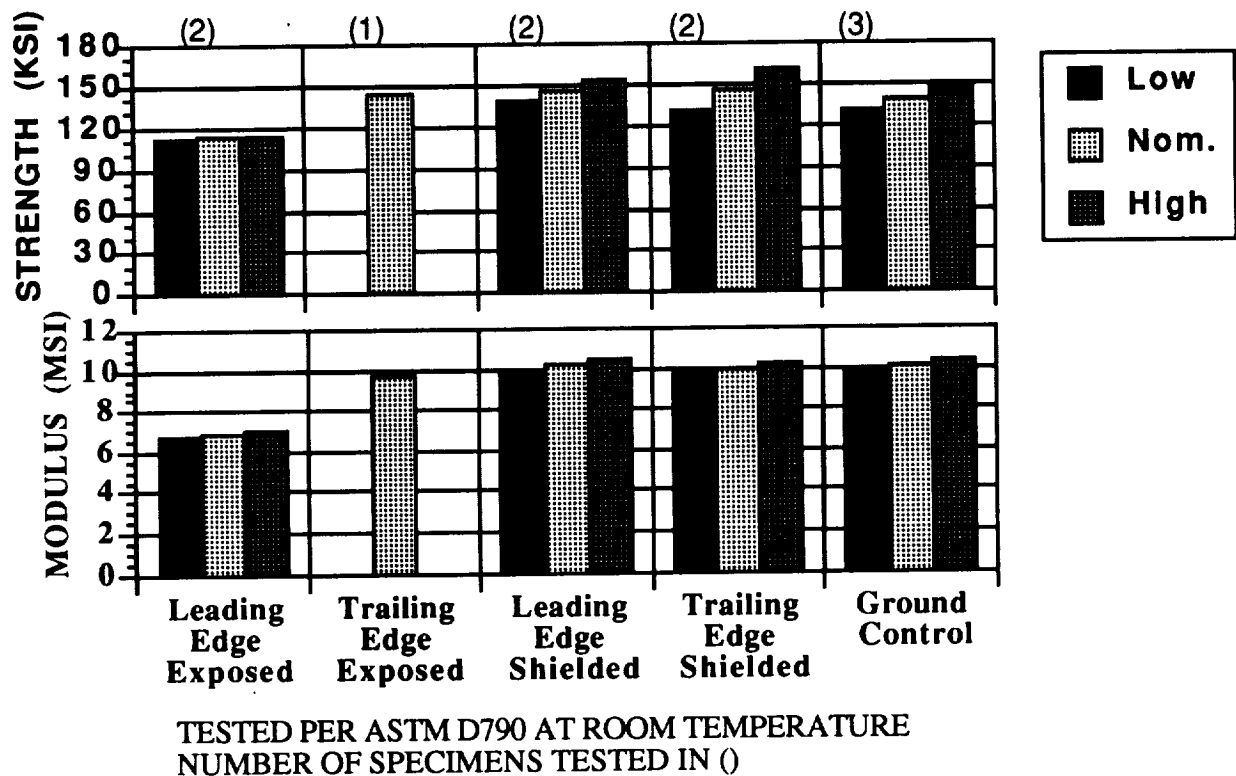


Figure 7. Flexure strength and modulus for PMR-15/C6000 specimens $(0^\circ, \pm 45^\circ, 0^\circ, \pm 45^\circ)_s$

The LARC 160 polyimide/ graphite flexure test results show very little change in modulus values among the different exposure conditions and the ground control. The strength values show some variation from position to position, most likely due to the inherent scatter with PMC strength measurements and the small sample size. Once again the 0° orientation of the reinforcement allows the underlying plies to pick up the load from the eroded surface ply on the leading edge exposed specimens. This is a similar situation to the other unidirectionally reinforced material results where mechanical performance reductions are due to erosion of material on the leading edge specimens.

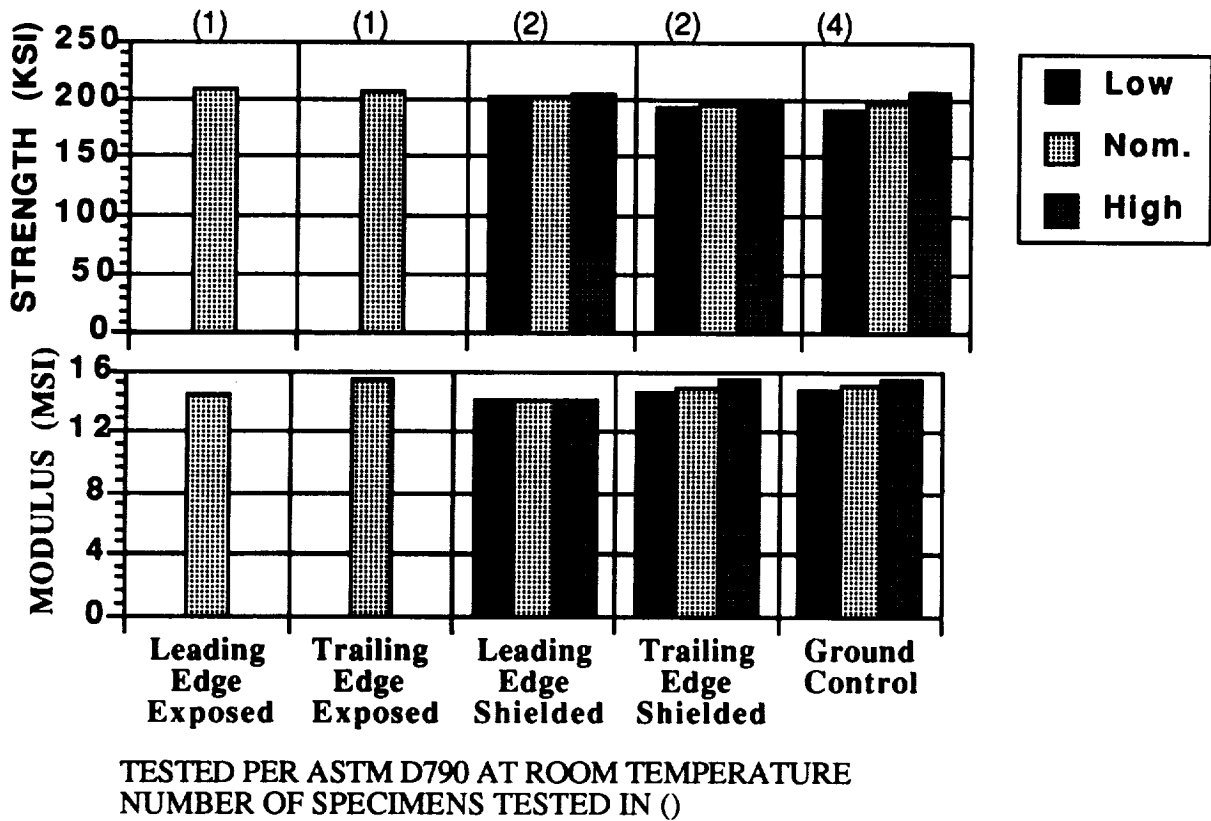


Figure 8. Flexure strength and modulus for LARC 160/graphite specimens, (0°)

Total mass loss (TML) and volatile condensable materials (VCM) measurements were made using the NASA-SP-R-0022A outgassing test. The test samples were held at 125°C and the collection plate at 25°C for 24 hours at 10⁻⁶ torr. The trailing edge 934/T300 specimens were not tested as this material was used for other purposes. The test results are presented in Table 2.

The exposed and shielded values compare favorably with the ground control values. After 5.8 years of space exposure including vacuum and temperature extremes one would expect these specimens to have thoroughly outgassed. Therefore the outgassing measured here is most likely due to moisture reabsorbed by the specimens during the 18 months between retrieval and testing. This phenomenon has been observed in dimensional change measurements performed on LDEF specimens by Tennyson.³

The TML outgassing levels for P1700 polysulfone/T300 graphite were an order of magnitude less than the other materials. This can be expected due to the thermoplastic nature and low polarity of the matrix resin.

TABLE 2. VOLATILE CONDENSABLE MATERIALS AND TOTAL MASS LOSS TEST RESULTS

LOCATION	934/T300 EPOXY		3501-6/AS EPOXY		PMR15/C6000 POLYIMIDE		LARC160/Gr. POLYIMIDE		P1700/T-300 POLYSULFONE	
	TML	VCM	TML	VCM	TML	VCM	TML	VCM	TML	VCM
LEADING EDGE EXPOSED	0.52	0.02	0.57	0.01	0.56	0.01	0.51	0.01	0.05	0.01
TRAILING EDGE EXPOSED	N.T.	N.T.	0.43	0.03	0.56	0.00	N.T.	N.T.	0.03	0.00
LEADING EDGE SHIELDED	0.43	0.00	0.41	0.02	0.57	0.02	0.71	0.01	0.08	0.00
TRAILING EDGE SHIELDED	N.T.	N.T.	0.43	0.01	0.59	0.00	0.63	0.02	0.04	0.01
GROUND CONTROL	0.39	0.01	0.56	0.02	0.53	0.02	0.68	0.01	0.06	0.01

NASA SP-R-0022A OUTGASSING TEST, 24 HOUR EXPOSURE

Thermomechanical analysis (TMA) in flexure was performed on specimen samples from each position including the ground controls. The trailing edge 934/T300 specimens were not tested as this material was used for other purposes. Testing was performed using a Perkin Elmer System 7 thermomechanical analysis unit using a 10° C /minute temperature ramp. The test results are presented in Table 3.

The exposed and shielded values compare favorably with the ground control values and with each other. This indicates that no significant thermal degradation of bulk polymer properties has occurred. No clear trends are perceivable concerning specimen position or material type. The value for the ground control P1700 polysulfone/T300 graphite sample is in doubt as the TMA trace curve began falling off in slope at the initiation of the temperature ramp indicating a sample mounting or measuring anomaly.

TABLE 3. GLASS TRANSITION TEMPERATURES

LOCATION	934/T300 EPOXY	3501-6/AS EPOXY	PMR15/C6000 POLYIMIDE	LARC160/Gr. POLYIMIDE	P1700/T-300 POLYSULFONE
LEADING EDGE EXPOSED	189°C	211°C	340°C	354°C	190°C
TRAILING EDGE EXPOSED	N.T.	216°C	336°C	340°C	180°C
LEADING EDGE SHIELDED	193°C	213°C	331°C	361°C	190°C
TRAILING EDGE SHIELDED	N.T.	214°C	336°C	354°C	180°C
GROUND CONTROL	191°C	211°C	335°C	352°C	167°C*

* This data point suspect due to possible mounting or measuring anomaly

Thermal expansion coefficients were measured in the 0° direction for each material using a Netzsch model 402 dilatometer. The dimensional change vs. temperature plots for the PMR-15 polyimide/C6000 graphite specimens shown in Figure 9 are representative of all the composite specimens. This plot includes values for leading and trailing edge shielded and exposed specimens as well as the ground control. The accuracy of this measurement technique is approximately 0.001% relative expansion as plotted. Therefore these measurements indicate no significant change in thermal expansion properties. However, as will be discussed in the following section, significant variations in microcracking in the PMR-15 polyimide / C6000 graphite specimens were found. This technique for measuring thermal expansion properties is not sensitive enough to measure the impact of this microcracking.

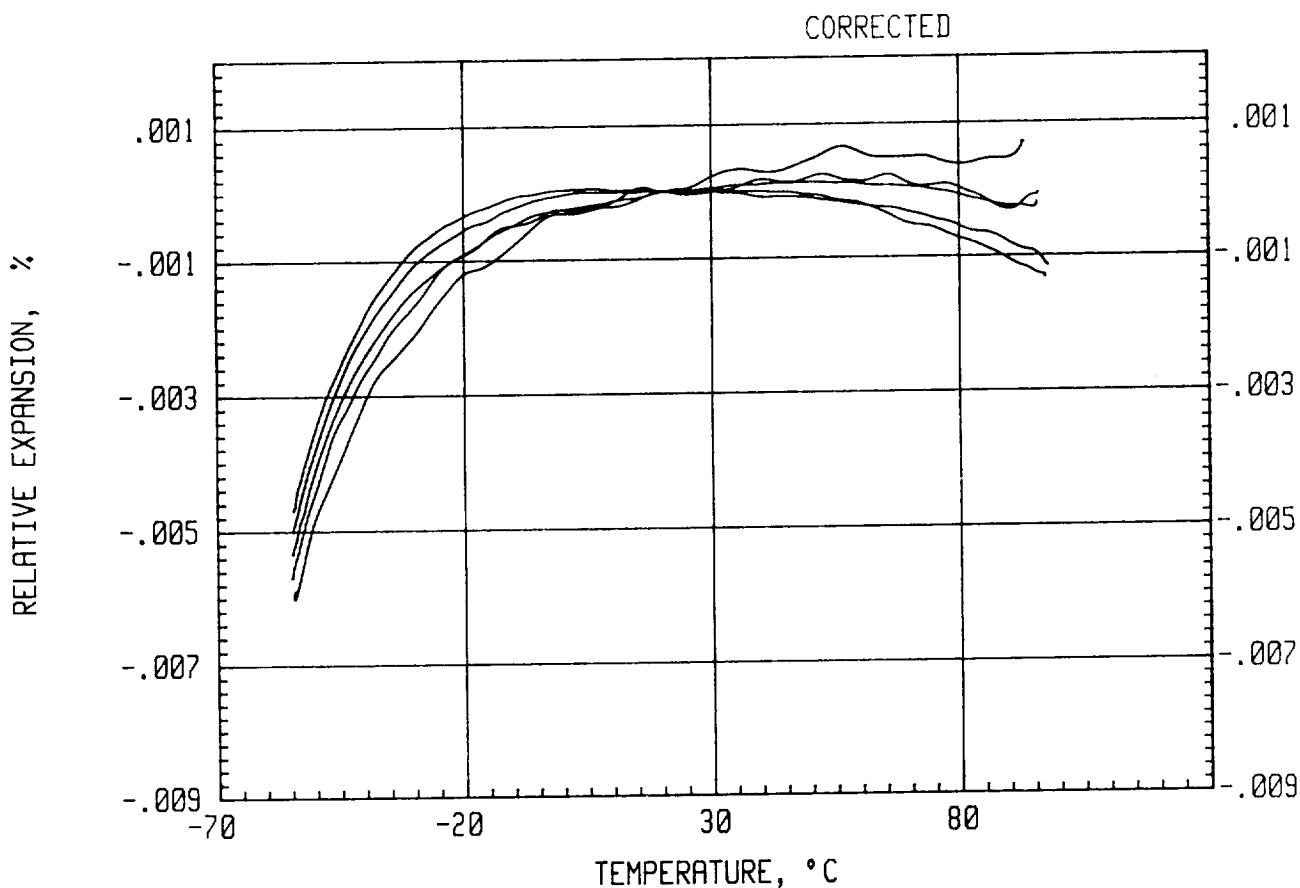


Figure 9.- Thermal expansion properties of PMR 15 polyimide/C6000 graphite LDEF specimens

Quantitative microcracking analysis was performed using optical microscopy on polished cross sections. These cross sections were taken perpendicular to the 0 degree direction and were examined at 100x magnification with the aid of a dye penetrant to enhance the contrast of the cracks. A total of 0.55 inches of lineal cross section was examined and the count of cracks was normalized to cracks per inch. Most of the surface ply of the leading edge exposed PMR-15 polyimide/C6000 graphite specimen was eroded away. The number of cracks per inch for the PMR-15 specimen was extrapolated to an estimated value as given in parenthesis in Table 4. Enough material remained for the leading edge exposed polysulfone specimen to obtain a crack count for the surface ply.

Most of the microcracks observed were intraply (within an individual ply). However some cracks in the PMR-15 polyimide/C6000 graphite did extend through two plies. Microcracking was only detected in the laminates with a nonunidirectional layup orientation. These laminates were the PMR-15 polyimide/C6000 graphite and the P1700 polysulfone/T300 graphite specimens which had $(0^\circ, \pm 45^\circ, 0^\circ, \pm 45^\circ)_S$ and $(0^\circ, 90^\circ)$ layup orientations respectively. The exposed (A-deck) PMR-15 and polysulfone PMC laminates specimens displayed the most microcracking. A smaller but significant level of cracking was found for the leading edge shielded (B-deck) PMR-15 and polysulfone PMC specimens. The trailing edge shielded (B-deck) PMR-15 and polysulfone PMC specimens displayed little or no microcracking. Ground controls did not display any microcracking.

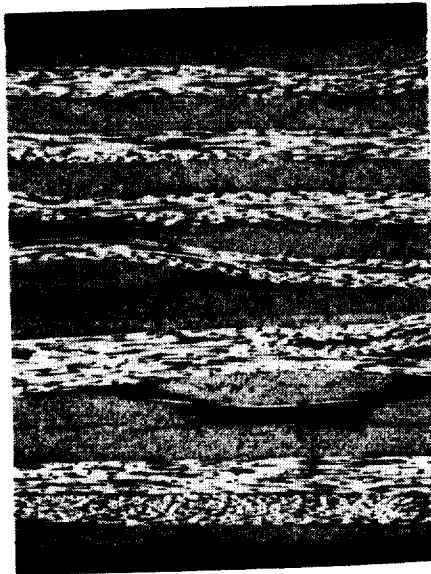
The non unidirectional layup produces greater thermally induced stresses as the part experiences thermal cycling. Also, the leading edge exposed specimens have a significantly higher emmissivity due to the rough texture produced by atomic oxygen erosion.³ This may account for the colder extremes reported for the leading edge exposed specimens.² The shielded specimens may have experienced milder thermal cycling extremes as their microcrack densities were significantly lower than the exposed specimens.

TABLE 4. MICROCRACKING (MICROCRACKS/INCH)

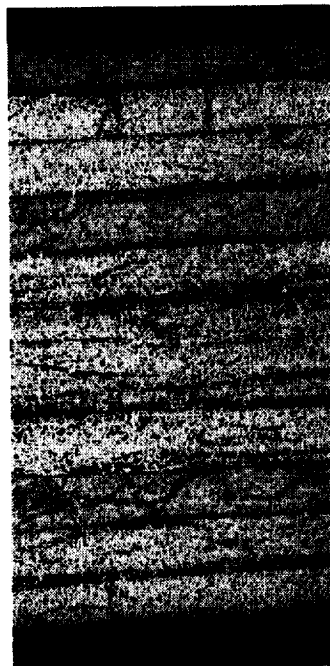
LOCATION	LDEF THERMAL CYCLING	934/T300 EPOXY (0°)	3501-6/AS EPOXY (0°)	PMR15/C6000 POLYIMIDE $(0^\circ, \pm 45^\circ, 0^\circ, \pm 45^\circ)_S$	LARC160/Gr. POLYIMIDE (0°)	P1700/T-300 POLYSULFONE (0°, 90°)
LEADING EDGE EXPOSED	-53°F to 183°F	0	0	33(45*)	0	35
TRAILING EDGE EXPOSED	-27°F to 170°F	0	0	47	0	35
LEADING EDGE SHIELDED	Less Than Above?	0	0	7	0	6
TRAILING EDGE SHIELDED	Less Than Above?	0	0	0	0	2
GROUND CONTROL	None	0	0	0	0	0

* extrapolation to account for eroded ply

Figure 10 shows a magnified cross sectional view of the leading edge P-1700 polysulfone/T300 graphite and PMR 15 polyimide/C6000 graphite specimens. These photomicrographs were taken at 50X and 100X magnification respectively. Intralaminar cracking can be seen in the outer plies of both specimens.



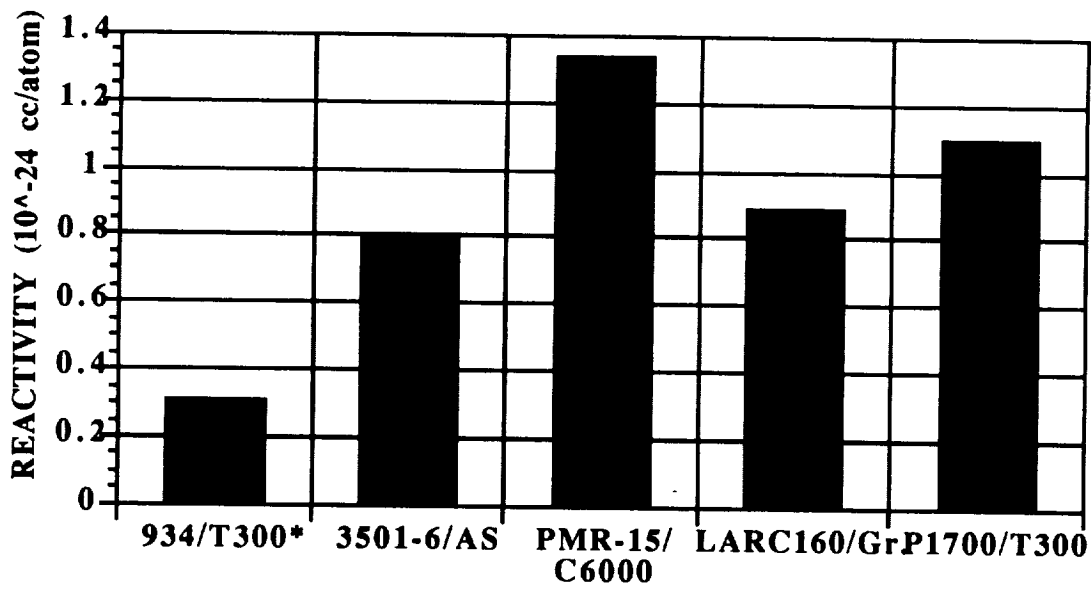
P-1700 polysulfone/T300



PMR 15 polyimide/C6000

Figure 10. Cross sectional micrograph of graphite reinforced polysulfone and polyimide specimens from the exposed leading edge position

Atomic oxygen reactivity values shown in Figure 11 for the five composite systems flown were calculated based on mass loss data. These values do not correspond well to the relative levels of local material loss as observed using optical microscopy. This suggests that other factors are involved in the mass loss of the whole specimen. Local areas of surface contamination were observed using scanning electron microscopy on many of the specimens. These areas appear to have experienced reduced or no erosion due to shielding by the contaminants. Other areas were observed with reduced erosion and no surface contaminant suggesting that a contaminant may have provided temporary shielding from atomic oxygen attack. Reactivity values for composite systems and any other material may best be obtained through local thickness loss measurements near a shielded area by microscopy or profilometry.



Calculated from weight loss data measured at the Aerospace corporation

* This value not consistent with cross sectional analysis

Figure 11. Atomic oxygen reactivity for leading edge exposed specimens

Figures 12 through 16 are scanning electron photomicrographs of leading edge specimens. Metallic coating of the specimens was not necessary as the conductivity of the graphite reinforcement was found to be sufficient. Perspectives and magnifications for each figure are similar allowing qualitative comparison of features.

Figure 12 shows the surface of a 934 epoxy/T300 graphite specimen. A jagged peak like structure exists with a stringy, "ash" like material concentrated in clumps around the peaks. The jagged peaks and "ash" structures are ubiquitous among the graphite reinforced specimens. However the level and texture of these features differ from composite type to composite type.

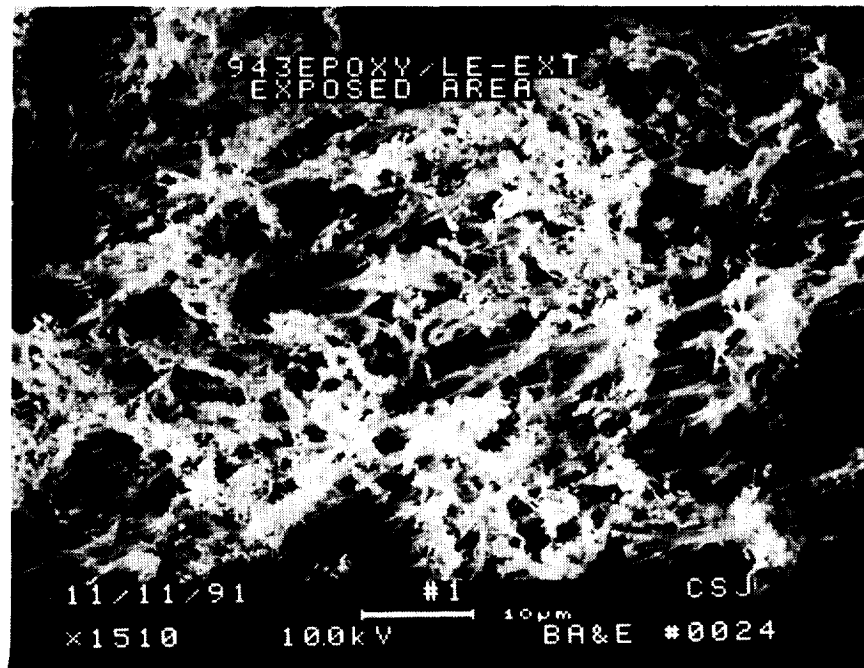


Figure 12. Scanning electron photomicrograph of leading edge exposed 934 epoxy/T300 graphite surface

ORIGINAL PAGE
BLACK AND WHITE PHOTOGRAPH

Figure 13 shows the surface of a 3501-6/AS graphite specimen. This material is very similar in chemistry to the 934 epoxy system. The jagged peak like structure and stringy, "ash" like material are present here in about the same level.

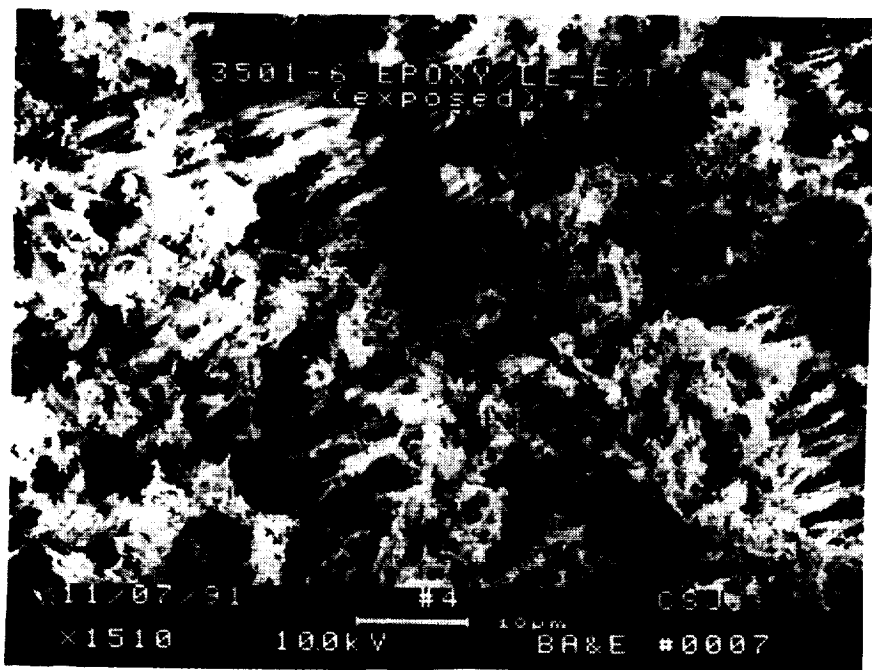


Figure 13. Scanning electron photomicrograph of leading edge exposed 3501-6/AS graphite surface

ORIGINAL PAGE
BLACK AND WHITE PHOTOGRAPH

Figure 14 shows the surface of a leading edge exposed P1700 polysulfone/ T300 graphite specimen. The size and texture of the jagged peaks and "ash" structure are more similar to the epoxies than the polyimides. The "ash" level appears to be less than with the epoxies and greater than the polyimides. Also visible in the photomicrograph are lines along the walls of the jagged peaks. It is not known whether these lines correspond to the fiber direction.

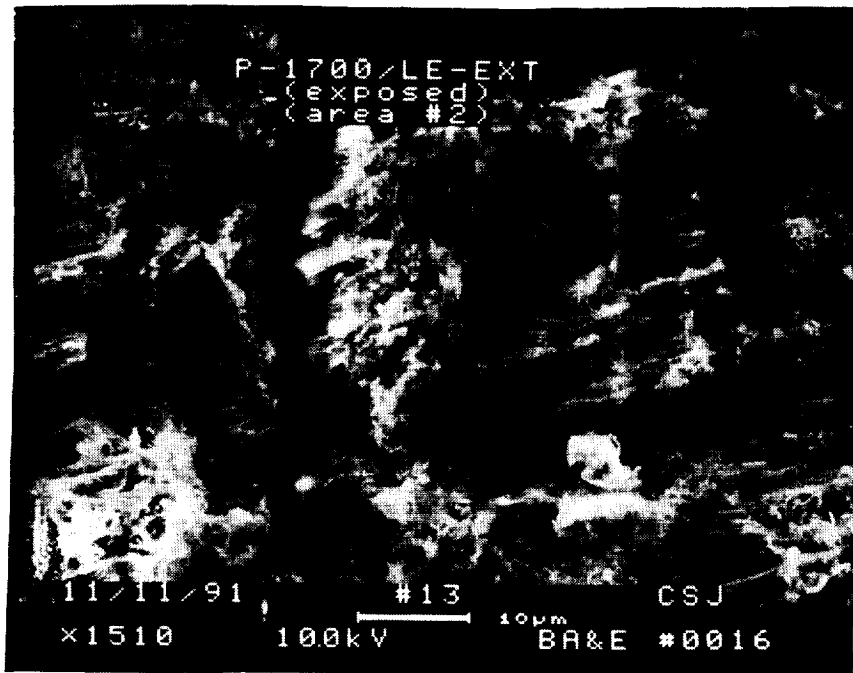


Figure 14. Scanning electron photomicrograph of leading edge exposed P1700 polysulfone/ T300 graphite surface

ORIGINAL PAGE
BLACK AND WHITE PHOTOGRAPH

The "ash" level for the PMR-15 polyimide/C6000 graphite shown in Figure 15 appears to be significantly lower than that of the epoxies. This "ash" is of a much finer texture resembling "cobwebs". Previous SEM work with LDEF specimens using metallic coatings to reduce charging did not reveal this structure for the PMR-15 polyimide.² The "ash" structure for the 934 epoxy specimens employing a metallic coating was visible and intact. This indicates that the "ash" structure for the PMR-15 polyimide is extremely delicate. The size and spacing of the jagged peaks for the PMR-15 polyimide appear larger than that of the epoxies.

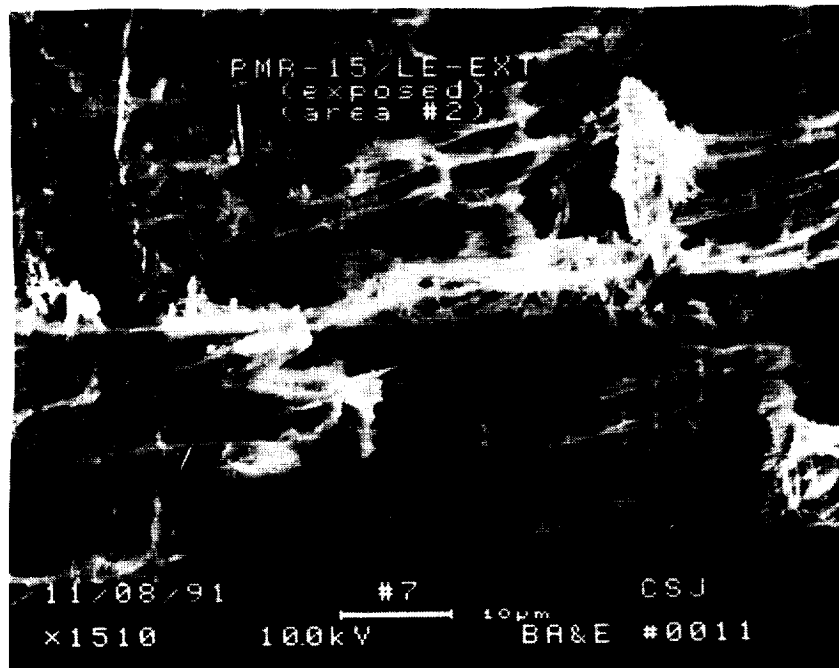


Figure 15. Scanning electron photomicrograph of leading edge exposed PMR-15 polyimide/C6000 graphite surface

Figure 16 shows the surface of a leading edge exposed LARC 160 polyimide/graphite specimen. The jagged peak size and spacing appear similar to the PMR-15 polyimide. The "ash" structure also appears similar with more "clumps" present. An area of contamination can be seen just to the left of the center. These areas were common on all leading edge exposed surfaces.



Figure 16. Scanning electron photomicrograph of leading edge exposed LARC 160 polyimide/graphite surface

ORIGINAL PAGE
BLACK AND WHITE PHOTOGRAPH

Figure 17 shows post flight infrared spectroscopy (IR) traces for material taken from two areas on the leading edge exposed surface of the 934 epoxy/T300 graphite specimen. An IR trace for the ground control specimen is also included. A Bio Rad Digilab FTS-60 fourier transform IR spectrometer equipped with a UMA 300A IR microscope was used to make all IR measurements.

Some obviously significant changes have occurred to the surface of these specimens during LEO exposure. The two leading edge exposed surface traces indicate that little if any of the original matrix material is present on the surface. Both traces are dominated by broad single peaks with various shoulders. The "long flaking coating" trace peak matches that of a silicate indicating that this material may be a contaminant. The "long flaking" appearance is consistent with that of other ubiquitous LDEF silicate contaminants.

The peak for the "particles on surface" trace is clearly shifted to the right compared to the silicate peak. This material is the "ash" seen on the surface of the exposed 934 epoxy specimen SEM photomicrographs.

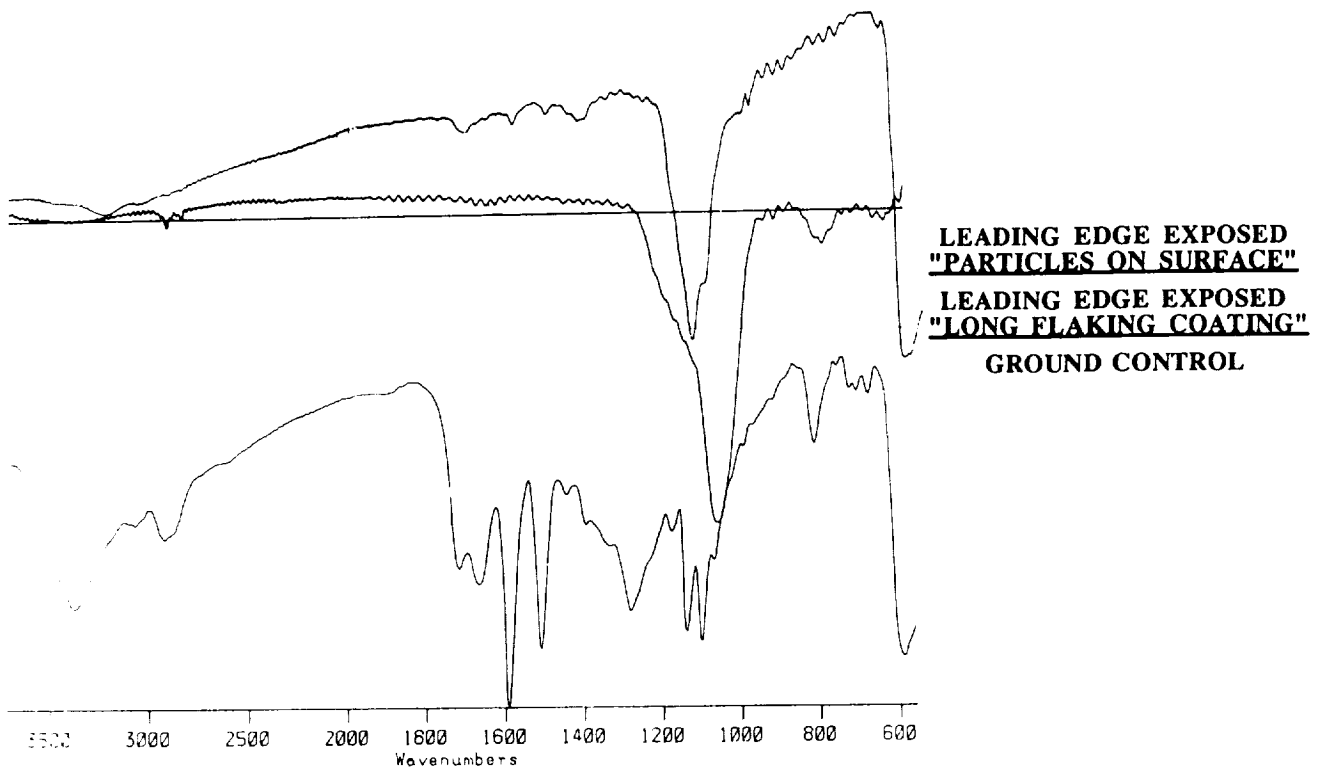


Figure 17. FTIR spectroscopy trace for 934 epoxy/T300 graphite specimens

The IR spectroscopy traces for the 3501-6 epoxy/AS graphite in Figure 18 resemble those of the 934 epoxy. The peak on the "surface scrape" trace occurring in the 1100-1200 wavenumber region matches that of the peak from the 934 epoxy "particles" trace. These peaks match the IR spectra of sodium sulfate very well as reported in earlier efforts.² The presence of a peak in this area has also been reported for 5208 epoxy/T300 graphite leading edge exposed specimens.⁴ The presence of sodium and sulfur on the 934 epoxy surface has been detected by EDX and is reported later in this paper. Also, X-ray diffraction techniques have confirmed the presence of orthorhombic crystalline sodium sulfate with a high degree of confidence for both the 934 epoxy and P1700 polysulfone composites. This suggests that sodium sulfate is present in the ash of both the 934 epoxy and P1700 polysulfone leading edge exposed specimens.

The presence of sodium sulfate on only certain polymer matrix composites suggests that contamination from other LDEF sources is improbable. One possible source of this compound is that residual sodium contamination from manufacture of graphite fiber tows is combining with sulfur from the composite matrix material curing agent to form AO resistant sodium sulfate. This may offer an explanation for the light and dark banded pattern reported for a 5208 epoxy/T300 graphite specimen flown on LDEF.⁵ The banding may be due to variations in the residual levels of sodium in or on the carbon fiber tows from the manufacturing process.

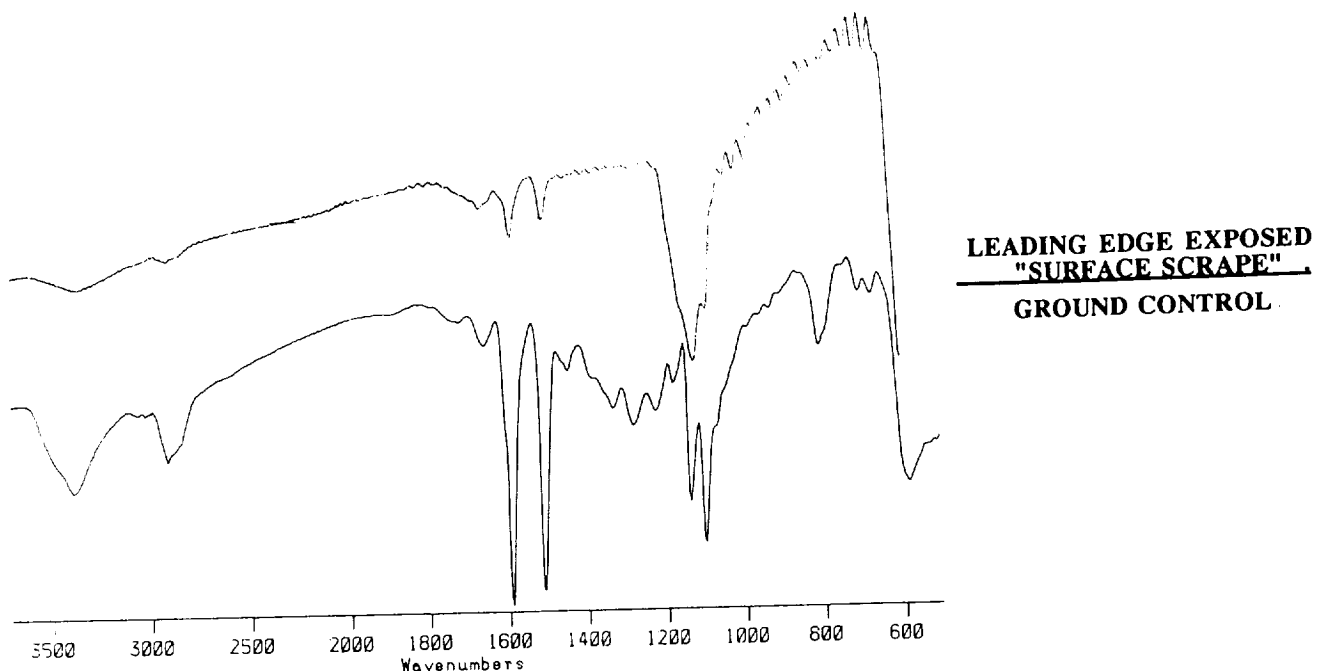


Figure 18. FTIR spectroscopy trace for 3501-6 epoxy/AS graphite specimens

The IR trace for the leading edge exposed P1700 polysulfone/T300 graphite as shown in Figure 19 also shows the presence of a broad peak in the 1100 to 1200 wave number region. Comparison to the ground control indicates that most of the matrix resin has been eroded from the surface. As mentioned previously the presence of sodium sulfate has been found on the surface of the P1700 polysulfone/T300 graphite leading edge exposed specimens using X-ray diffraction. The source of sulfur in this case may be the sulfur incorporated into the backbone of this polymer system.

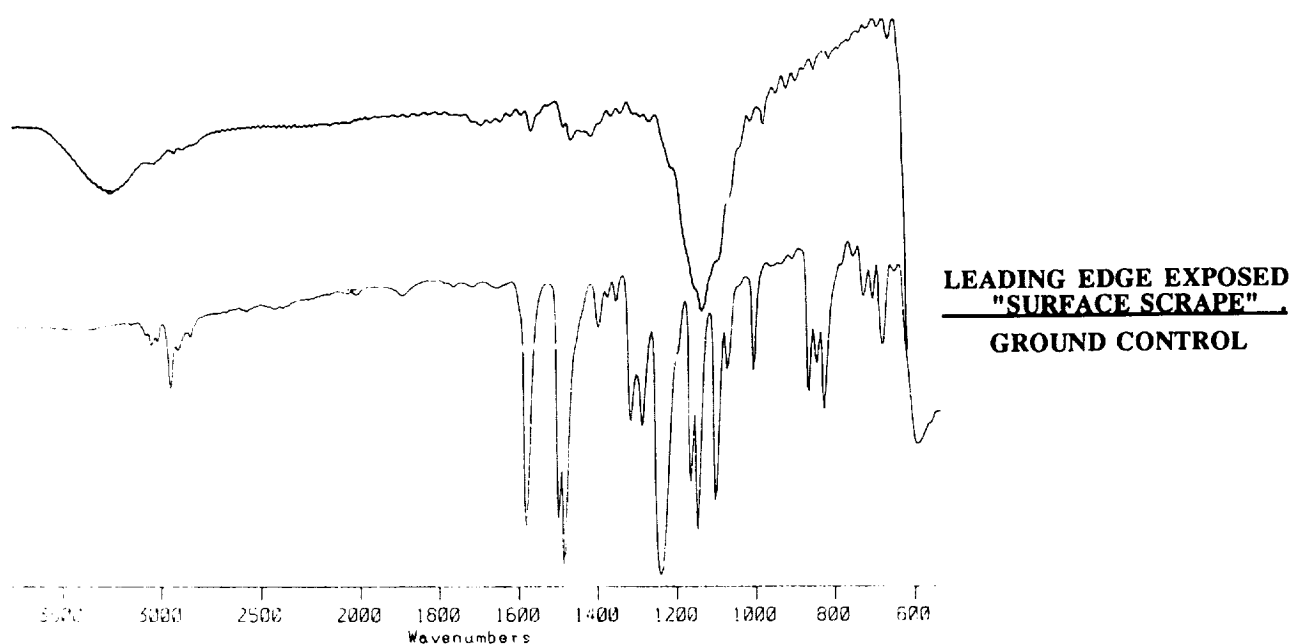


Figure 19. FTIR spectroscopy trace for P1700 polysulfone/T300 graphite specimens

Figures 20 and 21 show the IR traces for the PMR-15 polyimide/C6000 graphite and LARC160 polyimide/graphite leading edge exposed surface and ground control specimens. These spectra are very similar reflecting their similar chemistry. Unlike the epoxy and polysulfone exposed surfaces the polyimides appear to have retained more characteristic peaks for the matrix material indicating more exposed polymer remaining on the surface. The only significant differences are disappearance and/or weakening of peaks and shoulders at 1660, 1600, and 930 wave numbers from the ground control to the exposed trace. These differences were also present for the PMR-15 polyimide/C6000 graphite specimens examined from experiment M0003-8.² Changes in absorption in these bands may be attributable to changes in the carbonyl linkages between the phenyl rings.⁶ This area warrants further investigation as these changes may offer insight into the chemical breakdown mechanism of polyimides in an atomic oxygen environment.

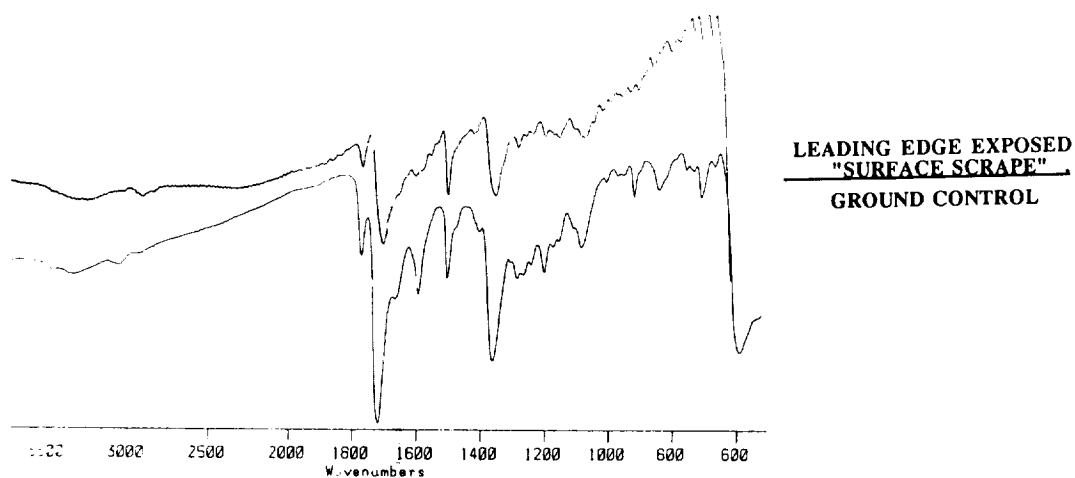


Figure 20 . FTIR spectroscopy trace for PMR-15 polyimide/C6000 graphite specimens

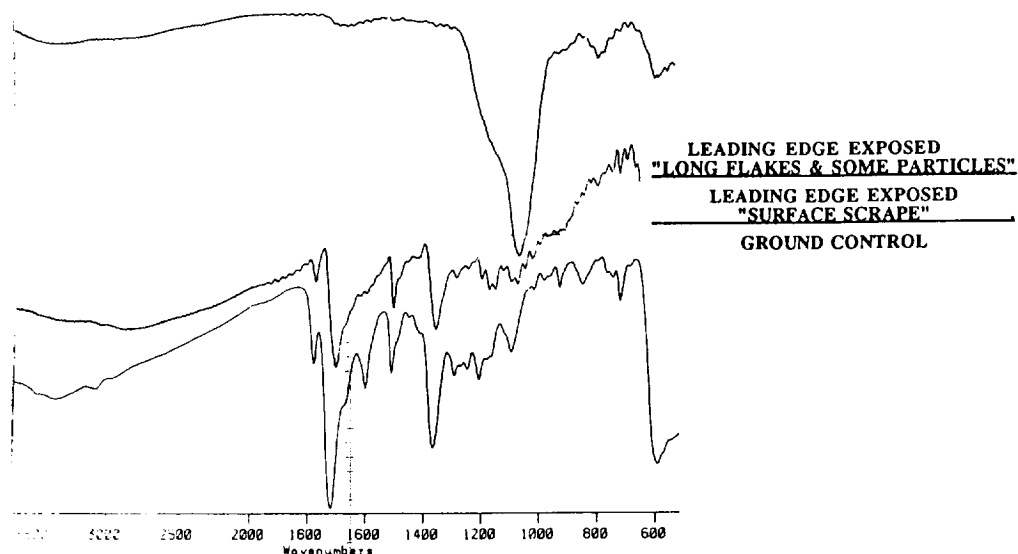


Figure 21. FTIR spectroscopy trace for LARC 160 polyimide/ graphite specimens

Energy Dispersive X-ray spectroscopy was performed on shielded, exposed and ground control specimens. Also, portions of the ground control were split open to reveal fresh material. Figure 22 summarizes the results. Contamination was found on all of the surfaces making comparison of test results difficult. However some clear trends were distinguishable.

Sulfur and silicon were present to some extent on all surfaces. The epoxy and polysulfone specimens displayed a strong presence of both sulfur and sodium on the surfaces. However, the polyimides did not have sodium present and only a trace of sulfur was found. Other than the heavy background noise associated with carbon the only distinguishable material found on the freshly exposed interior surfaces of the ground controls was silicon. This presence of silicon was extremely weak.

These test results agree with the previously mentioned findings of sodium sulfate on the surfaces of the epoxy and polysulfone specimens. The silicon contamination found on most surfaces of LDEF was also present on these specimens.

- STRONG SULFUR AND SODIUM PEAKS FOR EXPOSED LEADING EDGE SURFACE "ASH" OF EPOXIES, POLYSULFONE.
- SODIUM NOT PRESENT, SULFUR VERY WEAK FOR EXPOSED LEADING EDGE SURFACE "ASH" OF POLYIMIDES.
- SULFUR, SILICON PRESENT TO SOME EXTENT ON ALL SURFACES.
- SPECIMENS SPLIT OPEN TO REVEAL "FRESH SURFACES;" ONLY TRACE OF SILICON FOUND.

FIGURE 22. EDX TEST RESULTS

Figure 23 summarizes the test results and observations for the Boeing portion of sub experiment M0003-10. The most significant finding was the impact of atomic oxygen on mechanical properties. Thickness reductions for all the leading edge exposed composites resulted in reduced mechanical strength and modulus for a given specimen. Also, for the PMR-15 specimens with non 0 degree plies directly beneath a 0 degree surface ply an additional mechanical property reduction was observed. Atomic oxygen erosion resulted in unique surface textures which varied between composite types.

A residual "ash" material was observed for all atomic oxygen eroded surfaces. The level and texture of this "ash" varied between composite types. The epoxies and polysulfones displayed significantly higher levels of "ash" than the polyimides. This corresponded to the visual appearance and optical properties of the materials. Sodium sulfate was identified as a component of this "ash" for the epoxy and polysulfone composites. Attempts to isolate and identify the polyimide "ash" were unsuccessful due to the small quantities. Silicate contamination was found on all surfaces.

The only non atomic oxygen change identified was microcracking of multi-direction reinforced composites from the leading and trailing edge exposed positions. This indicates that the exposed specimens experienced higher thermal cycling extremes and/or thermal shock.

MECHANICAL: REDUCTION IN FLEXURAL PROPERTIES DUE TO AO EROSION

- Thickness loss for all leading edge exposed specimens
- Severe reduction in performance of PMR15/C6000 due to ply orientation

CHEMICAL: RESIDUAL ASH ON AO EXPOSED SURFACES

- Epoxy, polysulfone ash contains high levels of sulfur, possibly from DDS curing agent and sulfone respectively
- Polyimides had less ash on surface and could not be identified
- Silicates found on surfaces in form of "Flakes"

PHYSICAL: MICROCRACKING ONLY "NON AO" CHANGE DETECTED

- Relative reactivities (thickness reductions) of composites hard to compare due to local fiber volume and contamination variations
- No significant changes in glass transition temperatures, outgassing or thermal expansion properties.
- Microcracking occurred in multi-direction reinforced laminates
- Level of microcracking varied with severity of temperature fluctuations

FIGURE 23. SUMMARY

The author would like to acknowledge the following persons for their invaluable assistance: S. G. Hill, H. G. Pippin and H. W. Dursch of the Composites and Adhesives Group of Boeing Defense and Space; W. L. Plagemann and D. B. Skoropinski of the Analytical Engineering Group of Boeing Defense and Space; and E. R. Crutcher of the Image and Particle Analysis Group of Boeing Defense and Space.

REFERENCES

1. Bourassa, R.J.; Atomic Oxygen and Ultra Violet Radiation Mission Total Exposures for LDEF Experiments. First LDEF Post-Retrieval Symposium, NASA CP-3134, Feb.1992.
2. George, P. E., and Hill, S. H.; Results From Analysis of Boeing Composite Specimens Flown on LDEF Experiment M0003-8. First LDEF Post-Retrieval Symposium, NASA CP-3134, Feb.1992.
3. Tennyson, R.C., Mabson, G.E., Morison, W. D., and Klieman, J.; Preliminary Results From the LDEF UTIAS Composite Materials Experiment. First LDEF Post-Retrieval Symposium, NASA CP-3134, Feb.1992.
4. Steckel, G. L., and Le, T. D.; M0003-10: LDEF Advanced Composites Experiment. First LDEF Post-Retrieval Symposium, NASA CP-3134, Feb.1992.
5. Young, P.R.; Slemper, W.S.; Witt, W.G. Jr; and Shen, J. Y.: Characterization of selected LDEF Polymer Matrix Resin Composite Materials; 36th International SAMPE Symposium, April, 1991.
6. Young, P. R., and Chang, A. C. ; FTIR Characterization of Thermally Cycled PMR-15 Composites. 33rd International SAMPE Symposium proceedings. March 7-10, 1988.

ADDITIONAL RESULTS ON SPACE ENVIRONMENTAL EFFECTS ON
POLYMER MATRIX COMPOSITES — EXPERIMENT AO180

R. C. Tennyson
University of Toronto Institute for Aerospace Studies
Toronto, Ontario, Canada
M3H 5T6

ABSTRACT

This report presents additional experimental results on the atomic oxygen erosion of boron, Kevlar® and graphite fiber reinforced epoxy matrix composites. Damage of composite laminates due to micrometeoroid /debris impacts is also examined with particular emphasis on the relationship between damage area and actual hole size due to particle penetration. Special attention is given to one micrometeoroid impact on an aluminum base plate which resulted in ejecta visible on an adjoining vertical flange structure.

EROSION OF POLYMER MATRIX COMPOSITES

Experiment AO180 was located at station D-12 on LDEF, about 82° relative to its velocity vector. NASA estimates the atomic oxygen (AO) fluence at $\sim 1.2 \times 10^{21}$ atoms/cm² and the total equivalent sun hours of VUV radiation at ~ 6900 hours. It should be noted that the erosion data presented may well result from combined AO/VUV exposure. However, at the present time, the possible synergistic effects cannot be separated.

BORON/EPOXY LAMINATES (SP-290)

The erosion of boron/epoxy laminates was restricted to the outer epoxy layer. Figure 1 shows a comparison of the unexposed (a) and exposed (b) areas, where it is evident that loss of the outer epoxy layer reveals the woven glass fiber cloth (used as a binder material) and the unidirectional boron (coating over tungsten) fibers. Cross-sectional views (Figure 2) show the outer resin layer, glass fibers and composition of the reinforcing 'boron' fiber with its tungsten core. Figure 3 presents a similar view including the AO erosion profiles of the epoxy layer. For a tube structure, the erosion angle varies with circumferential position around the tube, as demonstrated by the results plotted in Figure 4. Finally, close-up examination of the boron fibers exposed to AO reveals a grain structure (Figure 5) that has formed in the boron coating, although no loss of boron material due to erosion was observed. The combination of boron reinforcing fibers overlaid with glass fiber scrim cloth yields a laminate that is significantly less sensitive to AO erosion than graphite and Kevlar® reinforcements.

KEVLAR®/EPOXY LAMINATES (SP-328)

Kevlar®/epoxy flat plate laminates were mounted on the exterior of the UTIAS LDEF experiment. The schematic shown in Figure 6 illustrates a shadow region (A) adjacent to an aluminum (Al) end tab, the outer exposed face (B) and erosion areas (C) on the bottom face (D) which resulted from AO reflection off cylindrical aluminum end fixtures mounted on adjacent tube specimens. Figure 7 presents SEM photographs of two unexposed regions, A and D. These can be compared to the AO erosion surface morphologies found in the exposed areas, B and C. The fibrous nature of the eroded Kevlar® is clearly evident in B, with C more typical of non-directional AO attack on the outer resin layer. Note the difference in texture of the Kevlar® fibers between B and C. In photograph B, the outer epoxy layer is gone and only the partially eroded Kevlar® fibers in the first layer remain.

GRAPHITE/EPOXY LAMINATES

The surface erosion morphology observed on graphite/epoxy laminates due to AO is shown in Figure 8 for a 90°, 4 ply tube (934/T300). When viewing the cross-section of a laminate, one finds that the AO fluence at station D-12 was sufficient to erode the outer epoxy layer and a portion of the reinforcing graphite fibers. Figure 9 presents SEM photographs of unexposed and exposed regions for a (±43°)_{4s} tube (SP288/T300). Erosion of the graphite fibers is clearly evident.

XPS measurements have also been made on the surface composition of a graphite/epoxy flat plate laminate (934/T300).* Comparing "unexposed" with "exposed" surface data (Table I), it is interesting to note a substantial reduction in the C-O content and a large increase in the O composition on the exposed surface. Furthermore, the exposed region also exhibits a large increase in the Si content, probably due to contamination.

TABLE I. APPROXIMATE ATOM % SURFACE COMPOSITION OF GRAPHITE/EPOXY COMPOSITE (934/T300) FROM LDEF AS MEASURED BY XPS

Sample	C			O	N	Na	Si	S
	C=O	C-O	CH					
Unexposed								
#1	5.8	19.0	41.3	23.3	4.4	0.4	3.6	2.2
#2	6.7	16.0	41.8	25.7	3.8	0.5	4.3	1.2
Exposed								
#1	4.6	6.2	38.9	34.0	1.8	0.5	13.0	0.9
#2	4.0	6.6	42.1	32.1	1.7	0.9	11.8	0.6

Courtesy: T. Wittberg, Research Institute
Nonmetallic Materials Division
University of Dayton

* Courtesy of T. Wittberg, Research Institute, Nonmetallic Materials Division, University of Dayton.

MICROMETEOROID/DEBRIS IMPACTS

Micrometeoroid Impact on Aluminum Support Structure

The largest impact found on experiment AO180 occurred on an aluminum base plate, with an ejecta splash observed on an adjacent flange structure (Figure 10). A view of the 1 mm diameter crater is shown in Figure 11. EDS spectra of the crater rim material composition (Figure 12) exhibits a strong Fe peak along with the Al substrate. Based on this evidence it is assumed that the crater resulted from a micrometeoroid impact. Figure 13 contains a SEM photograph of the surface ejecta splash pattern on the flange structure. Details of the different splash patterns in this region are shown in Figure 14. An aluminum ejecta particle, visible in Figure 14, is enlarged in Figure 15 and Figure 16 (lower photograph). Figure 16 presents two different forms of aluminum ejecta particles and their associated splash patterns. The lower photograph shows the remnants of a molten particle while the upper photograph shows the full spherical form of an aluminum particle.

Impact Damage on Composite Laminates

Micrometeoroid/debris impacts on polymer matrix composites do not produce the typical hemispherical craters found on metallic structures. Rather, because of the brittle nature of the resin matrix, one generally finds penetration holes with adjacent surface damage, some internal ply delamination and local fiber fractures. For brittle fibers such as graphite, the impact and exit holes exhibit brittle fiber fractures such as shown in Figure 17. On the other hand, tough non-brittle fibers such as aramid fail in a "brush or broom" mode surrounding the impact damage region. Figure 18 presents four impacts on a single Kevlar®/epoxy tube [SP-328, (± 45)_{4s}]. Enlargements of the damage areas are given in Figure 19 where it can be seen that three penetrations occurred with one grazing (or low energy) impact that produced only local surface damage. Note the fiber failure mode in photo 4. From the enlargements, it was possible to scan the images to calculate the surface damage area and impact hole size. Using an image enhancement backlighting technique that works well on translucent materials, one can also estimate the penetration depth of the impacting particle. Figure 20 presents the images and data obtained for these four impact sites. At this point in time, only 10 impact sites (out of 84) have been found on the composite samples, a summary of which is given in Table II with estimates of surface damage area, hole size and penetration. Such data will be useful for estimating total damage on composite structures that arises from micrometeoroids/debris.

TABLE II. SUMMARY OF IMPACT FEATURES ON COMPOSITE SPECIMENS
(EXPERIMENT AO 180)

Material Type	Sample Type	Number of Plies	Sample No.	Surface Damage Area (mm ²)	Hole Area (mm ²)	Particle Penetration Depth (Number of plies)
Graphite/Epoxy (T300/5208)	Plate	4		0.222	0.222	>4
Graphite/Epoxy (SP 288/T300)	Tube	4	1T10	1.064	0.083	>4
Aramid* Fiber/Epoxy (SP 328)	Tube	4	2T2	1.162	0.036	1 - 2
"	Tube	4	2T4	0.498	0.015	-1
"	Tube	4	2T11	0.423	0.018	-1
"	Tube	4	2T16	1.253	0.076	2 - 3
"	Tube	4	2T17(1)	0.223	—	1 - 2
			2T17(2)	1.445	0.033	2 - 3
			2T17(3)	0.370	—	-1
			2T17(4)	0.881	0.020	2 - 3

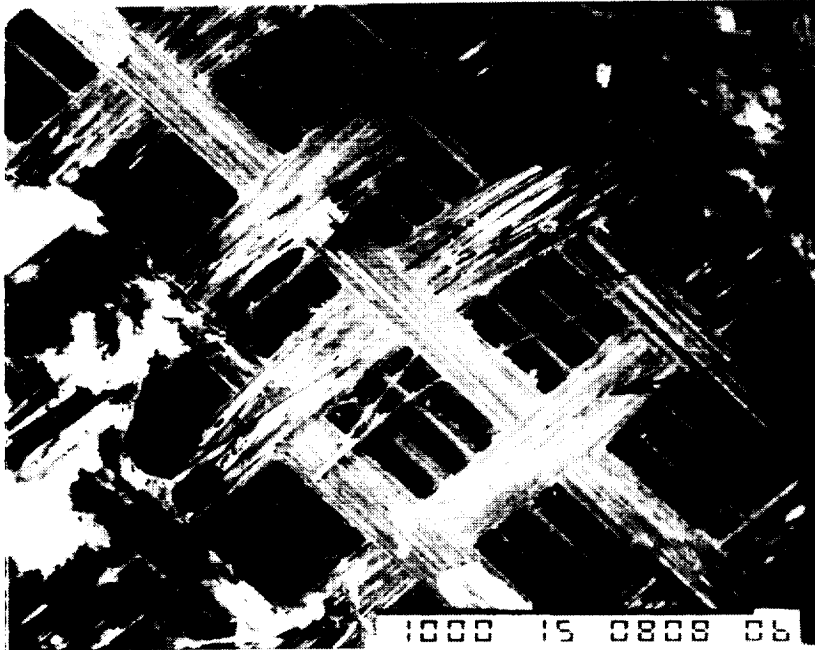
*Kevlar

(a)



Epoxy Layer

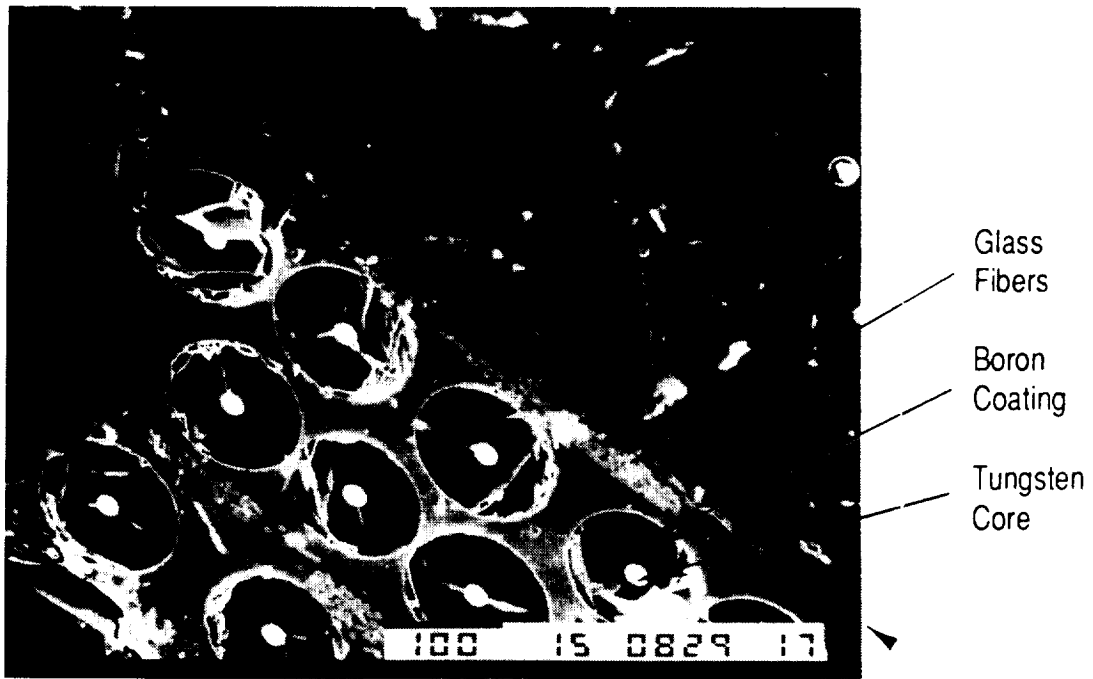
(b)



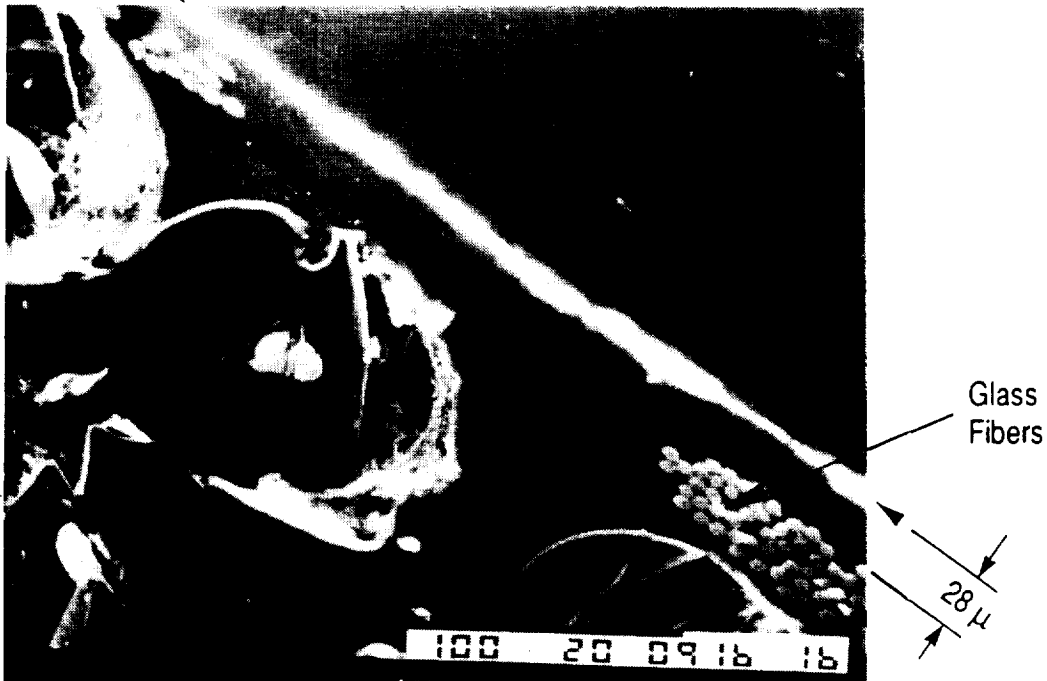
B/W Fiber

Glass Fibers

Fig. 1 SEM Photographs of Boron/Epoxy Tube Surface [SP-290, $(\pm 45^\circ)_4S$] (a) Unexposed (x50), (b) Exposed to Atomic Oxygen (x50)



(x150)



(x350)

Fig. 2 SEM Photographs of Cross-Section of Unexposed Boron/Epoxy Tube [SP-290, $(\pm 45^\circ)_{4S}$]. (Arrows delineate boundary between outer epoxy layer and potting compound)

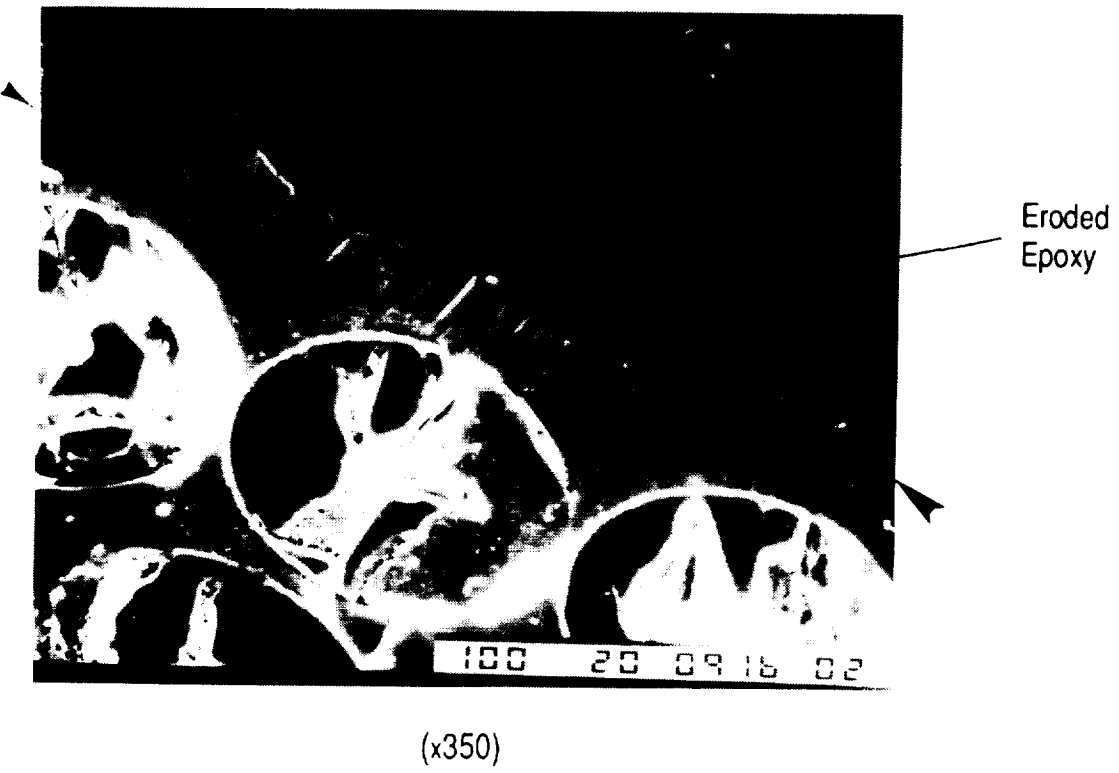
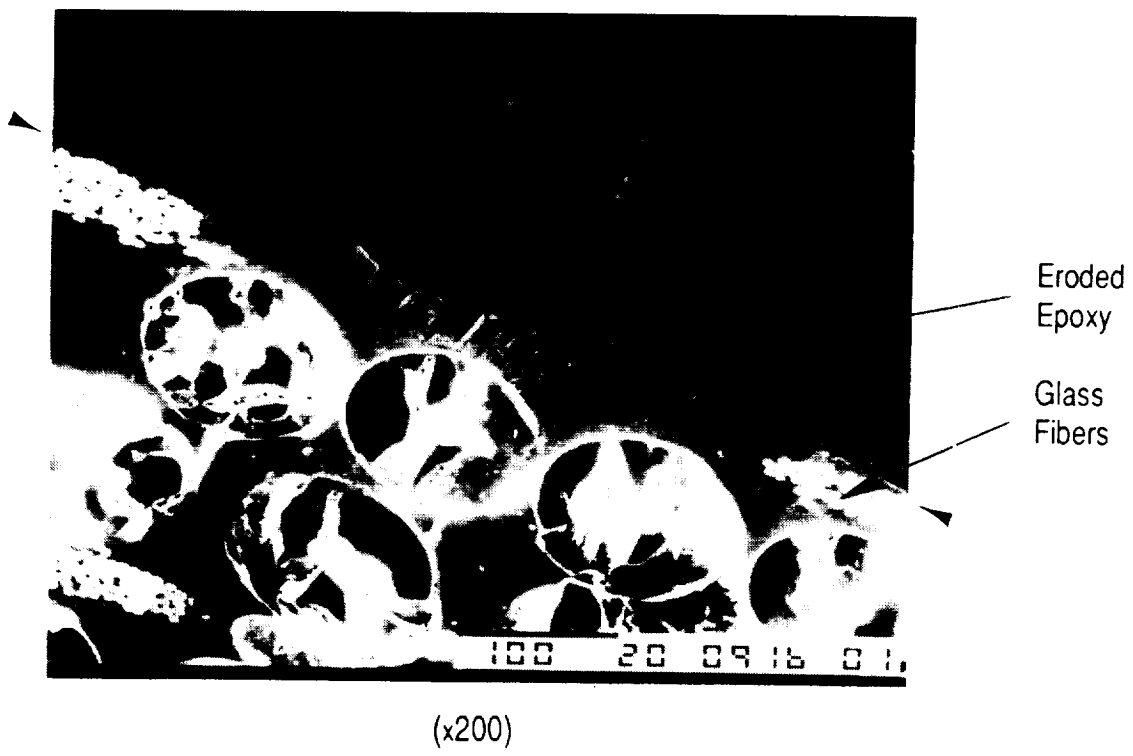


Fig. 3 SEM Photographs of Eroded Cross-Section of Boron/Epoxy Tube [SP-290, ($\pm 45^\circ$)_{4S}] Exposed to Atomic Oxygen. (Arrows delineate boundary between outer epoxy layer and potting compound)

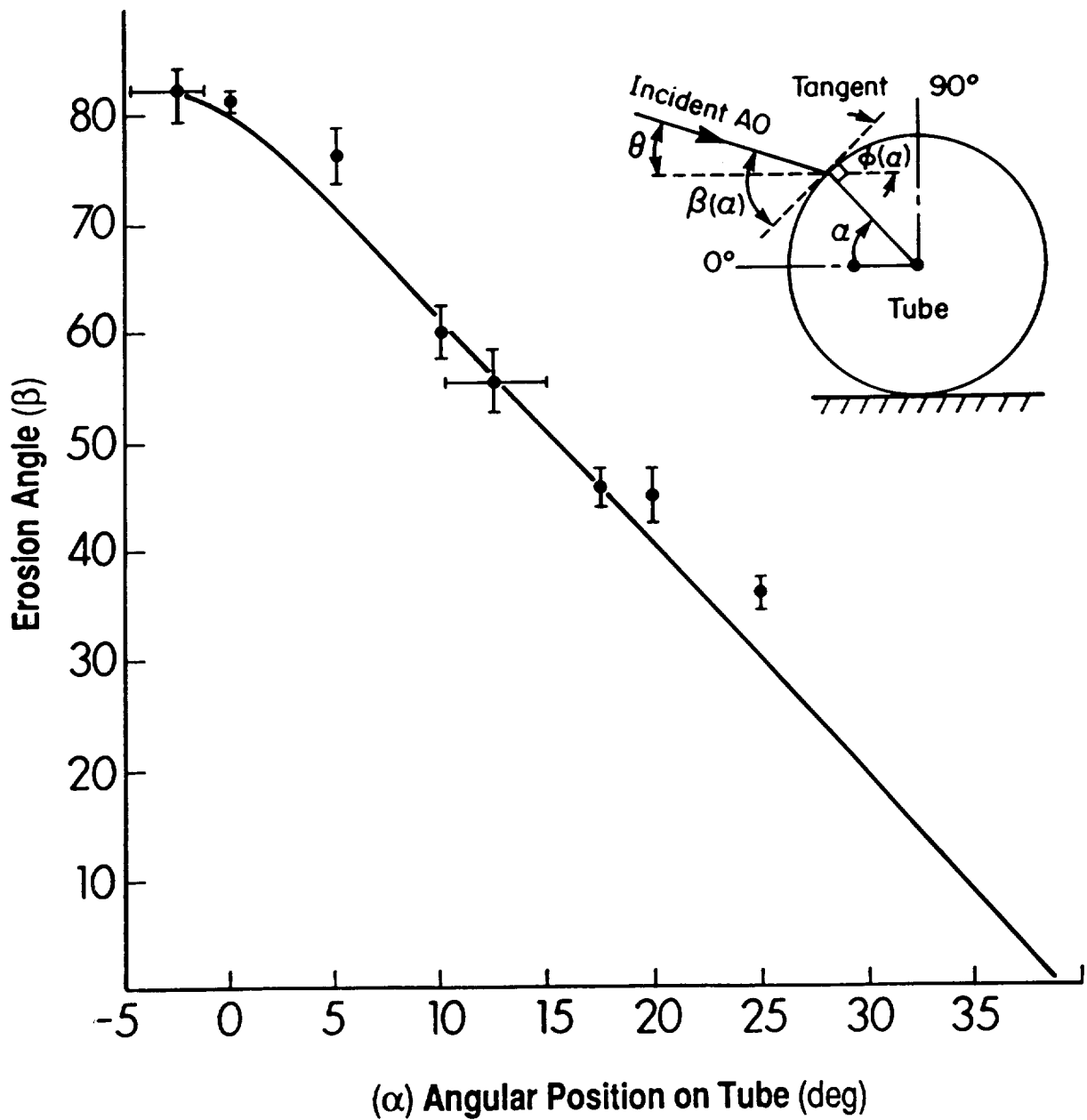


Fig. 4 Variation in Erosion Angle (β) with Angular Position (α) around Boron/Epoxy Tube [SP-290, ($\pm 45^\circ$)_{4S}]

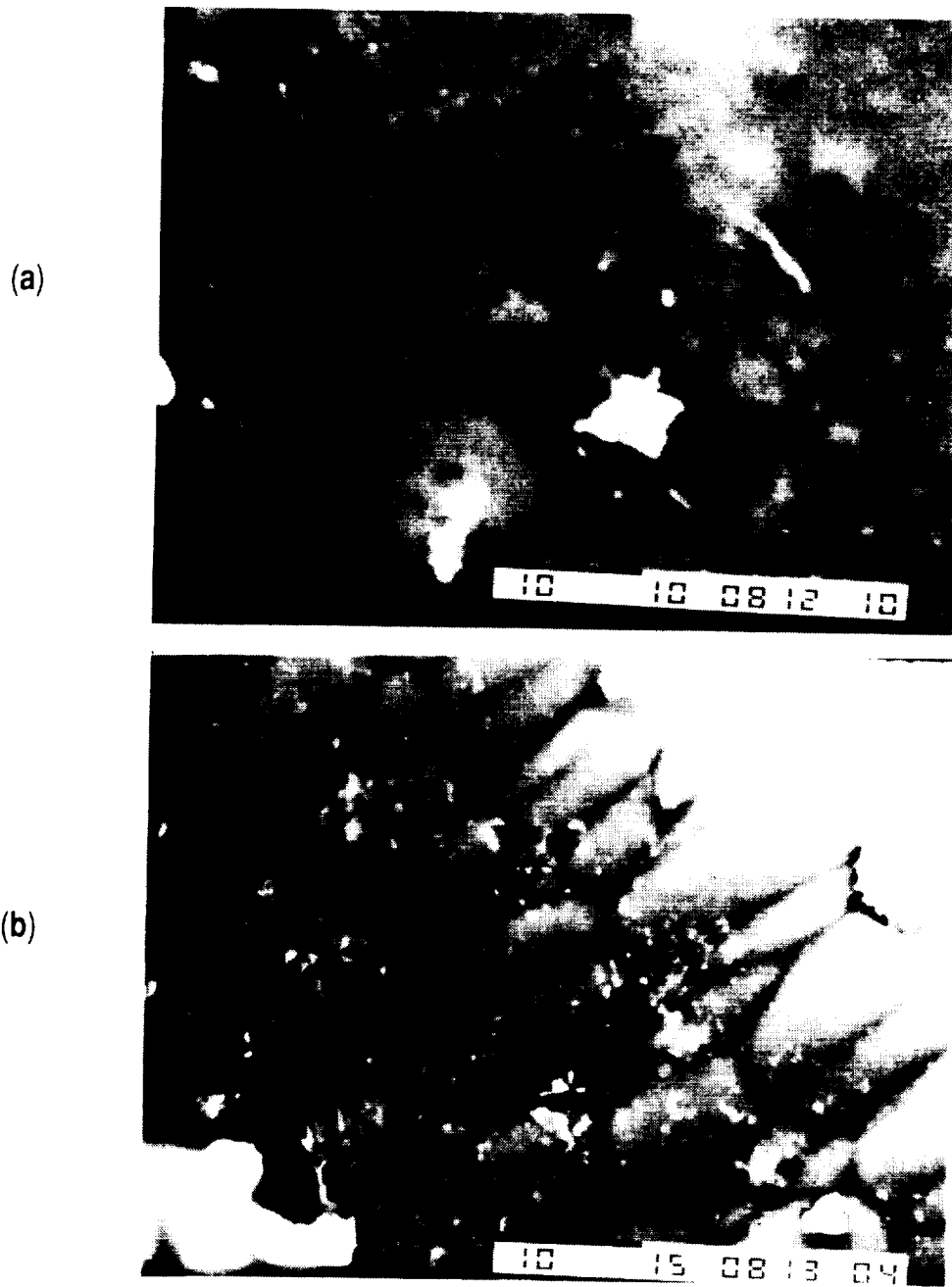


Fig. 5 SEM Photographs of the surface texture of a B/W fiber in a Boron/Epoxy Tube [SP-290, $(\pm 45^\circ)_{4S}$] (a) Unexposed (x2000), (b) Exposed to Atomic Oxygen (x2000)

ORIGINAL PAGE
BLACK AND WHITE PHOTOGRAPH

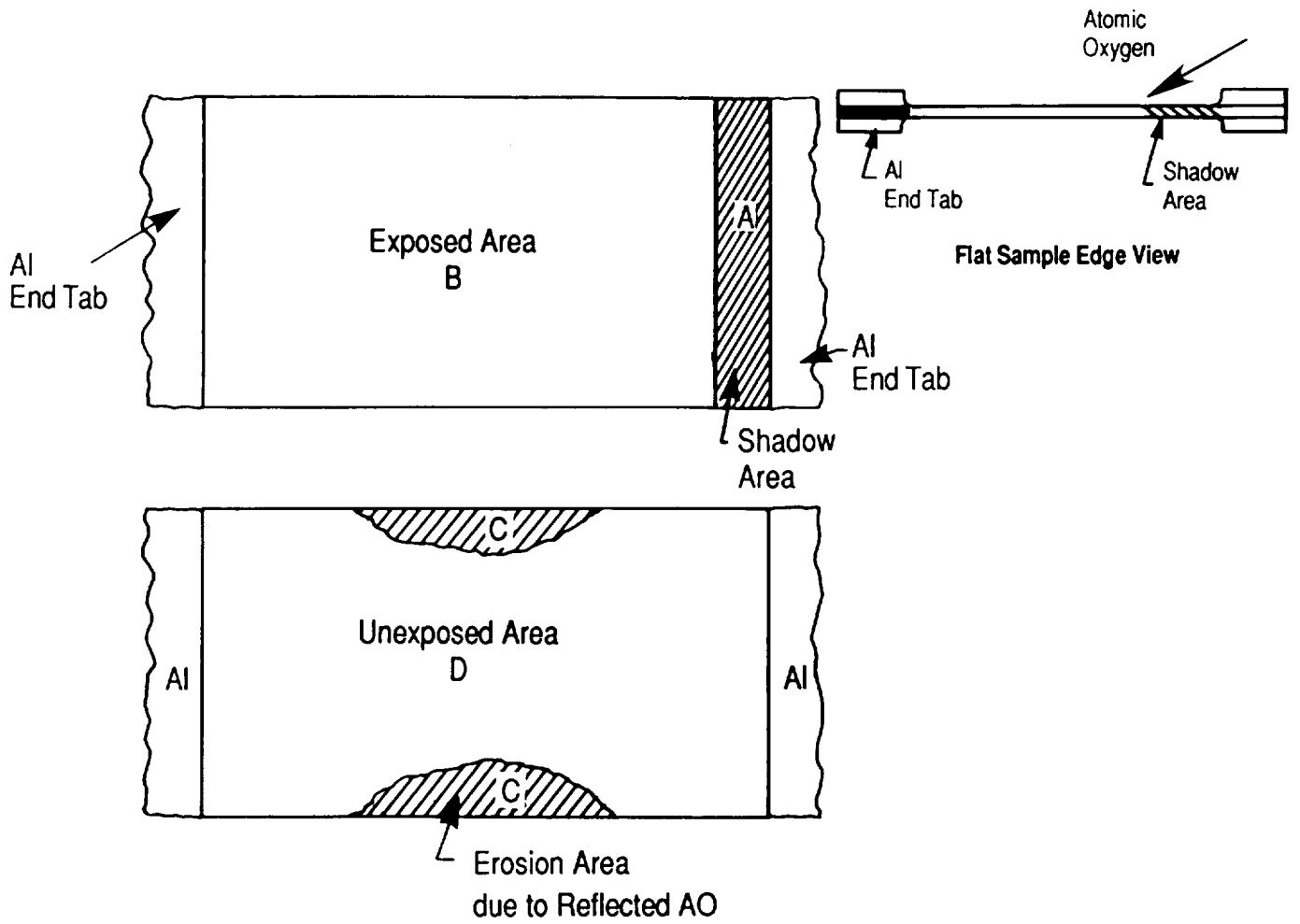


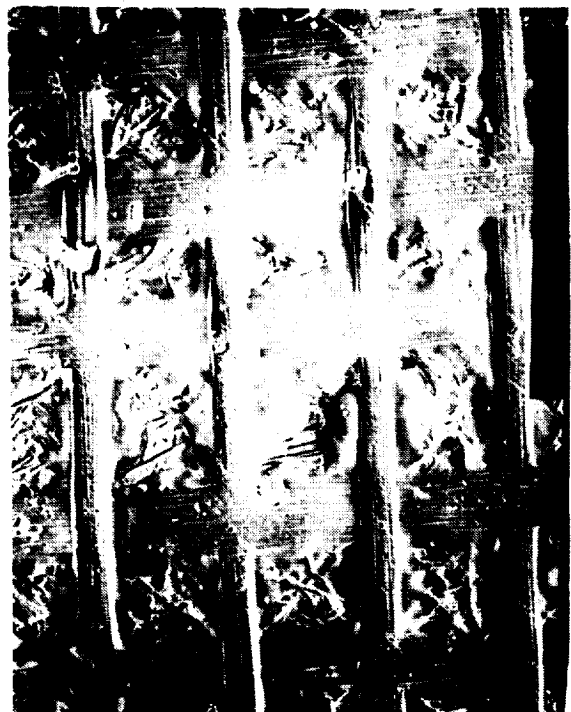
Fig. 6 Kevlar®/Epoxy (SP-328) Flat Plate Laminate



Exposed Area B (x750)



Erosion Area C (x750)



Shadow Area A (x50)



Unexposed Area D (x50)

Fig. 7 SEM Photographs of Kevlar®/Epoxy Laminate [SP-328, ($\pm 43^\circ$)_{4S}]



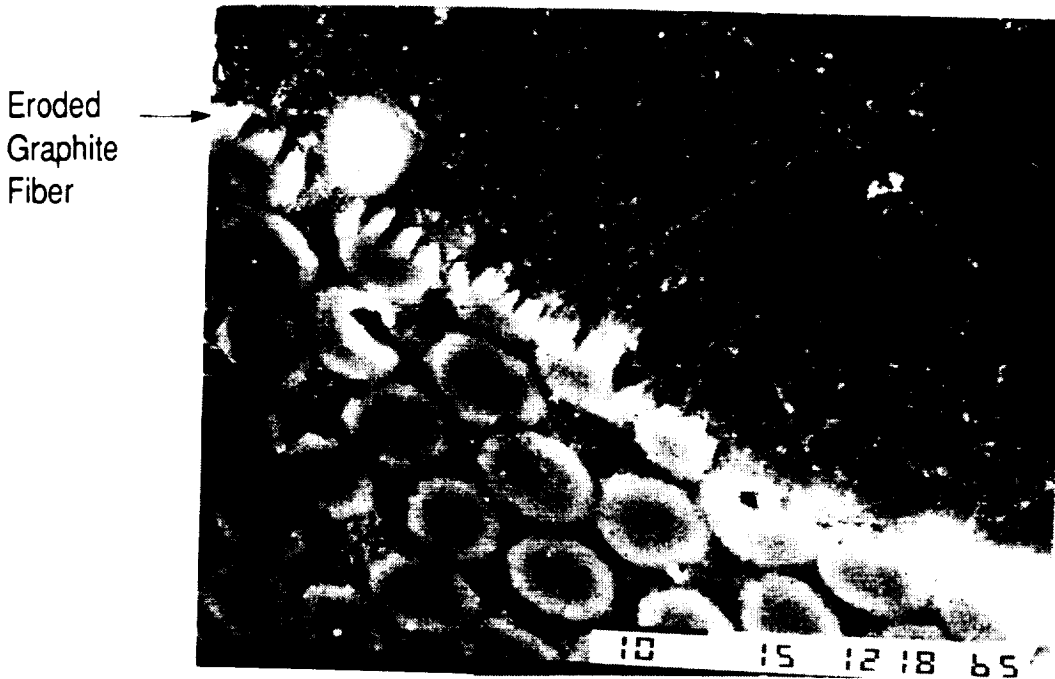
Fig. 8 SEM Photograph of Surface Morphology on Exposed Graphite/Epoxy Tube [934/T300, (90°)_{4S}]

ORIGINAL IMAGE
BLACK AND WHITE PHOTOGRAPH

ORIGINAL IMAGE
BLACK AND WHITE PHOTOGRAPH



Unexposed Region



Exposed Region

Fig. 9 SEM Cross-Sectional Photographs of Graphite/Epoxy Tube Subjected to AO Erosion [SP-288/T300, ($\pm 43^\circ$)_{4S}]

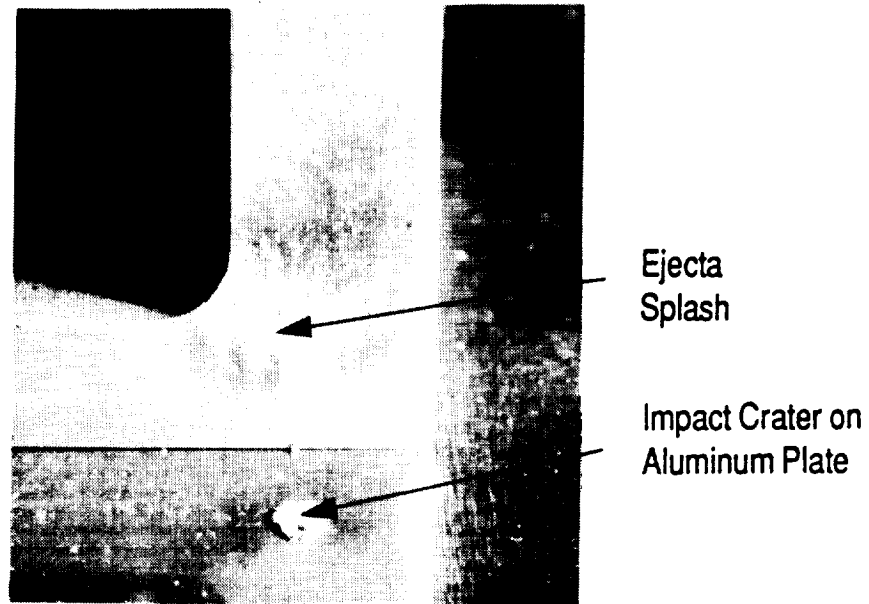


Fig. 10 View of Micrometeoroid Impact Crater and Ejecta Splash Pattern on Adjacent Vertical Flange Structure

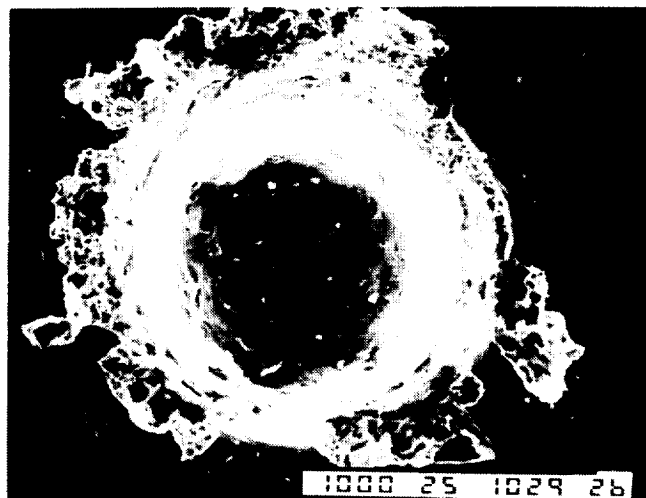
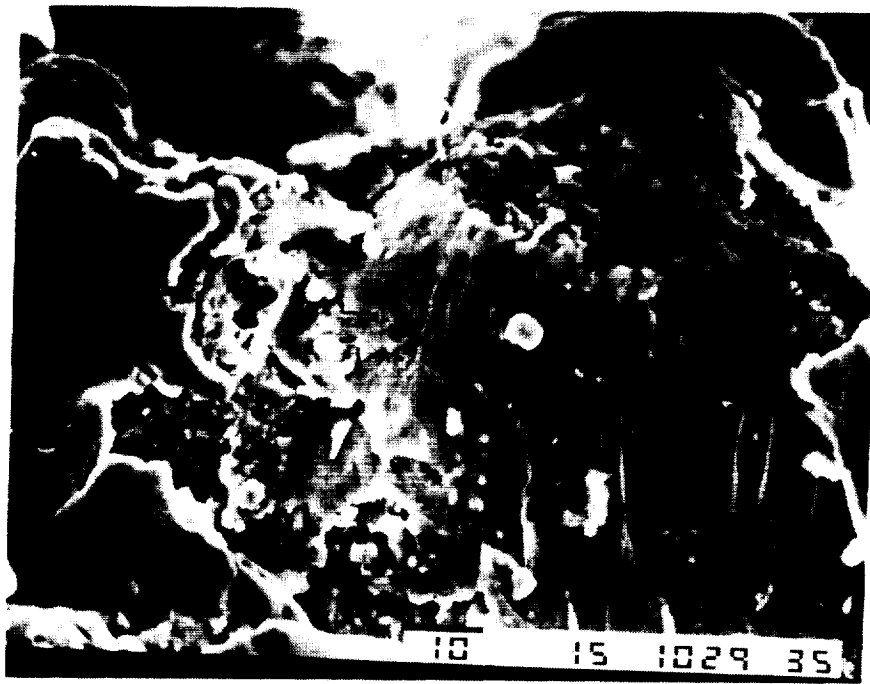


Fig. 11 View of Micrometeoroid Crater on Aluminum Base Plate



Crater
Rim
Ejecta

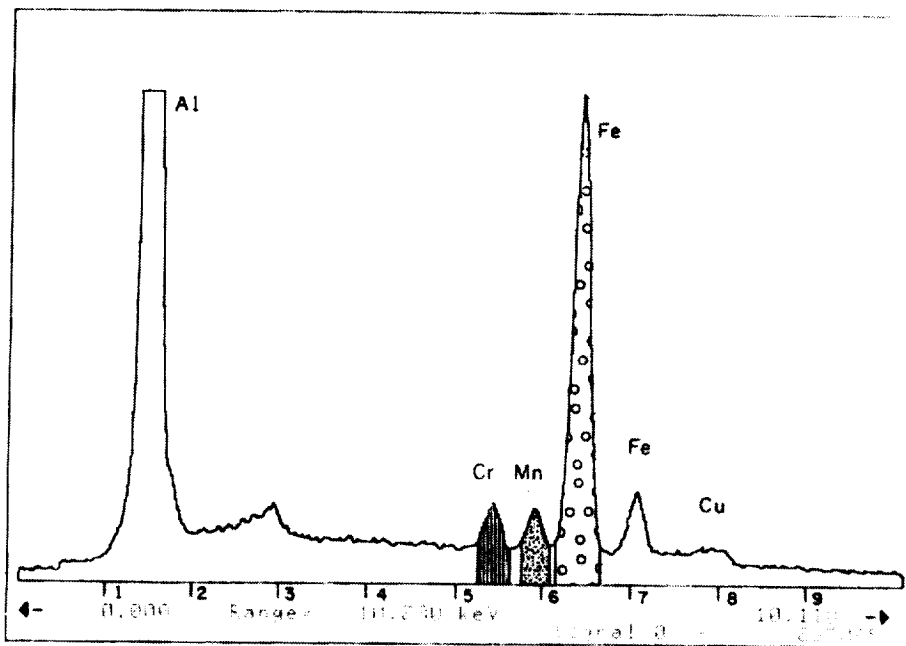


Fig. 12 Crater Ejecta and Elemental Composition (EDS Spectra)

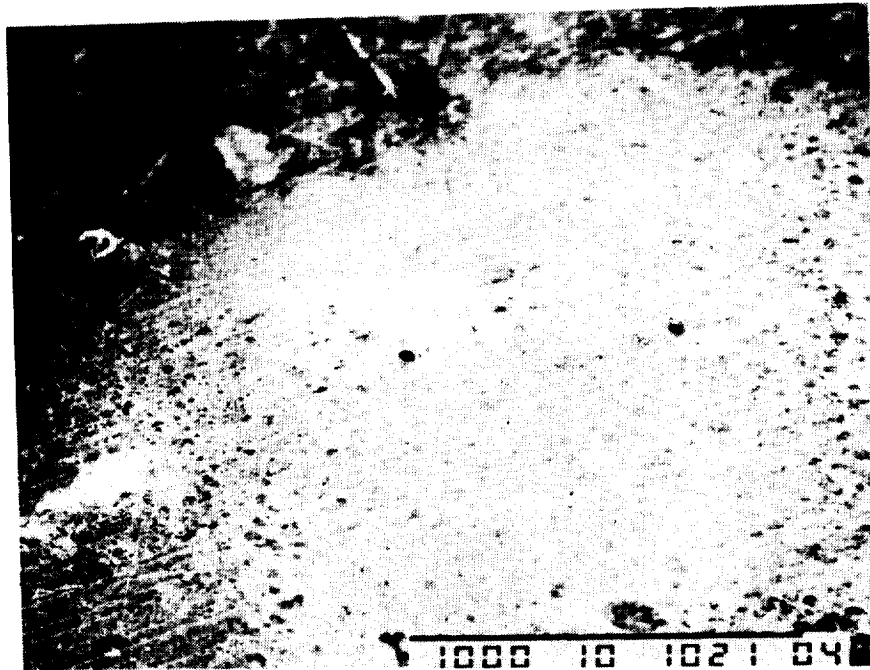
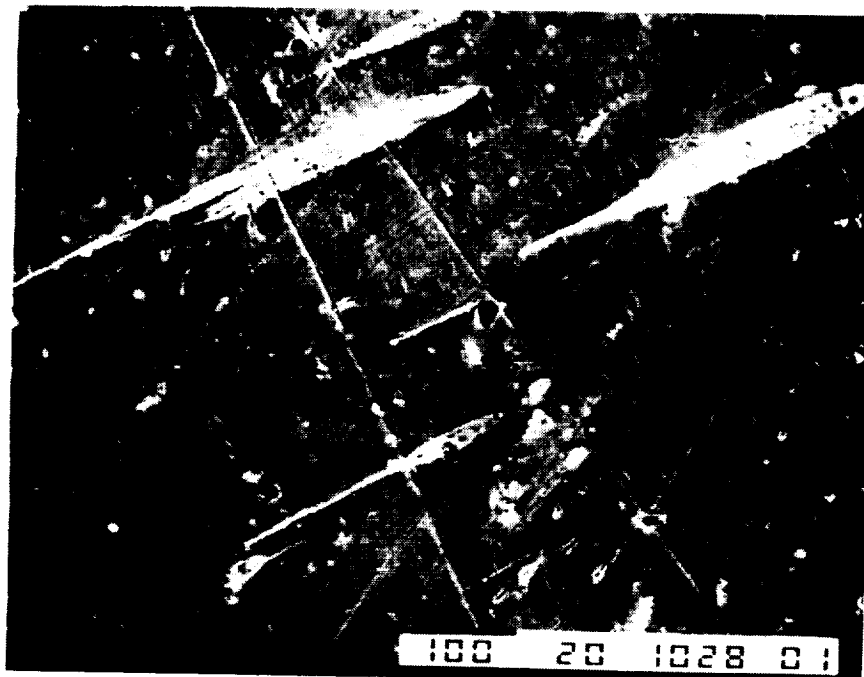
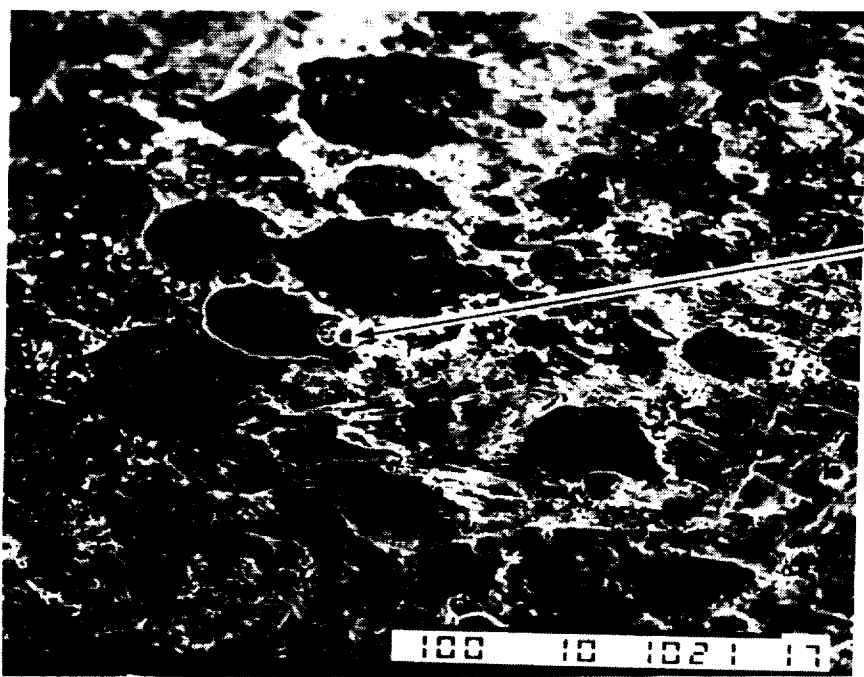


Fig. 13 Ejecta Splash Pattern on Vertical Flange Structure Adjacent to Crater

ORIGINAL PAGE
BLACK AND WHITE PHOTOGRAPH



Splash
Pattern



Al Particle and its
Splash Pattern

Fig. 14 Different Splash Patterns formed by Ejecta from Micrometeoroid Impact

ORIGINAL PAGE
BLACK AND WHITE PHOTOGRAPH

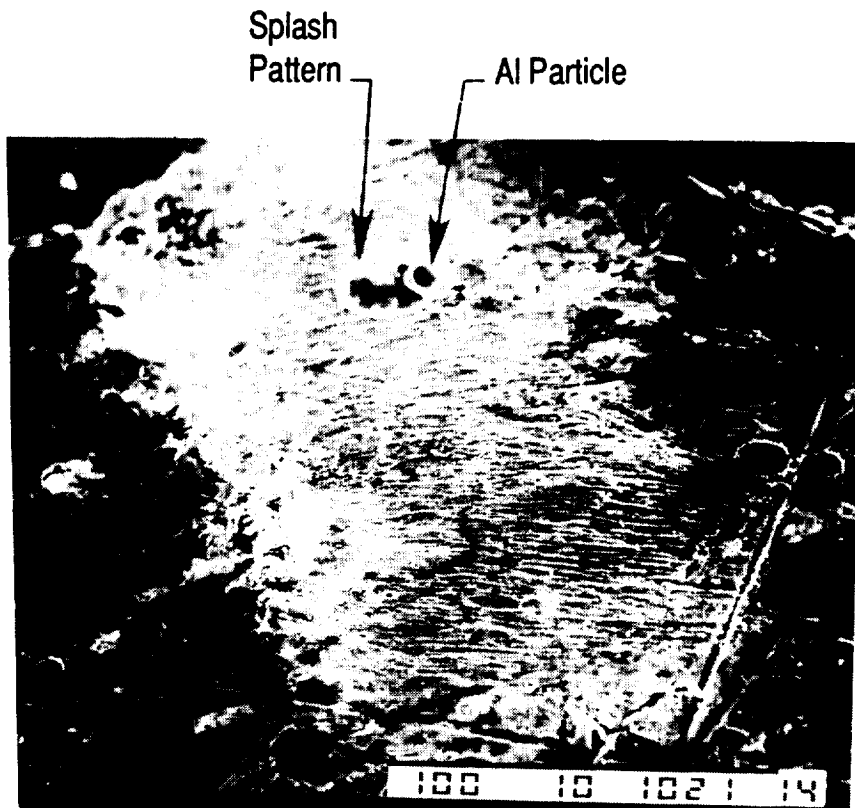


Fig. 15 Superposition of Aluminum Ejecta Particle on Splash Pattern

ORIGINAL PAGE
BLACK AND WHITE PHOTOGRAPH

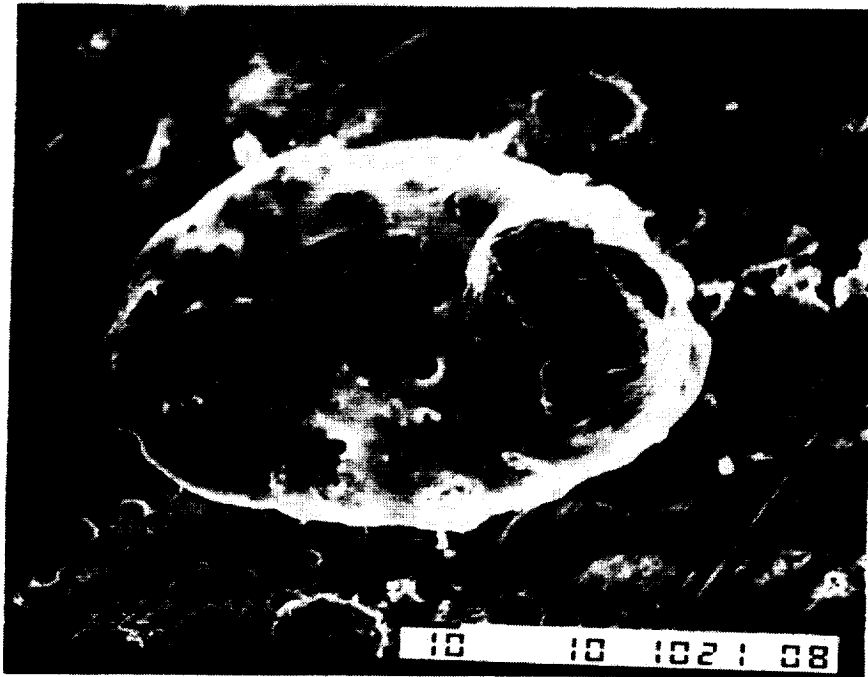
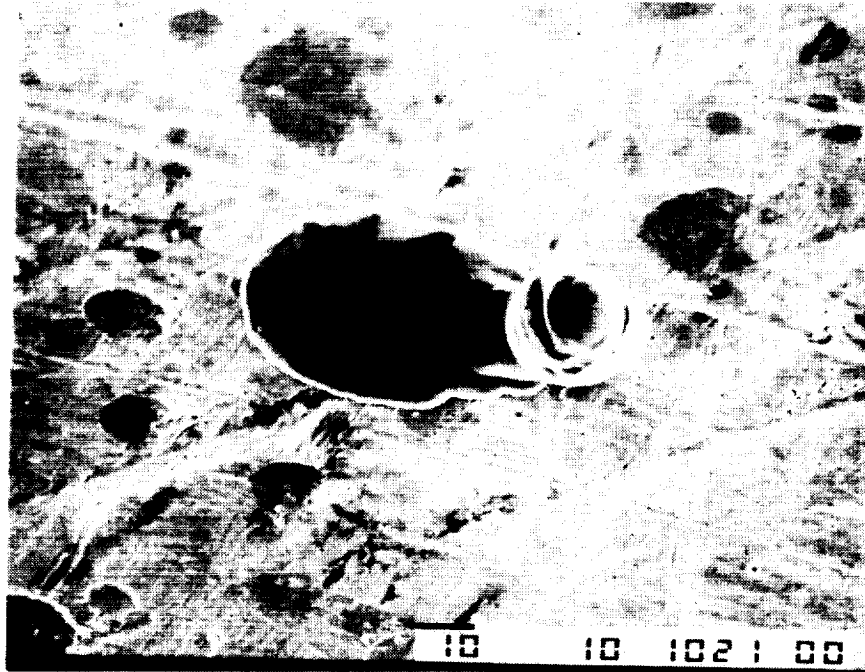
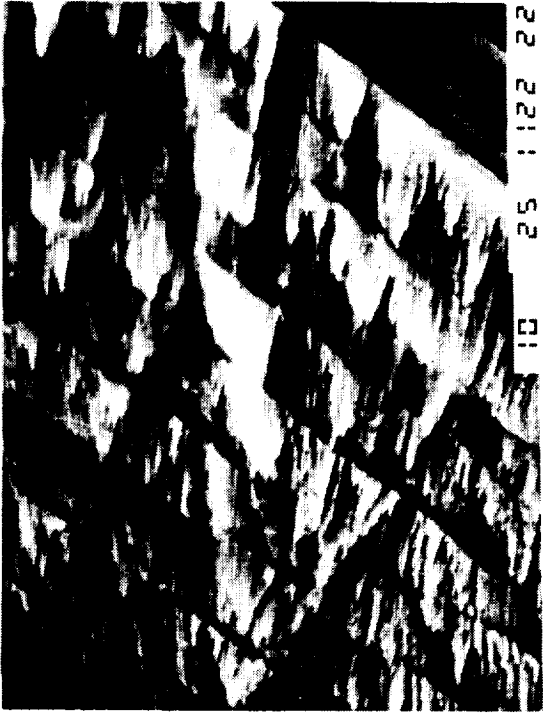


Fig. 16 Aluminum Ejecta Particles with Associated Splash Patterns

ORIGINAL PAGE
BLACK AND WHITE PHOTOGRAPH



Impact Hole - Exposed Surface
(x100)

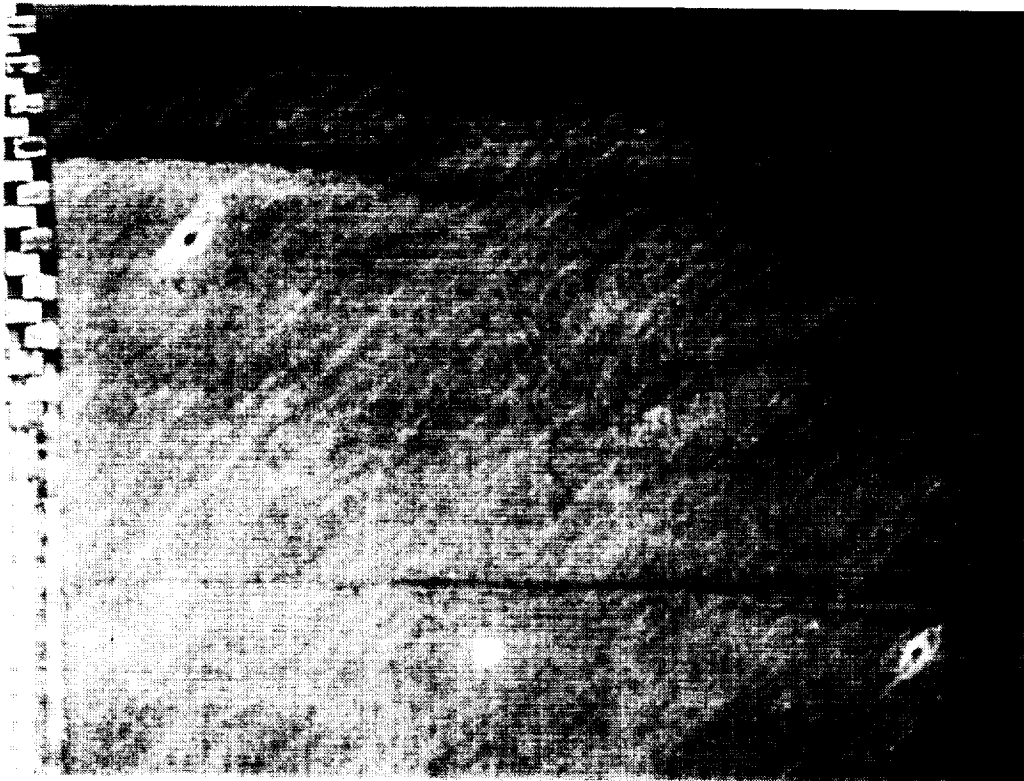
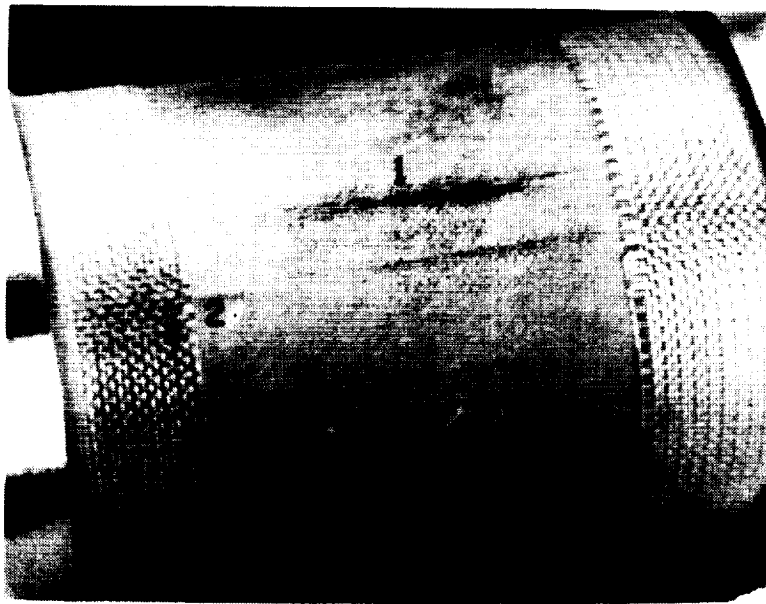


AO Erosion Morphology
(x1500)



Exit Hole on
Inside Tube Wall
(x75)

Fig. 17 SEM Photographs of Micrometeoroid/Debris Impact/Exit Holes and AO Erosion Morphology for Graphite/Epoxy Tube [SP-288/T300, ($\pm 43^\circ$)_{4S}]



(x5)

Fig. 18 Micrometeoroid/Debris Impacts on Kevlar®/Epoxy Tube [SP-328, ($\pm 45^\circ$)_{4S}]



1



2

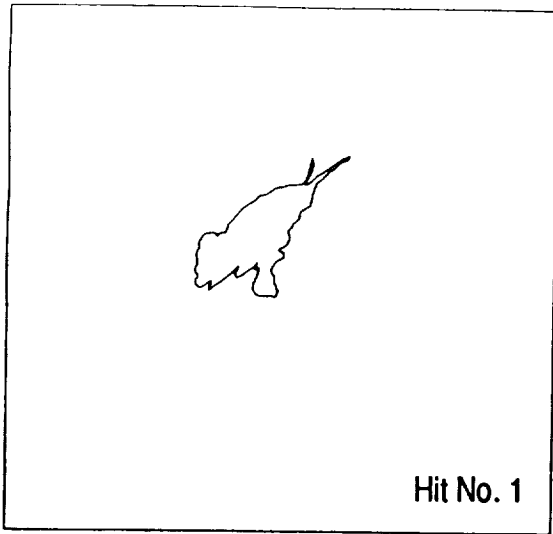


3



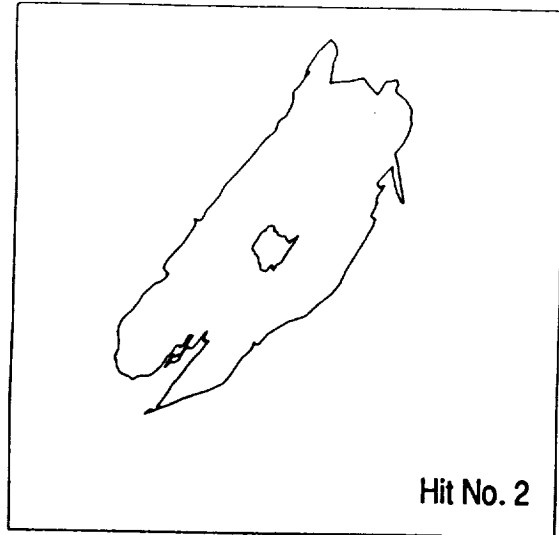
4

Fig. 19 Micrometeoroid/Debris Impact Damage (x100) on Kevlar®/Epoxy Tube [SP-328, $(\pm 45^\circ)_4S$]



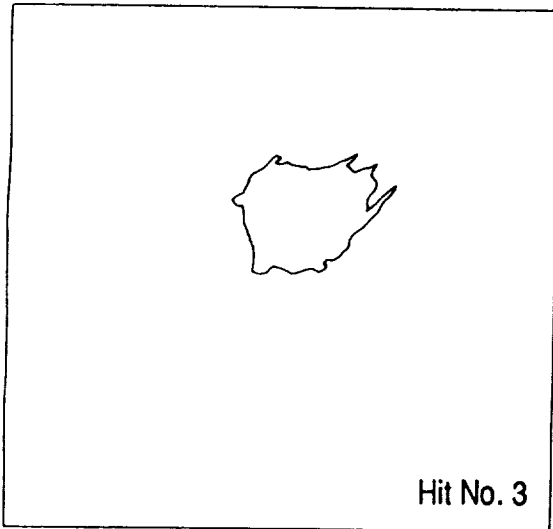
Hit No. 1

Surface Damage Area = 0.223 mm^2
Extent of Penetration = 1 - 2 plies



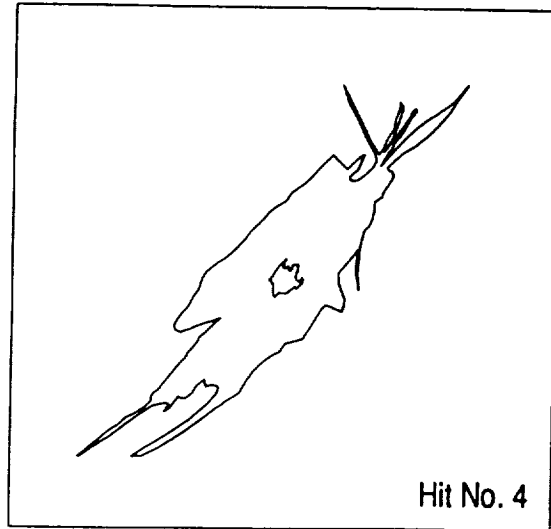
Hit No. 2

Surface Damage Area = 1.445 mm^2
Crater Area = 0.033 mm^2
Crater Diameter = 0.204 mm
Extent of Penetration = 2 - 3 plies



Hit No. 3

Surface Damage Area = 0.370 mm^2
Extent of Penetration = 0 - 1 plies



Hit No. 4

Surface Damage Area = 0.881 mm^2
Crater Area = 0.020 mm^2
Crater Diameter = 0.159 mm
Extent of Penetration = 2 - 3 plies

Fig. 20 Micrometeoroid/Debris Impact Damage SP328 Kevlar®/Epoxy Tube (2T17)

**PROPOSED TEST PROGRAM AND DATA BASE
FOR LDEF POLYMER MATRIX COMPOSITES**

R. C. Tennyson
University of Toronto Institute for Aerospace Studies

P. George
Boeing Defense and Space Group

G. Steckel
The Aerospace Corporation

D. G. Zimcik
Canadian Space Agency

INTRODUCTION

The purpose of this report is to present a survey of the polymer matrix composite materials that were flown on LDEF with particular attention to the effect of circumferential location (α) on the measured degradation and property changes. Specifically, it is known that atomic oxygen fluence (AO), VUV radiation dose and number of impacts by micrometeoroids/debris vary with α . Thus it is possible to assess material degradation and property changes with α for those materials that are common to three or more locations. Once the α -dependence functions have been defined, other material samples will provide data that can readily be used to predict damage and property changes as a function of α as well.

Another objective of this report is to summarize what data can be realistically obtained from these materials, how this data can be obtained and the scientific/design value of the data to the user community. Finally, a proposed test plan is presented with recommended characterization methodologies that should be employed by all investigators to ensure consistency in the data base that will result from this exercise.

LDEF POLYMER MATRIX COMPOSITES — TYPES AND LOCATION

Table 1 summarizes the extensive number of polymer matrix composites that were distributed over nine different circumferential locations around LDEF. Also shown is the variation in atomic oxygen fluence (atoms/cm²) and the total VUV radiation exposure at each location, measured in "equivalent sun hours" (ESH). For reference purposes, each experiment is defined by its NASA LDEF code and the experimenters identified.

Of particular interest are those materials which are common to three or more locations. From Table 2 it can be seen that 5 different materials meet this criterion and thus it is expected that any angular dependence of degradation mechanisms or property changes can be determined. Once the angular dependence functions are known, one can then utilize material data obtained from any of the LDEF samples to assess "worst

case" scenarios regardless of the sample location on LDEF. For example, mass loss due to AO erosion can be calculated for the "ram" direction based on measurements made on samples located at any α , providing $0 \leq |\alpha| \leq 90^\circ$.

Another example relates to the damage done to composite laminates due to impacts by micrometeoroids/debris. It is known that the number of "hits" is indeed a function of ' α ' (and time in orbit). Consequently, if one knew the correlation between "surface damage area" as a function of micrometeoroid/debris impact, one could then calculate "total damage area" for a given location on a satellite.

DATA BASE REQUIREMENTS

The usefulness of a data base is often determined by the presentation format employed. Processing of the raw data can take different forms, ranging from a fully catalogued "library," thus enabling full access to the raw data, to a condensed and "interpreted" handbook form which enables a user to apply the information directly. The need and usefulness of each of these forms will depend on the specific user community.

In the case of LDEF data, it is possible to identify a spectrum of likely users, ranging from researchers and scientists who are interested in the raw data necessary to further the science in this area, to the design engineer interested mainly in the direct application of the data to a specific problem. While being careful not to oversimplify this at either extreme, the needs of each community are quite distinct and different. In addition, the data base generated from LDEF must ensure completeness, integrity and traceability to enable future scientists to explore those "peculiar" results of today that will invariably find explanation or interpretation in future work. The complete LDEF data base must be multi-dimensional.

In creating a data base from LDEF data it is therefore imperative that the user community for which it is targeted be clearly identified and consulted (or at least considered) in its generation. The first requirement for such a data base must be to establish the user's needs in order to define the format of the presentation.

Technical requirements of a data base are determined by two factors:

- particular space environment effect on material damage or specific property,
- importance of specific material property on structural/component design and performance.

Table 3 summarizes the characteristics of materials that are deemed important in terms of their applications to spacecraft systems and components. The "degree of importance" can be assessed by the "value of the data" for design purposes, which is also described in Table 3. In addition, the "scientific value" is also noted. It should also be stressed that any of the property data obtained from flight samples is always useful for validating ground-based simulation tests and for providing a comparative basis on material performance for long term space applications.

Included in Table 3 is a listing of the quantities that would have to be measured to provide the proper characterization of each material.

PROPOSED TEST PLAN

Once the material characteristics have been defined based on their relevance to the user community, Table 3 provides a summary of the quantities that need to be measured. Table 4 can then be employed to define the “methodology” by which each quantity can be measured to determine the specific material characteristic. It is essential in the compilation of a consistent data base that each of the experimenters agree on the methodology.

TABLE 1. LDEF ORGANIC COMPOSITES

Row #	Angle off Ram	AO fluence x10 ²¹ a/sq.cm.	VUV ESHx10 ³	Experiment No.	Principal Investigator	Materials
9	8°	8.32	11.1	AO134	Wayne Slomp, NASA Langley Res. C. (804) 864-1334	5208/T300, 934/T300, P1700/C6000, P1700/C3000, 930/GY70
				M0003-9	Brian Petrie, Lockheed (408) 742-8244	CE-339/GY70, F263/T50, 934/T50, X904B/T50, E788/T50, 3501-5A/HMS, E788/C6000, 934/HMF176, CE-339/E-Glass, F593/P75, 934/P75
				M0003-8	Pete George, Boeing (206) 234-2679	934/T300, P1700/T300, PMR15/C6000
10	22°	7.78	10.7	A0054	TRW	Epoxy/Fiberglass
8	-38°	6.63	9.4	AO171	Ann Whitaker, NASA-MSFC (205) 544-2510	934/HMS, 934/P75S, P1700/HMF, Epoxy/S-Glass
				M0003-10**	Brian Petrie, Lockheed (408) 742-8244	X904B/GY70, 3501-5A/HMS, X904B/E-glass
				M0003-10**	Thomas Cookson, General Dynamics (619) 547-5081	X-30/GY70*, CE-339/GY70, CE-339/P75S, 934/P75S, 934/GY70, P1700/W722*, V378A/T300
				M0003-10**	Charles Smith, McDonnell Douglas (714) 896-5580	5208/T300*, P1700/T300*, PES/T300*, Polyimide/C6000*
				M0003-10**	Pete George, Boeing (206) 234-2679	934/T300, 3501-6/AS, P1700/T300, PMR15/C6000, LARC 160/Graphite
7	-68°	3.16	7.2	AO175	Dick Vynhal, Rockwell (918) 835-3111, Ext. 2252	F178/T300, PMR15/C6000
12	82°	1.2	6.9	AO180	Rod Tennyson, U. of Toronto (416) 667-7710	934/T300, 5208/T300, SP288T300, SP328 Kevlar/Epoxy, SP290 Boron/Epoxy
				AO019	David Felbeck, U. of Michigan (313) 994-6662*	5208/T300 interleafed w. Kapton
1	112°	0.06	7.5	AO175	Dick Vynhal, Rockwell (918) 835-3111 Ext. 2252	934/T300, LARC 160/C6000
5	-128°	0	8.2	P0005	Dean Lester, Morton Thiokol (801) 863-6809	Carbon/Carbon, Epoxy/Graphite, Epoxy/Kevlar, Epoxy/Glass (all mounted internally)
4	-158°	0	10.4	AO054	TRW	Epoxy/Fiberglass
3	172°	0	11.1	M0003-10 M0003-9 M0003-8 AO138	(See Row 8 List for M0003-10) (See Row 9 List for M0003-9) (See Row 9 List for M0003-8) Heinrich Jabs Matra Espace, France (33)-1-61-39-72-73	934/GY70, V-108/Kevlar, V108/T300, V108/GY70, V108/G837

* Some specimens flown with protective coating

** Part of Advanced Composites experiment integrated by Aerospace Corp., Gary Steckel (213) 336-7116

TABLE 2. COMMON MATERIALS

Row No.	Angle off RAM (°)	AO Fluence (10^{21} a/cm ² .)	VUV (ESH x 10 ³)	Materials				
				934 T300	5208 T300	PMR C6000	CE 339 GY70	934 P75
9	8	8.32	11.1	✓	✓	✓	✓	✓
8	-38	6.63	9.4	✓	✓	✓	✓	✓
7	-68	3.16	7.2			✓		
12	82	1.2	6.9	✓	✓			
1	112	.06	7.5	✓				
3	172	0	11.1	✓	✓	✓	✓	✓

Table 3

Polymer-Matrix Composites - Data Base Requirements*

Characterization	Quantities Measured	Value of Data (Scientific & Design)
Atomic Oxygen (AO) Erosion	<ul style="list-style-type: none"> • thickness loss • mass loss • surface morphology • surface molecular structure changes • optical property changes 	<ul style="list-style-type: none"> • material selection criteria based on erosion yield(cm^3/atom) • material lifetime predictions • synergistic effects due to VUV & AO • angular dependence effects • shadow effects • changes in structural CTE, strength, stiffness & buckling load • validate theoretical AO erosion models • degradation in system performance • guide for new material formulations & coatings
Coefficient of Thermal Expansion (CTE)	<ul style="list-style-type: none"> • strain/displacement as function of temperature 	<ul style="list-style-type: none"> • change in CTE with vacuum outgassing • effects of combined VUV & AO on changes in CTE • effect of thermal fatigue & microcracking on CTE • validation of zero CTE configurations for long term space exposure
Outgassing and Dimensional Changes	<ul style="list-style-type: none"> • outgassing products • strain/displacement changes with time and temperature • mass loss 	<ul style="list-style-type: none"> • contamination • long term "permanent" dimensional changes (important for zero CTE design) • validation of theoretical desorption models • times to reach equilibrium state
Micrometeoroid/Debris Impacts & Damage	<ul style="list-style-type: none"> • number & size distributions • surface damage area • number of penetrations • rear surface spallation 	<ul style="list-style-type: none"> • probability of hits based on size and damage zone • effectiveness of coatings • probable cumulative damage to structural elements • angular dependence

Table 3 (cont'd)

Polymer-Matrix Composites - Data Base Requirements*

Characterization	Quantities Measured	Value of Data (Scientific & Design)
Mechanical Properties		
- Microcracking	<ul style="list-style-type: none"> number and extent of transverse & interlaminar cracks 	<ul style="list-style-type: none"> damage effects on strength, stiffness of laminates thermal fatigue data validation of micromechanics models design of stiffness/strength critical laminates change in properties due to combined space environmental effects
- Modulus & Damping	<ul style="list-style-type: none"> variation of modulus & damping with frequency and temperature 	
- Transverse & Interlaminar Shear Strength	<ul style="list-style-type: none"> shear strength & modulus 	
- Tensile & Compression Strength	<ul style="list-style-type: none"> tensile and compression strength and modulus 	
Solar Absorptance & Infrared Emittance	<ul style="list-style-type: none"> absorptance & emittance 	<ul style="list-style-type: none"> thermal property changes due to long term space environmental effects system thermal design data
Molecular Structure Changes	<ul style="list-style-type: none"> surface molecular structure changes 	<ul style="list-style-type: none"> reaction of resin systems with A0 & VUV radiation resin long term stability & property retention validation of theoretical reaction models

* **Note:**

All data useful for:

1. Validating ground-based space simulation systems and tests
2. Comparing relative material performance characteristics for long term space applications

Table 4

Polymer-Matrix Composites Proposed Test Plan

Characterization	Methodology
Atomic Oxygen Erosion	SEM Cross-Section Profilimetry, Gravimetric
Coefficient of Thermal Expansion	Laser interferometer, strain gauges dilatometer (in vacuum)
Outgassing and Dimensional Changes	Laser interferometer, strain gauges dilatometer (in vacuum)
Micrometeoroid/Debris Impacts & Damage	Optical microscope SEM
Mechanical Properties <ul style="list-style-type: none"> • Microcracking • Modulus & Damping • Transverse & Interlaminar Shear Strength • Tensile & Compression Strength 	SEM Cross-Section DMA test system, various T ASTM D1002 ASTM D638, D695
Solar Absorptance & Infrared Emittance	ASTM E- 424, A ASTM E- 408, A
Molecular Structure Changes	Diffuse Reflectance <ul style="list-style-type: none"> • Solid State NMR

Lubricants, Adhesives, Seals, Fasteners, Solar Cells, and Batteries

Co-Chairmen: James Mason and Joel Edelman
Recorder: Harry Dursch



Identification and Evaluation of Lubricants, Adhesives, and Seals used on LDEF

**Bruce Keough
Boeing Aerospace**

A variety of lubricants, adhesives and seals were flown on LDEF. They were used in the fabrication and assembly of the experiments similar to other spacecraft applications. Typically, these materials were not exposed to U.V. radiation or atomic oxygen, except possibly around the perimeter of the joints.

Most of these materials were of secondary interest and were only investigated by visual examination and a "Did they fail?" criteria. Because of this role, most applications had only a few specimens, not enough for statistical data generation. Often, no control samples were kept, and documentation of what was used was occasionally sketchy.

LDEF Lubricants

VENDOR	MATERIAL	DESCRIPTION	EXPERIMENT	TRAY
	Cetyl Alcohol		A0175	A1, A7
	MIL-L-23398	Air cured solid film lubricant	EECC'S	
	MoS ₂		A0138 A0175	A1 A7
	WS ₂		GRAPPLE	C1
Apiezon	H	Petroleum based thermal grease	A0076	F9
Apiezon	L	Petroleum based lubricant	A0180	D12
Apiezon	T	Petroleum based lubricant	M0001	H3, H12
Ball Aerospace Systems Group	VacKote 18.07	MoS ₂ with polyimide binder	S0069	A9
Ball Aerospace Systems Group	VacKote 21207	MoS ₂	S0069	A9
Ball Brothers	44177	Hydrocarbon oil with lead naphthanate and clay thickener	EECC'S	
Castrol	Braycote 601	PTFE filled perfluorinated polyether lubricant	A0187	A3
Dow Corning	340	Silicone heat sink compound	A0133 M0001	H7 H3, H12
Dow Corning	1102	Mineral oil filled with Bentonite and MoS ₂	S1001	F12, H1
Dow Corning	Molykote Z	MoS ₂ powder	A0138	

Cetyl alcohol and a molybdenum disulfide (MoS_2) dry film lubricant were used on some of the fasteners on experiment A0175, Evaluation of Long-Duration Exposure to the Natural Space Environment on Graphite-Polyimide and Graphite-Epoxy Mechanical Properties. The dry film lubricant was provided on some of the nutplates and the cetyl alcohol was used to aid in fastener installation. Fasteners installed into nutplates with MoS_2 dry film lubricant showed no thread damage while fasteners installed without the lubricant sustained substantial thread damage. Post-flight FTIR examination of the lubricated treads found no remaining traces of cetyl alcohol.

MIL-L-23398 air cured solid film lubricant was used on several places on the Experimental Environment Control Canisters (EECC). The lubricant was applied to the Belleville washers, drive shafts, and linkages. Examination of the hardware revealed no signs of abnormal wear or coating degradation. Some bare areas where the washers rubbed on each other were apparent on surfaces not exposed to U.V. radiation. Portions of the drive shaft exposed to U.V. radiation were slightly discolored.

Tungsten disulfide (WS_2) dry film lubricant was used as the lubricant on both active and passive grapple shafts to insure successful release of the grapple from the RMS during deployment and retrieval of LDEF. The lubricant on the grapple used for both deployment and retrieval performed as designed. Because the tray was located 22 degrees to the ram, the base of the grapple saw limited atomic oxygen exposure (7.78×10^{21} impacts per square centimeter). However, because the shaft extended three to four inches beyond the LDEF surface, portions of the shaft were exposed to a greater fluence. During post-flight analysis at Johnson Space Center, samples of WS_2 were removed from both grapple shafts for SEM and EDX analysis. This analysis showed the bulk lubricant to be intact with no discernable difference between the lubricant exposed on the ram surfaces of the shafts and the lubricant exposed on the trailing edges. No surface analysis was performed. To date, the tribological properties of the WS_2 have not been determined.

Apiezon L was used on experiment A0180, The Effect of Space Environment Exposure on the Properties of Polymer Matrix Composite Materials, as a lubricant during fastener installation. It was not examined after LDEF retrieval.

Apiezon T was used on experiment M0001, Heavy Ions in Space, as a lubricant for installation of a large o-ring in a flange seal. Examination of the lubricant/o-ring by optical microscopy revealed some slight separation of the oil from the filler. Infrared spectroscopy of the lubricant showed no changes from the control. The o-ring was entirely wetted with the oil and showed no evidence of attack. Post-flight examination of the

flange revealed migration of the Apiezon T onto the flange. This migration was not quantified.

VacKote 18.07 and 21207 were used on experiment S0069, Thermal Control Surfaces Experiment. No post-flight examination of the lubricant has been performed.

Castrol Braycote 601 was used to lubricate the four drive shafts which opened and closed the clam shells of experiment A0187-1, Chemistry of Micrometeoroids. Since these drive shafts were exposed to space when the clam shells were in their open position, the Braycote 601 was exposed to some U.V. radiation. However, the experiment was located on the trailing edge of LDEF so the lubricant was not exposed to atomic oxygen. The lubricant had picked up a black color, thought to be contamination. This has not been identified. Castrol examined the Braycote 601 with the following results. Infrared analysis showed no new carbonyl groups, indicating that no oxidation took place. New peaks were found in the 1100 to 1400 range. These might be attributed to C-F bonds indicating some degradation of the PTFE filler but additional investigation is warranted. Some of the LDEF sample was separated into oil and filler by filtration. The viscosity of the base oil was lower than that of a control sample. This would indicate chain scissioning of the polyether and is consistent with exposure to U.V. radiation. Thermal analysis (differential scanning calorimetry and thermal gravimetric analysis) of the extracted oil revealed a new endotherm at approximately 106 C. This may be attributable to moisture effects. The LDEF exposed grease also had an endotherm at 211 C, which was not present in the non-flight sample.

Dow Corning 340 heat sink compound was used on two experiments on LDEF: A0133, Effect of Space Environment on Space Based Radar Phased Array Antenna, and M0001, Heavy Ions in Space. The heat sink compound in both experiments performed as expected, transferring heat from one surface to another. Neither application exposed the Dow Corning 340 to U.V. radiation or to atomic oxygen, but both experiments saw hard vacuum and mild thermal cycling. The infrared spectra of a sample of Dow Corning 340 from experiment M0001 was unchanged compared to that of a control sample.

Dow Corning 1102, used on experiment S1001, Low Temperature Heat Pipe, is an obsolete heat sink compound that was composed of 85 percent mineral oil, 10 percent Bentonite, 3 percent MoS₂, and 3 percent acetone. Post flight visual examination of the material showed no change from the initial condition.

Dow Corning Molykote Z was used on experiment A0138. No results have been reported.

Apiezon H was used as a heat sink grease on experiment A0076, Cascade Variable Conductance Heat Pipe. The grease was not exposed to atomic oxygen or to U.V. radiation. To determine the effect of extended hard vacuum on the grease, a sample was tested for outgassing in accordance with NASA SP-R-0022A. The LDEF sample had considerably higher total mass loss than the control sample, but the volatile condensible material was similar. It was postulated that this was due to the LDEF sample picking up moisture between satellite retrieval and sample test. Therefore, a series of tests were performed to determine the propensity of Apiezon H to absorb atmospheric moisture. A thin film of the grease was exposed to 100 percent humidity at room temperature prior to testing. The absorbed moisture caused a total mass loss similar to the difference between the LDEF sample and the control sample. Chemical analysis of the grease indicates that both the grease and the condensible materials from the volatility test match those of a control sample. This implies that changes noted in the LDEF exposed Apiezon were caused by storage on earth, not by space.

Apiezon H Volatility

TEST SAMPLE	DURATION	TOTAL MASS LOSS	VOLATILE CONDENSIBLE MATERIAL
LDEF	7 DAYS	2.32%	0.66%
LDEF	1 DAY	1.42%	0.44%
CONTROL	7 DAYS	0.97%	0.58%
CONTROL	1 DAY	0.53%	0.18%
CONTROL WITH 2 DAYS HUMIDITY	1 DAY	0.72%	0.21%
CONTROL WITH 1 MONTH HUMIDITY	1 DAY	1.38%	0.25%
MSFC HDBK 527	1 DAY	0.86%	0.16%

Ball Brothers Lubricant 44177 was used to lubricate a thrust washer on the EECC's. A nearby bracket was found to have a diffraction pattern due to off-gassing of the volatile component of the lubricant. Although 44177 is still used on previously designed spacecraft, Ball Brothers no longer recommends it for new design.

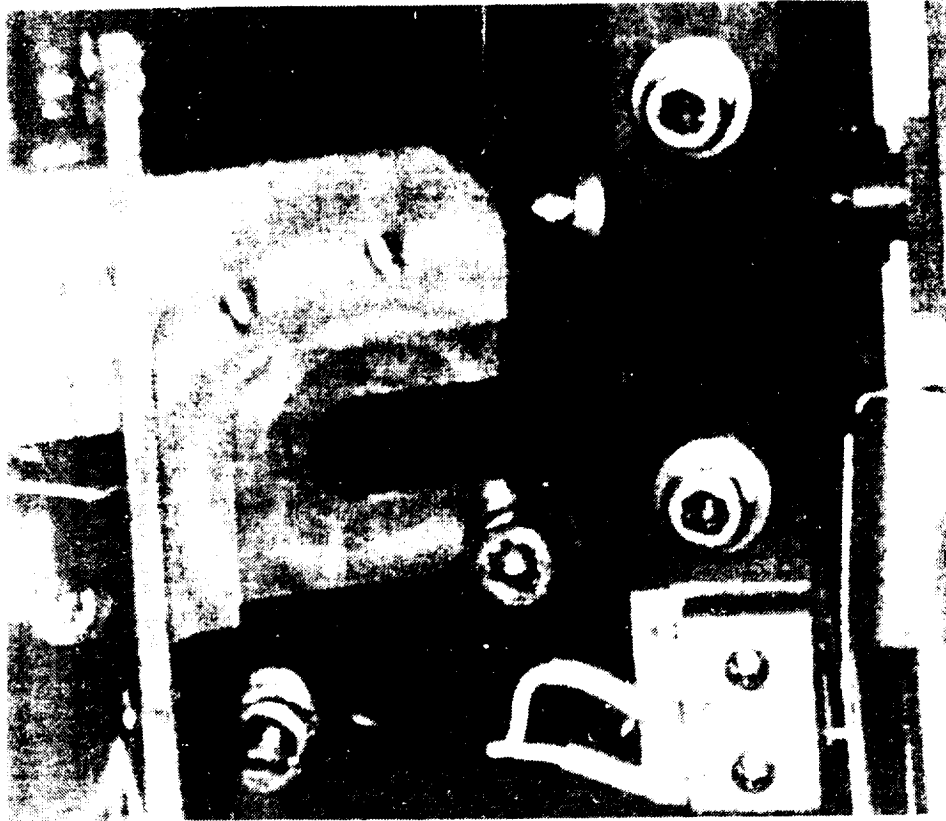


Figure 1. Offgassing Diffraction Pattern of Ball Brothers Lubricant 44177

(Original photograph unavailable)

Vespel bushings were used in experiments A0147, Passive Exposure of Earth Radiation Budget Experiment Components, A0187, and S1002, Investigation of Critical Surface Degradation Effects on Coatings and Solar Cells Developed in Germany. None of the bushings were exposed to U.V. radiation or to atomic oxygen. All Vespel bushings performed as expected.

Everlube 620 was also tested in experiment M0003. Post flight visual inspection of the sample showed that none of the lubricant remained on the test specimens. EDX examination of the surface showed traces of MoS₂ remaining in the bottom of the machining grooves, but not enough material remained to provide lubrication. The binder, a proprietary organic compound, was apparently completely consumed by the environment. Since the experiment was on the trailing edge, the Everlube saw U.V. radiation, but no atomic oxygen. No mechanism for the degradation has been proposed.

Exxon Andok C was used on the carousel of experiment S0069, Thermal Control Surfaces Experiment and Mobil Grease 28 was used on the magnetic tape memories (MTM's). Both applications were in sealed enclosures backfilled with inert atmospheres. The hardware was tested and compared to pre-flight performances. No changes were expected or found.

Rod end bearings were tested in experiment M0003. The bearings were exposed to U.V. radiation, but not to atomic oxygen. The bearings were tested to the original requirements by the manufacturer, New Hampshire Ball Bearing. All test requirements were met. One of the tests involved removing the PTFE coated Nomex liner from the bearing body. The force required to remove the liner was similar to virgin bearings. Inspection of the Nomex/PTFE liner showed no degradation. The bearing bodies were cadmium plated in accordance with QQ-P-35 Class 2 Type II. The Type II designation requires that the parts receive a chromate conversion coating after plating. The conversion coating, which is an iridescent yellow brown color, was mostly removed from parts of the rod end bearings flown on LDEF. Other areas of the bearings that received similar exposure did not exhibit similar chromate coating color loss. No explanation for this phenomena has been proposed.

LDEF Lubricants

VENDOR	MATERIAL	DESCRIPTION	EXPERIMENT	TRAY
DuPont	Vespel 21	Graphite-filled polyimide	M0003	D3
DuPont	Vespel	Polyimide	A0147 A0187-1 S1002	B8, G12 E3
Everlube	620	Heat cured, bonded dry film lubricant	M0003	D3
Exxon	Andok C	Channeling petroleum grease	S0069	A9
Mobil	Grease 28	Nonchanneling silicone grease		mtm
		Rod End Bearings	M0003	D3

With few exceptions, the adhesives performed as expected, that is, they held the hardware together. Several experimenters noted that the adhesives had darkened in areas that were exposed to U.V. radiation.

Epoxy Adhesives

Vendor	Product	Experiment	Comments
Ciba-Geigy	Araldite AV 100/HV 100	A0056 A0139	
	Araldite AV 138/HV 998	A0023 A0056 A0138-1 S1002	
	Araldite AV 138/HW 2951	A0138-1	
	Araldite AW 136/HY994	M0002	
	Araldite AW 2101/HW 2951	A0138-1	
	Araldite MY 750/HY 956	A0056	
Crest	3135/7111	A0180	1, 2, 3

Key to comments

- 1: Performed as expected.
- 2: Discolored where exposed to U.V.
- 3: Further testing is planned. Results to be published later.

Epoxy Adhesives (Continued)

Vendor	Product	Experiment	Comments	
Emerson & Cuming	Eccobond 55	A0056 A0139 A0147 S0014	1 1,2	
		Eccobond 55 + 10% Ecosil	S1002	
	Eccobond 56C	A0076 A0171 S0069	1 1, 3 1	
	Eccobond 56C + Silver Powder	S1002		
Epoxy Technology	Epo-Tec 301	A0147 S0014	1 1	
	Epo-Tec 331	M0004	1	
Furane	Epi-Bond 104	S0014	1	
Hysol	EA 934	A0180 M0004 S1001	1, 2, 3 1 1	
		EA 956	A0054	1
		EA 9210/109519	M0004	1
	EA 9628	M0003	1, 3	

Key to comments

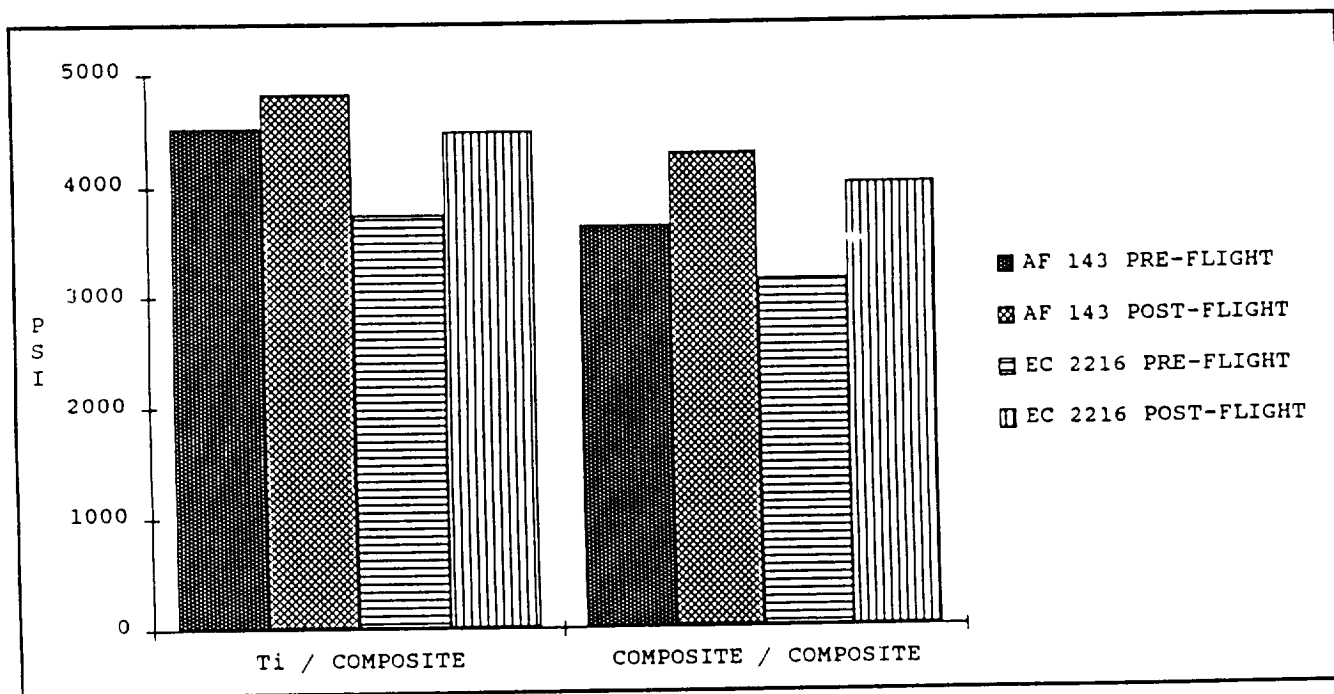
- 1: Performed as expected.
- 2: Discolored where exposed to U.V.
- 3: Further testing is planned. Results to be published later.

Vendor	Product	Experiment	Comments
Rome & Haas	K-14	A0171	1, 3
	N-580	A0171	1, 3
Shell	Epon 828	A0056 A0180 P0003 S1001	1, 2, 3 1 1
3M	AF-143	M0003	1
	EC 2216	A0076 A0138-1 A0178 M0003 S1005 Viscous Damper	1 1 1 1
Varian	Torrseal	M0006	

The most obvious adhesive failure on LDEF was on experiment M0003, Space Environment Effects on Spacecraft Materials. In this experiment, solar cells were bonded to an aluminum substrate using an unfilled low viscosity epoxy, Shell Epon 828. Photographs taken in space of the LDEF prior to retrieval show that the solar cells were no longer bonded to LDEF. No adhesive remained on the leading edge tray but some remained on the trailing edge tray. This indicates that the bond failed at the solar cell interface, and then the adhesive was attacked by atomic oxygen. Epon 828 was used successfully on other experiments so no conclusions have been drawn as to the failure mode. Possibilities include surface contamination prior to bonding, excessive loading during takeoff, and excessive thermal cycling and high loads due to different thermal expansion coefficients between the solar cell and the aluminum.

Two 3M adhesives, AF 143 film adhesive and EC 2216 room temperature epoxy, were tested in experiment M0003. Lap shear specimens using graphite epoxy substrates and the test adhesives were exposed on the trailing edge of LDEF. The reason for the slight increase in strength compared to a ground aged sample is not known at this time.

Shear Strength of 3M Adhesives



The only failure of the silicone adhesives was a debond of an FEP film/RTV 560/Kapton film joint. General Electric has postulated that the failure was due to lack of primer rather than to a failure of the adhesive.

Silicone Adhesive

Vendor	Product	Experiment	Comments
Dennison	Densil Silicone PSA	A0076	1
Dow Corning	6-1104	A0178 A0187 P0005	
	43-117	A0171	1, 3
	93-500	A0171 S1002	1, 3
	RTV 3140	S1001	1
General Electric	RTV 560	M0003	
	RTV 566	A0076	1
		A0171	1, 3
		S0014	1
		S1002	
	RTV 567	A0054	1
RTV 555	A0171	1, 3	
SR 585 PSA	A0076	1	

Key to comments

- 1: Performed as expected.
- 2: Discolored where exposed to U.V.
- 3: Further testing is planned. Results to be published later.

There were no failures of conformal coatings or potting compounds. All electronic hardware looked very good in post-flight examination.

Conformal Coatings and Potting Compounds

Vendor	Product	Experiment	Comments
Conap	CE-1155	A0201 P0005	
Dow Corning	Sylgard 182	S1001	1
	Sylgard 186	S1001	1
Emerson & Cuming	Stycast 1090	A0056	
	Stycast 2850	P0003	1
	Stycast 3050	S0069	1
General Electric	RTV 411/511	S0014	1
Products Research	PR 1535	A0038	
	PR 1568	A0201	
Thiokol	Solithane 112	A0178	
	Solithane 113	A0038 A0178 A0187-2 S0001 S1001 S1002	
3M	Scotchcast 280	A0139	

Key to comments

- 1: Performed as expected.
- 2: Discolored where exposed to U.V.
- 3: Further testing is planned. Results to be published later.

A variety of tapes were flown on LDEF. No adhesive failures of the tapes occurred.

Tapes and Other Materials

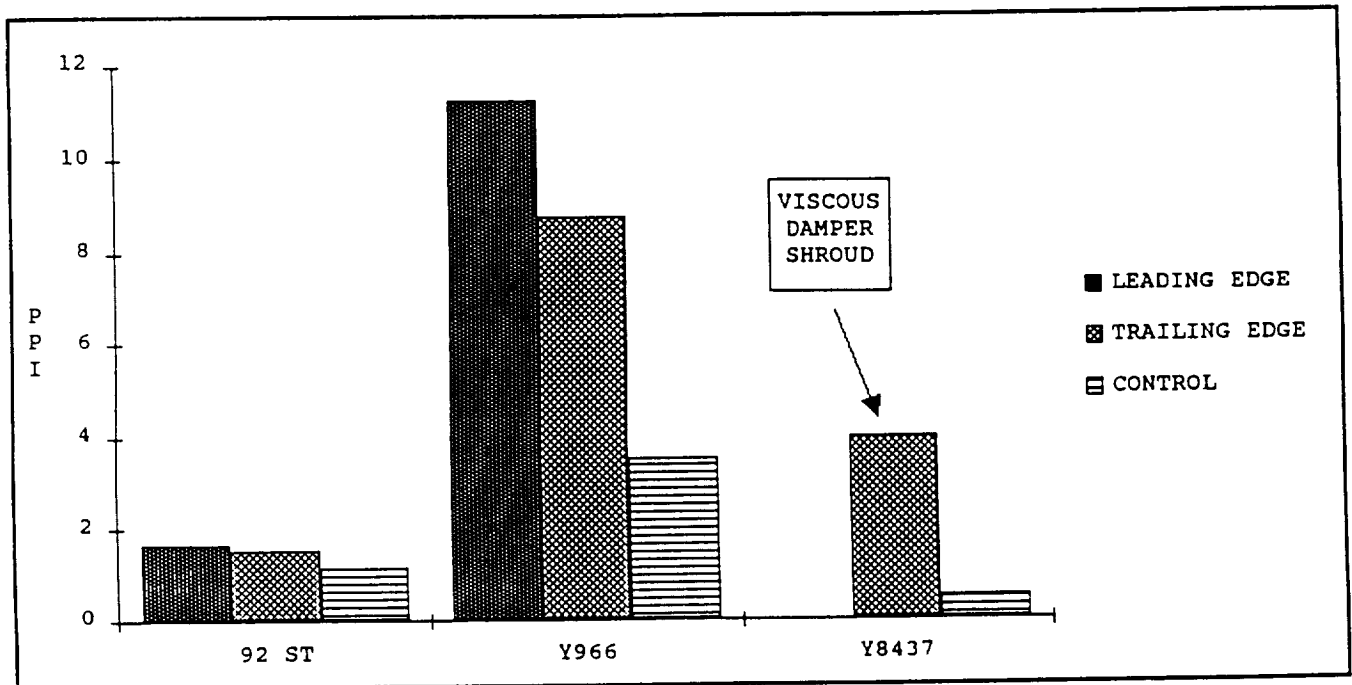
Vendor	Product	Experiment	Comments	
Emerson & Cuming	Eccoshield PST-C	M0003		
Loctite		A0119 A0138-1		
Mystic Tapes	7355	M0001	1	
	7452	P0003	1	
3M	5	A0139		
	56	S0069	1	
	74	S0069	1	
	92 ST	A0054	1	
	433	A0076	1	
	X-1181	A0178 M0001	1	
	Y966	A0054 M0003 S0069	1 1 1	
	Y8437	A0076 VISCOUS DAMPER	1 1	
		Polyester Hot Melt Adhesive	A0133	1, 3

Key to comments

- 1: Performed as expected.
- 2: Discolored where exposed to U.V.
- 3: Further testing is planned. Results to be published later.

3M tape Y966 on a silverized FEP film was also used to hold the thermal blankets to the tray frame on experiment M0001. The blankets apparently shrunk in flight causing the blankets to detach from the frame. Portions of the tape were attached to both the blanket and to the frame, having failed in tension. The film and Y966 remained pliable. Attempts to fail the tape to frame joint in shear were unsuccessful even though a load of roughly 100 pounds was applied to a piece of tape less than a quarter inch wide. The tape was then tested in peel. The Y966 bonded to the aluminum and to the silver on the film well enough to cause delamination of the silver from the film.

Peel Strength of 3M Tapes



3M tape 92 ST, a Kapton tape with a silicone adhesive was tested on experiment A0054, Space Plasma High Voltage Drainage. Peel strength of tape 0.787 inch wide bonded to aluminum was 1.3 pounds on a leading edge tray, 1.2 pounds on a trailing edge tray, and 0.9 pounds for a fresh, unflown tape.

3M tape X-1181, a copper foil tape with a conductive adhesive, was used as grounding straps for the silver/Teflon blankets. The grounding straps were constructed by plying two layers of tape, the adhesives together, with an area of adhesive remaining on each end. A peel test was performed on a sample of the ground strap and compared to a control sample of a freshly constructed strap made from the same roll of tape. All samples had a peel strength of 3.5 to 3.9 pounds per inch. No difference was found between space hardware and ground hardware.

3M tape Y966, an acrylic transfer tape, was tested in experiment A0054. The tape was used to bond vapor deposited aluminum (VDA) Kapton film to the aluminum trays. The tape was tested using a 90° peel test similar to ASTM D1000 except that tape width was 0.4 inches. Tape from the leading edge tray had a 4.5 pound peel strength while tape from the trailing edge tray had a 3.5 pound peel strength. A ground control specimen made from a different lot of material had a peel strength of 1.4 pounds. The differences may be attributable to tape variations from batch to batch, additional "cure" of the space exposed tape, and experimental variation. Comparison of the failure mode of the tapes from the leading and trailing edge trays showed significant variation. On the trailing edge tray approximately 75 percent of the adhesive stuck to the VDA Kapton while on the leading edge, 85 percent of the adhesive stuck to the aluminum tray and pulled the VDA from the Kapton film.

3M tape Y8437, a VDA Mylar tape, was used as a coating on the viscous damper shroud, a fiberglass epoxy structure. The tape used on LDEF had a 90° peel strength of approximately 4 pounds per inch. After the LDEF tape had been removed, a new piece of the same type of tape (different batch and manufacture time) was applied to the shroud. This tape had a peel strength of only 0.5 pounds per inch. Apparently, the adhesive on the tape sets up with time to give increased adhesion. Space did not appear to have any adverse effect on the tape.

A variety of seals were used on LDEF. These were generally o-rings, although sheet rubber was also used for seals. These materials performed as anticipated, sustaining little or no degradation. In addition, materials that are commonly used for seals were used as cushioning pads.

Butyl o-rings were used in face seals on experiment P0004, Seeds in Space Experiment. Because the o-rings were sandwiched between metal surfaces, their exposure was limited to vacuum only. The o-rings were apparently installed without lubricant and sustained some scuff marks and pinching upon installation. There was no evidence of space induced degradation and the performance of the o-ring seal was as predicted.

Ethylene propylene (EP) o-rings were used to seal the lithium batteries on experiment S0069, Thermal Control Surfaces Experiment. These seals failed due to excessive compression set of the o-rings as shown in Figure 1. The temperatures seen by the batteries, 13 to 27 C, were well within the limits of EP o-ring capabilities. Therefore, failure has been attributed to attack of the o-ring by the battery electrolyte, dimethyl sulfite.

Silicone rubber was used as a cushioning gasket between the sunscreen and the tray in experiment S0050, Investigation of the Effects on Active Optical System Components. Portions of the gasket were exposed through holes in the sunscreen. Since the experiment was on the trailing side of LDEF, the gasket saw U.V. radiation, but not atomic oxygen. The exposed areas of the gasket were slightly darkened, as shown in Figure 3, but did not show any other signs of degradation. The hardness of the gasket was the same in exposed and unexposed areas, and all material was very pliable. Although control specimens were not available, tensile strength and elongation were determined and found to be within the range of other silicone elastomers.

Silicone rubber was also used as a cushioning pad between a metal clamp and some optical fibers in experiment M0004, Space Environment Effects on Fiber Optics Systems. The rubber was mostly shielded, but some edges were exposed to U.V. radiation and atomic oxygen. The rubber remained pliable and free of cracks. Some darkening of the rubber was observed in the exposed areas.

A large number of Viton o-rings were used on LDEF. Post flight examination of these found that they were all in pristine condition. No Viton o-rings seals failed to maintain a seal. None of the Viton o-rings were exposed to U.V. radiation or to atomic oxygen.

LDEF Seals

ELASTOMERIC PARTS	EXPERIMENT	TRAY
Butyl o-ring	P0004	F2
Butyl rubber seal	A0138	B3
EP o-ring	S0069	A9
EPDM rubber	P0005	CENTER RING
NBR rubber	P0005	CENTER RING
Neoprene gasket	A0139	G6
Nitrile o-ring	M0006	C2
Nitrile butadiene rubber	P0005	CENTER RING
Silicone gasket	S0050	E5
Silicone pad	M0004	F8
Viton o-ring	A0015	G2
	A0134	
	A0138-2	B3
	A0139	G6
	A0180	D12
	M0001	H3, H12
	M0002	LOTS?
	P0005	CENTER RING
	S0010	
	S0069	A9
Viton washer	A0189	D2
Metal "V" seal	EECC'S	

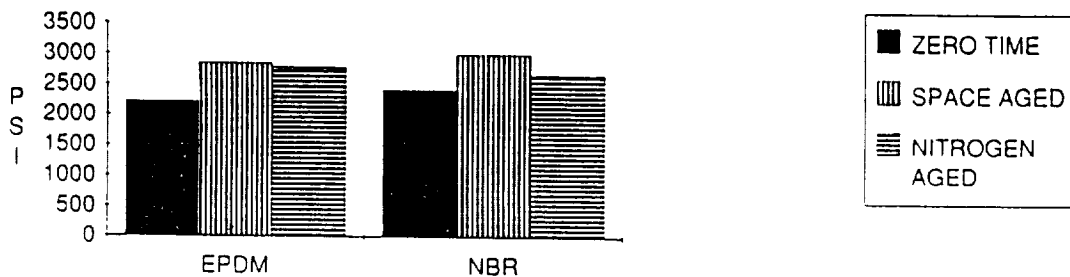
A group of Viton washers was used to pad the quartz crystal oscillators in experiment A0189, Study of the Factors Determining the Radiation Sensitivity of Quartz Crystal Oscillators. The washers were apparently dinked out of sheet stock as a fabric texture was apparent on the flat surfaces. Many of the washers had indentations on one or both of the contacting surfaces, indicating compression set. A quantitative analysis of this is not meaningful since the original compression is not known.

A metal "v" seal was used to seal the pressure valve in the EECC's. The seal was made of gold plated Inconel 750. It was sealing the stainless steel valve to an aluminum surface. There was no evidence of cold welding between the valve, the seal, and the contacting aluminum surface. No metal transferred between the surfaces.

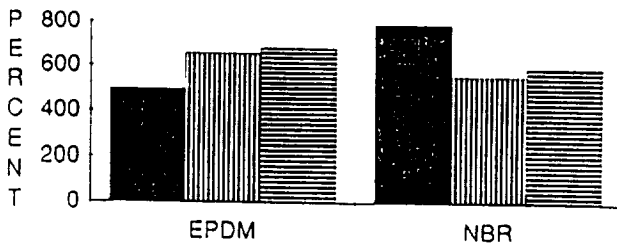
Ethylene propylene diene monomer rubber, EPDM, and acrylonitrile butadiene rubber, NBR, were tested in experiment P0005, Space Aging of Solid Rocket Materials. The elastomers were not exposed to U.V. radiation or to atomic oxygen, but had extended exposure to hard vacuum. Both elastomers exhibited slight changes in strength, modulus and ultimate elongation.

Properties of EPDM and NBR

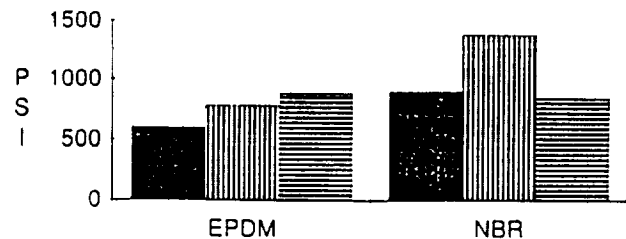
TENSILE STRENGTH



ULTIMATE ELONGATION



TENSILE MODULUS



Results from the Testing and Analysis of LDEF Batteries

**Steve Spear
Harry Dursch
Chris Johnson**

Boeing Aerospace

Results from Testing and Analysis of LDEF Batteries

Batteries were used on LDEF to provide power to both the active experiments and the experiment support equipment such as the Experiment Initiate System, Experiment Power and Data System (data acquisition system), and the Environment Exposure Control Canisters.

Three different types of batteries were used: lithium sulfur dioxide (LiSO_2), lithium carbon monofluoride (LiCF), and nickel cadmium (NiCd). A total of 92 LiSO_2 , 10 LiCF , and 1 NiCd batteries were flown on LDEF. In addition, approximately 20 LiSO_2 batteries were kept in cold storage at NASA LaRC. This presentation reviews the various investigations and post-flight analyses of the flight and control batteries.

The primary objective of these studies was to identify degradation modes (if any) of the batteries and to provide information useful to future spacecraft missions. Systems SIG involvement in the post-flight evaluation of LDEF batteries has been two-fold: (1) funding SAFT (original manufacturer of the LiSO_2 batteries) to perform characterization of 13 LiSO_2 batteries (10 flight and 3 control batteries) and (2) integrate investigator results. No testing of LDEF batteries occurred at Boeing.

LiSO₂ Batteries

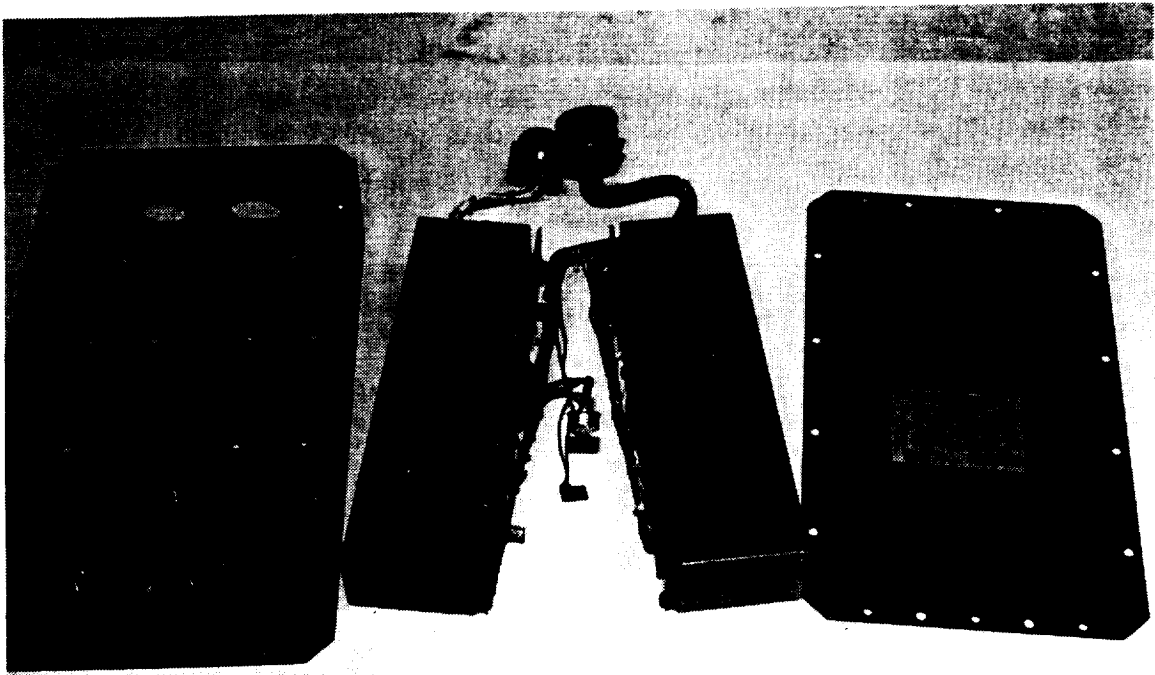
A total of 92 LiSO₂ battery packages (provided by NASA LaRC) were flown on LDEF. These batteries were divided into three voltages: 7.5, 12, and 28 volts. The individual cells were D-size and manufactured by Duracell (the Duracell LiSO₂ division has been purchased by SAFT America). Because many of the active experiments and LDEF support systems experienced cutoff prior to expending the total battery capacity, a large number of batteries had substantial remaining charge when LDEF was retrieved. Several control batteries were kept in cold storage at NASA LaRC throughout LDEF's mission and were then made available to the battery community.

During LDEF de-integration at Kennedy Space Center, all batteries were checked for evidence of leaks and post-flight voltages determined. No remaining capacity measurements were made.

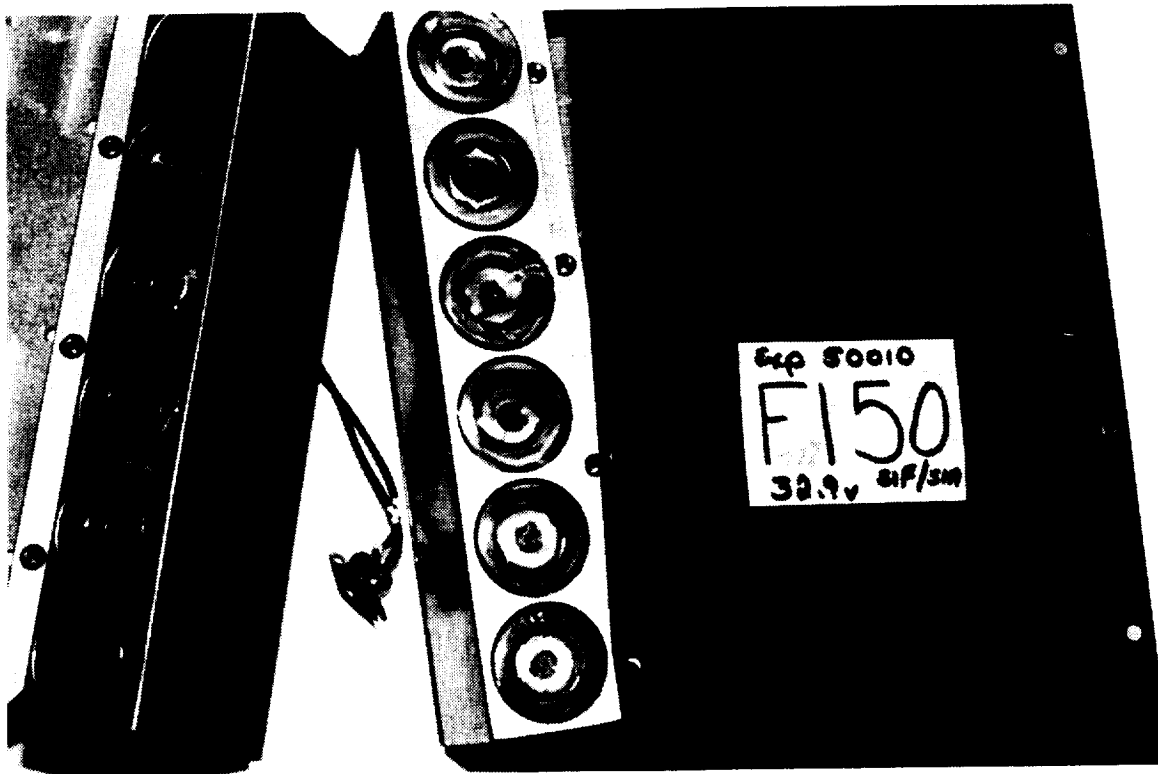
SAFT America received 10 flight batteries and 3 control batteries for comparative evaluation and destructive physical analysis. The results are contained in the footnoted reference. The retained capacity testing of three control batteries showed that the capacity loss over approximately 69 months was around 11%. The one unused battery flown on LDEF suffered an almost 30% capacity loss. The difference in capacity loss is attributed to differences in ambient temperatures. The ground-stored batteries did not see temperatures above 40° F whereas the flight batteries were subjected to temperature ranges from 40° F to over 95° F during the LDEF mission. The LiSO₂ batteries suffered capacity loss due to parasitic reactions.

The following four figures show representative photographs of the LiSO₂ battery disassemblies performed at SAFT. This figure shows both a LiSO₂ battery case disassembled and a close up of a LiSO₂ cell block.

* Raman, "Experimentation and Destructive Physical Analysis for the Space-Exposed LiSO₂ Batteries from the LDEF," SAFT America, Inc., 1991.



LISO₂ Battery Case Disassembled

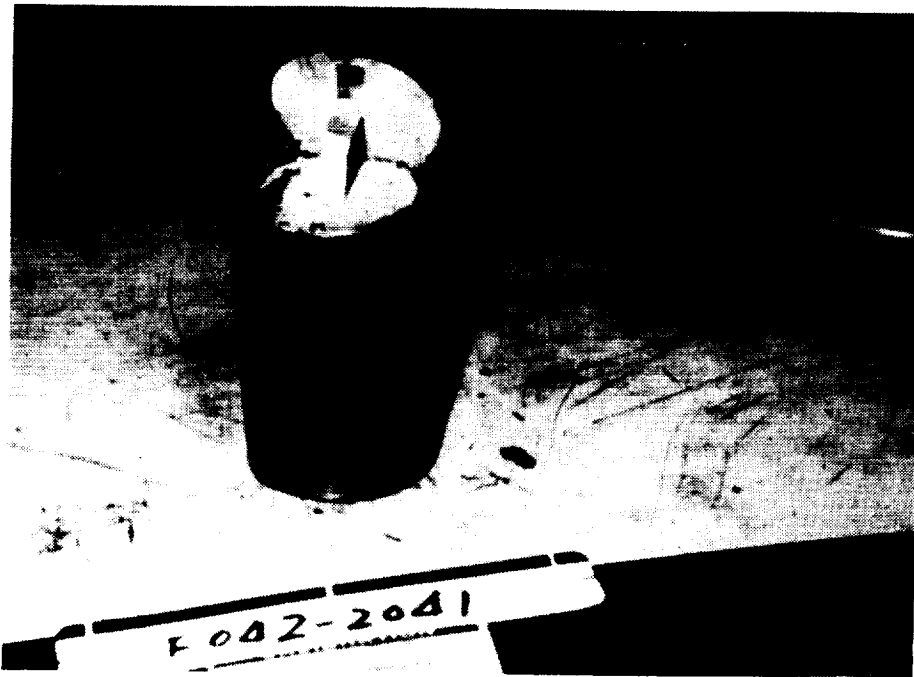


Closeup of LISO₂ Cell Block

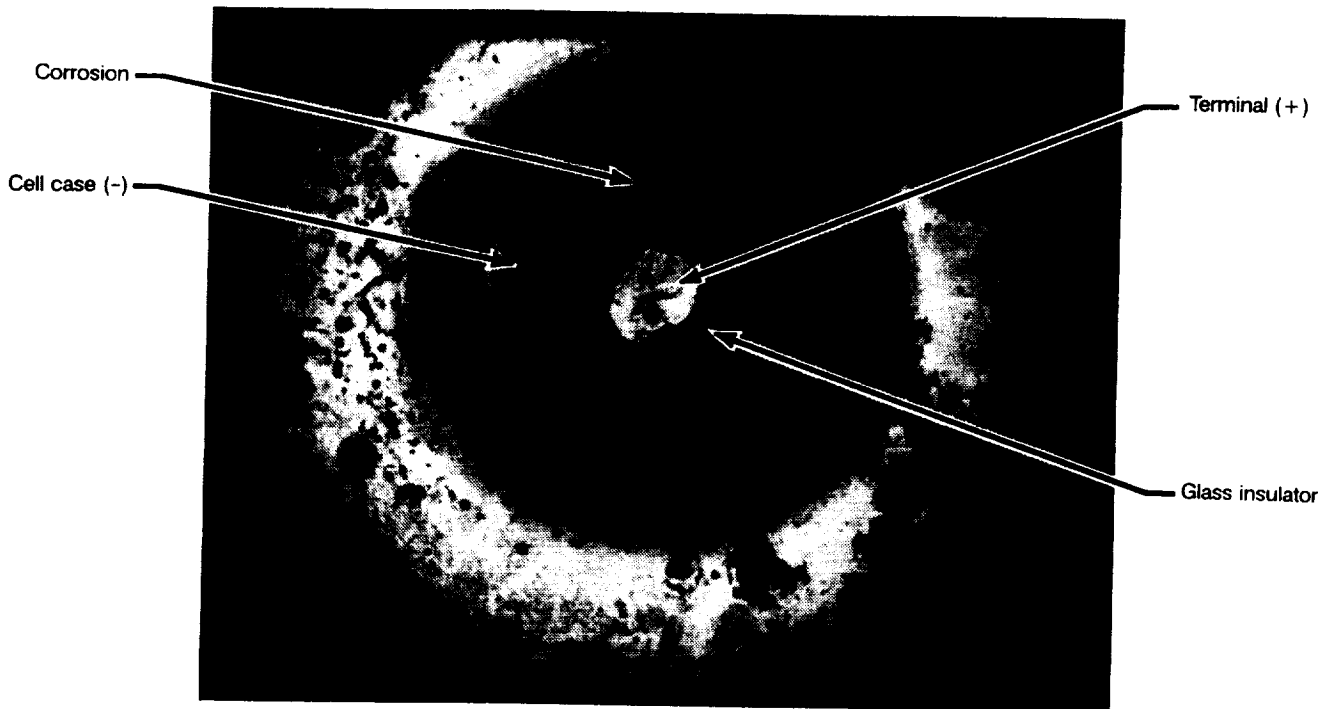
ORIGINAL TYPE
BLACK AND WHITE PHOTOGRAPH

Results of LISO₂ Investigations Con't

This figure shows a LISO₂ cell opened and a close up of the corrosion around the glass to metal seal. The corrosion around the seal was expected and was also found on the control batteries.



LISO₂ Cell Opened



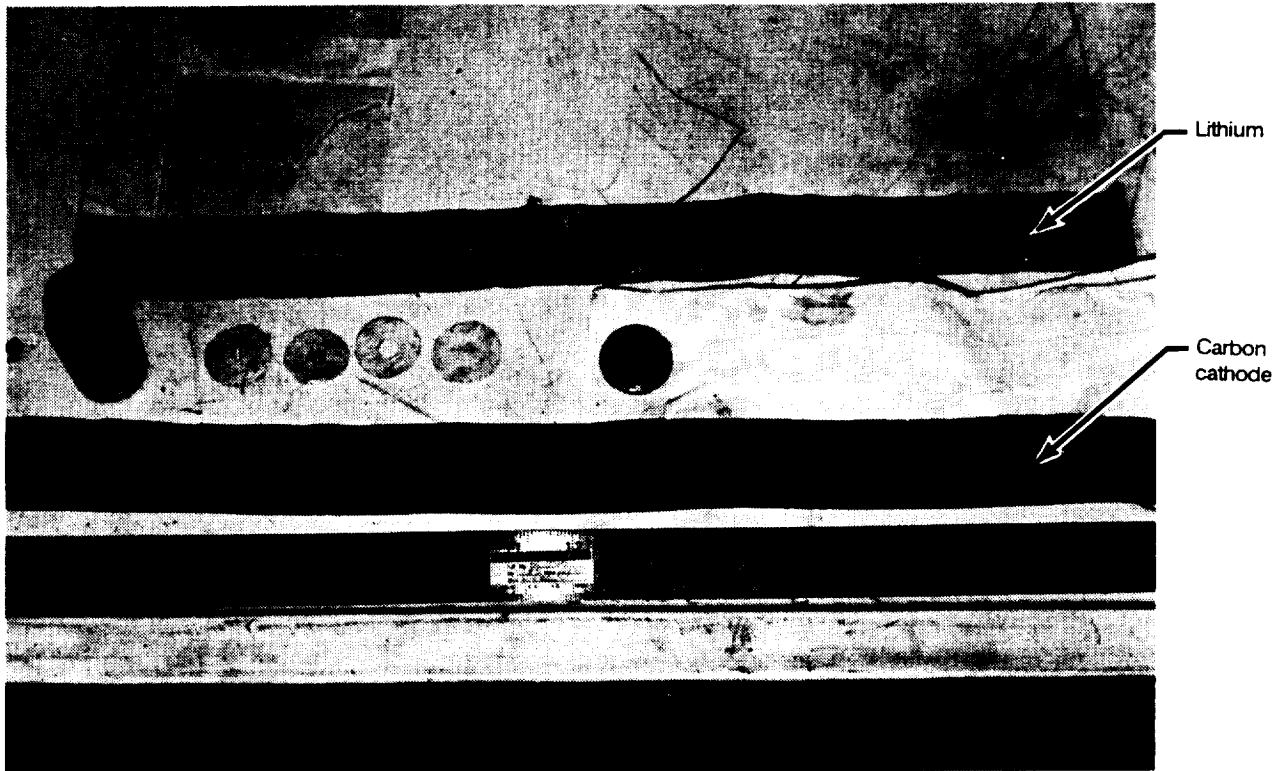
Closeup of Glass to Metal Seal

Results of LiSO_2 Investigations Con't

Shown is the condition of the lithium anode and the carbon cathode from a control battery. Note the good condition of the lithium strip.



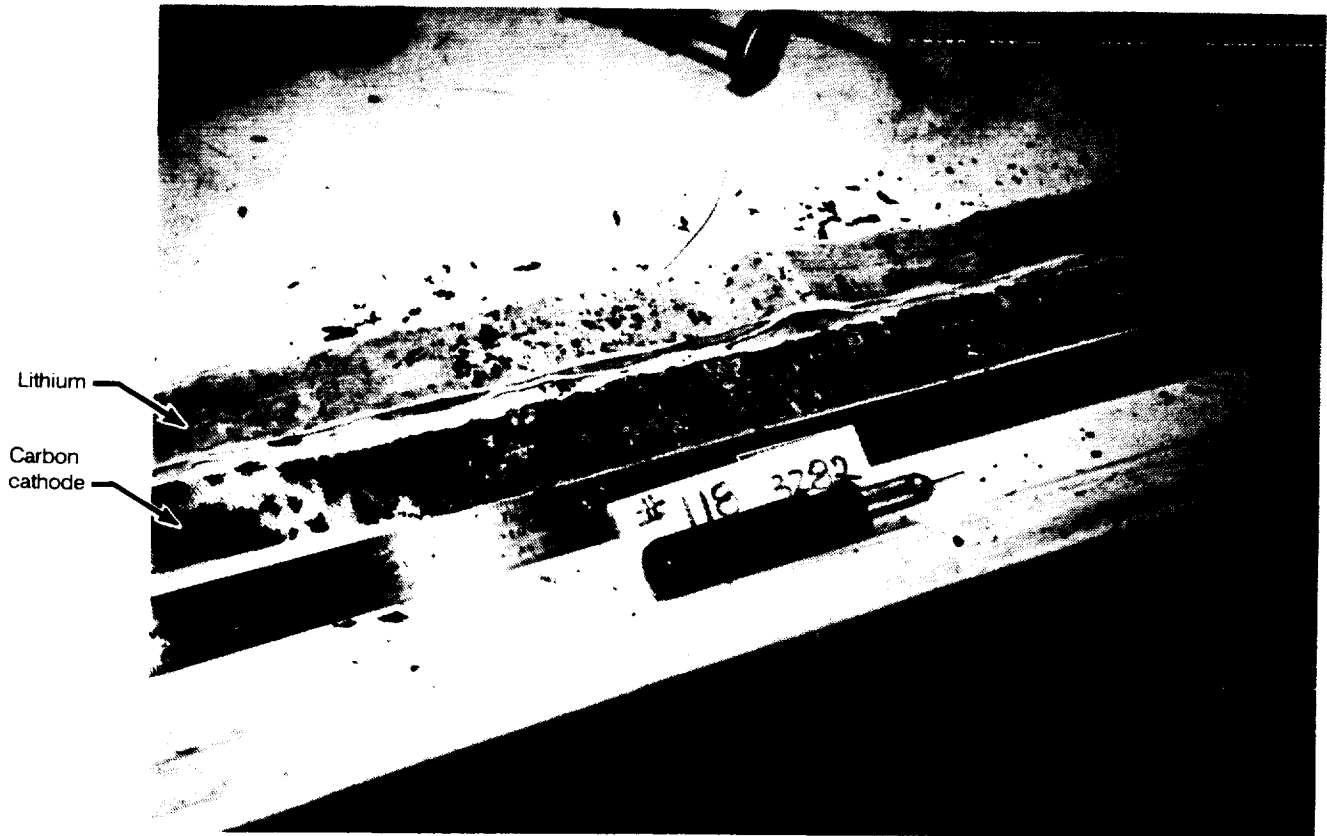
LiSO_2 Cell Electrode Materials



LiSO_2 Cell Components - Control Cell

Results of LiSO_2 Investigations Con't

This photo shows the lithium and carbon from a flight battery that was at a 35% state of charge. Note the absence of lithium.



LiSO_2 Cell Components – Flight Battery With a 35% State of Charge

ORIGINAL PAGE
BLACK AND WHITE PHOTOGRAPH

Investigation of LiCF Batteries

Investigation of the LiCF batteries has been performed by AZ Technology, NASA MSFC, and Naval Weapons Support Center. All ten LiCF batteries were used on the two active MSFC experiments: four batteries were used on the MSFC heat pipe experiment (Experiment S1005) and the other six were used on the Thermal Control Surface Experiment (Experiment S0069). As predicted, all ten batteries were depleted on return of LDEF. The required experiment life was 12 months, with an expected life of 15 to 18 months. All ten batteries met or exceeded life expectations

The cells were roughly double D size having vented construction with a rated capacity of 25 Ah and a nominal voltage of 3 volts. The cells were potted in a plastic block and hermetically sealed with a "can opener" vent for relief of cell over-pressure.

LICF BATTERIES

- **Used on MSFC experiments**
 - **S0069 & S1005**

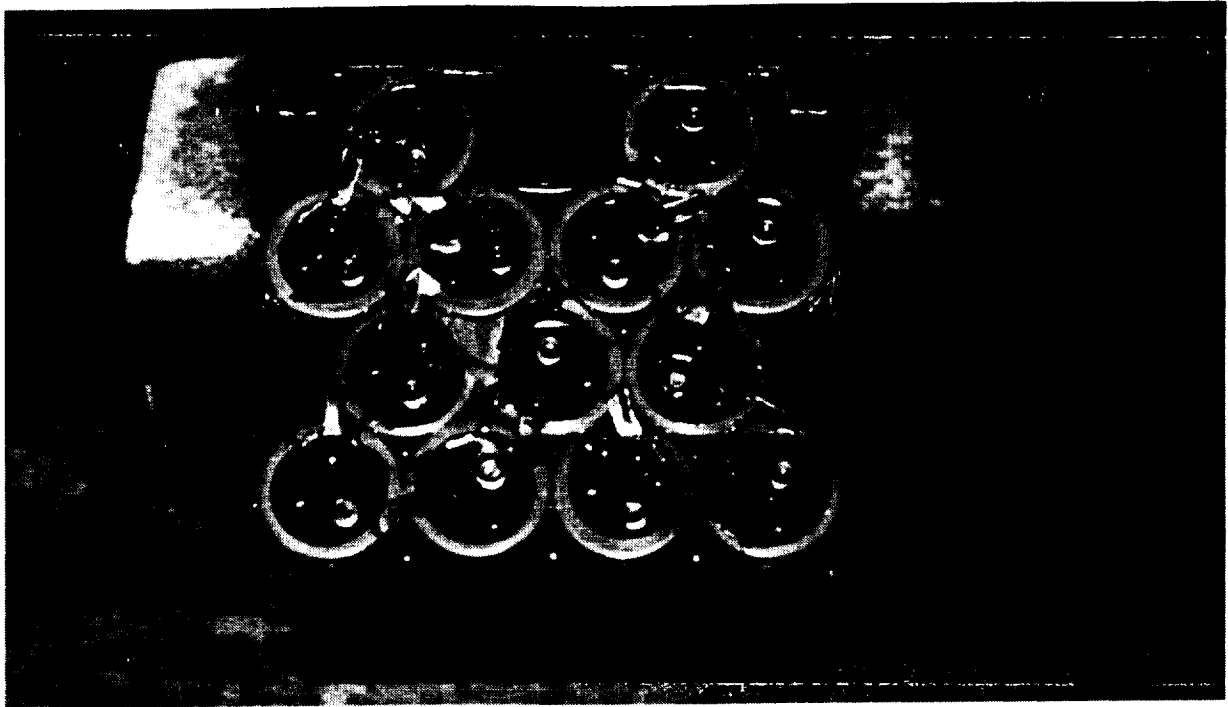
- **All ten batteries returned depleted**

- **S0069 battery life was 19.5 months**
 - **Anticipated lifetime was 15-18 months**

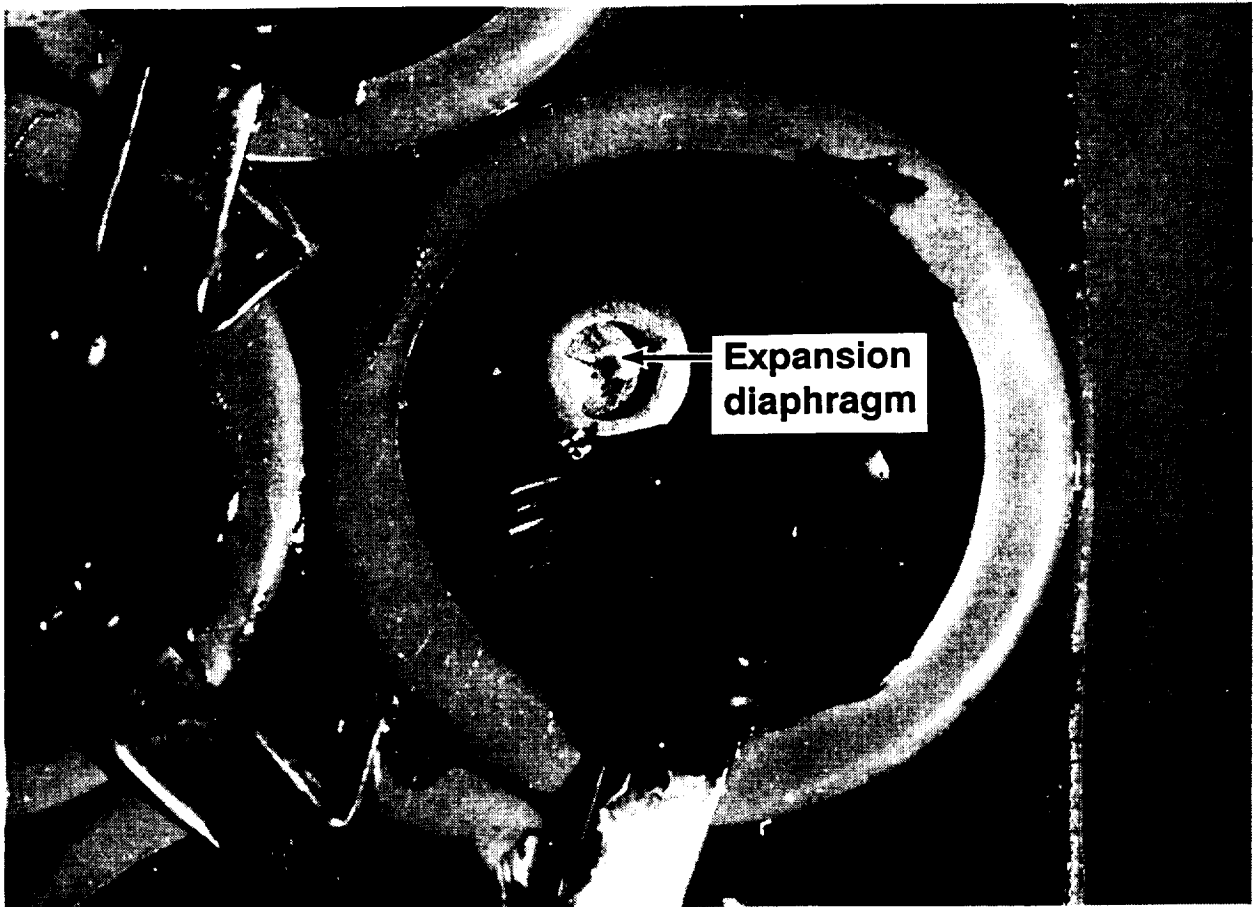
- **Noticeable order evident for all batteries**
 - **Source identified as the electrolyte**
 - **O-ring did not operate as designed**

LiCF Electrolyte Leakage

All ten LiCF batteries possessed a strong odor, first noticed during the deintegration of S0069 and S1005 at MSFC. The electrolyte used in the Eagle-Picher Industries LiCF batteries is dimethyl sulfite, which contains small amounts of other sulfur compounds that can be quite odorous. AZ Technology investigated the cause and effect of the leaked electrolyte vapors from the ethylene propylene battery containment case. The presence of the odor was determined to be the normal byproduct of the discharge process. The LiCF cell is designed with an expansion diaphragm on the top of the cell with a sharp, rigid protrusion adjacent to the diaphragm. This photo shows a LiCF battery (made up of 13 individual cells) removed from the battery case. The diaphragm expanded during the slow discharge process when internal cell pressure increased. Eventually the diaphragm was punctured, releasing the electrolyte vapors. The cells were sealed in battery boxes. The O-ring seal experienced softening and deformation due to the extended exposure to the electrolyte vapors which allowed the vapors to leak from the battery box. However, this created no performance problem for the battery or associated experiment hardware. It is important to note that the ground-stored LiCF batteries experienced the same phenomena.



LiCF Cells Removed From Battery Case



LiCF Cell

ORIGINAL FILE
BLACK AND WHITE PHOTOGRAPH

LICF Voltage Versus Time On-orbit

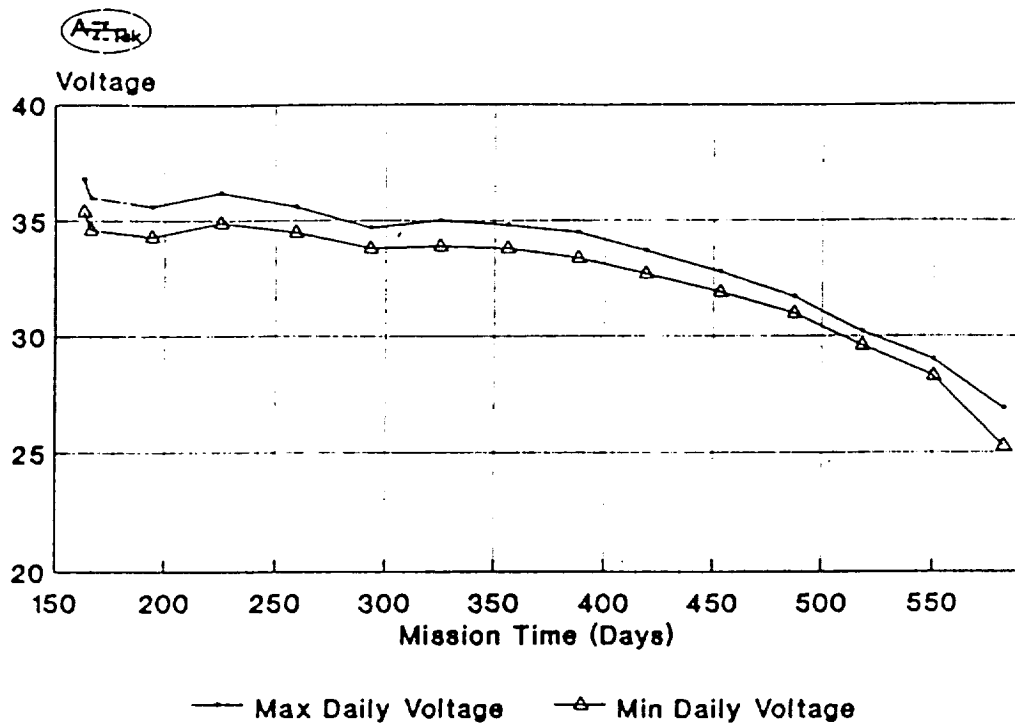
This figure, provided by AZ Technology, shows the gradual degradation of battery voltage versus time for one of the four batteries used on S0069.

Lithium Carbon Monofluoride Batteries - LDEF Flight Data

Gradual Degradation of Voltage with Flight Duration

12 Month Mission - Achieved

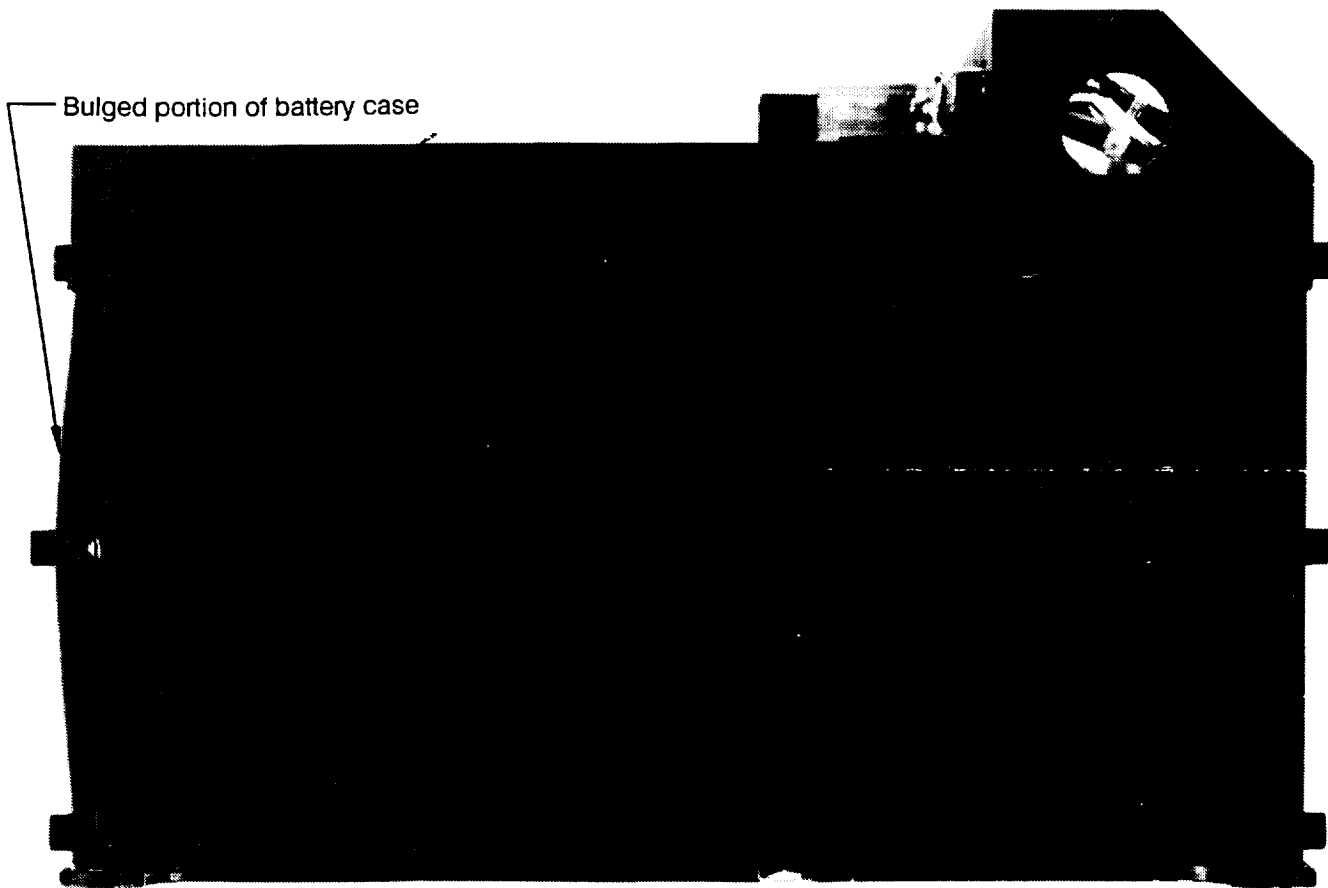
12 to 18 Month Expected Life - Achieved



Investigation of the Nickel Cadmium Battery

One NiCd battery manufactured by General Electric was flown on the Low Temperature Heat Pipe Experiment (Experiment S1001). This battery was continuously charged by a four arrays of solar cells which were located on the space end of LDEF. Analysis and testing of the battery was performed by S. Tiller and D. Sullivan of NASA GSFC. The battery consisted of 18 cells, which were mounted on an aluminum baseplate. Pre-flight power analysis for the 12 Ah NiCd battery indicated a need for 2 to 3 amp discharge. However, reduction in the experiment current requirements during flight resulted in much lower power demand. This led to an overcharging situation that caused the development of internal pressure, resulting in the bulging of the cell case. This bulging is especially noticeable on one end of the cell pack, as shown in this figure.

LDEF/HEPP
POWER SYSTEM BATTERY
(12-AH NiCd)



Bulged portion of battery case

Bulging of NiCd Battery Case

ORIGINAL PAGE
BLACK AND WHITE PHOTOGRAPH

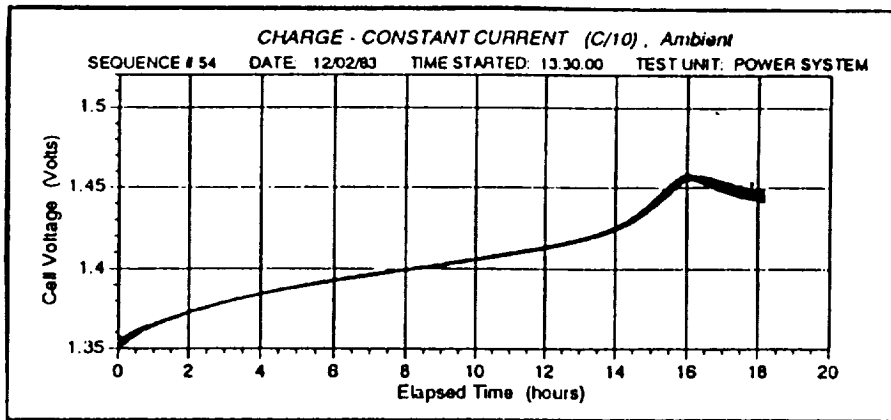
Loss of NiCd Overcharge Protection

The loss of overcharge protection is obvious from the difference in voltage performance shown for the pre-flight and post-flight measurements of cells on constant current, as shown in this figure. Pre-flight charge profile showed all cells were matched and reached full state of charge in 18 hours, while maintaining voltage below 1.46 volts. Post-flight data showed considerable differences between cells with cell #10 (this cell bulged the most during the mission) reaching a high voltage of 1.52 volts which tripped the charge for the battery off at 14 hours of charge. Discharge testing produced similar results.

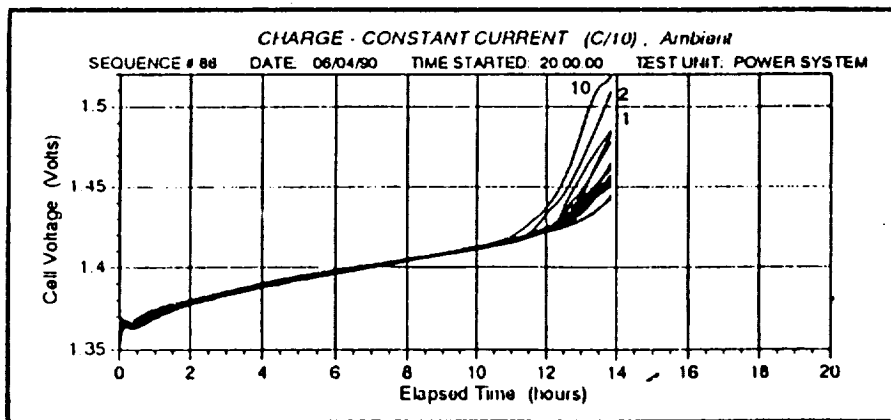
Despite the obvious bulging of some cells, loss of overcharge protection, and failure of cell #10 during the open circuit recovery test, the battery still had the capability to provide output current in excess of the cell manufacturer's rated capacity of 12 Ah.

NiCd Battery

Constant Current Charge Indicates Loss of Overcharge Protection



Pre-flight Capacity Charge



Post-flight Capacity Charge showing loss of overcharge protection

Summary of LDEF Battery Findings

All LDEF batteries were mounted on interior surfaces of LDEF and, therefore, experienced a mild temperature environment. All batteries met or exceeded their predicted post-flight state-of-charge.

The LiSO₂ batteries exhibited good charge retention, with a loss in capacity of an unused flight battery of less than 5% per year. The LDEF LiSO₂ batteries showed charge retention properties commensurate with that expected, based on the temperatures experienced by these batteries. The favorable performance underscores the merit of the selection of LiSO₂ batteries of similar design for the Galileo mission.

Testing completed at the Naval Weapons Support Center investigated the post-flight condition of three LiCF batteries: one flight battery provided by MSFC, one control battery discharged to 0 volts prior to dissection, and one control battery dissected as received. Their findings showed that no significant changes occurred in the chemistry or function of the LiCF cells as a result of operation on LDEF. The differences found in material compositions were either trivial, or when significant, a result of long term degradation of cell electrolyte in storage prior to discharge.

The NiCd battery showed the effect of loss of overcharge protection. However, this did not affect the on-orbit performance.

For additional information, the reader is referred to the Systems SIG report dated February, 1992.

LDEF BATTERY SUMMARY

- **LDEF batteries met and exceeded design requirements and predicted lifetimes.**
- **LiCF flight batteries experienced leakage of electrolyte vapors.**
 - **Similar phenomena occurred for ground stored LiCF batteries.**
- **NiCd battery suffered loss of overcharge protection.**

**EFFECTS OF LONG-TERM EXPOSURE ON LDEF
FASTENER ASSEMBLIES****Steve Spear
Harry Dursch****Boeing Aerospace****Effects of Long Term Exposure on LDEF Fastener Assemblies**

This presentation summarizes Systems SIG findings from testing and analysis of fastener assemblies used on the LDEF structure, the tray mounting clamps, and by the various experimenters.

PRIMARY STRUCTURE FASTENERS

- **STAINLESS STEEL BOLTS**
 - 1/4 to 7/8 inch diameters
 - Silver-plated nuts
- **All primary structure fasteners were re-torqued to pre-flight values following experiment deintegration**
 - Only 4% (119 of 2,928) assemblies had relaxed
 - Nut rotations required to re-establish pre-flight torque levels ranged from 5 to 20 degrees
 - Small number of relaxed assemblies indicates high reliability of bolted joints in space applications
- **Intercostal fastener assembly cross-section**

(Original figures unavailable)

Primary Structure Fasteners

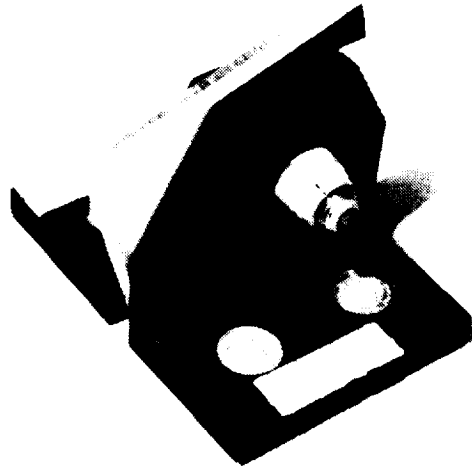
The LDEF structure consisted of a welded center ring and aluminum beams called longerons connecting the center ring frame to the two end frames. Aluminum intercostals were used to connect longeron to longeron. The longerons were bolted to the end frames and center ring. The intercostals were bolted to the longerons. This provided flexibility in adapting the LDEF structure to meet future Shuttle payload manifest requirements (LDEF was designed as a reusable structure). For overall stiffness, eight tubular structural members stretch diagonally through the interior of LDEF from the center ring to the end frames. These components of the LDEF structure were also bolted into place. Stainless steel bolts and silver plated nuts were used to bolt the structural components together.

As one of the last deintegration activities, all LDEF primary structure fastener assemblies were re-torqued to pre-flight values. Only approximately 4% of the 2928 fastener assemblies showed any sign of relaxation. Nut rotations required to re-establish the pre-flight torque values were closely monitored. These values ranged from 5 to 20 degrees.

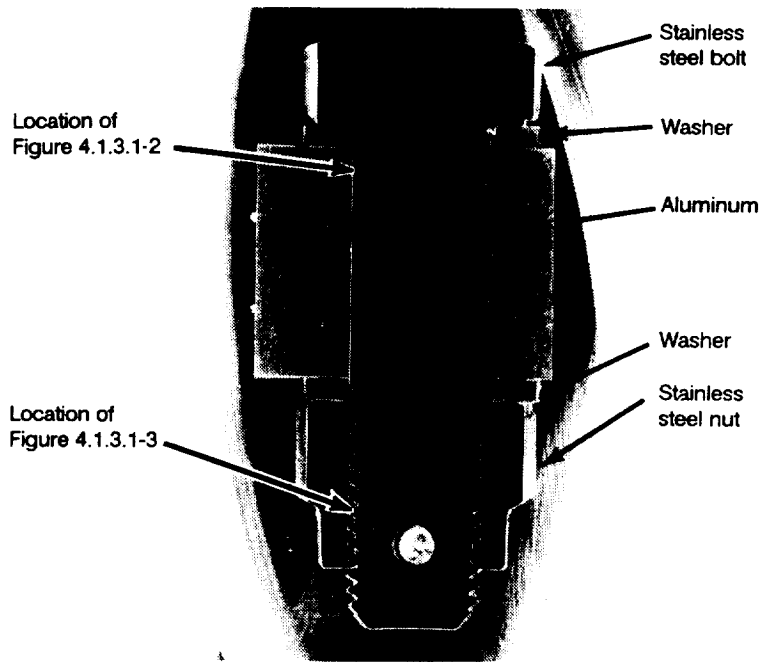
This small number of relaxed assemblies indicates the high reliability of bolted assemblies for spacecraft applications. See figure 1.

Intercostal Fastener Assembly

An undisturbed intercostal fastener assembly (shown in figure 2) was removed from the LDEF structure to investigate its post-flight condition. This fastener was selected because of its availability and not because of any evidence of coldwelding, galling or any other suspect condition.



Fastener Assembly



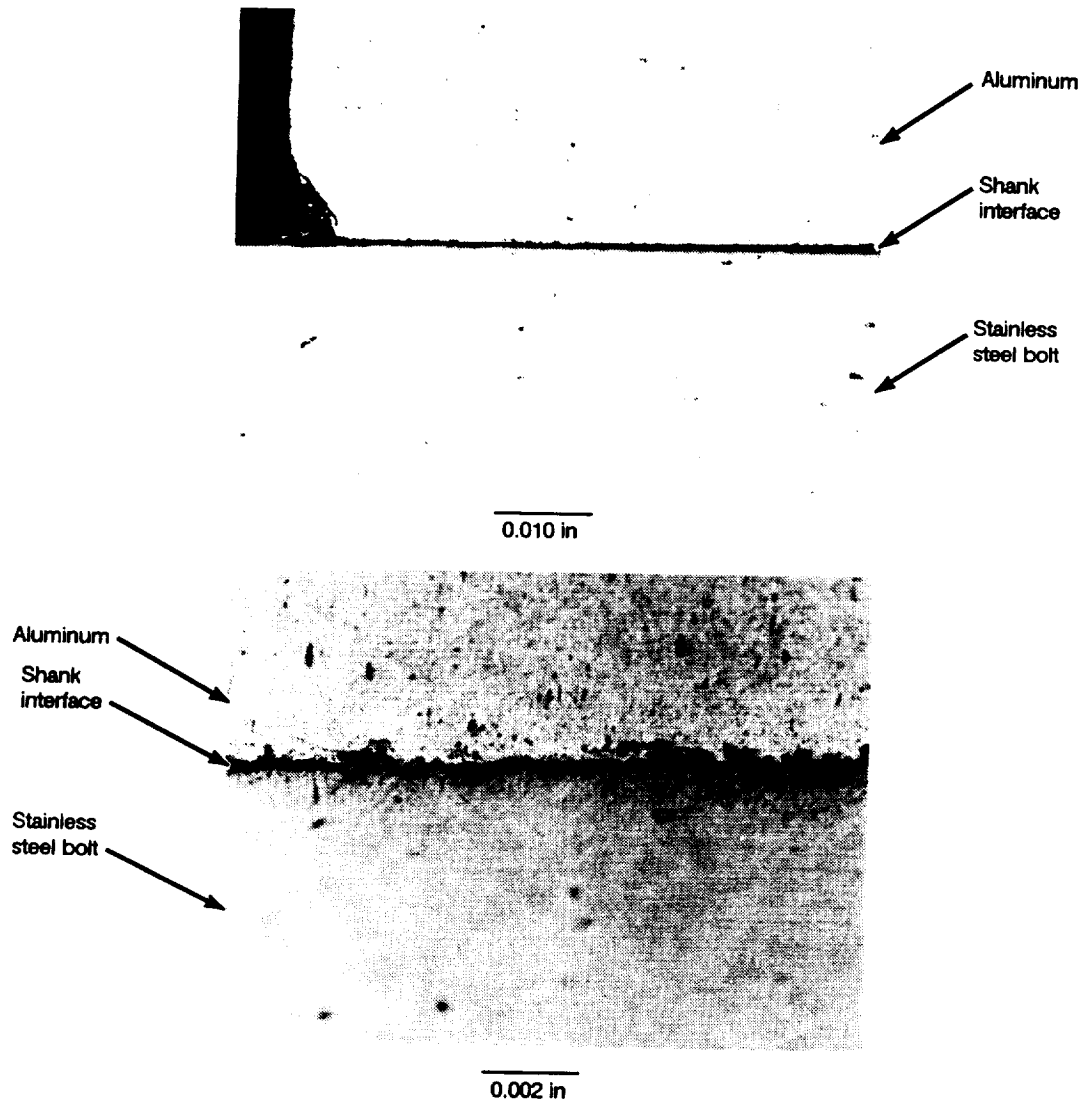
Metallographic Cross-Section

0.040 in

Figure 2 Unassembled Intercostal Fastener Assembly

Intercostal Fastener Assembly Cross-Section

The stainless steel/aluminum interfaces and bolt/nut interfaces were examined for indications of damage. Closeups of these areas are shown in figures 3 and 4. Metallographic examination of the bolt shank interface revealed no evidence of galling or coldwelding.

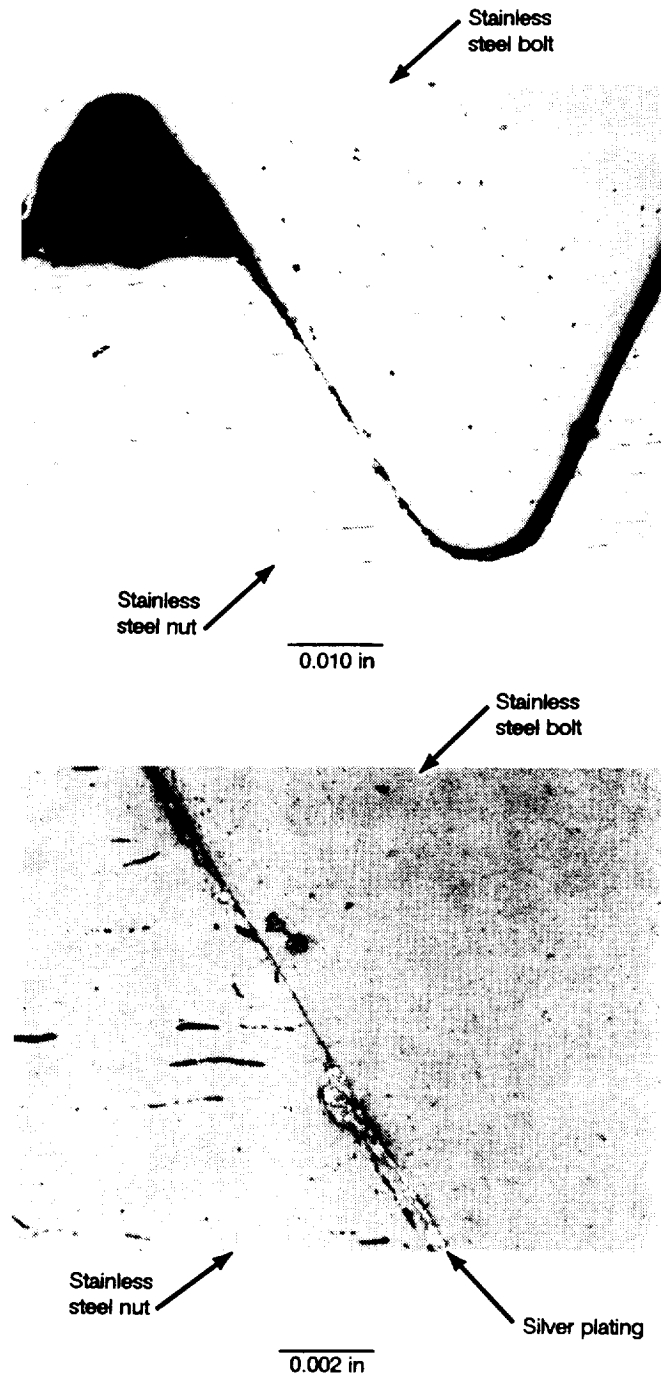


Intercostal Fastener Assembly Cross-Section

Figure 3 Closeup of Shank Interface Area Indicated in Figure 2

Intercostal Fastener Assembly Cross-Section

The thread mating surfaces also show no evidence of coldwelding; however, some minor galling and smearing of the silver plating is evident. The behavior of the plating is normal because it is specified to act as a lubricant during both installation and removal to prevent galling and seizure of the nut to the bolt (fig. 4).



Intercostal Fastener Assembly Cross-Section

Figure 4 Closeup of Nut/Bolt Thread Faying Surfaces as Indicated in Figure 2 (Note Smearing of Ag-Plating Which Acts as a Lubricant Between the Nut and Bolt.)

Experiment Tray Clamp Fasteners

The experiment trays were held to the longerons and intercostals by aluminum clamps. These clamps consisted of flat 0.25" thick rectangular or "L" shaped plates with three mounting holes in them. They were attached to the structure with NAS1004-4 hexagon head 0.25-28 bolts. The bolts, with alodined aluminum washers under the head, were installed into self-locking threaded inserts mounted in the primary structure. Installation torque was 75 in-lb, plus or minus 5 in-lb. See figure 5.

INSTALLATION DETAILS

- **Trays held in structure by 1/4" aluminum clamps**
- **Clamps mounted to structure with three A286 heat-resistant steel bolts**
 - **0.25-28 UNF-3A**
 - **Heat-treated to 140 KSI and passivated**
 - **Alodined aluminum washers**
 - **Self-locking threaded inserts installed on structure**
 - **Bolts cleaned with alcohol prior to installation**
 - **Pre-flight installation torque 75 ± 5 in-lb**
 - **Bolts installed into inserts 2 or 3 times**

Experiment Tray Clamp Fasteners Cont.

During the experiment tray removal portion of deintegration, unseating (breakaway) torque values were recorded for 2,159 of the 2,232 tray clamp fasteners. Prevailing (running) torque values were obtained for every third bolt (the middle of the three bolts in each tray clamp). A database was created that contained all unseating and prevailing torques as a function of the bolt and its location on LDEF.

The results in figure 6 show that the unseating torques averaged 72 in-lbs and ranged between 10 and 205 in-lbs. The averages of the 20 lowest and 20 highest values were 31 and 175 in-lbs. The average unseating torques were similar throughout LDEF, indicating no pronounced effect of the different LEO exposures on bolt behavior. The prevailing torques averaged 17 in-lbs and ranged between 2 and 132 in-lbs. The average of the 20 highest prevailing torques was 58 in-lbs. There was little correlation between high unseating torques and high prevailing torques. Only one bolt possessed both one of the 20 highest prevailing torques and one of the 20 highest unseating torques.

The threaded insert vendor stated that they were not surprised by the wide variation and range of unseating torques. These values are very unpredictable due to fatigue, bolt stretching, corrosion, particle contamination, etc. The prevailing torque specification for these self locking inserts is a maximum of 30 in-lbs. Approximately 10% of the prevailing torques exceeded this maximum value. Further testing and analysis was performed in an attempt to understand why.

LDEF DEINTEGRATION BOLT TORQUE DATA BASE

- **Data base contains all 2,232 tray clamp bolts**
- **Unseating (breakaway) torques measured for all fasteners**
 - **Average 72 in-lb**
 - **Range 10 to 205 in-lb**
 - **No location effects**
- **Prevailing (running) torques measured for one third of the fasteners**
 - **Average 17 in-lb**
 - **Range 2 to 132 in-lb**
 - **No correlation between high running and high breakaway torques**

Tray Clamp Fastener Rating System

A tray clamp bolt and washer rating system was developed to further characterize the tray clamp fasteners. The various codes used for this rating system are shown in figure 7. Eighty-nine fasteners were examined using 8x magnification and then coded. These codes, along with the associated bolt torque data and associated parameters were entered into another database.

- Bolts**
- B1 = No galling, very little scoring on threads.**
 - B2 = Light galling or thread wear, no metal deposits, threads crests may be sharpened or rounded.**
 - B3 = Medium galling, threads may be sharpened or rounded, a few deposits and smears, a few areas of metal removal.**
 - B4 = Heavy galling, threads sharpened or rounded, several metal deposits, smears of areas of metal removal, slivers.**
 - B5 = Threads mostly removed, much smearing, deposits, metal removal.**

Note: Some bolts were given mixed codes i.e. B2/B3, to better describe them.

- Washers**
- W1 = Very little smearing or scoring.**
 - W2 = Moderate smearing or scoring.**
 - W3 = Heavy smearing or scoring.**

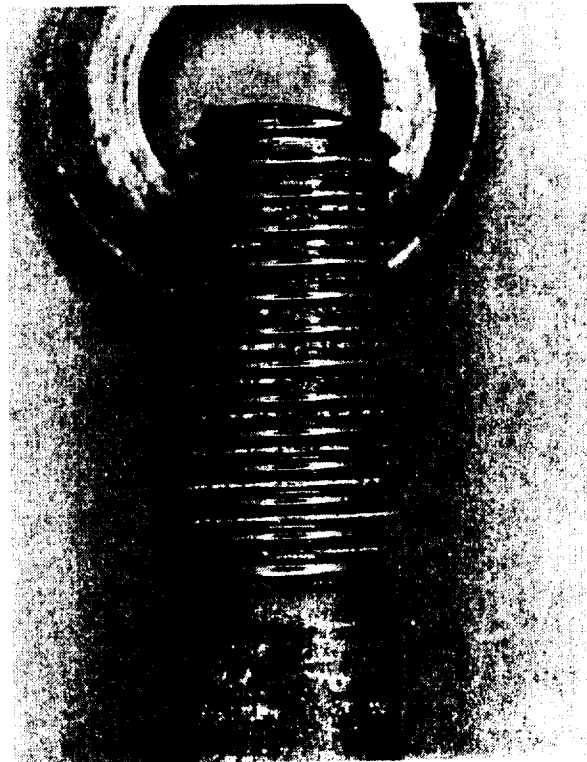
Tray Clamp Fastener with a "B1" Rating

These two photos (fig. 8) show a typical "B1" tray clamp bolt. Both the unseating and prevailing torques were close to the average values. The condition of the bolt threads is nominal.



G4-6B

2.5X



G4-6B

4.5X

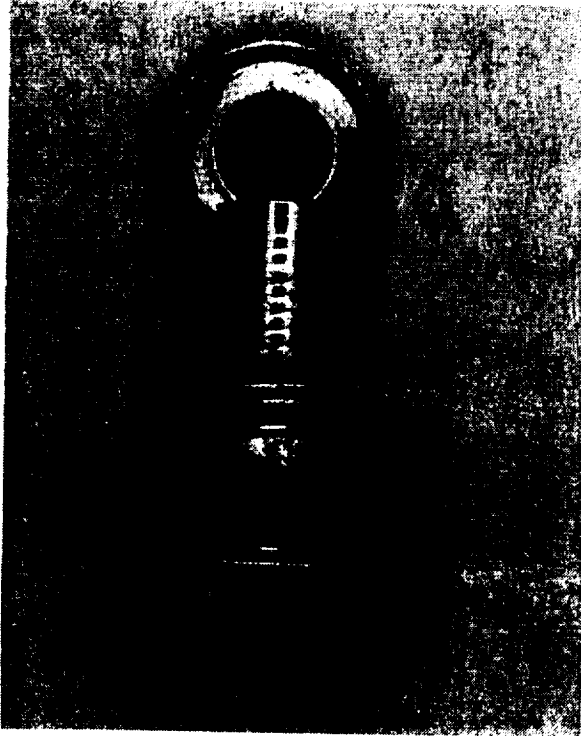
Unseating torque = 70 in-lb

Prevailing torque = 15 in-lb

Tray Clamp Fastener With a "B1" Rating

Tray Clamp Fastener with a "B5" Rating

These two photos (fig. 9) show a typical "B5" tray clamp bolt. While the unseating torque was actually below average, the prevailing torque was almost twice the maximum specification value. Note the severely damaged (stripped) threads.



C1-8B

2.5X



C1-8B

4.5X

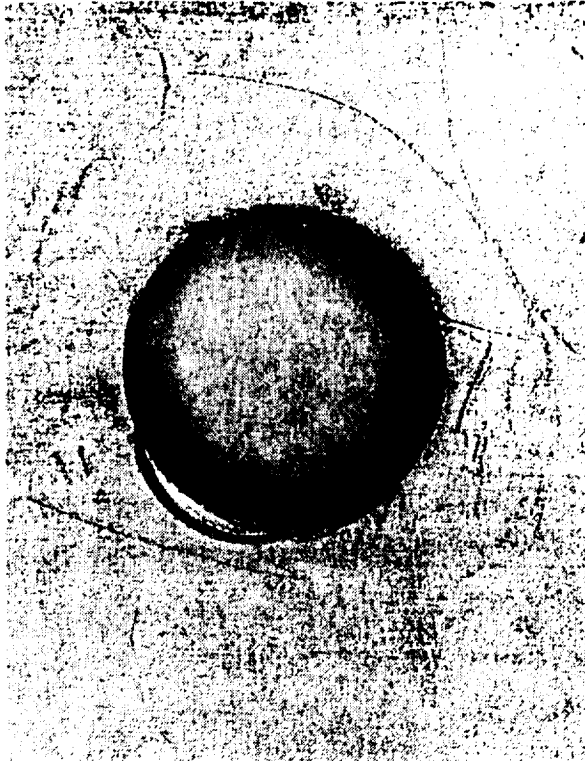
Unseating torque = 190 in-lb

Prevailing torque = 35 in-lb

Tray Clamp Fastener With a "B5" Rating

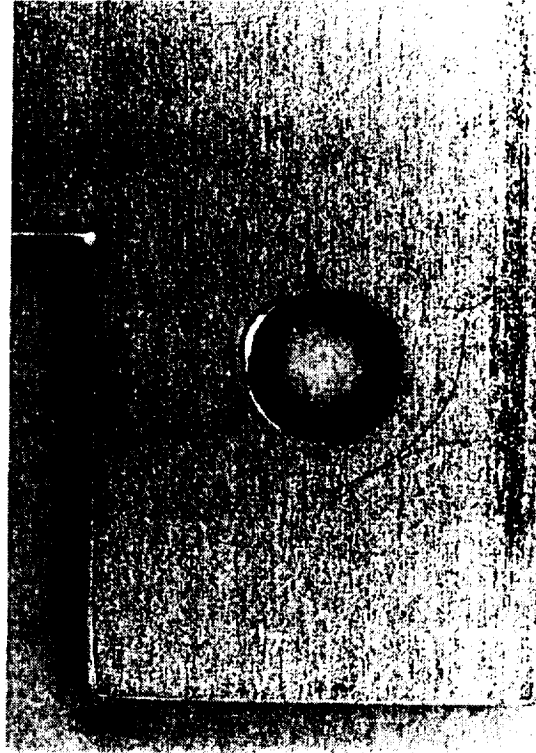
Tray Clamp Shim

As would be expected, the threads of the bolts with the higher prevailing torques generally exhibited greater thread damage. Most of the bolts examined have varying amounts of smears or deposits of aluminum on the grip (unthreaded) portion of the bolt shank, suggesting that there was a hole misalignment between the clamp and structure. Visual examination of a few clamps revealed varying amounts of burnishing in most of the holes. A visual examination of 21 shims (used between the tray clamp and structure) revealed varying degrees of bolt thread contact in the holes. It is thought that this apparent misalignment may have contributed to the high prevailing torques noted for some of the bolts. See figure 10.



E1-3

2.5X



E1-3

5.5X

Unseating torque of bolt = 62 in-lb

Prevailing torque = Unknown

Tray Clamp Shim

ORIGINAL PAGE
BLACK AND WHITE PHOTOGRAPH

Tray Clamp Fastener Conclusions

It is believed that an unusually high percentage of bolts exhibited prevailing torques above the 30 in-lb maximum required for the self-locking inserts, especially for only two or possibly three installation/removal cycles. It is unknown how much bolt contact with the clamp and shim holes and the relative softness of these bolts (140,000 psi versus the more commonly used 160,000 psi ultimate tensile strength) may have contributed to this result.

No clear correlation has been made between thread condition, washer damage, and unseating torques. No evidence of coldwelding was observed. All thread damage was consistent with galling damage generated during installation and removal. See figure 11.

- **Threads of high prevailing torque bolts generally exhibited greater galling damage**
- **Most bolts examined have varying amounts of smears or deposits of aluminum on shanks**
 - **Suggests hole misalignment between clamp holes and structure inserts**
 - **Apparent clamp misalignment may have contributed to high unseating and high prevailing torques upon removal of some bolts**
- **Unusually high percentage of bolts exhibited prevailing torques greater than 30-in lb max permitted for self-locking inserts**
- **No clear correlation thus far between thread condition, washer condition and unseating torques**
- **No evidence of cold-welding. All damage consistent with galling damage**

Experimenter Fasteners

The LDEF Project Office suggested that experimenters use type 303 stainless steel bolts combined with self-locking fasteners. In fact, a wide variety of fastener assemblies and lubrication schemes were used. (fig. 12).

Dr. Richard Vyhna (Experiment A0175) reported severe difficulties with seizure and thread stripping during fastener removal. Typical fastener damage is shown in figure 13.

Further investigation determined that the nut plates had the original MoS₂ dry-film lubricant removed by acid stripping prior to installation. This was done because of possible concerns about volatilization and contamination while on-orbit. The MoS₂ was replaced with cetyl alcohol. Initial speculation was that the fasteners may have coldwelded on-orbit because of insufficient lubrication provided by the cetyl alcohol.

Unseating and prevailing torques were obtained for the majority of the fasteners by Dr. Vyhna. Several fasteners were left undisturbed for analysis by the System SIG. Examination of one of the two trays at Boeing revealed that some of the nutplates had not been stripped of their dry-film lubricant. Correlation of the torque data with the nutplate lubrication conditions (with or without MoS₂) showed that the average prevailing torques associated with the MoS₂ nut plates was 15 in-lbs as opposed to 64 in-lbs for the bare nutplates. The specification for these types of nut plates (with MoS₂) requires a prevailing torque range of 2 to 18 in-lbs. The average unseating torques were the same for both the MoS₂ and cetyl alcohol nutplates at 31 in-lbs. If coldwelding had occurred in the cetyl alcohol lubricated nutplates (as was initially speculated), the unseating torques would have been substantially higher and there would have been a difference in unseating torque values between the MoS₂ and cetyl alcohol nutplates. The excessively high cetyl alcohol nutplate prevailing torques were a result of severe galling. The removal difficulties were a direct result of lack of adequate lubrication during removal that caused additional galling. This resulted in seizure, thread stripping, and sheared bolts.

Fasteners and clamps located graphite-reinforced composite panels

- A286 bolts, no finish
- A286 self-locking nut plates
 - Majority had MoS₂ dri-lube removed by acid-stripping
 - Cetyl alcohol used as lubricant during installation

Experienced severe seizure/thread stripping during post flight removal

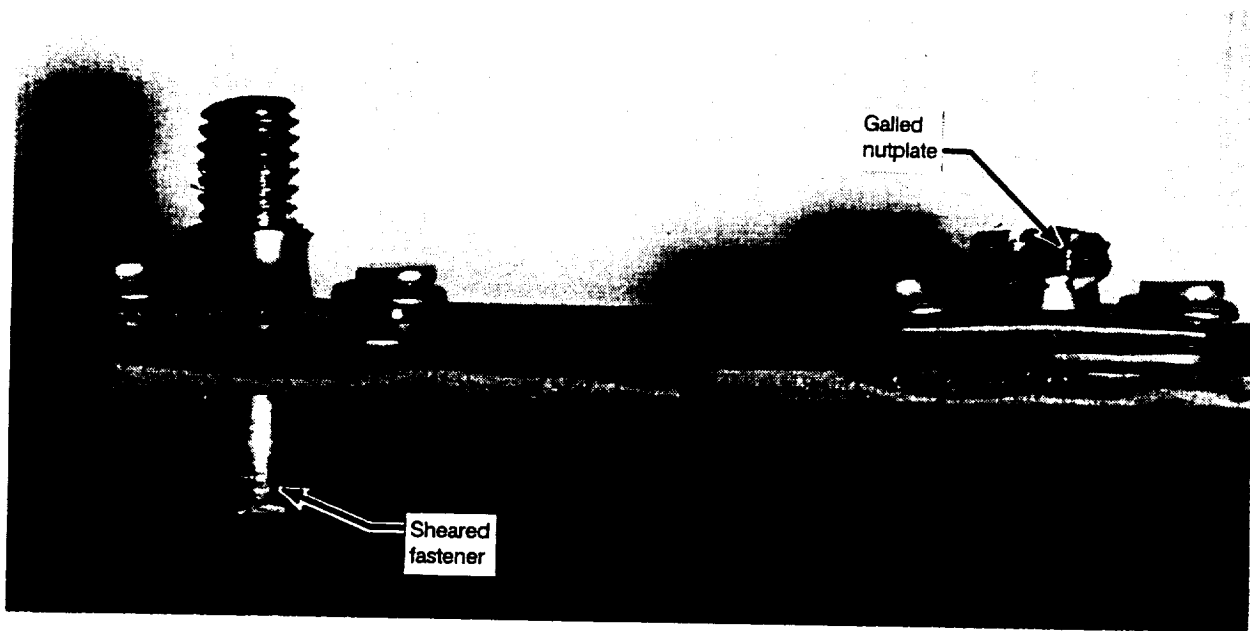
- Average breaking torques:
w/MoS₂: 31 in-lb, w/o MoS₂ : 31 in-lb.
- Average running torques:
w/MoS₂: 15 in-lb, w/o MoS₂: 65 in-lb.

Post flight examination

- Correlated seizure with galling during installation caused by lack of MoS₂
- No evidence of coldwelding

Severely Damaged Experimenter Fastener Assemblies

This photo (fig. 13) shows two of the severely damaged fastener assemblies from Experiment A0175. Note the severely damaged nut plate and sheared fastener. One of the Boeing fastener experts stated that this was the worst galling he had seen in his 30 years of working with fasteners.

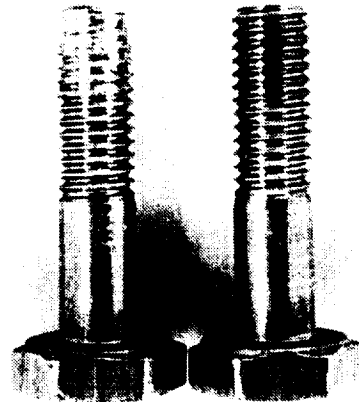


A0175 Sheared Fastener and Galled Nutplate

ORIGINAL PAGE
BLACK AND WHITE PHOTOGRAPH

Experiment A0175 Tray Fasteners

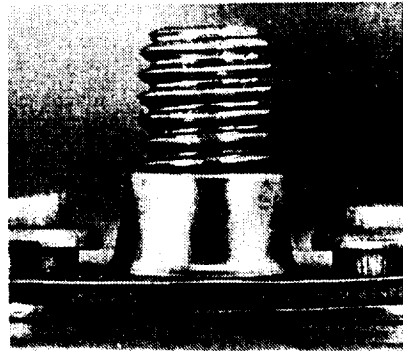
Figure 14 shows typical bolts removed from nutplates that had the MoS2 removed prior to bolt installation and removed from nutplates that had the MoS2 intact. Fourier transform infrared spectroscopy (FTIR) found no traces of the cetyl alcohol remaining in either the nutplates or bolts.



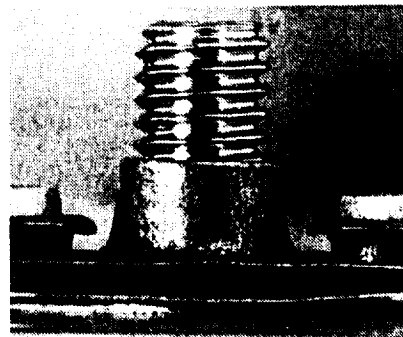
No MoS2

MoS2

(Top) – Comparison of Thread Conditions of AO175 Tray Bolts Removed from Nut Plates. Undisturbed Assemblies Were Cross-Sectioned. Note Thread Galling Damage on Fastener That Had MoS2 Removed (Center).



No MoS2



Fastener Conclusions

The LDEF deintegration team and several experimenters noted severe fastener damage and hardware removal difficulties during post-flight activities. The System SIG has investigated all reported instances, and in all cases examined to date, the difficulties were attributed to galling during installation or post-flight removal. To date, no evidence of coldwelding has been found. Correct selection of materials and lubricants as well as proper mechanical procedures is essential to ensure successful on-orbit or post-flight installation and removal of hardware (fig. 15). For additional details on the investigation of fasteners flown on LDEF, the reader is referred to the February, 1992, Systems SIG Interim Report.

- **Fastener removal difficulties in all cases have been related to galling damage on installation or during removal**
- **No evidence of cold-welding**
- **Stainless steel fasteners are very susceptible to galling**
 - **Success application on orbital replacement units (ORU 's)**
 - **High thread quality and, most importantly,**
 - **Effective lubrication schemes or surface modifications**
- **Simulated space effects testing, in conjunction with tribology studies, is required to determine optimal lubrication schemes for long-term space exposure for high-reliability fasteners to be employed on ORU's**

**Results From Testing And Analysis Of Solar Cells
Flown on LDEF**

**Harry Dursch
Boeing Aerospace**

Results from Testing and Analysis of Solar Cells Flown on LDEF

This presentation provides a brief discussion of the solar cell experiments flown on LDEF. The information presented is a collation of results published by the various experimenters. This process of collation and documentation is an ongoing Systems SIG effort. No testing of solar cells has occurred at Boeing.

OUTLINE

- Overview of solar cells flown**
- Description of the various cell experiments and results to date**
- Summary of findings**

SOLAR CELLS FLOWN FOR VARIETY OF PURPOSES

- **Four arrays actively charged a NiCd battery**
- **Cells actively monitored for first 325 days of mission**
- **Cells were functioning components of active experiments**
- **Cells, coverglasses, adhesives, and array materials passively exposed**
- **Variety of LEO exposures**
 - **Leading edge**
 - **Trailing edge**
 - **Space end**

Solar Cells Flown for a Variety of Reasons

There were nine LDEF experiments that possessed solar cells, solar cell components, and/or solar array materials. The complexity of experiments ranged from active on-orbit monitoring of solar cells (Experiment S0014) to recharging a nickel-cadmium battery used to power a heat pipe experiment (Experiment S1001) to passive exposure. The vast majority of solar cells were silicon based but two experiments flew GaAs solar cells (Experiments S0014 and M0003-4).

Table of Experiments Possessing Solar Cells

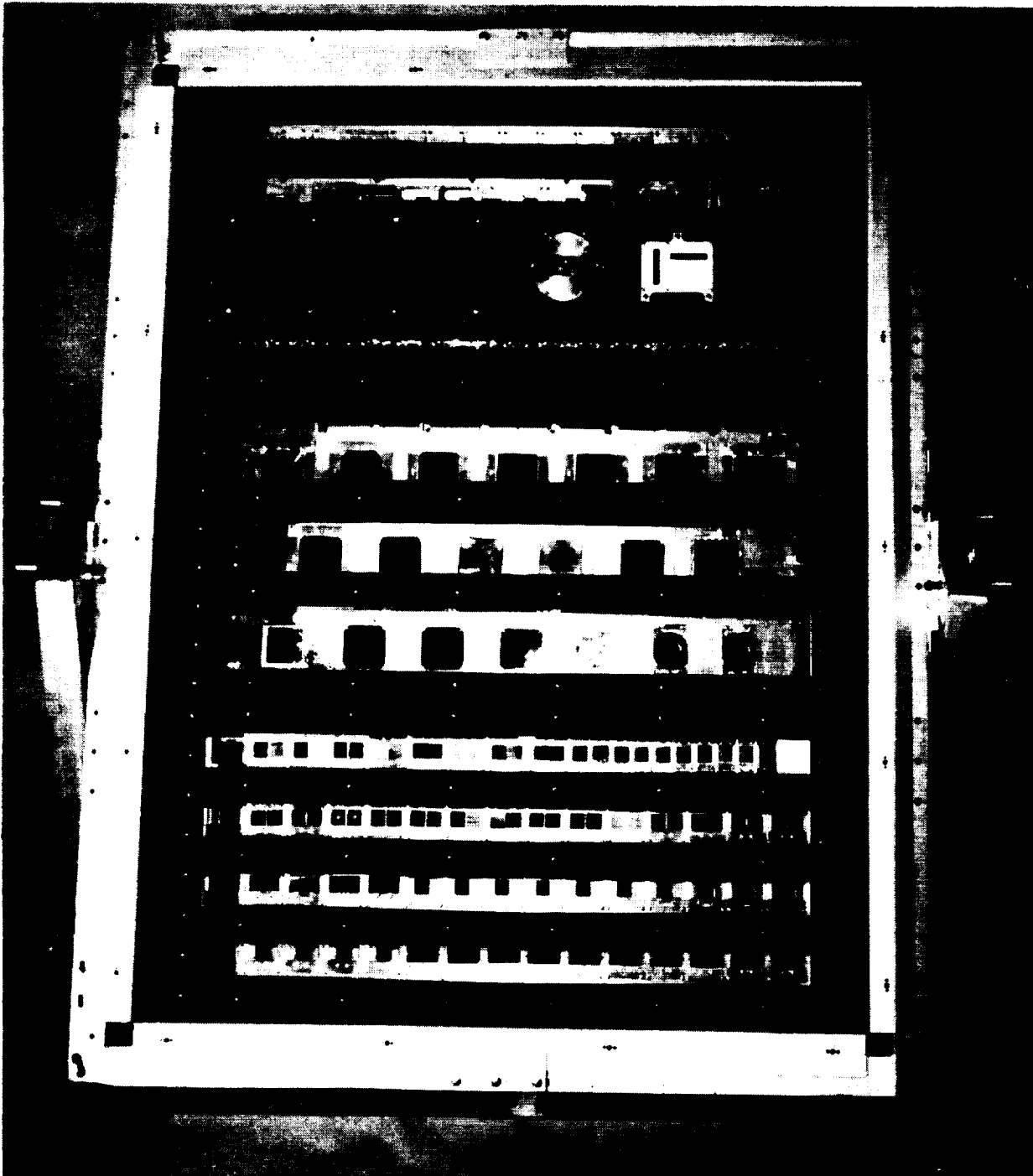
This chart shows the various solar cell experiments that were flown on LDEF. Information provided on this chart includes the current principal investigator, type and number of cells flown, name of experiment and location of experiment on LDEF. The degrees from ram take into account LDEF's constant 8 degree offset to ram. This presentation does not describe the specific types of cells and solar cell/array materials flown on LDEF. These details can be obtained from the individual experimenter or the LDEF Project Office. The Systems SIG has given the development of a solar cell database high priority but this activity is dependent upon 1992 funding.

List of LDEF Experiments Possessing Solar Cells

Principal Investigator	Type of Cells	Number of Cells	Experiment	Experiment Location
NASA LeRC - D. Brinker	Si & GaAs	155	S0014 - Advanced Photovoltaic Experiment	Tray E9 (8° from ram)
NASA MSFC - A. Whitaker	Si	4 modules & 5 cells	A0171 - Solar Array Materials Passive LDEF Experiment	Tray A8 (38° from ram)
NASA LeRC - D. Brinker	Si	20	A0171 - Solar Array Materials Passive LDEF Experiment	Tray A8 (38° from ram)
JPL - P. Stella	Si	30	A0171 - Solar Array Materials Passive LDEF Experiment	Tray A8 (38° from ram)
NASA GSFC - E. Gaddy	Si	45	A0171 - Solar Array Materials Passive LDEF Experiment	Tray A8 (38° from ram)
Wright Pat AFB - T. Trumble	Si & GaAs	70	M0003-4 - Advanced Solar Cell and Coverglass Analysis	Trays D9 & D3 (8° & 172° from ram)
NASA GSFC - S. Tiller	Si	4 arrays	S1001 - LDEF Heat Pipe Power System	Tray H1 (space end)
MBB - L. Preuss	Si	3	S1002 - Evaluation of Thermal Control Coatings/Solar Cells	Tray E3 (172° from ram)
TRW - J. Young	Si	12	A0054 - Space Plasma High Voltage Experiment	Trays B10 & D4 (22° & 158° from ram)

Advanced Photovoltaic Experiment (S0014)

This a pre-flight photo of the S0014 experiment. This experiment was designed to provide reference solar cell standards for laboratory measurements. This was to be accomplished by placing individual solar cells in orbit, measuring their current-voltage characteristics or short circuit current values while in orbit, and returning solar cells to the respective organizations for use as reference standards. On-orbit data acquisition took place once per day for the first 325 days of the LDEF mission. At day 326, the data acquisition batteries had discharged to the point that they were unable to further power the data recording system.



Preflight Photo of S0014

Advanced Photovoltaic Experiment Results To Date

The on-orbit data has been successfully read from the data acquisition system. Analysis of this data has been initiated. Post-flight I-V curves are being taken and comparison to pre-flight data has begun. Results to date include:

- The contamination film found on much of the cell surfaces has minimal effect on solar cell performance.
- Some discoloration in the RTV used to bond the cell wiring harness was observed.
- Degradation in I-V curves for individual cells was found to be mainly attributable to the severity of meteoroid or debris impact damage.

S0014 RESULTS TO DATE

Post flight I-V curves taken and comparison to pre-flight data underway

Analysis of on-orbit data has begun

Degradation in I-V curves proportional to severity of M&D damage

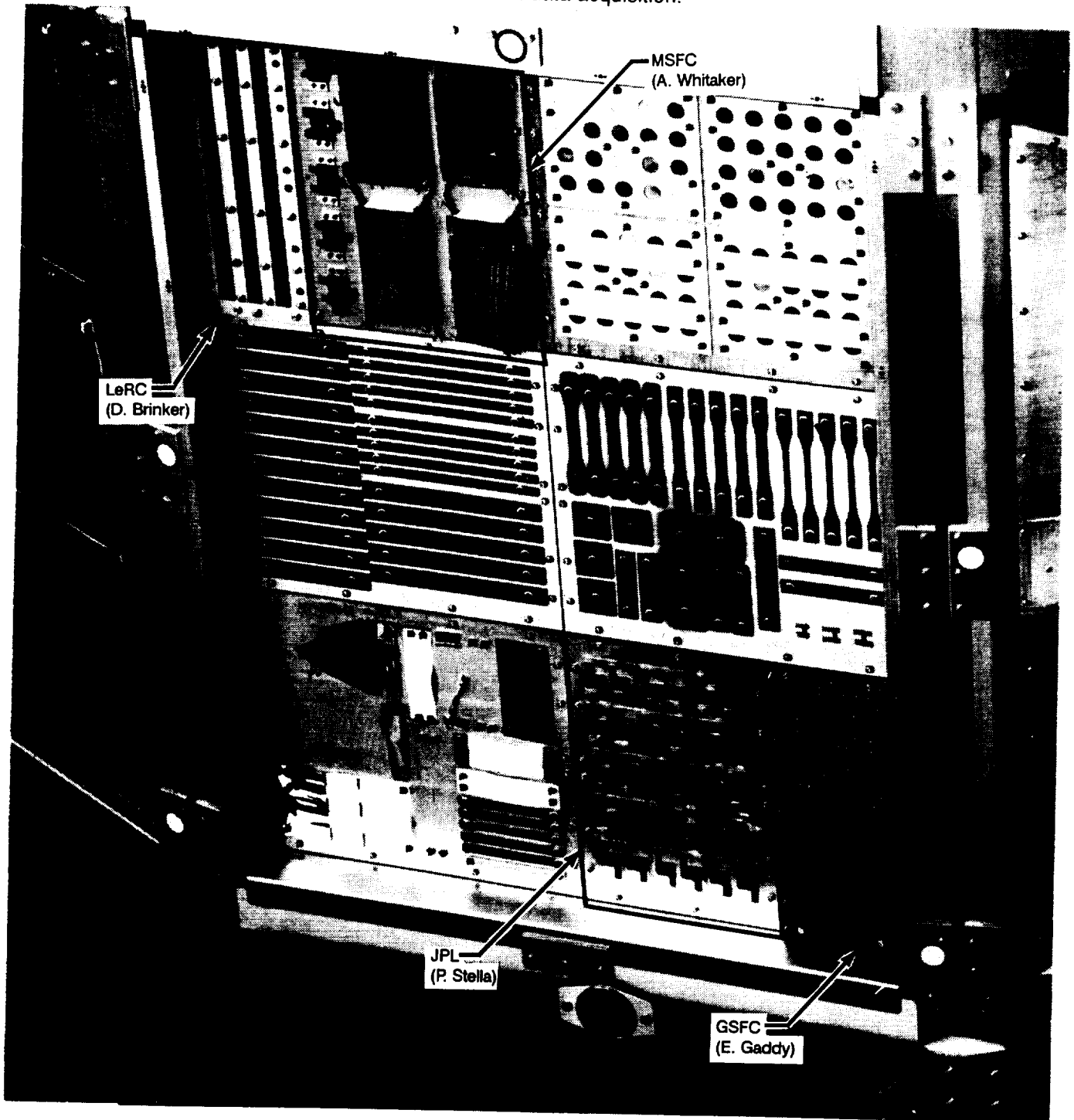
- **Cells with only coverglass damage showed minimal change**
- **Cells with damage to the structure show changes in fill factors**

Solar Array Passive LDEF Experiment (A0171)

This figure is an on-orbit photograph of Tray A8. The following four solar cell experiments were flown on this tray:

- MSFC experiment consisting of four solar cell modules and five solar cells
- JPL experiment consisting of 30 different combinations of cells/covers
- GSFC experiment consisting of testing solar cells, covers, encapsulants, and adhesives
- LeRC experiment consisted of solar cells with covers

This was a totally passive experiment with no on-orbit data acquisition.



On-Orbit photograph of Tray A8 which contained four different solar cell experiments.

A0171 Results to Date (MSFC portion)

Design of the four solar cell modules included the use of Kapton substrates. As a result of the longer than planned mission, the atomic oxygen caused erosion of the Kapton substrate resulted in two of the four modules becoming separated from the experiment prior to grappling and, therefore, not retrieved. The first of these two was lost prior to Shuttle rendezvous with LDEF, and the second one was still within close proximity during the grappling of LDEF. The third module was attached at one corner when LDEF was retrieved (as can be seen in the previous figure). This module (M3) was later found on the Shuttle cargo bay floor after LDEF was removed. This module was found to have five of the twelve cells containing cracks in either the solar cell or cell cover. The fourth module (M4) remained attached to the tray.

Solar cell and solar cell module maximum power (Pmp) output degradation ranged from 4.3% to 80% but over three-quarters of the individual cells tested had less than 10% degradation. There were 4 cells out of the 18 tested (including the twelve cells from M3) which had a Pmp degradation of greater than 20%. Three of these cells were from the M3 module and the fourth cell was flown without a coverglass. Discounting these four cells, the average cell Pmp degradation was 6.5%.

A0171 RESULTS TO DATE (MSFC portion of A0171)

- **Extended exposure caused loss of modules using Kapton substrate**
- **Solar modules performance degradations ranged between 4% and 80%**
 - **75% of the single cells exhibited < 10% degradation**
- **Exact degradation mechanisms yet to be determined**

A0171 Results to Date (JPL Portion)

This experiment studied the effects of exposure to the LEO environment on 30 different combinations of solar cells and coverglasses. The solar cell material for the 30 cells was Solarex Corporation 50-micron thick 2x2 cm silicon. Results to date include:

- The test plate and cells exhibited brownish-orange stains, which are residues of adhesives and encapsulates that had reacted to the LDEF and LEO environment.

- Large numbers of meteoroid and debris impacts are apparent ranging in size from 0.05 mm to 1.0 mm in diameter with > 157 total impacts over the 180 square inches of JPL's portion of the A0171 experiment.

- No impact damage was found to have caused any significant degradation to the solar cells. The degradation in cell performance for all samples was due to a loss of cell current due to darkening of the adhesive and/or coverglass due to exposure to UV, charged particles, and/or atomic oxygen.

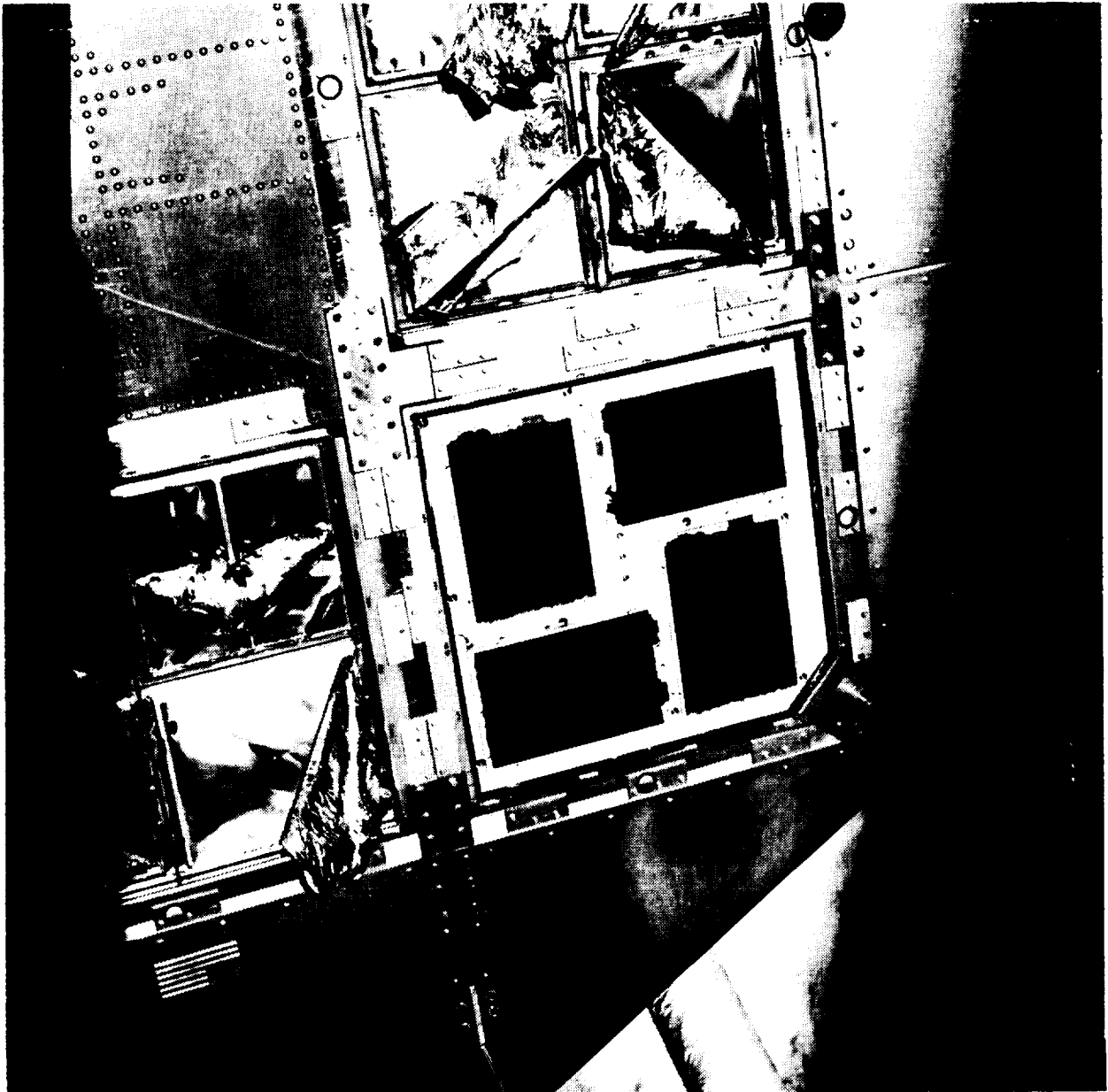
- Short-circuit current loss ranged from 3% for the cerium doped microsheet coverglass cells to 22% for the Teflon encapsulated solar cells.

A0171 RESULTS TO DATE (JPL portion of A0171)

- **No significant degradation caused by M & D impacts**
- **Degradation caused by darkening of adhesive and/or coverglass due to exposure to AO, UV, and radiation**

LDEF Heat Pipe Power System Solar Arrays (S1001)

The LDEF Heat Pipe Power System Experiment included a self-contained direct-energy transfer power system which functioned properly during the entire mission lifetime. This power system was designed to provide power to the Low Temperature Heat Pipe Experiment and was located on the space end of LDEF. The power system included four solar array panels and one 18-cell, 12 amp-hr, nickel-cadmium battery. This figure is an on-orbit photograph of the four arrays.



On-Orbit Photo of S1001 Solar Arrays

S1001 Results to Date

A detailed visual inspection of the four arrays found that most cell damage could be attributed to the 99 meteoroid and debris impacts, of which 29 impacts caused coverglass cracks. Post-flight IV analysis made five months after LDEF retrieval indicated that the solar panel's current and voltage performance had degraded an average of 1.5% and 3.3% respectively. The degradation was concluded to be caused by darkening of coverglass adhesive and impact damage. The extent of damage due to any one of the mechanisms is currently unknown.

S1001 RESULTS TO DATE

Visual Inspection

- 99 M&D impacts**
- 22 impacts caused coverglass cracks**
- Adhesive migration**

Electrical Characterization

- Average of four modules**
 - Current degraded 1.5%**
 - Voltage degraded 3.3%**
- Control module**
 - Current degraded 0.3%**
 - Voltage degraded 0.6%**
- Flight degradation due to darkening of coverglass adhesive and M&D damage**

Advanced Solar Cell and Coverglass Analysis (M0003-4) Results to Date

This experiment consisted of 63 coverglass samples and 12 solar cell strings (5 cell/string). Of the 63 coverglasses, 16 were on the leading edge, 16 on the trailing edge, 16 on the backside of a tray protected from direct exposure to the LEO environment, and 15 were used as control samples and not flown. 5 of the cell strings were on the leading edge, 5 on the trailing edge and 2 were used as control strings.

The surface contamination found on all specimens did not interfere to a significant degree with the optical characteristics, but the contamination film does increase the absorption by moving the short wavelength transmission of the top surface to longer wavelengths.

Visual comparisons of cell strings indicated that the metallization process will have a large effect on the lifetime of arrays in LEO orbit. Metal migration and contamination between the coverglass and cell are two of the main concerns. Electrical characterization of these cell strings has not yet been initiated.

M0003-4 RESULTS TO DATE

Coverglass

- **Optical properties determined. No significant changes. Trailing edge specimens "dirtier" than leading edge specimens.**

Solar Cells

- **Oxidation of silver; contamination; discoloration on cell contacts and interconnects.**
- **Electrical characterization not yet begun.**

Solar Cell Conclusions

There are four LEO environments, operating individually and/or synergistically, that cause performance loss in solar cells:

- Meteoroid and space debris
- Atomic oxygen
- Ultraviolet radiation
- Charged particle radiation

In addition, the effects of contamination caused by outgassing of materials used on the specific spacecraft play a role in decreasing the light being transmitted through the coverglass and adhesive to the solar cell.

From the results presented on the solar cells aboard LDEF, the most extensive degradation of the solar cells came from impacts and the resulting cratering. The extent of the damage to the solar cells was largely dependent upon the size and energy of the meteoroids or space debris.

The other cause of degradation was reduced light reaching the solar cell. This was caused by contamination, UV degradation of coverglass adhesive, and/or atomic oxygen/UV degradation of antireflection coatings.

For additional information, the reader is referred to either the individual papers presented at the First LDEF Post-Retrieval Symposium or the Systems SIG report dated February, 1992.

CONCLUSIONS, SOLAR CELLS

- **Approx. 340 Si & GaAs solar cells flown on LDEF**
- **Over half were actively monitored on-orbit**
- **Most degradation of cells caused by M&D impacts**
 - **Performance loss dependent on size and energy of impacts**
- **Minor degradation caused by decreased amount of light reaching cell**
 - **Contamination**
 - **UV degradation of coverglass adhesive**
 - **Atomic oxygen/UV degradation of antireflection coatings**
- **To date, radiation effects not discernible from other degradation factors**

SYSTEM RELATED TESTING AND
ANALYSIS OF FRECOPA

Christian DURIN (System SIG Member)
CNES Toulouse FRANCE
18, av E. BELIN 31055
Phone: (33) 61 28 14 39, Fax: (33) 61 27 47 32

SUMMARY

This paper presents a new part of the results from FRECOPA system analysis. It was one of the numerous experiments which were flown on the LDEF satellite. In our flight configuration (LEO orbit, trailing edge), the environment was a better vacuum than the leading edge, with many thermal cycles (32000) and U.V. radiations (11100 equivalent sun hours). The satellite was also bombarded by mainly natural micro-particles. It saw a low atomic flux and minor doses of protons and electrons.

INTRODUCTION

The subjects of our analyses are the studies of: canisters and their seals, organic and metallic fasteners, and the study of adhesion between two metallic parts. The canisters were used to protect samples during launch and return to Earth. The butyl seal provided vacuum tightness. The glues were used to bond metallic fasteners and the velcro tapes to fix the thermal blankets. The adhesion phenomenon was found between a small steel spring and an aluminium plate used to fix samples. At the end, we will show two contamination phenomena which will be the subject of our future investigations. The following results are based on comparisons between components after flight and those stored on ground in laboratory conditions.

SEALS

Butyl rubber seals were used to provide vacuum tightness inside the canisters. The seal was bonded to one of the face-plates of the half canisters as seen in figure 1. In the closed position (during launch and return to earth) a compression force was exerted on the canister to guarantee global cohesion. An aluminium shield was placed on the top of the canister to protect the seal during opening (10 months). According to this position, their exposure was limited to hard vacuum and thermal conditions. We performed two tests on the seal:

- Micro-Hardness M.H. (NF-T 46-003)
- Compression Set C.S. (NF-T 46-011) 22 hours, 100°C and 25% set

We measured

	M.H.(DIDC)	C.S.(%)
Flight model B3	55	5.5
Reference model B6	53	8.3

The increase in micro-hardness values show a slight ageing of the seal confirmed by the decrease in compression set values.

We conclude good behaviour; the seal is still in good working order, and it adheres efficiently to the metal and has not changed aspect.

CANISTER

Measurements of pressures inside the canisters 70 days after return of FRECOPA show the excellent behaviour of canister n°5 which has an improved vacuum, 0.045 mbar for 0.66 mbar equivalent nitrogen before flight. Canisters 3 and 4 have pressures of approximately 1.6 and 4.1 mbar respectively, slightly less than at the beginning. We performed leak tests after removal of the samples with a new pressure in the canister of 10^{-3} mbar. We measured:

- canister 3 after 500 hours, $4 \cdot 10^{-6}$ mbar.dm³.s⁻¹ equivalent N₂
- canister 4 after 800 hours, $2 \cdot 10^{-6}$ mbar.dm³.s⁻¹ equivalent N₂
- canister 5 after 500 hours, $3 \cdot 10^{-6}$ mbar.dm³.s⁻¹ equivalent N₂

For canister 4 after 7200 hours we had the value of $3 \cdot 10^{-7}$ mbar.dm³.s⁻¹ equivalent N₂.

This value shows the good behaviour of the butyl seal. The pressure differences between

canisters after flight can be explained by the fact that canisters 3 and 4 contained organic materials which may have outgassed even after the canisters were closed.

This technique for protecting samples operated correctly, but the thermal conditions inside the canisters after they were closed may have contributed to the materials' ageing.

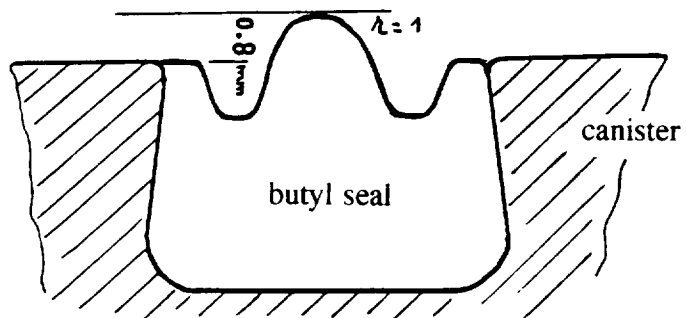
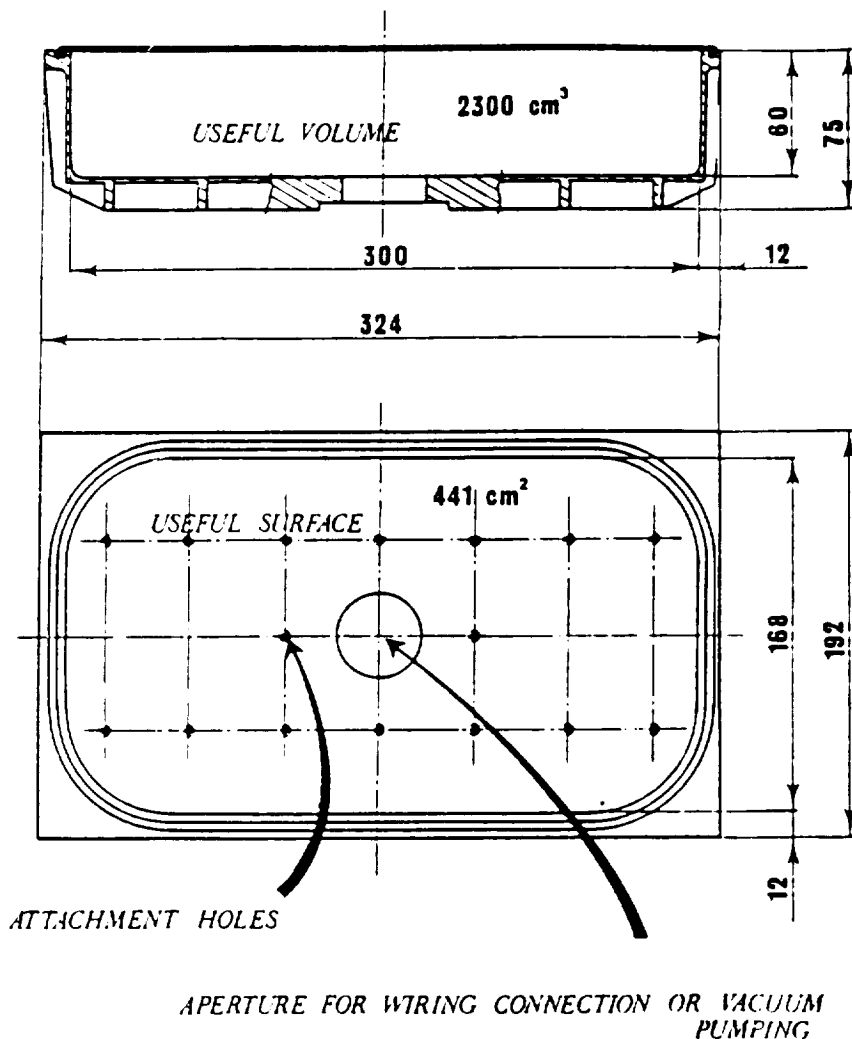


Figure 1. Canister dimensions and Butyl seal cutting out

VELCRO TAPES

The behaviour of the velcro tapes was highly satisfactory when used to attach flexible shields. Qualitative tests carried out upon disassembly showed a high level of resistance for assemblies using these materials. Quantitative tests show no change in tensile strength but a decrease of 50 % in opening strength. Visual observations show a change in color (yellowing as seen in figure 2). Analysis of surface constituents (R.B.S.) reveals silicon contamination, along with the presence an other element not yet definitely identified (as seen in figure 3). Thermal analysis (D.S.C.) shows no significant change in transition temperature (3%) but a second peak appears on the flight sample curves (as seen in figure 4). The type of transition or the element producing it are not yet known.

GLUES

All structure attachments were secured by bonding (bolts, screws). The Velcro strips were bonded to the structure by EC 2216 glue. Traces of adhesive, although cleaned for assembly, reappeared under the effect of U.V. (as seen in figure 2). The adhesives themselves changed color (grey to green) but variations in their transition temperature (Tg) depended on the type of support and the thermal conditions to which they were subject (as seen in figure 5*).

SILVER-PLATED BOLTS

All the screw torques were nominal during disassembly but we detected a pollution on certain bolts holding the batteries. Sulfur and oxygen were detected in the layer of silver, and this had a granular appearance (as seen in figure 6). This may be due to in-flight contamination by other experiments. Contamination after the return of FRECOPA is also possible, as the satellite travels in the cargo bay of the space shuttle and this is not sealed. This pollution is only slight but it could generate small conductor particles on the bolts. These are harmful not only to electronics and components but more generally to any manned flight.

In our flight conditions, these attachment techniques were proved to be high performance. This would not be the case on the side exposed to atomic oxygen.

*Photographs are not shown in color.

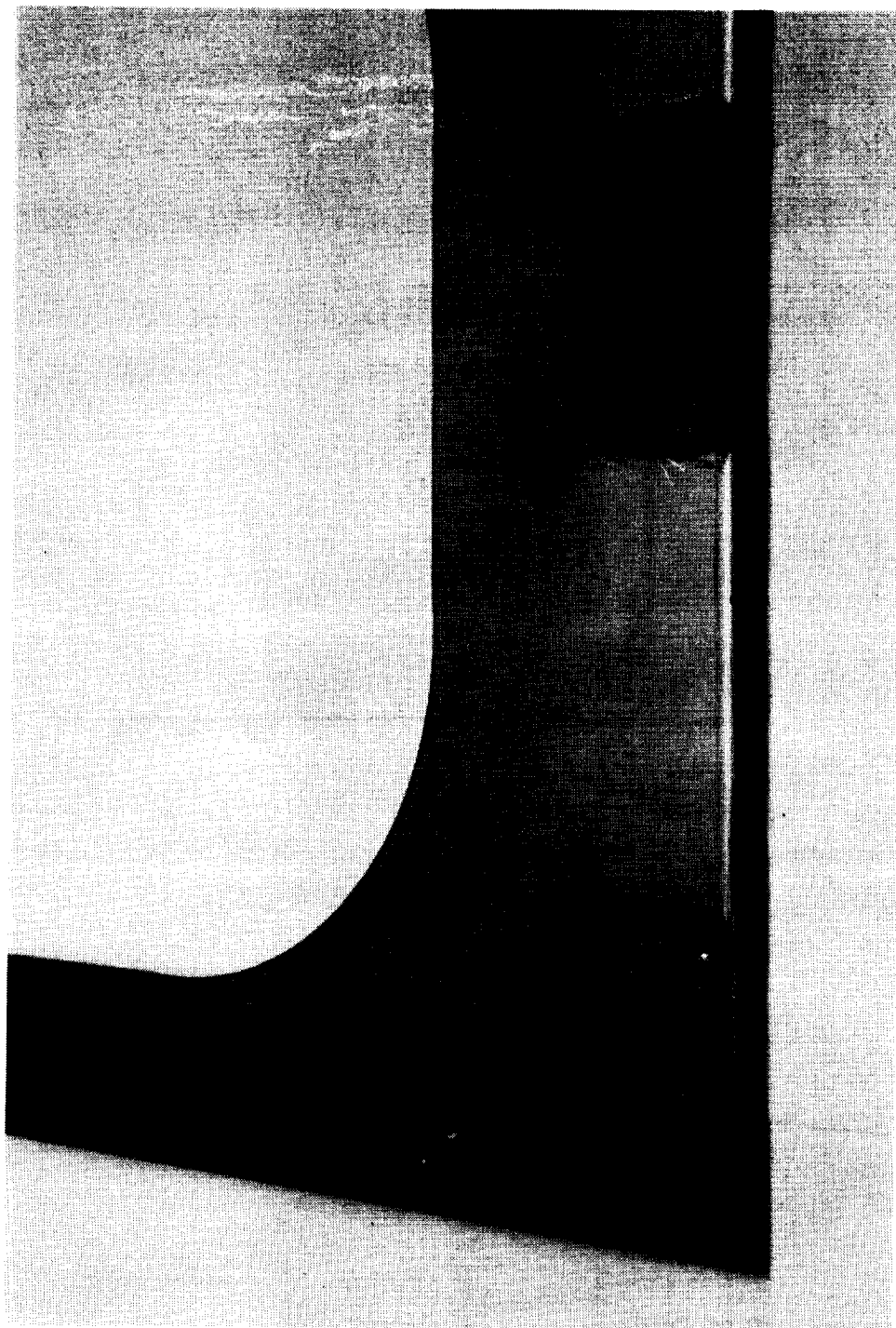
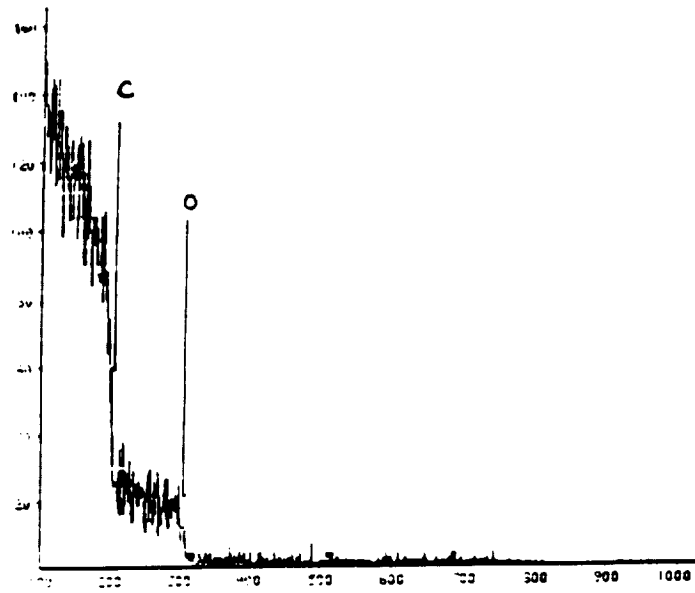


Figure 2. Velcro color change and glue trace
on rigid shield

ORIGINAL PAGE
BLACK AND WHITE PHOTOGRAPH

Reference



Flight

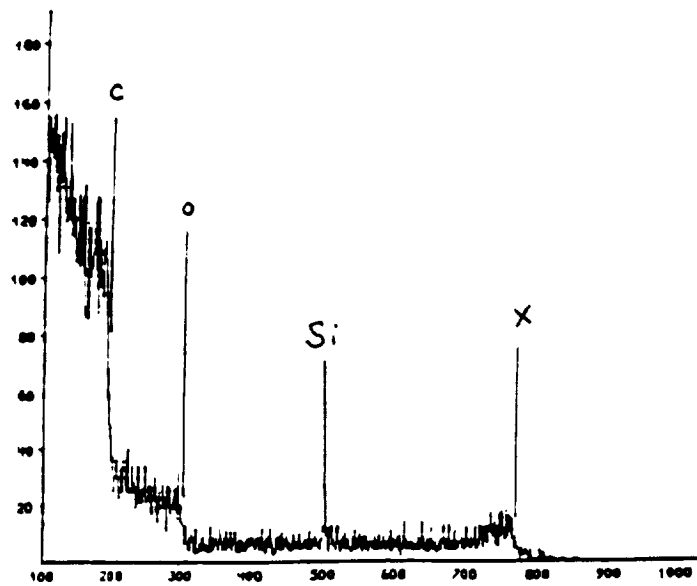


Figure 3. R.B.S. results on velcro tapes

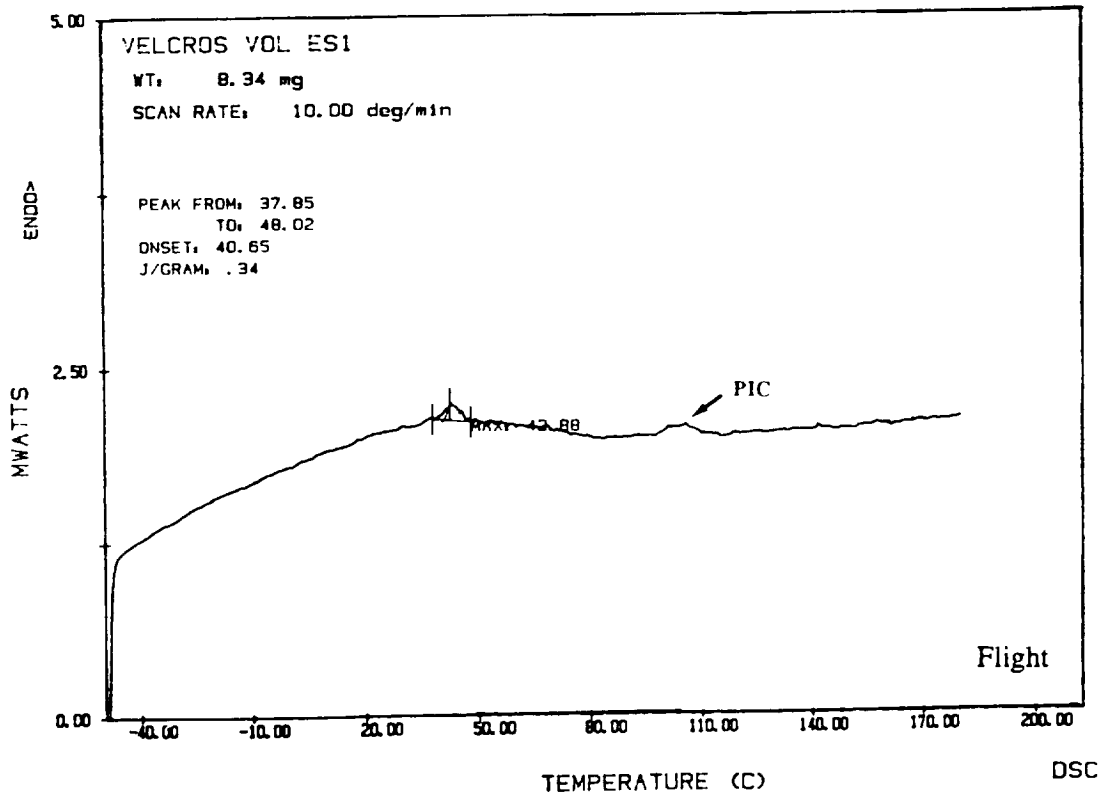
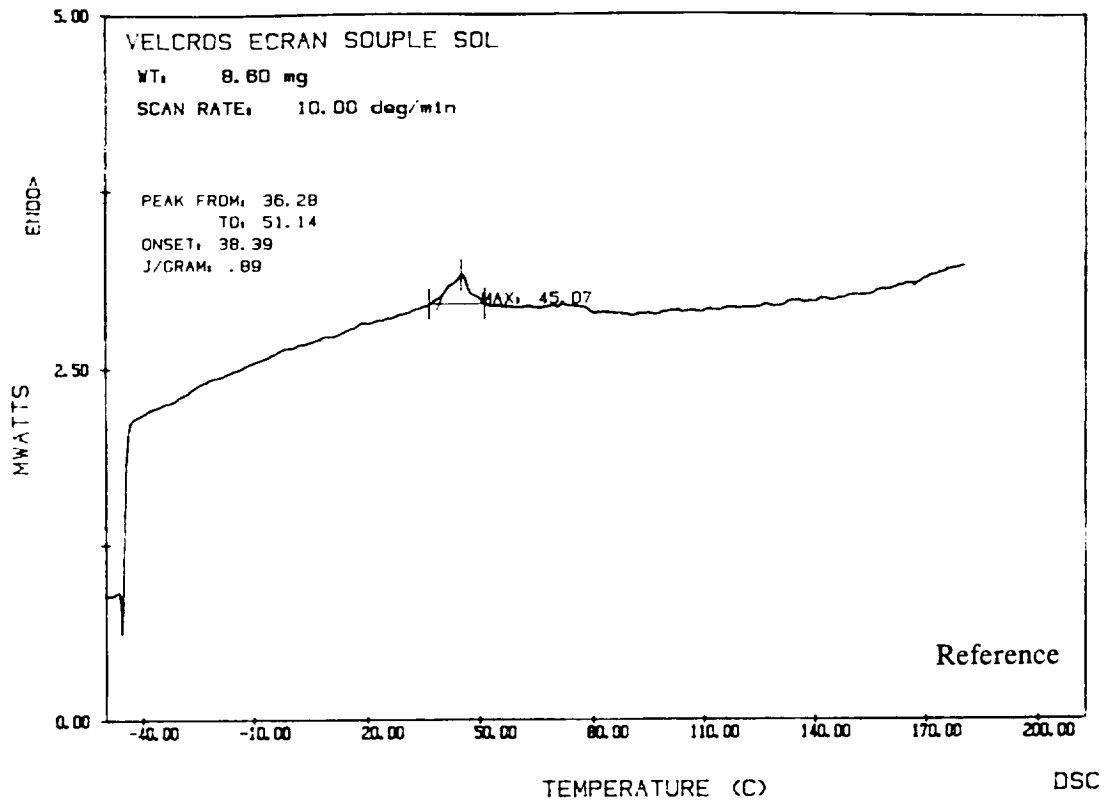


Figure 4. D.S.C. results on velcro tapes

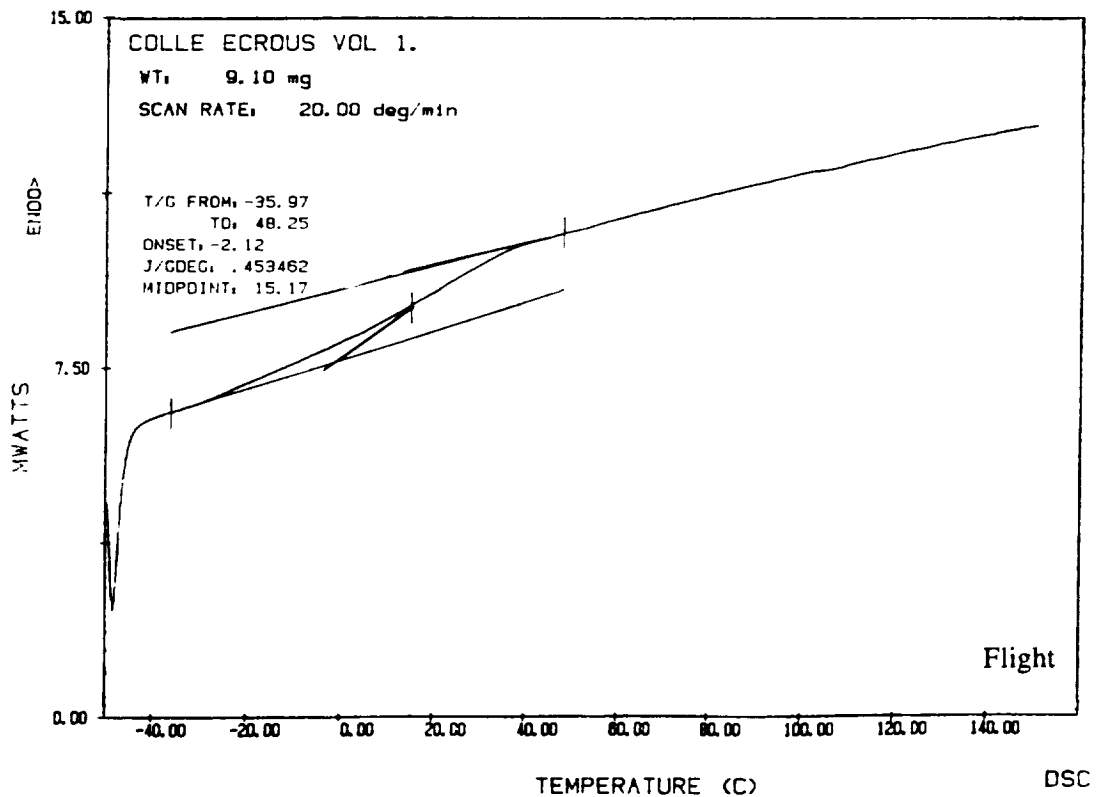
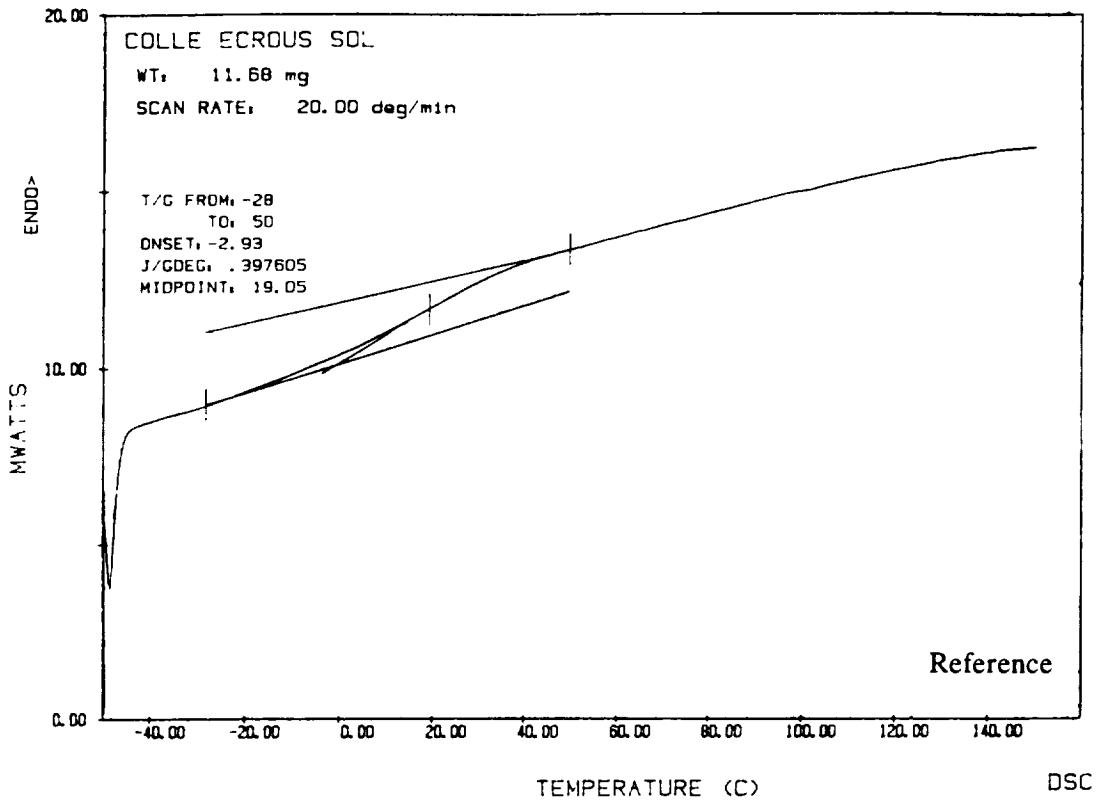
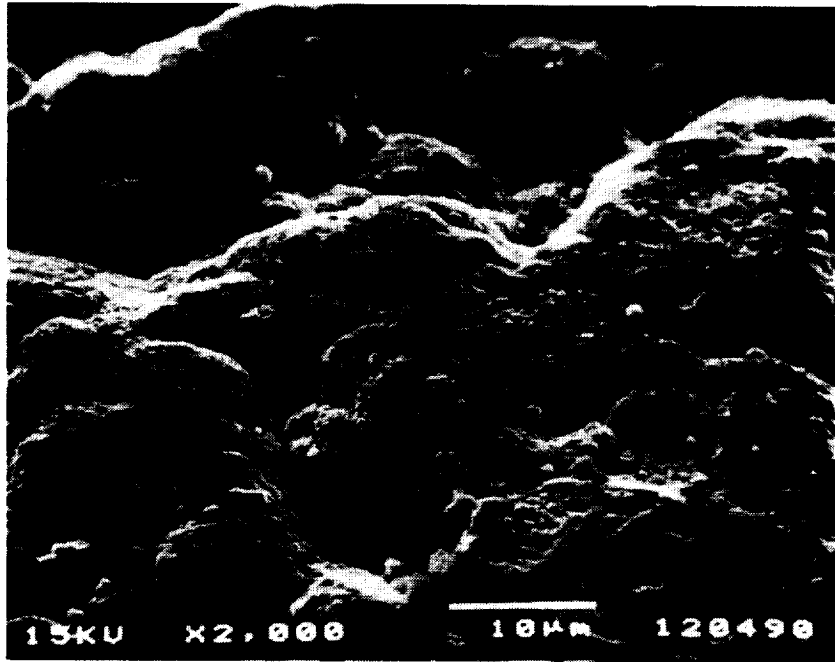
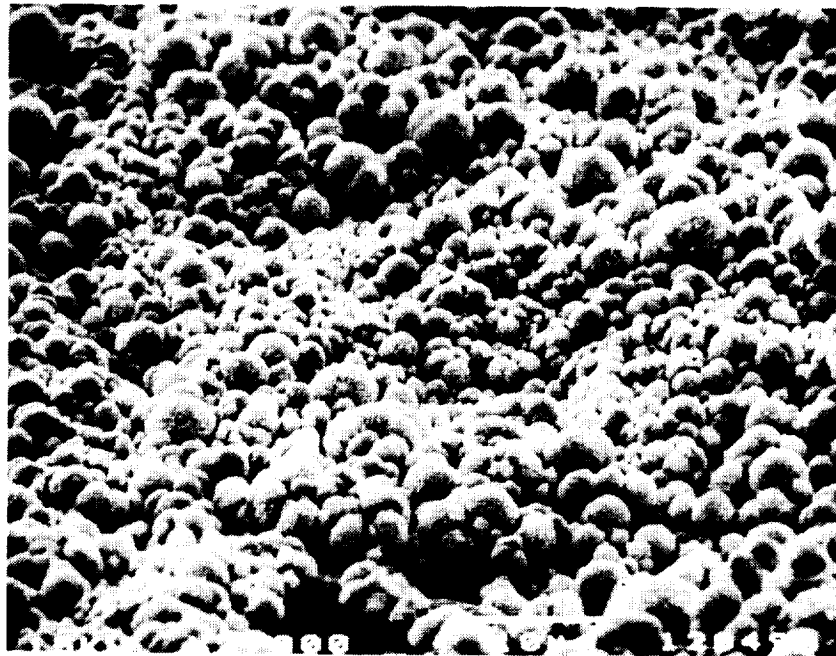


Figure 5. D.S.C. results on glue



Reference



Flight

Figure 6. Contamination aspect on silver-plated bolt

ADHESION PHENOMENON

This phenomenon concerns a welding problem. We noticed the adhesion between a steel spring and a small aluminium plate. The disassembly force was very slight and we only observed a single outright case of bonding. These items come from experiment AO138-1 or AO138-6 and were used to support the samples (as seen in figure 7). Visual inspection reveals local shiny marks on the spring (as seen in figure 8). X analysis and the electronic microscope reveal a transfer of aluminum material to the steel (as seen in figure 9). This phenomenon could have been produced by a machining problem (unevenness of the spring), which, under launch and environment constraints, was locally "welded" to the aluminum.

This last paragraph highlights the importance of choosing the right metallic and organic materials, and the possible consequences in terms of pollution and/or faulty mechanical operation.

WORK IN PROGRESS

The former phenomenon concerns the shadow of a canister which can only be seen on one side of the plate (as seen in figure 10). We put its origin down to the outgassing of organic materials in vacuum and to the thermal conditions. The products of evaporation were condensed over all the cold surfaces of FRECOPA during the night. At sunrise, one side of the plate was more rapidly illuminated. The combined action of this illumination and U.V.'s radiations led to polymerization of these products. On the opposite side, which was slower to heat up, the contaminants had time to re-evaporate before polymerization by the U.V.'s.

When studying this contamination problem, we also noted the shadows of a connector wire, a bolt and of rivets on the FRECOPA structure (as seen in figure 11). This time, orientation of the contaminating flows seems to come from inside the LDEF towards space. It is far more difficult to explain this phenomenon. A study will be carried out, along with surface analysis.

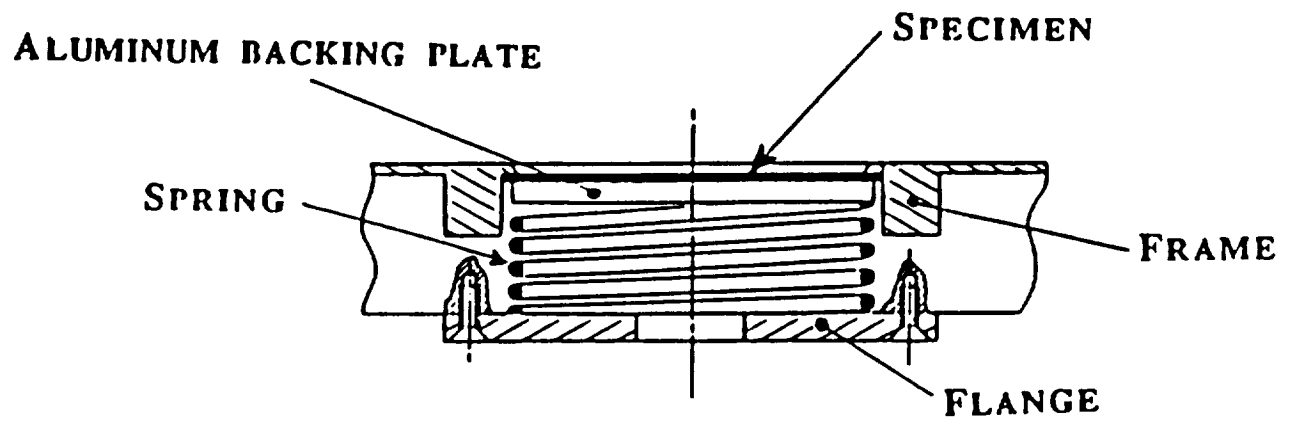


Figure 7. Steel spring and aluminum plate configurations

Aluminum

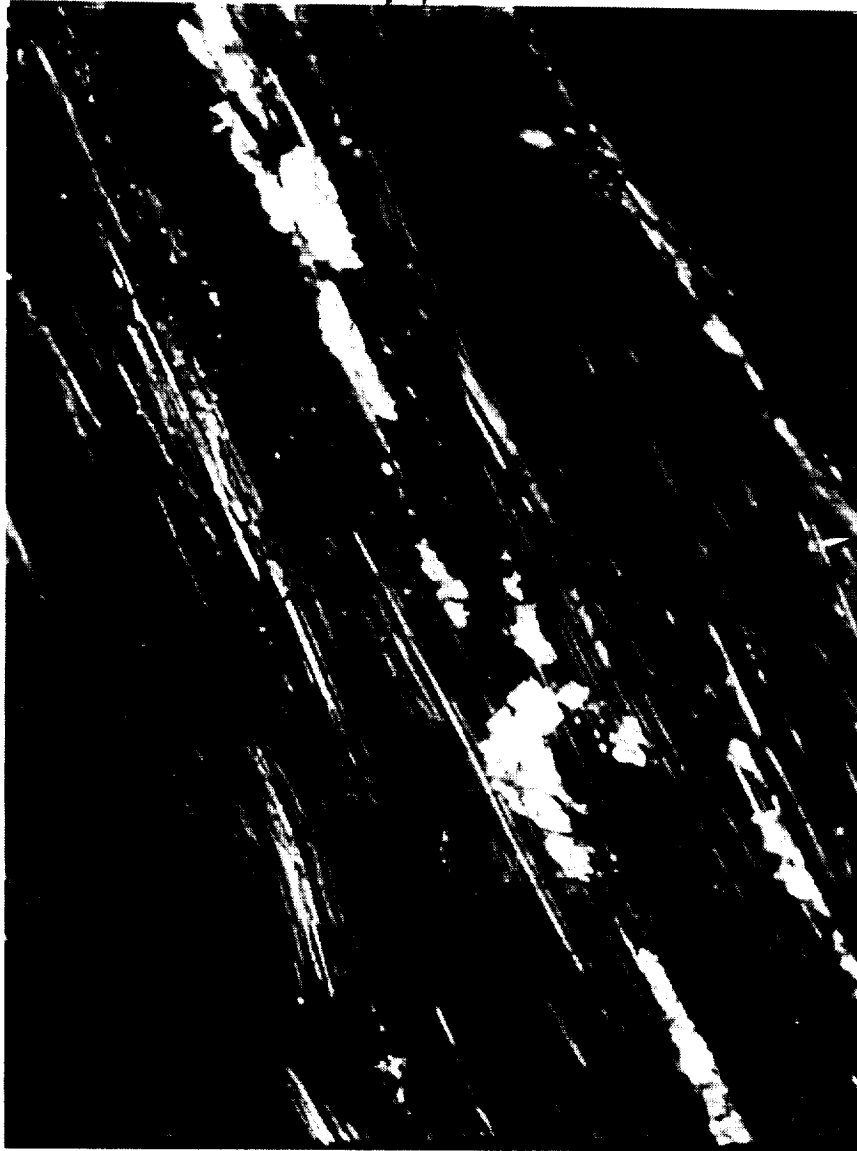
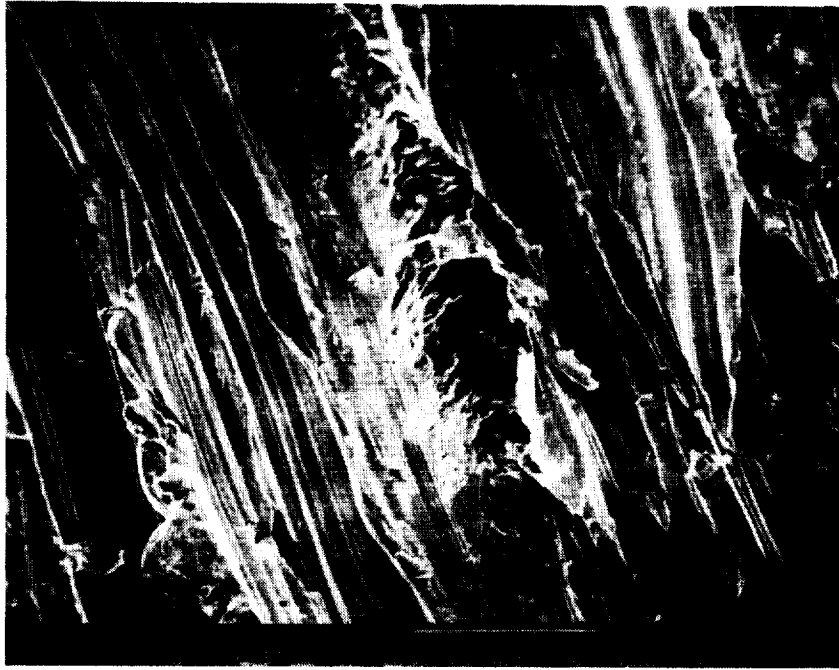
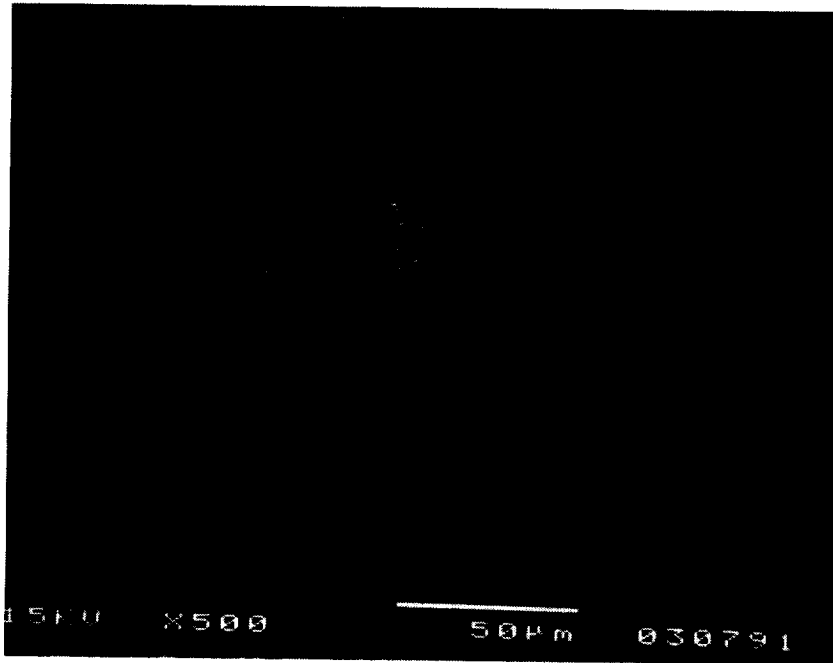


Figure 8. Aluminum transfer on steel spring



SEM picture



Aluminum element map

Figure 9. Aluminum transfer on steel spring (SEM)

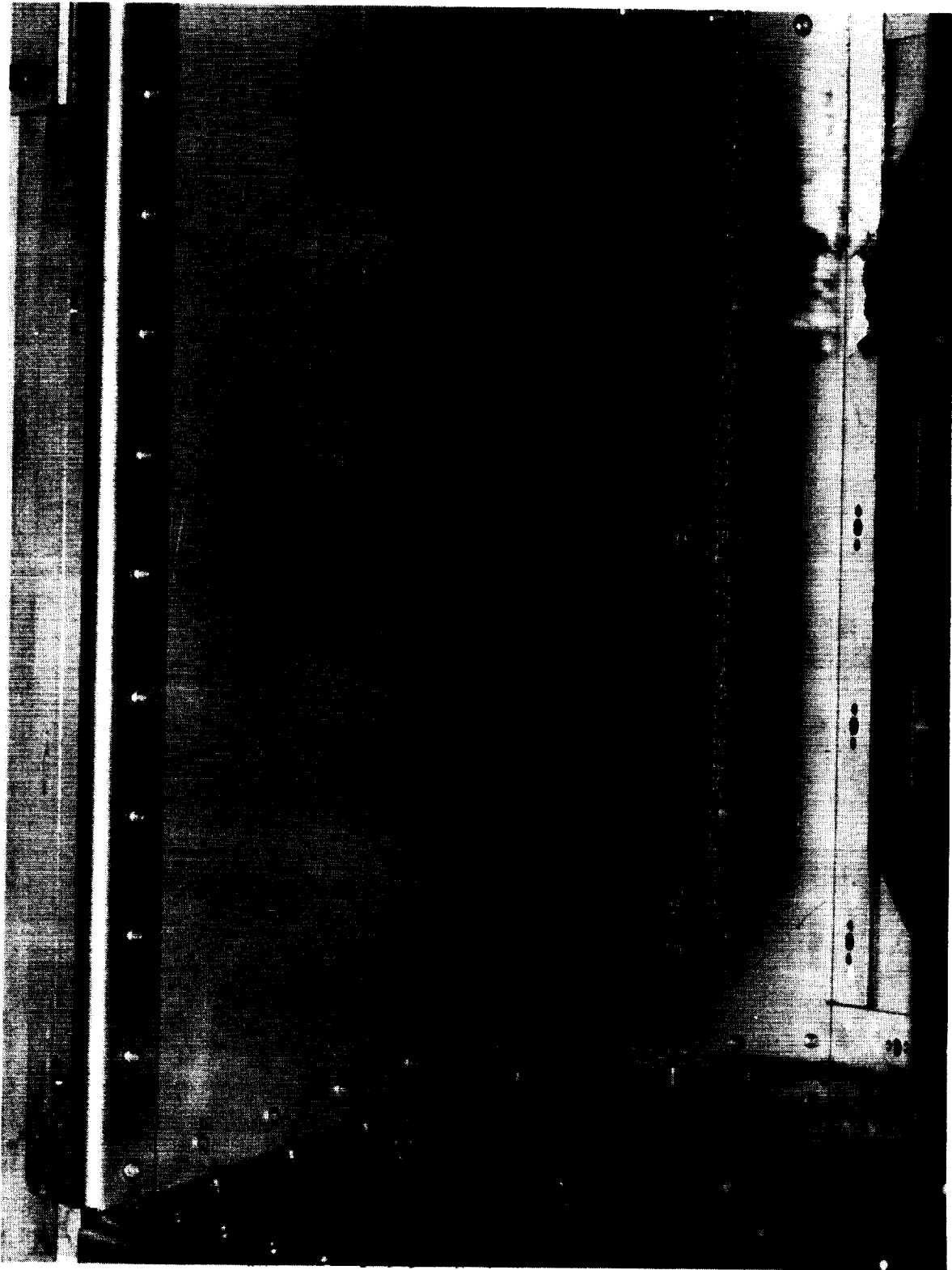


Figure 10. Canister shadow inside the tray

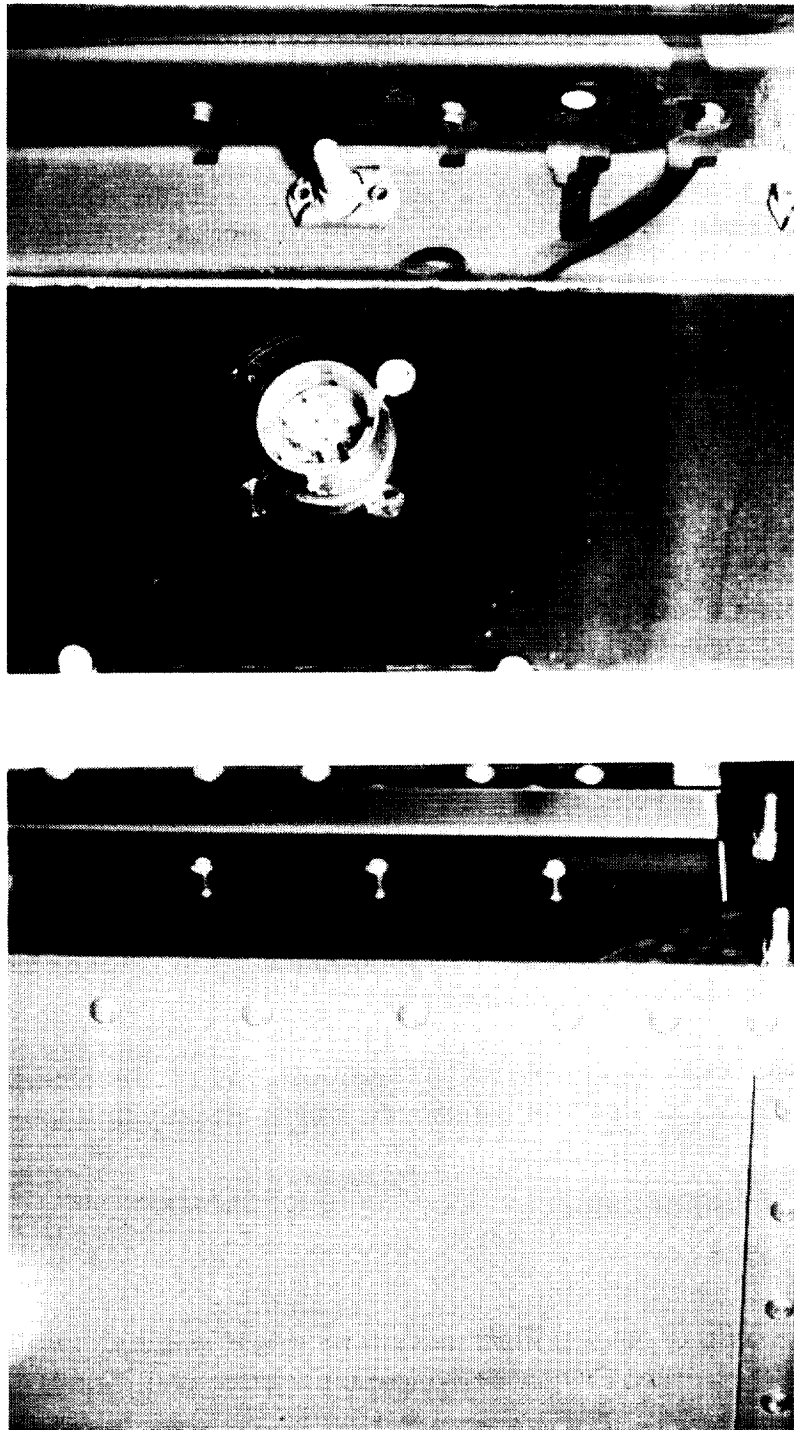


Figure 11. Bolts, wire and rivet shadows on the back of the tray

ORIGINAL FACE
BLACK AND WHITE PHOTOGRAPH

CONCLUSIONS

The FRECOPA experiment was a success. All systems operated correctly. The mechanisms and electronics of the sealed canisters worked correctly and provided ten months' exposure as planned. The extension to the mission enabled us to study the behaviour of a large number of materials after nearly 6 years' exposure. The overall result is positive. Materials resisted well in the environment, even if some of them show evidence of ageing which could have been harmful to a longer mission. We must use the results obtained to improve dimensioning or to protect the materials used for longer missions.

We noticed the good behaviour of the butyl seal despite a slight ageing.

For organic materials (velcro tapes, glues) we observed an ageing and some noticeable changes in mechanical and physico-chemical properties. We also noted a contamination by Si. The mechanical functions have been nevertheless executed.

Certain combinations of metallic materials must be prohibited, as local welding phenomena may occur under certain mechanical and/or environmental conditions. Combinations such as the organic/metallic used for FRECOPA gears might be a solution. Machining of parts are also important conditions affecting the appearance of this phenomenon.

Despite selection and the tests carried out, organic materials produce contamination which is likely to polymerize on cold surfaces. Protection and stringent outgassing tests before flight are the only remedies for using these materials.

Validation through tests is perhaps not sufficient at present for modelling the synergic complexity of all space environment parameters, which can only be approached through in-orbit tests.

References

1. Ch. DURIN, *Results of the post flight analysis on system materials for the LDEF/FRECOPA experiment*, Cinquieme Symposium International, Sep 91 Cannes-Mandelieu, France.
2. J.GUILLIN, *Les matériaux en environnement Spatial*, Cinquieme Symposium International, Mandelieu, France, Septembre 1991.

PANEL DISCUSSION SUMMARY

THEME PANEL DISCUSSION TOPICS

**Bland A. Stein and Philip R. Young
Workshop Coordinators
NASA - Langley Research Center**

Considering your theme / discipline, how have initial LDEF results affected:

- Potential space applications of specific classes / types of materials?
- Understanding of environmental parameters / synergism?
- Understanding of mechanisms of materials degradation?
- New materials development requirements?
- Ground simulation testing requirements?
- Space environmental effects analytical modeling requirements?

Considering your theme / discipline:

- What are the LDEF data-basing requirements? How would you like to see the data compiled / presented?
- What are the general needs for future flight experiments?
- What level of information should be presented for this discipline (and in what format should it be presented) at the Second LDEF Post-Retrieval Symposium, June 1992?

Considering your theme / discipline:

- Which LDEF findings are clear, indisputable, unambiguous?
- Which LDEF findings are confusing, ambiguous, obscure?
- Additional comments, concerns, recommendations?

LDEF Materials, Environmental Parameters, and Data Bases

Co-Chairmen: Bruce Banks and Mike Meshishnek
Recorder: Roger Bourassa

Consistent with the theme assigned, a wide range of topics was discussed by the Panel. The consensus of opinions and comments expressed by the various part-time and full-time panel attendees are summarized herein.

Initial LDEF results have affected and will continue to affect the application of specific classes of materials to spacecraft design. Unprotected polymers were shown to be unsuitable for long duration exposure in low earth orbit. The need has been shown for protective coatings for organic materials. The results also show that other materials may be employed with greater confidence than was realized before. For example, silicate binder Z-93 and YB-71 thermal control coatings survived and functioned well even under severe exposure conditions. LDEF data indicates both spatial and temporal nonuniformity in debris and micrometeoroid impact rates. This finding may significantly affect Space Station *Freedom* reliability assessments.

The availability of actual material samples exposed to low earth orbit environment for laboratory examination has both answered questions and raised new questions. Understanding of environmental parameters has been expanded to include synergistic effects that were not widely known outside the research laboratories. For example, atomic oxygen flux and ultraviolet radiation interact in degradation of silver/FEP and silicone materials. These interactions verify ground simulations and thus help to validate research methods. However we do not understand the mechanisms of atomic oxygen reactions with polymers. LDEF samples show that materials with volatile oxides develop surfaces textured with conical shapes. No satisfactory explanation has been advanced.

Differences between leading and trailing surfaces of LDEF reveal a role for atomic oxygen in contamination. Atomic oxygen is active in both depositing contamination layers and in their subsequent chemical change and removal. We do not understand how contamination layers are deposited. At this juncture LDEF is supplying clues that will help to focus future research.

No cold welding of fastener mating surfaces was observed on LDEF which could be attributed to space exposure. Only the occasional galling of threaded surfaces, commonly associated with assembly operations, was observed on post-flight examination of fasteners. However, the possibility that cold welding may occur between cleaned surfaces or between surfaces of threaded fasteners assembled and disassembled in space is not ruled out.

A few instances of adhesive failures on LDEF have been documented. These failures may be associated with thermal cycling. But, for the most part adhesives employed on LDEF functioned satisfactorily.

The need for on-board monitoring of several material properties and flight parameters has been revealed. These measurements include solar absorptance, thermal emittance, temperature, impacts, strain, yaw, pitch and roll because time dependent factors are important to analysis. Also, post-flight degradation of samples occurs. The need is

evident for even more careful preparation and preflight handling of samples than was the practice for LDEF.

New material needs demonstrated by LDEF include: (1) protective coatings for organic materials; (2) a replacement for silver/FEP thermal control film; (3) a flexible white paint replacement for S13G/LO; (4) a durable flexible polymer electrical insulation; and (4) improved bumper designs for increased micrometeoroid and debris impact tolerance.

The panel recommends that ground simulation test requirements include synergistic effects. Analytical means need to be developed to extrapolate from ground testing to in-space performance of materials. Acceleration artifacts, ultraviolet radiation, atomic oxygen, thermal cycling and ground facility contamination effects are items of concern. Comparative ground testing of materials flown on LDEF is recommended. The environments simulated in ground facilities must be better characterized.

Modeling requirements for space behavior of materials depends on reliable reporting of LDEF exposures and are dependent on observed behavior of materials. As of now, not all data is available. Thermal models appear adequate. Return flux and trailing edge contamination effects must be modeled to accurately predict results. All models must be user friendly, accessible, and accepted by the user community.

Data bases developed for LDEF must acknowledge the divergent needs of different user groups; scientists, engineers, designers, etc. The user community needs to be able to electronically alert MAPTIS when the need for data updating is identified. The medium and procedures for forwarding data for inclusion in MAPTIS need to be defined. The data base must include sources and references for information. LDEF photographs need to be archived and the location of LDEF hardware needs to be made available to users.

Throughout the LDEF post-flight investigation a requirement has existed for individual investigators to collate and exchange results in a simple data base prior to more careful checkout and incorporation of data into MAPTIS. While not presented in this session, such a data base was reported on by the Systems Special Investigation Group, Optics Study and is worthy of note for use by others.

Recommendations by the Panel for future flight experiments are as follows: (1) provide for on-board measurement of spacecraft health and time dependent test parameters; (2) continue testing of actively monitored solar cells; (3) standardize test practices for characterization of materials; (4) allow for development of methods for extrapolation of test results; (4) test new higher performance, more durable materials to meet the critical needs identified by LDEF; (5) include validation as well as phenomenology levels of test; and, (6) be responsive to LDEF lessons learned.

At the Second LDEF Post-Retrieval Symposium, the Panel recommends that results and interpretations be presented in concurrent, narrow discipline sessions. Presentations on lessons learned and recommendations for LDEF data users should be prepared. Presentations should focus on quantitative results and new information. Qualitative overviews should be omitted. A view graph format should be followed and advanced copies of view graphs should be handed out at the start of the conference. Photographs should have scale bars. Appropriate acknowledgements should be made for materials used. The Second Symposium should feature a MAPTIS data base presentation.

Of the various LDEF findings the Panel noted that those most clear, indisputable and unambiguous are the following: (1) all polymers including organic paint binders are attacked by atomic oxygen; (2) most metal oxides protect materials from atomic oxygen

attack; (3) silicate binder Z-93 and YB-71 thermal control coatings are durable in low earth orbit; (4) silicones are crazed on exposure in low earth orbit; (4) the Space Shuttle produces debris; (5) the majority of impacts occur in temporal bursts; and, (6) synergistic contamination and environmental effects are significant to materials behavior. The Panel also noted that there were unanticipated bond failures, these occurring with acrylic adhesives. The most confusing, ambiguous, and obscure finding was the extensive surface contamination of experiments and structure. What is the source of this contamination and by what mechanism is it deposited?

Concerns and recommendations for LDEF included the following items: (1) that LDEF lessons learned be captured and summarized; (2) the need for selectivity in deciding what to do with limited funding; (3) that completion of testing be timely because of aging of retrieved samples; (4) that the preflight condition of samples including processing details be more carefully documented; (5) that the location of LDEF control samples be documented; and, (6) that LDEF's value be recognized for ultraviolet radiation effects, thermal cycling, micrometeoroid and debris impact as well as for atomic oxygen effects.

LDEF MATERIALS, ENVIRONMENTAL PARAMETERS, AND DATA BASES

Bruce Banks and Mike Meshishnek, Co-Chairmen
Roger Bourassa, Recorder

- + **Spacecraft on-board monitoring needed for (α , ϵ , T, impacts strain, yaw, pitch, roll) monitors needed**
- **Post-flight degradation occurs**
- **Preflight and post-flight handling is important**
- **New Materials Development Requirements**
 - **Potassium silicate binder paints are durable for α , ϵ (Z-93, YB-71)**
 - **Protective coatings are needed for long term durability of organic materials**
 - **Bumpers or improved designs needed for micrometeoroid and debris tolerance**
 - **Large new data base is emerging from flown LDEF materials which may be baseline for future spacecraft**
 - **AO durable flexible polymer (electrical insulation)**
 - **Replacement for Ag/FEP with low α/ϵ**
 - **Flexible white paint replacement for S13G/L0**
- **Ground Simulation Testing Requirements**
 - **Must be capable of simulating observed LDEF results**
 - **Synergistic effects must be included (simultaneous or sequential)**
 - **How do you extrapolate from ground testing to predict in-space performance?**
 - **Acceleration artifacts for UV, AO, thermal cycling--How much is okay?**
 - **Ground facility contamination effects must be considered**
 - **Ground facility comparative testing on materials flown on LDEF**
 - **Better characterization of ground facilities**
- **Space Environmental Effects Analytical Modeling Requirements**
 - **Data must be available to be modeled - not all is available yet**
 - **Exposures must be reliably reported for LDEF**
 - **Models must predict observed results**
 - **Return flux, trailing edge contamination effects must have models which accurately predict results**
 - **Models must be user-friendly and accepted by the user community**
 - **Thermal models appear adequate**

- **Potential Space Applications**
 - SSF, EOS
- **Understanding of Environmental Parameters**
 - Debris, spatial and temporal non-uniformity may have big impact on SSF reliability
 - AO-UV synergism not previously known especially for Ag/FEP and silicones
- **Understanding of Mechanisms**
 - AO Mechanisms not understood (details of micro-cone structure)
 - Contamination mechanisms not understood
 - + Leading-Trailing surface contamination differences
 - + AO/UV silicone interactions verify ground simulations
 - + Thermal cycling effects in space
 - o No cold welding possibly due to contamination
 - o Adhesive failures
- **LDEF Data-Basing Requirements**
 - Need for LDEF community to be able to electronically alert MAPTIS that data needs updating
 - Two kinds of users' needs should be met
 - Scientists
 - Engineers, Designers
 - LDEF data needs to be sent to
 - Joan Funk, NASA LaRC, for MAPTIS inclusion in any form (hard copy, magnetic disk)
 - Data base must have data source and paper title identified
 - Archiving of photos needs to be carried out
 - Knowledge of location of all LDEF hardware must be capable of being made available to those who may have need it
- **General Needs For Future Flight Experiments**
 - Monitoring of spacecraft
 - Study effects of active vs passive solar cells

- Separation of synergistic phenomena
- List of "LDEF Lessons Learned" must be considered in future spacecraft designs
- Use standard recommended test practices for characterization of materials
- Need to know how to extrapolate results of short flight experiments to long duration
- Need to test new, higher performance, more durable materials
- Need validation as well as phenomenology tests
- **Presentations At Second LDEF Post-Retrieval Symposium**
 - Results and interpretations be presented in narrow discipline, concurrent sessions
 - Organization committee should have presentations on:
 - lessons learned
 - recommendations for users
 - Presentation of quantitative results (new data) not qualitative overviews
 - Advance copy of transparencies should be handed out at start of conference
 - Suggested viewgraph format (include scale bars and appropriate acknowledgments)
 - MAPTIS data base presentation
- **Confusing, ambiguous findings**
 - Sources of contamination
 - Mechanisms--what caused what
- **Additional Recommendations, Concerns**
 - Need to be selective in deciding what to do with limited funds
 - LDEF's value for combined UV, thermal cycling, micrometeoroid, and debris, etc. needs to be recognized
 - Timeliness of aging material samples
 - Initial conditions (preflight) of samples be more carefully documented
 - Processing details are important
 - Capture LDEF lessons learned
 - Location of LDEF control samples needs to be documented

LDEF Contamination

Co-Chairmen: Wayne Stuckey and Steve Koontz
Recorder: Russell Crutcher

The contamination panel consisted of nineteen individuals representing a variety of NASA, DOD, and corporate centers (see attached). The meeting commenced at 12:55 PM, November 21, 1991. This session covered the following agenda topics:

1. What have we learned?
What are we sure of and what is still in question?
2. How have initial results affected Aerospace Technology?
3. How should the data generated be stored to facilitate retrieval?
4. What future requirements have been indicated?

The items listed under what we had learned included things confirmed by LDEF, new information from LDEF, and things suggested by LDEF with data from, other projects strengthening the inference.

WHAT HAVE WE LEARNED

Most of the molecular film deposition was not line of sight. The deposits exhibited a geometry that did not point toward any specific outgassing source. Much of the contaminant film was found deposited on surfaces that faced outward from LDEF, indicating some of the deposition was the result of return flux. The interesting geometry seen in the deposited films were all related to the 'fixing' mechanisms, ultraviolet radiation and atomic oxygen, and not to an obvious surface collection mechanism. The infrared spectra of the most common molecular films indicated that the film was a mixture of functional groups from the variety of materials found on LDEF with modification as would be expected from the ultraviolet and atomic oxygen exposure. Urethane and silicone modalities were very common along with various other nitrogen containing functional groups and carbonyls. Large amounts of urethane paint, Z306 and A276, and silicone containing materials had been used on LDEF. The outgassing products from these materials, if blended and modified, would be consistent with what has been found using infrared analysis. This leads to the conclusion that most of the molecular contamination was outgassed from material intentionally used on LDEF. Infrared analysis of residues under tray clamps and shims and under materials fixed in location prior to flight indicated the presence of silicones and organics. Witness plates in the shuttle bay on other missions have indicated a deposition of silicones and organics during payload integration and vertical assembly. It is reasonable to assume that the molecular contaminants present prior to launch included both organic and silicone films and that these materials may have been widely distributed.

Silicones were a significant part of the final molecular film seen on LDEF surfaces. Atomic oxygen reacted with these molecular films removing most of the carbon and creating an oxidized silicon film. On surfaces with high atomic oxygen exposure the resultant film was thoroughly oxidized and became an invisible, porous, glassy layer. With less atomic oxygen exposure the characteristic brown film persisted underneath the silicon oxide surface layer. All exposed surfaces were contaminated with this film except for those being eroded by atomic oxygen.

The initial deposition of the molecular film was cyclic in nature, depositing the film with as many as 34 discrete layers as seen on tray C-12 and Earth and Space end films. Deposition patterns on the sample canisters indicate that most of the molecular film deposition occurred in the first thirty days though materials continued to accumulate throughout the mission at a reduced rate. A Quartz Crystal Microbalance

active over the first 400 days of orbit on the trailing edge tray D-3 recorded a steady accumulation of mass. This is consistent with the experience of other satellites with sensors in a trailing or UV shadowed orientation.

The film was not uniformly distributed. Inside LDEF the film was concentrated wherever ultraviolet light could penetrate as LDEF came out of the earth's shadow. These surfaces were oriented toward the ram direction so they also received atomic oxygen. The vent openings tended to have heavy deposits on the more ram directed sides. The films over much of LDEF were thin and often perforated. Atomic oxygen, ultraviolet light, the thermal condition of the surface and the cyclic inter-relationships of these parameters influenced deposition. Different surfaces also exhibited different collection efficiencies. Particulate contaminants on the surface of LDEF created holes in the contaminant film nearly an order of magnitude greater in area than that of the particle. This was exhibited as halos of relatively "clean" surface or "clean" shadows associated with the presence of particulate contaminants.

Cross contamination from the Shuttle to LDEF and from LDEF to the Shuttle was evident based on particle types collected from the surface of both. Many of the Shuttle particle types found on LDEF were present while LDEF was in orbit. These particles were deposited on LDEF prior to and during launch. Others were not associated with orbital artifacts and may have been deposited post orbit during the recovery operations. LDEF was a major source of contamination for the Shuttle bay during recovery. There may have also been molecular cross contamination both during the original preorbit exposure of LDEF to the Shuttle bay and during the recovery. Current evidence from the HALO program suggests a low level of silicones may have deposited on LDEF prior to release into orbit from the silicones used on the Shuttle Bay liner and the Shuttle tiles.

Small circular deposits made by liquid aerosols have been found on every tray and most of the tray clamps of LDEF's surface. The concentration of these deposits varies widely from hundreds per square inch in a few locations to less than one per square inch in other areas. The deposits also vary in size from about a millimeter in diameter or larger to a few micrometers. Some of these materials were deposited prior to integrating the trays to LDEF and are consistent with "sneeze" droplets. These exhibit the highest local concentrations. Others are more complex and exhibit a pattern characteristic of an orbital environment. Some of these on the ram surfaces are oxidized and have no residual organic compounds. Others on the ram surface contain significant amounts of organics and could not have been present for any extended duration during the free orbit of LDEF.

The importance of contamination control plans and the need for detailed material reviews have been reemphasized as a result of the LDEF findings. Contaminants generated in any one area of LDEF contributed to the contamination of the entire structure. The concept of having sensitive surfaces out of the line of sight of contaminating materials is not sufficient to protect sensitive surfaces.

There are a number of questions that are not yet resolved. The sources of the silicone component of the molecular films have not all been identified. Many materials have been suggested but no detailed inventory of silicone containing materials has been produced. The Z306 black paint contained a very low level of silicones (0.05% or less). There were silicone contaminant films on the surface of some trays prior to launch. Silicone RTV's were used to stabilize some components so that they could better tolerate launch vibration; a ring of silicone contamination was deposited on every tray by the gasket of the tray covers; cross-contamination of silicones used on the shuttle to payload surfaces has been suggested with some support based on witness plate studies. The relative contribution of all these sources to the final film has not been determined.

Another unresolved question is the time and the mechanism of molecular film deposition. There was a major deposition sequence early in the mission but deposition continued over at least the first 400 days and probably over the entire mission. Atomic oxygen and ultraviolet light degraded more stable materials creating new outgassing species throughout the mission. The proportion of the outgassing materials that returned to LDEF as a stable surface film has not been determined nor has the mechanism for creating the

film in its various locations. Ultraviolet light and atomic oxygen are both implicated as important to the creation of the film but the relative role of each has yet to be resolved.

There still remains much work to be done in quantifying the amount and distribution of the molecular films on LDEF. Models for the return flux and for the effects of vent geometry cannot be validated without such a detailed map. Electrical or magnetic field effects and other possible effects also need such a map to be adequately investigated.

INITIAL EFFECTS ON AEROSPACE TECHNOLOGY

Aluminized Kapton has been used frequently for low earth orbit (LEO) applications. On LDEF Kapton used on the ram surfaces eroded on exposure to atomic oxygen, leaving a very thin layer of aluminum foil. Some of the residual foil migrated in orbit, obscuring areas of previously exposed surface. Use of this material for future low earth orbit missions should be reconsidered in the light of the LDEF experience. The Z306 paint and its primer was one of the major contributors to the molecular film deposit on LDEF. The Z306 has a very favorable volatile/condensable material (VCM) rating based on the NASA standard outgassing test. This should not be considered a reasonable measure of the VCM during nearly six years of actual orbital exposure. Large areas on the interior and some of the exterior surface of LDEF were covered with this paint, so even low VCM values could contribute significant amounts of condensed material. The primer had a much higher VCM value and the volatile species did diffuse through the Z306, which also contributed to the total material outgassing from the painted surfaces. A more general concern is the possible formation of volatile condensable materials by the interaction of ultraviolet (UV) light and atomic oxygen (AO) on exterior exposed polymers. The frequency with which fluorine, presumably from the Teflon blankets on LDEF, was found by surface elemental analysis on surfaces far removed from any Teflon suggests such a mechanism. A list of likely reaction products from ultraviolet and atomic oxygen exposure for most polymer materials also includes many materials that could condense on surfaces in an orbital environment.

LDEF provides an opportunity to better understand the environment in low earth orbit and the synergistic relationships between the various environmental parameters. One example is the apparent UV enhanced atomic oxygen erosion rate of Teflon materials in LEO. Teflon surfaces exposed to UV alone exhibited surface modification and texturing that suggests chemical modification.

Another example is the AO cleaning effect. On ram surfaces that were attacked by AO there was no accumulation of molecular contaminants. On ram oriented metal or ceramic surfaces a contaminant film was present, though it tended to be invisible, making the surface appear 'clean'. When a surface analysis was performed on such materials, a layer of silicate contamination was invariably found. This silicate layer is the oxidized remnant of the molecular film found elsewhere on LDEF.

LDEF underscored the importance of synergistic effects in the performance of materials in LEO. Molecular films were not found necessarily on the most efficient collection surface or on surfaces that experienced the greatest exposures to outgassing materials but rather on surfaces where the conditions were conducive to the formation of stable films. These were surfaces that were cool at the time of their exposure to ultraviolet light and that had direct or indirect exposure to atomic oxygen. The relative role of UV and AO to the formation of these films may be indicated by the distribution of the film on LDEF but they have not yet been deciphered. The migration of particles during orbit has been documented on LDEF, but the conditions that cause the movement away and back or along the surface have not been determined. The distribution of debris from impacts to other surfaces on the satellite is another well documented effect on LDEF. Impact generated, spattered molten metal has been found on the surface of LDEF tens of centimeters from its source.

The whole field of combined effects needs to be more closely examined in light of LDEF findings. UV, AO, thermal effects, charging, field effects, outgassing and offgassing rates, the path of impact ejecta, degradation product yield in response to UV, AO, and combined UV-AO at various surface temperatures are environmental parameters that require more evaluation as indicated by the distribution and flight dynamics of contaminants on LDEF. Other parameters such as electrical fields, magnetic fields, and plasma may also have left distinguishable marks on LDEF.

The LDEF findings have emphasized the desirability of eliminating silicones and of minimizing organic materials on spacecraft. Exterior surfaces are the most susceptible to degradation caused by the exposure of silicones or organics to UV and AO. Venting from the interior of LDEF was responsible for much of the exterior deposit. Careful design of vents would help eliminate these problems as would the reduced application of organic or silicone materials on the interior of the spacecraft.

LDEF verified the need for greater flexibility in the testing of materials for specific orbital applications. ASTM E595 is a step in the right direction but more is needed. Combined exposure testing is needed for surfaces exposed to UV and AO. After all the components have been evaluated, a system level test would show the result of the interaction between contaminants from different components and their joint response to the environment. The panel stressed that acceptable performance of a material in these tests does not eliminate the concern for contamination; it simply helps to quantify the risk. Current materials carefully used can be acceptable, provided all recommended guidelines for restricted use and special processing are followed. The term "Space Qualified" for materials that meet a particular performance level should not be interpreted as license to use such a material freely.

LDEF results have also had an effect on contamination modeling. Most of the molecular deposition occurred at surfaces where the conditions were conducive to the formation of a stable film and not in the direct line of sight from specific sources. Current models model condensation on surfaces and not 'fixing' of the condensed materials to surfaces. Return flux was also an important contributor to the surface film. The role of vent configuration needs more detailed consideration. Larger trailing edge vents on satellites could reduce return flux. On the ground the poor correlation between airborne monitoring, small area fallout collection plates, and the actual accumulation of contaminants on the surface of large spacecraft was again verified.

DATA BASE REQUIREMENTS

The effects of contaminants on LDEF materials need to be documented by material type and/or system. Optical, thermal control surfaces, solar cells, and other key references must be one mode of access. The effects must also be accessible by type of contaminant, source of contaminant, time of contamination, and analytical method. The analytical method should be cross referenced to results from other methods of analysis. The test methods used to measure the changes in the material and those to identify and quantify the contaminant must be specified along with the raw data, the time of the analysis, sample preparation, conditions of storage prior to the test, and any other information that would have an effect on the measurements taken.

Much valuable information about the dynamics of contaminants on Shuttle missions and on the dynamics of contaminants in low earth orbit has been gained by the study of LDEF, but there is much more that can still be learned. LDEF has been a rare opportunity to glimpse the actual dynamics of contaminants in low earth orbit. These lessons learned must now be communicated to the aerospace community in general. The database is an important part of that communication but so also are the papers being generated by the various LDEF conferences. Much of the analytical work already accomplished has yet to be evaluated and disseminated. The upcoming June, 1992 LDEF meeting will be an opportunity to continue to disseminate the lessons learned from LDEF to the entire community and not just to those in our own particular area of aerospace technology.

PANEL MEMBERS

Brian Blakkolb	TRW Space and Defense	(310) 813-8960
David Brenza	JPL	(818) 354-6836
Richard W. Cahill	Lockheed Missiles & Space Co.	(408) 743-2739
Robert J. Christie	Rockwell International	(216) 734-2550
Joan Cranmer	JHU/APL	(301) 953-5000 X3810
Russ Crutcher	Boeing Defense & Space Group	(206) 773-7002
Capt. Deidra Dykeman	RL/OCPC	(315) 330-3145
Frederick C. Gross	NASA Goddard Space Flight Ctr.	(301) 286-8349
Gale Harvey	NASA Langley Research Ctr.	(804) 864-6742
Carol Hemminger	The Aerospace Corp.	(213) 336-7666
James L. Jones	NASA Langley Research Ctr.	(804) 864-3795
Michele D. Jones	MLBT, Wright Laboratory	(513) 255-8097
Chia-Shih Lee	SSD/CNSE, Los Angles AFB	(213) 363-6867
Francois Levadou	ESA/ESTEC	31/1719-83915
Joe McKenzie	Grumman-SSEIC	(713) 929-7467
Michael Rodriguez	MDSSC, NASA Goddard Space Flight Ctr.	(301) 286-9296
David Schwam	Case Western Reserve University	(216) 368-3864
Wayne K. Stuckey	The Aerospace Corp.	(310) 336-7389
Bob Turner	W. J. Schafer	(703) 558-7900

LDEF CONTAMINATION

Wayne Stuckey and Steve Koontz, Co-Chairmen
Russell Crutcher, Recorder

DISCUSSION TOPICS

What Have We Learned?

Clear

Needed

How Have Initial LDEF Results Affected

Potential Space Applications

Understanding of Parameters/Synergisms

Materials Degradation

New Materials Development

Ground Simulation Testing

Analytical Models

Data Bases

Future Requirements

WHAT HAVE WE LEARNED (Clear, Indisputable)

Not Line-of-Sight - Notable return flux

Self Contaminating

Confirmed environmental interactions - Atomic Oxygen, UV, Temperature

Silicone Contamination

Contamination continued to accumulate

Non-Uniform deposition - Not always visible

Contamination layers present

Importance of Multiple Sources

Leading Edge deposits are more transparent

Cross Contamination from Shuttle Sources

Droplets from pre- and post-orbit operations

Importance of Contamination Control Plans and Materials Review

WHAT HAVE WE LEARNED (Needs Clarification)

Sources of Silicones/Silicates
Deposition profile for entire mission
Deposition Mechanisms
Thickness, Amounts of Contaminants on LDEF Surfaces
Contribution of AO Degradation Products
Models for Return Flux, Vents
Sources of Other Contaminants from LDEF Interior
Electrical Interaction with Contaminant Deposition

How Have Initial LDEF Results Affected

Potential Space Applications

Aluminized Kapton
Erosion may be Contaminant Source

How Have Initial LDEF Results Affected

Understanding of Environmental Parameters/Synergisms

Particulate Migration
UV Enhanced Deposition
AO/UV Synergism for Deposition
AO "Cleaning" or Deposition
Impact Debris
Non Line-of-Sight Deposition
Other Parameters to be considered
 Electrical Fields
 Plasma
 Magnetic Fields
Particulates from AO/UV Interactions

How Have Initial LDEF Results Affected

New Materials Development Requirements

Alternate Non-Silicone Materials
Current Materials generally acceptable with proper usage/processing

How Have Initial LDEF Results Affected

Ground Simulation Testing Requirements

Verified Need for Materials Testing for Contamination (E595)
New ASTM Method Available for Materials
Need for Combined Exposure Testing
System Level Contamination Tests

"Space Qualified" (E595) does not eliminate contamination concern

How Have Initial LDEF Results Affected

Space Environmental Effects Analytical Modeling

Line-of-Sight versus Monte Carlo - Importance of Return Flux
Venting Source Analysis Needed
Airborne particulate results do not correlate with surface cleanliness

How Have Initial LDEF Results Affected

Data Base Requirements

Effects of Contamination on Materials Performance
 Optics
 Thermal Control
 Others
Document Results and Analysis Technique
Analyze Reference Areas by Multiple Techniques
Note Potential Sources
Note Contamination Analysis and Effects of Contamination
Include other relevant data whenever possible
Time of Analysis, Storage Conditions, Removal, Sample Preparation,
 History
Document Lessons Learned

Thermal Control Coatings, Protective Coatings, and Surface Treatments

Co-Chairmen: Ann Whitaker and Wayne Slempp
Recorder: Johnny Golden

Applicability of Results:

The initial LDEF results on thermal control coatings have direct applicability to all LEO spacecraft. The environmental conditions provided by LDEF, including the contamination environment, will also be partially applicable to other spacecraft working altitudes.

Understanding Of Environment/Synergism:

Although the LDEF results greatly increased our knowledge of long-term LEO effects on materials, we still do not fully understand the LEO environment in terms of synergistic effects. This deficiency is largely due to the lack of firm single environmental parameter effects data from LDEF. Most measured changes in thermal control materials have been related to combined environmental effects due to the nature of the LDEF mission.

Understanding of Degradation Mechanisms:

The mechanisms of materials degradation are likewise not well understood. Degradation (chemical) mechanisms are determined by understanding rate effects. However, the effect of temperature and thermal cycling has been largely ignored in the initial LDEF results. The temperature dependence of AO and UV effects must be ascertained to complete our understanding of materials degradation mechanisms. For LDEF in particular, we also need to express how contamination effects have interacted with surfaces when we interpret degradation mechanisms.

Materials Development Required:

LDEF results and recent world-wide focus on environmentally conscious manufacturing have affected requirements for new materials development. The inorganic white coatings Z93 and YB-71 were confirmed through LDEF data to have stable optical properties in the LEO environment. However, a new source for the silicate binder used in these coatings must be obtained. The requalification process is presently underway at IITRI. LDEF results indicate that thin silicates as overcoatings should be developed for AO protection of less stable thermal control surfaces. The continued use of organic coatings for passive thermal control will require the development and qualification of materials with environmentally compliant levels of volatile organic compounds (VOCs). Need was expressed for the development of new conductive and partially conductive coatings with acceptable optical properties. Finally, the UV degradation of silver/Teflon adhesive observed on LDEF warrants the evaluation and publication of an appropriate application procedure to avoid future problems.

Ground Simulation Testing:

The ability of ground simulation testing to be accelerated and still provide results comparable to that observed on long-life spacecraft is the ultimate goal of performance

life prediction. Examples where prediction did not meet performance, most notably with S-13G/LO, have been observed with LDEF. The ability to conduct combined effects testing is indicated, involving combined AO plus UV exposure at controlled temperature with in situ reflectance measurements. Serious work concerning the proportionality of AO and UV for such a system, in addition to the type of UV source, needs to be done. The use of calorimetry to obtain real time α/ϵ measurements would be an enhancement. The addition of electrons and protons to ground testing is also recommended.

Analytical Modelling:

The LDEF results have illustrated the need for adequate modelling of the contamination environment, to determine the sources and sinks of molecular contamination, and how this will affect the performance of thermal control coatings. The most useful contamination model would include interactions with AO and UV.

Data-Basing Requirements:

Data-basing of LDEF thermal control coating experience is essential. A format like that developed for the optical systems data, presented at the workshop, would be acceptable when modified to support thermal control coatings key words. However, it must be recognized that such a database will require a commitment for continued financial support in order to be maintained adequately.

Future Flight Experiments:

Future flight experiments suggested by the results of LDEF thermal control coatings analysis would be an "LDEF"-like vehicle and orientation, flown in polar or highly elliptical orbits. Such experiments would allow more separation of the individual environmental factors for elucidation of degradation mechanisms and synergisms, and would also provide enhanced particulate radiation for the study of spacecraft charging effects on thermal control coating degradation.

Second LDEF Post-Retrieval Symposium:

Information presented at the Second LDEF Post-Retrieval Symposium should draw conclusions and make recommendations. It is also preferable to see more comprehensive presentations, which provide data for materials considering the various environmental exposures available on LDEF when applicable. Another factor in these comprehensive presentations would be that they also include comparisons to ground test results reported in the open literature.

Clear Findings:

Clear findings from LDEF were few, but it is apparent that the silicate-based coatings Z93 and YB-71, and the chromic acid anodized aluminum are stable thermal control coatings for long-term space flight in LEO. Another clear finding is that for paints which are vulnerable to AO and UV degradation, such as in polyurethane paints (A276), the coating performance is principally controlled by AO erosion.

Confusing Findings:

Several results from LDEF appear confusing at this time. Urethanes, silicones, and epoxies exhibited changes in their fluorescence spectra after LDEF exposures, with reflectance of a UV illumination source shifting from the ultraviolet region to the visible region. LDEF AO fluence modelling has shown that most of the AO exposure occurred in the latter stages of the LDEF mission. It is not completely clear how this relatively rapid increase in AO flux has affected thermal control coating results. It is also apparent that we do not understand the degradation of the black chromium solar absorber coating, when it exhibited very stable optical properties in some areas but changed in other areas where the environment should not have been substantially different. And finally, has contamination contributed to some of the results which are not compatible with STS measurements? There is some confusion in determining which LDEF results are due to contamination, which are due to the "natural" space environment, and which involve interactions that protect or degrade the performance of thermal control coatings.

Other Concerns:

Several other concerns and comments were raised in the thermal control coatings theme panel discussion. One concern was post-flight handling, and how this has affected the data. Comment was made about the FEP Teflon AO erosion rate appearing to have been accelerated above STS predictions due to UV exposure, and if electron and proton radiation could also play a role in this effect. It was also observed that the S-13G/LO coating exhibited varying degrees of degradation, all within what could be considered as comparable environmental exposure conditions. There is some question as to how much of such effects are due to formulation and application technique, as opposed to contamination and environmental exposure.

THERMAL CONTROL COATINGS, PROTECTIVE COATINGS, AND SURFACE TREATMENTS

**Ann Whitaker and Wayne Slomp, Co-Chairmen
Johnny Golden, Recorder**

THERMAL CONTROL COATINGS

- **Applications:** Data directly applicable to all LEO spacecraft - partially applicable to some higher orbits without high radiation fluences
- **Understanding of environment/synergism:** Not fully understood - Need single parameter effects data mechanisms dependent upon rate effects - Need dependence data for AO, UV at temperature. Need contamination effects interaction data
- **Materials development required:** Thin silicates as overcoats for AO protection - Need source of silicate for Z-93 and requalification of coating
- **Materials development:** Evaluation and publication of application process for silvered Teflon
- **Ground simulation testing:** In-situ measurement capability for AO and UV testing, addition of electrons and protons to ground testing, and achievement of same results for long-life spacecraft
- **Analytical modeling:** Ability to model contamination and its effect on coatings

- **Data-basing requirements:** Optical systems data base is acceptable - use thermal control coating key word
 - This Data Base will need continued financial support to be maintained!
- **Future flight experiments:** Need polar and elliptical orbit data with high particulate radiation
- **Information should draw conclusions and make recommendations - need more comprehensive presentations looking at all environments on LDEF**
- **Clear Findings:**
 - Chromic acid anodized aluminum and Z-93, YB-71 paints are stable for long-term space flight
 - AO erosion is major factor in coating performance where paints are vulnerable to UV and AO degradation. Example--A276 (urethane binders)

- **Confusing Findings:**
 - Urethanes, silicones and epoxies change fluorescence spectrum after UV and AO exposure
 - Since LDEF had most of its AO exposure at end of life - how does this effect the results?
 - Black chromium had stable optical properties in some areas but changed in others where environment should be the same
 - How does contamination effect AO and UV degradation? What changes on LDEF are due to contamination vs natural space environment?
- **Concerns:**
 - How did post-flight handling affect data?
 - FEP Teflon coating AO erosion rate appears to accelerate with UV exposure. Do electron and proton radiation also play a role in this acceleration?
 - The S-13GLO exhibited varying degrees of degradation - Is this caused by formulation, application, or contamination and environmental exposure?

Polymers and Films (Including Ag/FEP)

Co-Chairmen: Philip R. Young and David Brinza
Recorder: Gary Pippin

This theme panel is conveniently separated into two subtopics, silvered teflon (Ag/FEP) and other thin film polymeric materials.

Potential Space Applications

The Ag/FEP blankets remained functional as a thermal control system over the lifetime of the LDEF. Several changes were observed which will limit the lifetimes of the blankets. The recession due to atomic oxygen will eventually leave the FEP layer thin enough so that the emissivity will decrease. Solar ultraviolet and vacuum ultraviolet radiation caused degradation of mechanical properties. Delamination zones were observed around all the impact sites. The above effects acted in concert at certain locations. Any one, or combination of these effects may ultimately limit the lifetime for a given application. The large number of thermal cycles endured by the spacecraft may have enhanced the delamination. The silver layer in the adhesive-backed Ag/FEP was cracked during the application onto the aluminum substrate, causing "bleed-through" and subsequent darkening of the adhesive under solar exposure. While this process increased the solar absorptance to thermal emittance ratio, the resulting temperature increases were not excessive. The roughening of the surface texture of the FEP layer dramatically increased the diffuse component of reflectance. The resulting increase in light scattering means that care should be taken when atomic oxygen susceptible materials are used near sensitive optics.

Unprotected, non-silicone containing organic polymers were heavily attacked by atomic oxygen. At least 0.010" thickness of Kapton was removed from near leading edge locations.

Siloxane containing materials are self-protecting as thin silicon dioxide layers are formed under atomic oxygen exposure. These materials outgas, and if the outgassed materials deposit on other surfaces, the surface optical properties can change.

Understanding of Environmental Parameters

The erosion rate of Ag/FEP was greater than rates observed on short-term shuttle flights. One possibility is that increased UV exposure will break bonds and provide more and more active sites for oxidation events. There is evidence for heating on a number of film specimens. The texture of some regions of the FEP, as viewed under SEM, looks like material which has been melted at some time. Some remaining strips of thin film materials are twisted and curled and appear to be shrunk. The thermal cycling can influence the erosion rate for oxidation processes which have some activation energy. The measured recession rates are global averages over the complete range of conditions, but the actual rates may have varied widely during even single orbits. Localized heating appears to have occurred where particles with particular optical properties have migrated onto surfaces with different optical properties. The Earth and space end thermal panels were coated differently, and the bicycle reflector near the trailing edge and at the Earth end of LDEF was severely eroded and very different in appearance from any of the other reflectors. On Ag/FEP blanket A4 there is evidence of indirect atomic oxygen scattering from the underside of a nearby scuff plate which extended beyond the end of the LDEF structure and was exposed to ram atomic oxygen. Surface roughening on the tucked edge portions of Ag/FEP blankets near the leading

edge was also observed, implying oxygen was scattered from tray and clamp edges. LDEF represents the first examination of material which has been exposed under all conditions of the solar cycle, from solar min to solar max. The solar vacuum ultraviolet radiation flux varies over the solar cycle. The influence of this variation on the thin polymer film samples has not been well characterized.

Understanding of Degradation Mechanisms

The erosion of Kapton is apparently linear with AO fluence; the observed recession on LDEF can be generally predicted by multiplying the STS-8 erosion yield with the calculated LDEF AO fluence. Significantly greater erosion yields are observed for FEP, polystyrene, and PMMA from LDEF in comparison with shuttle results, suggesting a strong atomic oxygen/ultraviolet radiation synergism in the degradation mechanism for these materials. The mechanical properties of FEP were affected by exposure to UV. The data indicate chain scission processes followed by crosslinking in the polymer under UV exposure. For the specimens which were highly eroded due to atomic oxygen exposure, little chemical change was observed relative to ground specimens. This suggests that UV may prepare free radical sites on or near the surface. The oxygen reacts at these sites, producing volatile species which then leave, exposing fresh material. There is concern that there may be post-retrieval material degradation; peroxide radicals may form on surfaces and continue oxidation and volatilization processes.

New Materials Development Requirements

LDEF confirmed the need for both atomic oxygen and ultraviolet radiation stabilized materials for long term missions. Polysiloxane modified materials and thermoset siloxane materials with high (> 200C) glass transition temperatures offer possibilities for atomic oxygen stabilized materials. Fluorocarbons have extended lifetimes relative to polyimides and hydrocarbons. Use of phosphate pendant groups on polymer chains should enhance oxidative stability because the phosphate group is already oxidized and is large enough to block access to main chain atoms. For ultraviolet stabilization, candidates include polyphosphazenes, UV stabilized fluorocarbons such as perfluorophenyls, low color polyimide polymers (UV transparent), and aromatic polyimides.

Ground Simulation Testing Requirements

The types of capabilities needed from test facilities are high fluence atomic oxygen exposure testing with directed beams, high fluence UV/VUV testing, simultaneous atomic oxygen/ultraviolet (including vacuum ultraviolet wavelengths) radiation exposures, in situ properties measurements, thermal cycling/temperature control and monitoring, and "large" exposure areas (perhaps 100 cm² or greater). Materials flown on LDEF which appear to be good candidate material types for use in calibration of test facilities include FEP, the type of polymers flown on experiment AO114, the graphite fiber/organic resin composites, and the polyurethane based A-276 white thermal control paint. This is a good range of pure materials and mixtures which degrade by a variety of mechanisms and will give a good gauge of the effectiveness of a space simulation test bed.

Space Environmental Effects Analytical Modeling Requirements

Spacecraft environmental models should be able to predict overall effects on satellites, atomic oxygen and UV flux, and particle impact rates vs location, and should be able to predict local effects, temperature variations, outgassing, and shadowing from nearby structures. Both direct and indirect scattering of atomic oxygen should be modeled. Experimental results from the LDEF provide a means to verify models for virtually every LEO environmental parameter. The orbit data generated by NORAD observations of LDEF can be used to test models of the atmosphere, particularly density predictions, to improve our knowledge of satellite drag coefficients. Materials degradation models can be produced from LDEF for several materials. We can make some empirical predictions about erosion yields for materials with up to six years exposure. Detailed mechanistic models will require more effort. The specific dependence of degradation and recession on atomic oxygen and ultraviolet fluxes varies by material type. These effects are likely strongly time and temperature dependent, activation energies will vary for different processes, and the fluxes of vacuum ultraviolet radiation and atomic oxygen change drastically over the solar cycle. At different times, different parameters likely dominate the rate limiting processes. This is a complex, material specific area. The goal is to be able to make accurate lifetime performance predictions for materials with specific applications. This would improve the reliability of spacecraft and therefore their chances of enduring and performing their missions over the long term. Good models would also minimize the cost of testing by guiding selection of test parameters to focus on critical conditions.

Data Basing Requirements

The following information is the minimum required for an effective compilation of materials data from LDEF. The trade name of the material; its chemical composition and structure; the locations on LDEF, including exposure details such as direct, indirect, internal, and likely thermal conditions; and availability of controls for each are desired, as well as a list of investigators who flew a particular material as part of their experiment, either as specimens or supporting hardware. A compilation of general observations should be obtained and should include notes on contamination, meteoroid and debris impacts, physical integrity of the hardware, and any evidence of melting or other visual changes. The available numerical data, with estimates of the uncertainty (error bars!) is of interest. Measurements of erosion are needed, as well as a surface analysis to obtain elemental analysis and to identify the functional groups present. Surface morphology should be documented, and a thermal analysis is needed to obtain glass transition temperatures, coefficient of thermal expansion, heat capacities, and melting temperatures. Mechanical and optical properties of interest are the moduli, strength, % elongation, solar absorptance, thermal emittance, and diffuse reflectance. Outgassing and weight loss of material should be included. Reports of measurements should include the laboratory and the date of analyses so that any terrestrial degradation may be accounted for. A reference list of photographs of SEM, AFM, and STM images should be compiled. A list of references to other flight data, laboratory data, and investigators working with this material for space applications should be compiled for each material.

Future Flight Experiments

There are several near term flight opportunities which may provide materials performance data. Shuttle flight STS-046 will contain the Energetic Oxygen Interaction with materials-3 (EOIM-3) experiment, which will provide a 40 hour exposure. This flight will also launch the EURECA free flyer experiment which will remain in orbit for between 6 and 11 months. The LDCE (gas can) sponsored by Case Western Reserve University, the IOCM and other gas can experiments represent additional opportunities. The SAMMES experiment will be an active experiment with telemetered data. Future opportunities may include other free flyers, RPC, and Space Station Freedom.

Measurement techniques on EOIM-3 will include recession measurements vs weight loss, stressed and loaded materials, temperature effects, thin films on reflective surfaces, UV synergism, and variable exposure. The SAMMES and OPM will have in situ monitoring of critical properties such as absorptance, emittance, and thickness, and SAMMES will have an in situ environment monitor. The SAMMES mission will be an extended duration exposure of between 6 and 18 months. Canister experiments will offer the advantage of controlled environments.

Suggestions for the Next Symposium

Submission of data packages at the symposium for data basing should be required. The presentations by the principal investigators should be detailed and include interpretations of their observations. The presentations by the special investigation groups should focus on the consequences of the observed condition of the hardware, a compilation of engineering lessons learned, and predictions for use by future missions. There should be plenary sessions for environments and for each of the special investigation groups. The conference should include a poster session and a mixer. Discussion periods are essential, and concurrent sessions should be conducted for the different subject themes and disciplines.

Summary of LDEF Findings

The clear findings are that the LDEF was retrieved, the funding was inadequate for postflight analysis, and the results were needed rapidly. The effects of atomic oxygen and solar ultraviolet acting in concert were evident for many materials. Contamination was widely present on this spacecraft. The effects of the thermal velocity component of atomic oxygen were verified by examination of FEP and Kapton films.

The LDEF findings that are not so clear are the impact of contamination, post-retrieval aging effects, thermal effects, and the atomic oxygen fluence estimate. We have several comments, concerns, and recommendations. This community of workers needs more access to each others' data and materials for additional testing. The methods of storage of materials, both flight and controls, may not have prevented aging effects. Both time and money are critical for obtaining the maximum information from this rather unique opportunity. We should try to target end-users for support and advocate continued investigations. Prime contractors on SSF should consider supporting these efforts with IR&D funding; we should also continue to solicit support from DoD and SDIO.

POLYMERS AND FILMS (INCLUDING AG/FEP)

Phil Young and David Brinza, Co-Chairmen
Gary Pippin, Recorder

- Potential space applications of materials affected by LDEF results
 - Ag/FEP:
 - Blankets remained functional over LDEF mission
 - AO erosion may limit life; diffuse reflectance may impact systems sensitive to light scattering
 - UV/VUV effects on FEP mechanical properties
 - Enhanced propensity for delamination of Ag/FEP can impact thermal control performance
 - "Bleed-through"/aging of bonded Ag/FEP affects α
 - Non-silicone-containing, unprotected polymers heavily attacked by AO (i.e. ~ 0.010" Kapton eroded)
 - Siloxane - modified materials are self-protecting survive AO attack outgassing concerns...chemical incorporation rather than blends effects on surface optical properties are a concern
- Understanding of environmental parameters/synergisms affected by LDEF results
 - Greater than expected erosion noted for some materials Enhanced UV/AO fluence ratio effect?
 - Indirect (scattered) AO effects observed Reflection from LDEF tray surfaces on Ag/FEP films
 - Extensive heating of films witnessed (melting of polyethylene) Effects on degradation due to UV/VUV exposure Effects on AO attack of carbon films
 - Local thermal effects noted Particles/surface debris on materials Earth, space end panels (melted bicycle reflector)
 - Variability of UV/VUV with solar cycle
- Understanding of mechanisms of materials degradation affected by LDEF results
 - Erosion of Kapton apparently linear with AO fluence data. Observed recession predicted by previous erosion yield from LDEF AO fluence
 - Significantly greater erosion yields for FEP, polystyrene, PMMA... suggests strong AO/UV synergism

- Mechanical properties significantly affected by UV
Crosslinking, chain scission processes in FEP, polyethylene
- Little chemical change noted in highly eroded materials;
Exception: ESCA of FEP
C8 - nearly same as control (+0.5% Oxygen)
C5 - CF, CF₃ enhanced with respect to control
C6 - intermediate to C8, C5
- Data for materials in canisters important for leading edge
Enhanced AO/UV fluence ratio
- Materials degrading since retrieval
Peroxide radical chemistry?
- New materials development requirements affected by LDEF results
 - Materials intrinsically stable against AO attack needed
Siloxane - modified polymers (polysiloxane/polyimides)
Thermoset siloxane materials - High Tg (>200°C)
Fluorocarbons have extended life compared to polyimides,
hydrocarbon polymers
 - UV--stabilized materials
Fluorocarbons with pendent and chain perfluoroaromatics
Aromatic polyimides
Colorless/low color polyimides
Polyphosphazines
Phosphate pendant groups on polymer chains
- Ground simulation testing requirements affected by LDEF results
 - High fluence AO testing (directed beam)
 - High fluence UV/VUV testing
 - Simultaneous AO/UV exposure testing
 - Quantify acceleration factors for testing
 - Large exposure areas - mechanical testing
 - Thermal cycling
 - Temperature effects
 - Potential "benchmarks":
A276 paint
Polymers being studied at UAH
FEP
Composite materials (matrices)
Canister materials

- **Space environmental effects analytical modeling requirements affected by LDEF results**
 - **Environment definition - global and local environments**
AO fluence estimates: direct, indirect (scattered AO)
UV/VUV fluence
Thermal environment
 - **Degradation models**
Empirical, simple models (erosion yield, optical and mechanical property changes, etc.)
Detailed mechanistic models
Dependent on:
 - AO fluence
 - UV/VUV fluence
 - Materials
 - Temperature
 - Time
 - Load
 - .
 - .
 - .
- Lifetime performance prediction - Complex!**

- **LDEF Data base needs, format, search strategy**
 - **Specimen:**
 - * Trade Name, MARTIS ID
 - * Chemical composition, structure
 - * LDEF location
 - * Investigator(s)
 - * Availability of flight, control materials
 - **Analytical data:**
 - * Erosion (recession) \Rightarrow erosion yield
 - * Surface analyses: ESCA, IR (functional groups, spectra references)
 - * Mechanical property changes (moduli, strength, percent elongation, etc.)
 - * Thermal analyses (T_g , T_m , C_p , CTE, ΔH fusion, decomposition)
 - * Optical properties (α , ϵ)
 - Mass loss (outgassing characteristics)
 - Reference (index) of photos, SEM, STM, AFM
 - Laboratories, techniques and dates of analyses
 - **General observations:**
Contamination, M&D impacts, melting, etc.
 - **References to other flight, laboratory simulation data with dates and investigators**
 - * **Search keywords**

- Needs for future flight experiments

Opportunities:

- Imminent:

Shuttle: EOIM-3 STS-46 (AO, 40+ hr.)
 LDCE-1 (GAS canister) STS-46 (AO, 40+ hr.)
 Other - IOCM, Canadian experiment (STS-52)

Free-flyers: EURECA-1 (STS-46, 6-11+ mo.)

- Future:

Shuttle: EOIM-4 ?
 LDCE, GAS can

Free-flyers: RPC ?
 MATLAB ?
 SSF ?

Active: SAMMES (SDIO) ?
 OPM (AZ-Tech) ?

Techniques, Approach:

EOIM-3 Recession measurements vs weight loss
 Stressed, loaded materials
 Temperature effects
 UV synergism
 Variable exposure

SAMMES, OPM In situ measurements (α/ϵ , erosion, environmental
 monitoring)

Extended exposure - SAMMES, Free-flyers, SSF
 Returned specimens - Canisters, controlled environment

- Suggestions for 2nd LDEF post-retrieval symposium

- Invited presentations:

P.I.'s - Details, interpretations, consequences
 SIG's - Lessons learned, predictions for future missions

- Submission of data packages for data basing activities
- Relevant ground simulations, flight experiment results
- Plenary sessions for environments, SIGS

- Concurrent sessions for disciplines
- Opportunities for discussion essential
 - Interpretation
 - Future focus of analyses, follow-on efforts
 - Mitigation of environmental degradation
- Poster session / mixer
- LDEF Findings: Clear, indisputable, unambiguous
 - General
 - LDEF retrieved
 - Funding inadequate
 - Results needed yesterday
 - AO/UV effects evident for many materials
 - Contamination evident
 - Thermal velocity of AO effects verified on Kapton, FEP films
- LDEF Findings: Confusing, ambiguous, obscure
 - Impact of contamination
 - Post-retrieval aging effects
 - Thermal effects
 - AO fluence estimates ⇒ erosion yields

- Comments, concerns, recommendations
 - Access to data, materials (additional testing)
 - Storage/disposition of flight and control materials
 - Time, \$ critical
 - Target end-users for advocacy/support
 - SSF prime contractors, IRAD
 - Material vendor analyses
 - DoD, SDIO Support

Metals, Ceramics, and Optical Materials

Co-Chairmen: Roger Linton and John Gregory
Recorder: Gail Bohnhoff-Hlavacek

Q. How have initial LDEF results affected potential space applications of specific optical, metals and ceramic materials?

LDEF is providing pertinent and previously unattainable information of long-term environmental effects on metals, optics, and ceramics for diverse space mission applications. For example, silver oxidation data from LDEF Experiment A0171 provided timely input to the Intelsat VI retrieval mission assessment study. Additional materials included in this and other LDEF experiments are contributing to the baseline selection of materials for future solar arrays and solar concentrators, optical telescope and sensors, and structure metals. Experiment A0114 is providing pertinent data for the selection of AXAF primary mirror coatings in the results for gold, nickel, and irridium coatings. The damage assessment of meteoroid and debris impacts, including ejecta deposit patterns, is providing data needed for evaluating the integrated optical performance.

Q. How have inital LDEF metal/optical/ceramic results affected the understanding of space environmental parameters and synergism?

New information was made possible by the unexpected long duration of LDEF in space. Several metallic materials whose oxidation or space environmental stability was either unknown or undetectable for short term exposure, were found to be measurably affected. For example: 1) the unexpected degree of copper and silver oxidation; 2) potential evidence of slight, though perceptible, reactivity in gold and, 3) evidence of natural environment degradation in the fluoride compound protective or antireflection coatings (e.g. MgF₂ and CaF₂).

Other results described the localized effects found on LDEF including the synergistic effects of atomic oxygen, solar UV, and contamination, resulting in polymerization and discrete flow patterns of contaminant deposits. Despite severe limitations on the utility of Trailing Edge specimens due to contamination, the range of LDEF results indicates that the microenvironment of individual experiments, resulting from environmental factors such as contamination and thermal excursions, are critical factors needing further study for Leading Edge and Trailing Edge experiments.

Finally, other very useful data, are the timed exposures on LDEF trays ranging from months to over five years. The timed intervals provided a new set of empirical data points along the LDEF five-year timeline, not available in the past. This proved useful in the comparisons for validation of ground-based environmental exposure simulations.

Q. How have LDEF optical/metal/ceramic results affected new material requirements?

LDEF underscores the need for new material research on environmental stability and protection schemes for long-term space exposed hardware. Few materials on LDEF were found to be completely unaffected, whether due to the extended exposure or the increased sensitivity of state-of-the-art analysis instrumentation. Even for those LDEF materials or optical elements whose degradation cannot presently be clearly attributed to specific environmental

factors, the need for further study is apparent. Some new, post-LDEF results were discussed concerning the apparent effectiveness of CVD-diamond coatings for optical element protection. LDEF also demonstrated the importance of ensuring quality and uniformity in the manufacturing of space hardware, since slight variations in hardware fabrication and materials processing can change performance. Evidence for this was seen in the results of selected solar cells.

Q. How have initial LDEF results affected analytical modeling?

LDEF initial results have provided new tools for analytical modeling and classifying materials. Radiation and meteoroid/debris damage are being incorporated into both empirical and analytical models. The degree and patterns of contamination, including the tray vent-hole deposition "plumes", the apparent cleaning of Leading Edge surfaces, and the general distribution of deposition around the LDEF are providing invaluable input to analytical modeling for contamination.

Q. What are the LDEF database requirements?

An LDEF database should have an accessible format that is easy-to-use, so that the distribution of LDEF findings will be timely, and enhance communication between principal investigators and space hardware designers. The Optical Experiments Database developed by the Optical Systems Special Investigative Group, provided essential information about the various optical experiments including: what optical materials flew, who was the principal investigator, results summaries, conclusions, the environmental conditions the samples were exposed to, future design considerations, and additional sources of information. It was developed as a library research tool, to enable researchers to quickly locate pertinent optical information from LDEF experiments. The database does not contain extensive data tables, graphs, etc. on each experiment; instead it summarizes many of the results and then directs researchers to the original source of information for details. The database layout is highly focused, using terminology and search queries that are appropriate for the optical applications. The data can also be easily downloaded into other types of files for reports and spreadsheets, or other more powerful databases.

Q. What are the general needs for future flight experiments?

Several topics were discussed including: 1) ensuring the statistical design of experiments with sample controls and preflight measurements; 2) requiring screening methodologies for outgassing materials on spaceborne hardware; 3) providing on-orbit monitoring (including temperature, radiation flux, UV, AO, contamination); 4) utilizing more active experiment measurements; and 5) completing a thorough recovery and post-flight examination. Without all of this information, it is difficult to make conclusions concerning which effects are due exclusively to space exposure on samples flown in space.

Q. What level of information should be presented for this discipline (and in what format should it be presented) at the second LDEF Post-Retrieval Symposium, June 1992?

Several panel members suggested that the proceedings from the November Materials Conference be available prior to the symposium. Secondly, they suggested that we emphasize the technical content, and suggested that speakers give more back-up information about their hypothesis to allow the audience to form their own opinions and ask specific questions. Along that same line, the panel thought concurrent sessions would be most appropriate to

allow time for the questions and discussion. The panel requested that speakers use a standardized experiment description (one viewfoil) prior to their talk, to assist first-time attendees. The viewfoil should include the experiment number, experiment title, principal investigators, location on LDEF, and the space environmental conditions it experienced.

METALS, CERAMICS, AND OPTICAL MATERIALS

Roger Linton and John Gregory, Co-Chairmen
Gail Bohnhoff-Hlavacek, Recorder

- **Potential Space Applications**
 - **Interference filter and detectors**
visible wavelength transmission altered
increased IR throughout
erosion/contamination caused "detuning"
 - **Reflecting films**
oxidation of metals (Ag, Cu, Au?)
mass changes
thicknesses determined
 - **Environmental parameters**
time intervals of exposure
microenvironments
comparison to ground simulation data
- **New Materials Development**
 - LDEF results underscore the need for new protection schemes
 - black coatings get more absorbing
- **Ground simulation**
 - LDEF enhances reliability
 - wide range of goals for new ground simulation
- **Analytical modeling**
 - provides new tools
 - classifying materials
 - considers M&D impacts
size distribution
density
damage
- **Data Base Requirements**
 - accessible format
 - electronic
 - easy to use
 - materials usage limitations
- **Level of Information for Second LDEF Conference**
 - proceedings from this conference available prior to next conference
 - emphasize technical content
 - standardize experiment description

- Findings
 - Clear
 - Presence of contamination
 - Unclear
 - Source of contamination
- General needs for future flights
 - Control samples
 - Preflight measurements
 - On-orbit monitoring
 - temperature
 - radiation flux
 - UV, AO
 - contamination
 - Active measurements

Polymer Matrix Composites

Co-Chairmen: Gary Steckel and Rod Tennyson
Recorder: Pete George

This summary narrative details summary charts from the Polymer Matrix Composites (PMC) theme panel discussion. The charts present the issues and preliminary conclusions from LDEF PMC test results and experiences. This narrative attempts to assign significance, supporting discussions, and priorities for the issues and conclusions.

Polymer matrix composite materials used in low earth orbit (LEO) applications with lengthy direct atomic oxygen (AO) exposure will likely require protective coatings. This conclusion was largely anticipated prior to the retrieval of LDEF based on ground based simulation and on orbit shuttle payload bay experiments. Graphite reinforced PMCs displayed 3 to 5 mils of erosion for leading edge (perpendicular to direction of orbit) exposure conditions on LDEF.

The AO erosion occurred over 5 3/4 years of flight exposure, during which the LDEF was losing altitude (thus entering higher AO concentrations). LDEF AO erosion data combined with ground based simulation and modeling can be used by designers to make the decision whether AO protective coatings will be required for their specific application. Leading edge applications for PMCs may not need a protective coating if only insignificant material loss to AO erosion is expected over its useful life. Factors such as resin content, fiber orientation of exposed plies and load bearing directions must be considered for PMC materials in direct AO environments. In addition, the potential contaminating effects of the erosion on the overall space system must be considered.

PMCs located on LDEF's trailing edge and in other AO shielded positions did not display any significant reductions in mechanical properties. Based on LDEF results, specific matrix and fiber systems appear suitable for non-AO-exposed LEO applications without protective coatings. Coatings may be required for thermal stability or other reasons.

PMC experiments have not provided any special insights to date into understanding LDEF environmental parameters or possible synergistic effects. However, cause and effect relationships have been fairly well established. Surface erosion with an accompanying reduction in mechanical properties is a direct effect of AO exposure. Some darkening of the PMC matrices has been observed for trailing edge exposed specimens and has been attributed to ultraviolet exposure. Although synergistic effects between AO and ultraviolet (UV) radiation are suspected for some polymer systems, none have been identified based on LDEF PMC experiment results.

A reversible shrinkage of LDEF PMCs was measured by inflight strain gauge instrumentation. This dimensional change has been attributed to moisture loss due to the microvacuum and thermal cycling environments. The thermal cycling environment is also believed to be responsible for increased microcrack

levels (compared to control specimens) which were reported for some multidirectional carbon fiber reinforced PMCs. Other than during the periods of shrinkage mentioned above, no changes in thermal expansion coefficients were reported. However, most of the post-flight thermal expansion data reported to date were acquired using techniques insufficient to resolve small CTE changes in low expansion materials. There is a need for more precise thermal expansion measurements.

The morphology of the AO eroded PMC surfaces does not resemble that of pure polymer specimens of similar chemistry as the PMC matrix resin. For example, surface morphology for AO eroded polyimide films reveals a rough surface with up to 5 μm features versus up to 75 μm features for graphite reinforced polyimides. Other graphite reinforced PMCs display similar size features. Also, "ash" like "residues" have been reported for most of the AO eroded PMC surfaces. These findings, along with some reported surface chemistry changes for AO eroded PMCs, may provide some insights into the AO erosion mechanism.

The need for AO protective coatings and scale up of coating processes for high AO flux LDEF polymer matrix composite applications has been strongly confirmed by LDEF test results. The AO protective coatings which flew on LDEF were applied to small coupons. The viability of scale up should be investigated to determine which coatings offer the most promise. Optical properties as well as coating durability are also important factors. Flexible structures such as PMC springs may require the development of flexible AO protective coatings.

Since LDEF integration over 10 years ago, significant advancements in materials for space applications have occurred. Evaluation of these new materials including PMCs using the the LDEF environment as a benchmark will help to identify potential performers while possibly avoiding costly material development programs.

Concerning ground based simulation the general consensus at the PMC theme panel discussion was that existing techniques are adequate for individual effects testing. However, availability and sample size capacity for quality AO exposure are inadequate. Ground based simulation testing will be necessary to validate models developed from LDEF experiences. LDEF AO recession rates can be used as a benchmark for future ground based studies. Atomic oxygen ground based simulation testing of LDEF UV exposed specimens which were shielded from AO during flight may help to identify AO/UV synergistic effects including a possible UV "induction" period.

Since AO erosion, microcracking, and dimensional stability properties appear to be the most significantly affected for PMCs, it is logical to concentrate analytical modeling efforts in these areas. Continuation of the existing efforts for development of local geometry AO fluence simulation with addition of reflection factors will hopefully allow experimenters to evaluate PMC specimens which may have been subjected to local geometry effects onboard LDEF. Also,

application of a model as described above to simulated inhomogeneous materials such as PMCs with reactivities assigned to the separate components may help explain the unique surface morphologies which have been observed. LDEF and ground based test results should be combined with analytical modeling in the areas of dimensional stability, microcrack density and thermal expansion properties. These properties are related and can be combined with other properties and orbital environment inputs for a comprehensive model. The output from this model could be subsequently used as input for fatigue life, structural and dimensional stability models. A general call for validation and refinement of LDEF AO environment modeling was also expressed during the discussion.

Data base requirements were discussed during the theme panel with the conclusion that both comprehensive archive and design data formats should be developed as separate but cross referenced databases. The archive should include property data, photos, and phenomenology. This database should have multiple path accessibility through material type, property range and application requirements. Also, an evaluation of the data including test methods, conflicting results etc. should be included to alert the database user to the confidence level associated with the reported values.

LDEF polymer matrix composite data which shows consistency and can be confidently interpolated and/or extrapolated to the ranges of concern for the designer in areas such as AO fluence, altitude, and exposure time. should be presented in a design handbook format. Both hard and electronic copies would present this data as design curves as a function of the above mentioned conditions.

During the PMC theme panel discussions the general needs for future flight experiments were discussed. On orbit measurement of AO flux vs. time would provide means for very accurate AO recession rate determination. In situ measurement of critical specimen properties would avoid the problems associated with retrieval and deintegration. Also, self opening and closing canisters, like the ones used on some LDEF trays, should be the preferred format for exposure duration critical experiments.

Comparison of LDEF data from experiment to experiment has been difficult. Future flight experiments should incorporate standard specimen configurations as well as standard methods for contamination, handling, and testing. Critical properties and their test methods should be identified and agreed upon prior to integration to allow consistent zero time control specimen testing. Strong integration guidance will be required to achieve these goals.

The second post retrieval symposium should have a full day session dedicated to polymer matrix composites. This session should include investigators presentations of test results as well as initial work on model development. Standard data formats for properties to be included in data basing should be established prior to the call for papers. A comprehensive summary

paper for PMCs with integrated test results, space systems relevance and additional test requirements should be presented.

Among the clear, indisputable initial LDEF findings for polymer matrix composites are susceptibility to material loss and surface roughening due to atomic oxygen for leading edge exposed PMCs. As a result of the material loss, mechanical property reductions have been observed. The surface roughening and perhaps the presence of "ash" has affected the optical properties for leading edge exposed graphite reinforced PMCs. Trailing edge PMCs did not display any measurable change in mechanical properties. Glass reinforced PMCs displayed significantly less AO erosion due to the AO resistant nature of the glass fiber reinforcement. Glass reinforced PMCs did display significant changes in optical properties. Micrometeoroid and debris impact damage did not result in any catastrophic failures of PMCs. However, through penetrations and reverse side spallation damage were observed at some impact sights. Polymer property changes were only "skin deep". No changes were found for bulk polymer properties.

Among the more confusing and obscure findings are the variations in color and texture of AO eroded PMC surfaces. Variations in graphite fiber reinforced PMC AO eroded surface morphologies were observed by scanning electron microscopy as a function of fiber modulus. Also, "ash" levels varied from PMC type to PMC type. In one case AO erosion characteristics varied within individual T300 graphite/934 epoxy specimen creating light and dark banding on the surface. Also, the effects of contamination on erosion rates and other properties are not clear.

In summary, the panel members felt that good progress was being made by the individual investigators. Areas in which additional data are required include microcracking analysis, detailed surface chemistry analysis of AO eroded surfaces, and precise thermal expansion measurements. There was a consensus that at this point greater emphasis should be placed on compiling and comparing the data from the different experimenters in order to identify trends, relationships, synergisms, and data gaps. More coordinated test planning and cooperative efforts should then follow.

POLYMER-MATRIX COMPOSITES

Gary Steckel and Rod Tennyson, Co-Chairmen
Pete George, Recorder

THEME PANEL DISCUSSION

- How have initial LDEF results affected:
 1. Potential space applications of specific classes/type of materials
 - A. Specific graphite reinforced composites for non AO LEO structural applications (both external and internal).
 - B. Coated composites for direct AO exposure LEO applications
 - C. Uncoated Composites for certain leading edge applications
 2. Understanding of environmental parameters/synergism
 - A. AO causes mechanical properties degradation
 - B. UV causes darkening of PMC matrix surfaces
 - C. Thermal cycling can cause microcracking
 - D. No synergistic effects identified to date
 - E. Sequential environmental effects of micrometeoroid impact/AO erosion observed on coated specimens
- How have initial LDEF results affected:
 3. Understanding of mechanisms of material degradation?
 - A. Thermal cycling/microcracking mechanism understood from previous efforts in general composites activities
 - B. Differences in AO eroded surface morphology, "ash" composition, and surface chemistry have been identified and may provide insights into AO erosion mechanisms
 - C. No specific mechanisms identified for AO or UV to date
- How have initial LDEF results affected:
 4. New materials and processes development requirements?
 - A. Coatings to protect composites - scale up of coating process to full scale parts
 - B. Flexible coatings for protection of composite springs, other flexible composite structures
 - C. Evaluation of post-LDEF-integration-developed materials
- How have initial LDEF results affected:
 5. Ground simulation testing requirements?

- A. Existing simulation techniques adequate for individual effects
 - B. Capacity and sample size for quality AO simulation currently inadequate
 - C. AO, UV, thermal cycling, vacuum, contamination simulation testing including synergistic effects
 - D. Use LDEF recession rates, etc. as benchmarks
 - E. AO simulation on UV degraded LDEF specimens etc.
- How have initial LDEF results affected:
 - 6. Space environmental effects analytical modeling requirements?
 - A. Validate/Improve AO environment modeling
 - B. Continue development of local geometry AO fluence simulation with addition of reflection factors. Apply to textured AO eroded surface geometry, post damaged composites
 - C. Microcrack density prediction modeling based on optical properties, thermal coupling, solar exposure, etc. Plug results into fatigue life, structural, and dimensional stability models

- DATA BASE REQUIREMENTS

- Archive

- Comprehensive LDEF Results

- Property Data
 - Photos
 - Phenomenology

- Multiple Access

- Material Type
 - Property Range
 - Application

- Data Evaluation

- Handbook Data

- Hardcopy/Electronic Copy present data as design curves; properties function of AO fluence, altitude, exposure time

- General Needs for Future Flight Experiment

 - On Orbit Measurements

 - Environmental Factors

 - AO, other species, UV, Thermal

 - In situ property measurement

 - Orbital parameters

 - Standardized samples

 - Standardized handling of controls

 - Strong integration/guidance contamination control

- 2nd Symposium Coverage

 - One day session

 - Investigators' presentations

 - Comprehensive summary paper

 - Integrated results

 - Space Systems Relevance

 - Additional Test Requirements

- CLEAR, INDISPUTABLE FINDINGS

 - PMC's on leading edge susceptible to material loss/surface roughening due to AO

 - No degradation of mechanical property except on leading edge from AO

 - Graphite/polymers show no changes in optical properties except on leading edge

 - Glass/polymers composites do show optical property changes

 - No catastrophic failures from impact damage

 - No bulk polymer property changes except outer skin

- CONFUSING, OBSCURE FINDINGS

 - Presence of stripes on T300/934 with 5 mil tape (experiment A0134)

 - Differences in AO erosion morphology

 - Differences in appearance and amount of "ash" on AO erosion surfaces

 - Effects of contamination on AO erosion rates and other properties

- ADDITIONAL COMMENTS

- Need to compile, compare and "filter" data to identify trends, relationships, gaps, and synergisms
- Use above results to establish test plan and integrated cooperative effort
- Need further data for
 - Thermal cycling/microcracking
 - AO Erosion surface chemistry
 - Precision CTE measurements
 - Interpretation of AO erosion mass loss data

Lubricants, Adhesives, Seals, Fasteners, Solar Cells, and Batteries

Co-Chairmen: James Mason and Joel Edelman
Recorder: Harry Dursch

General Findings:

Spacecraft designers need to consider both the effects of the space environment on materials or components and the effects of the material or component on the surrounding space environment. Examples of this include lubricant outgassing, location of high voltage power supplies, or the impact of degrading materials that could contaminate optics.

What one spacecraft designer might view as common knowledge might not be common knowledge to another designer. One LDEF related example was an experimenter changing his fastener assembly lubricant from MoS₂ dry film lubricant to cetyl alcohol. This change was made to avoid possible volatilization and contamination while on-orbit. However, it led to severe galling of the fasteners. To some designers, it would have been obvious that fastener seizure would result from the switch of lubricants but it wasn't "common knowledge" to the experimenter. This illustrates the need for timely and accurate development and distribution of design guidelines. LDEF presents a unique opportunity to make common knowledge more common.

Clear, Indisputable Findings:

Adhesives - Most adhesives that were flown on LDEF performed as designed. When PI's were contacted about the condition of adhesives used on their experiment, the vast majority stated that "it is still stuck, even though the adhesive turned brown". However, there have been two notable exceptions to the successful use of adhesives on LDEF. Four solar cells became disbonded and were lost sometime during the LDEF mission and several PI's noted darkening of solar cell coverglass adhesives, causing a loss of light to the solar cells. In addition, following the Theme Panel presentation, several additional adhesive failures were mentioned by members of the audience.

Seals - A wide variety of seals were flown on LDEF. No failures attributable to exposure to the space environment occurred. However, all seals were shielded from direct exposure to the space environment. The only known failure occurred on the ten LiCF batteries. Due to extended exposure to the electrolyte gas, the o-ring lost its resiliency, causing leakage of the electrolyte gas. This failure had no effect on the battery performance and similar failures occurred on control LiCF batteries.

Lubricants - There was a wide variety of lubricants flown on LDEF. All lubricants shielded from direct exposure to the space environment performed as designed. The lubricants that were unprotected from the space environment underwent viscosity changes, had organic binders disappear or disappeared completely. This points out the need to thoroughly test lubricants in a simulated combined effects chamber (including dynamic effects) to enable determination of service lifetimes.

Fasteners - As with the adhesives, seals, and lubricants, there was a variety of fasteners used on LDEF. During de-integration, there were widespread reports of fastener related anomalies. Instances of sheared fasteners, severely damaged nut plates, and excessive breakaway and/or prevailing torques were reported. To date,

all anomalies have been attributed to galling due to poor pre-flight installation practices and/or incorrect selection of lubricants. The most important finding has been the absence of any coldwelding.

Solar cells - Over 350 solar cells were flown on LDEF. The vast majority of the cells were silicon, but several GaAs cells were flown. While over half of the cells were actively monitored while on-orbit, very little electrical characterization results have been published. The leading cause of cell degradation was meteoroid or debris impacts. This performance loss was dependent upon the size and energy of the impacts. The type of loss ranged from a decrease in fill factor, to a loss of short circuit current caused by loss of active cell area from the impact crater, to a loss of open circuit voltage due to damage to the cell structure. Minor performance loss was caused by decreased amounts of light reaching the cell. This was caused by the cumulative effects of contamination, UV degradation of the coverglass adhesive, atomic oxygen/UV degradation of the anti-reflection coatings, and/or radiation damage.

Batteries - There were no space related failures of any of the LiSO₂, LiCF, or NiCd batteries flown on LDEF. All ten of the LiCF batteries used on LDEF suffered experienced an anticipated seal rupture which resulted in the leakage of the electrolyte gas. Corrosion of the glass seal interface took place on the LiSO₂ batteries. However, both of these degradations were duplicated in batteries kept in ground storage and thus this effect is not attributed to the spaceflight environment. Reliability and performance of these types of batteries proved to be quite satisfactory.

Confusing, Ambiguous or Obscure Findings:

The variations in the prevailing torques during removal of tray clamp fastener assemblies are greater than would be expected.

Integrated current leakage measurements on one experiment and erratic real-time charge loss measurements on large numbers of charged sensors on another experiment indicate the possibility of a complex plasma environment. Contributing factors are speculated to include outgassing molecular contamination, solar orientation, and local thermal dynamics

Ground Simulation Testing Requirements:

A need exists for a combined effects chamber that possesses the capabilities for temperature cycling, UV, atomic oxygen, and dynamic testing of lubricants and mechanisms. Dynamic testing not only needs to be performed on lubricant specimens but on the operating mechanism.

Future Flight Experiments:

A significant concern to the spacecraft designer is the successful on-orbit replacement of hardware. LDEF is providing valuable information towards the use of fasteners and mechanisms in space. However, because LDEF was primarily a "static" satellite, additional questions remain. These questions include the possibility of coldwelding occurring due to repeated on-orbit cycling of fastener

assemblies. Even if coldwelding doesn't occur, increases in friction due to galling will cause difficulties during EVA. Because of these concerns, there is a need to know the durability of the various lubricant schemes being suggested for long term space exposure. Formidable difficulties would be encountered in testing a fastener assembly or mechanism to the combined effects of the space environment while undergoing dynamic cycling in a ground simulation chamber. Only a future flight experiment will provide the required design data.

Because the operative factors in plasma effects are not well understood, it is not possible to design a ground simulation at this time. Thus it is of significance that future flight experiments be designed to characterize these effects. It is particularly important that some degree of uniformity and consistency be assured in future plasma measurements and observations on orbit. Every flight mission, at a minimum, will have a unique contamination environment and the subsequent correlation of data from separate missions will be difficult in the best circumstances.

Databasing Requirements:

Databases should contain the following information: 1) specific lubricant, adhesive, solar cell, and fasteners flown on LDEF, 2) environment seen by the specific component, 3) results and conclusions, 4) status of testing, 5) responsible experimenter, and 6) references for additional information. The amount of material will determine whether the database would consist of a paper version (handbook) or an electronics version (floppy disc). In many areas the quantity of data is expected to be compatible with hardcopy storage and distribution.

LUBRICANTS, ADHESIVES, SEALS, FASTENERS, SOLAR CELLS, AND BATTERIES

James Mason and Joel Edelman, Co-Chairmen
Harry Dursch, Recorder

LUBRICANTS, ADHESIVES, SEALS, AND FASTENERS

- RESULTS AFFECTED SPACE APPLICATION OF _____?

[Alternate View: What material does to environment vs. space environment effects on material]

ADHESIVES

- Failures, while few, not necessarily the result of space environment
- No evidence of failure due to space environment
 - Four solar cells fell off?
Thermal cycling?
Cohesive/adhesive?
Thermal cycling?
AO/UV/thermal/vacuum?
Kapton?
 - Exposure Questions
Angle of attack?
Sacrificial layer?
 - Darkening of Solar Cells?

LUBRICANTS

- Failures did occur due to space environment
- All "protected" lubes continued to do their job
- Contamination by lubricants must be considered

SEALS

- No failures attributed to the space environment (all seals protected)
- With one exception, all seals worked (one compression failure due to contamination)

FASTENERS

- No failures due to space environment
- No space environment-induced cold welding
- Extensive galling
- Lubricants for space servicing and assembly

SOLAR CELLS

- Approximately 300 silicon and GaAs cells flown
- Over half were actively monitored

FINDINGS TO DATE:

- Most degradation of cells caused by meteoroid or space debris impacts
 - Performance loss dependent upon size and energy of impacts
- Minor degradation caused by decreased amount of light reaching cell
 - Contamination
 - UV degradation of coverglass adhesive?
 - Atomic oxygen/UV degradation of antireflection coatings?
- To date, particle radiation effects not discernible from other degradation factors

BATTERIES: LiSO₂, LiCF_x, NiCd

- No space related failures of any battery. Anomalies duplicated in ground storage samples
- Reliability and performance of these types of batteries are satisfactory in unexposed space applications
- Summary and final conclusions to be presented in Systems SIG Phase I Final Report
- No requirements for additional testing

UNDERSTANDING OF ENVIRONMENTAL PARAMETERS?

- LDEF demonstrates importance of combined thermal/vacuum/AO/UV/thermal effects
- Results suggest thermal vacuum testing is required for characterization of adhesives, lubricants, seals. Angle of attack appears to be a factor.

UNDERSTANDING OF MECHANISMS OF MATERIAL DEGRADATION?

- Not yet addressed

NEW MATERIAL DEVELOPMENTS REQUIRED?

- Seals/Adhesives--Okay if not directly exposed to environment
- Lubricants
 - Shielded, are okay
 - Exposed dry films are a concern
 - Improved dry films for exposed situations

GROUND SIMULATION TESTING REQUIREMENTS?

- Need combined T/UV/AO/Dyn Testing
- LDEF II

ANALYTICAL MODELING REQUIREMENTS?

- Still need testing

DATA BASE REQUIREMENTS

- Publish A.S.A.P.
- Final report summarizing findings and presenting references (Paper/electronic forms)

LDEF CONFERENCE RECOMMENDATIONS

- Conclusions
- Design Recommendations/Guidelines
- Set standards for viewgraphs

CLEAR FINDINGS

- No cold welding
- Shielded lubricants, adhesives, seals work
- Several exposed lubricants failed
 - Everlube 620 - gone
 - Braycote 601 - decreased viscosity

AMBIGUOUS FINDINGS

- High prevailing (running) torques
- Dynamic effects on cold welding and lubricants
- No statistical data on seals, lubricants, and adhesives

CONCERNS

- Lubricant duty cycle vs periods of exposure
- Material impact on environment vs environment impact on material
- Moisture and ambient oxygen exposure of materials
- Development of guidelines for design engineers
- Testing of lubricants exposed to LEO on external surfaces
- Need to continue collation and integration of experimenter results
- Solar cell round robin
- Primary structure fasteners/silver lubricants

GENERAL FINDINGS REGARDING LDEF SYSTEMS

- "Common knowledge is not all that common."
- "I wish I didn't know now what I didn't know then."

LDEF MATERIALS WORKSHOP 1991

SPONSOR: Long Duration Exposure Facility - Materials Special Investigation Group

OBJECTIVES:

- In-depth exposition of LDEF Materials Findings from Principal Investigators and MSIG
- Workshop discussions and theme reports on LDEF materials disciplines, data-basing requirements, ground simulation testing and analytical modeling needs, and future flight experiments

TUTORIAL AND WORKSHOP DISCUSSION DISCIPLINES:

- LDEF Materials, Environmental Parameters, and Data Bases
- LDEF Contamination
- Metals, Ceramics, and Optical Materials
- Lubricants, Fasteners, Adhesives, Seals
- Thermal Control Coatings, Protective Coatings, and Surface Treatments
- Polymers and Films
- Polymer-Matrix Composites

ATTENDANCE:

- ~200 technologists from the International Space Materials Community
- Spacecraft materials analysts and designers
- Space Environmental Effects research and development scientists and engineers
- Spacecraft and space experiment program managers

LDEF MATERIALS - PRELIMINARY FINDINGS

- **PRELIMINARY DATA ON SIMILAR MATERIALS FROM TRAY TO TRAY IS REMARKABLY CONSISTENT:**
 - Data quality is excellent
 - LDEF will provide the "benchmark" for materials design data bases for LEO/SSF
- **SOME MATERIALS WERE IDENTIFIED TO BE ENCOURAGINGLY RESISTANT TO LEO SPACE ENVIRONMENTAL EFFECTS (E.G. - AO & VUV) FOR 5.8 YEARS:**
 - Chromic-acid anodized aluminum, other metals, ceramics
 - Some thermal control coatings (e.g.- YB-71, Z-93, PCB-Z, D-111)
 - Composites with inorganic coatings; siloxane-containing polymers
 - Aluminum coated stainless steel reflectors
- **OTHER MATERIALS DISPLAYED SIGNIFICANT ENVIRONMENTAL DEGRADATION:**
 - Various thermal control coatings and silicone conformal coatings
 - Uncoated polymers and polymeric-matrix composites, silver, copper
 - Silvered Teflon thermal blankets and second-surface mirrors
- **MOLECULAR CONTAMINATION WAS WIDESPREAD:**
 - LDEF offers an unprecedented opportunity to provide a unified perspective of LEO spacecraft contamination mechanisms / interactions / lessons learned
- **ABSOLUTELY ESSENTIAL TO SPACE STATION FREEDOM AND FUTURE SPACECRAFT DESIGNERS THAT LDEF MATERIALS RESULTS BE THOROUGHLY ANALYZED AND DOCUMENTED INTO A QUANTITATIVE DESIGN DATA BASE:**
 - Requires continued adequate funding to complete Materials Principal Investigator and MSIG analyses

LDEF MATERIALS WORKSHOP '91 AGENDA

NASA Langley Research Center
H. J. E. Reid Conference Center
14 Ames Road Building 1222
Hampton, Virginia 23665-5225
November 19 - 22, 1991

Tuesday, November 19, 1991

8:30 a.m. Introductions

William H. Kinard, LDEF Chief Scientist
Bland A. Stein, Workshop Coordinator
Philip R. Young, Workshop Coordinator

9:00 a.m. Technical Session

- LDEF Materials, Environmental Parameters, and Data Bases (Plenary Session)

Cochairman: Bruce Banks, NASA - Lewis Research Center
Cochairman: Mike Meshishnek, The Aerospace Corporation
Recorder: Roger Bourassa, Boeing Defense & Space Group

LDEF Atomic Oxygen Fluence Update

Roger Bourassa
Boeing Defense & Space Group

LDEF Yaw and Pitch Angle Estimates

Bruce Banks

LDEF Experiment M0003 Meteoroid and Debris Survey

Mike Meshishnek
The Aerospace Corporation

Atomic Oxygen Erosion Yields of LDEF Materials

Bruce Banks, LeRC for John Gregory
University of Alabama in Huntsville

The LDEF M0003 Experiment Deintegration Observation Data Base

Sandy Gyetvay
The Aerospace Corporation

Overview of Flight Data from LDEF M0003 Experiment Power and Data System

John Coggi
The Aerospace Corporation

12:00 Noon Lunch

Tuesday, November 19, 1991 continued

1:00 p.m. Technical Session

- LDEF Contamination (Plenary Session)

Cochairman: Steve Koontz, NASA Johnson Space Center
Cochairman: Wayne Stuckey, The Aerospace Corporation
Recorder: Russell Crutcher, Boeing Defense & Space Group

Introduction	Wayne Stuckey The Aerospace Corporation
Materials SIG Quantification and Characterization of Surface Contaminants	Russell Crutcher Boeing Defense & Space Group
Z-306 Molecular Contamination Ad-Hoc Committee Results	John Golden Boeing Defense & Space Group
LDEF Contamination Modelling	Tim Gordon Applied Science Technology and Ray Rantanen ROR Enterprises
M0003 Contamination Results	Wayne Stuckey and Carol Hemminger The Aerospace Corporation
Organic Contamination on LDEF	Gale Harvey NASA Langley Research Center
5:00 p.m. End Session	

Wednesday, November 20, 1991

8:00 a.m. Technical Session

- **Thermal Control Coatings, Protective Coatings and Surface Treatments (Plenary Session)**

Cochairman: Ann Whitaker, NASA Marshall Space Flight Center
 Cochairman: Wayne Slemp, NASA Langley Research Center
 Recorder: John Golden, Boeing Defense & Space Group

Thermal Control Materials on Thermal Control Surfaces (TCSE) Experiment	James Zwiener, NASA MSFC for Don Wilkes AZ Technology
Vacuum Deposited Coatings	Wayne Slemp NASA Langley Research Center
Anodized Aluminum on LDEF	John Golden Boeing Defense & Space Group
Thermal Control Tape	Rachel Kamenetsky NASA Marshall Space Flight Center
Fluorescence in Thermal Control Coatings	James Zwiener NASA Marshall Space Flight Center
Thermal Control Coatings on DoD Flight Experiment	William Lehn, Nichols Research Corp. for Charles Hurley Univ. of Dayton Research Institute and Michele Jones U.S.A.F Wright Laboratories
Next Generation LDEF: Retrieval Payload Carrier	Arthur Perry American Space Technologies, Inc.

Element Material Exposure Experiment
Experiment by EFFU

Yoshihiro Hashimoto
Ishikawajima- Harima Heavy Industries Co., Ltd. (IHI)

Skylab DO24 Thermal Control Coatings and
Polymer Films Experiment

William Lehn,
Nichols Research Corporation

12:00 Noon **Lunch**

Wednesday, November 20, 1991 continued

1:00 p.m.

Technical Session

• **Polymers and Films (including Ag/FEP) (Concurrent Session)**

Cochairman: Phil Young, NASA Langley Research Center
Cochairman: David Brinza, Jet Propulsion Laboratory
Recorder: Gary Pippin, Boeing Defense & Space Group

Ag/FEP Teflon

François Levadou
European Space Research & Technology Centre

Ag/FEP: Recent MSIG Results

Gary Pippin
Boeing Defense & Space Group

Polymer Films and Resins

Philip Young
NASA Langley Research Center

Texas A & M S1006 Balloon Materials Experiment

Alan Letton and Thomas Strganac
Texas A & M University

Depth Profiling of Orbital Exposure Damage to
Halar (A0171 Solar Array Materials Experiment)

William Brower
Marquette University

M0003: Recent Results on Polymer Films

Michele Jones
U.S.A.F Wright Laboratories

5:00 p.m. **End Session**

Wednesday, November 20, 1991 continued

1:00 p.m.

Technical Session

• **Metals, Ceramics, and Optical Materials (Concurrent Session)**

Cochairman: Roger Linton, NASA Marshall Space Flight Center
Cochairman: John Gregory, University of Alabama
Recorder: Gail Bohnhoff-Hlavacek, Boeing Defense & Space Group

Selected Results from Metals on LDEF
Experiment A0171

Ann Whitaker
NASA MSFC

Oxidation of Copper and Silver on LDEF

Ton de Rooij
European Space Research & Technology Centre

Optical Transmission and Reflection Measurements
of Thin Metal Films Exposed on LDEF

Roger Linton, NASA MSFC for John Gregory
University of Alabama in Huntsville and

Oxidation of Black Chromium Coatings on LDEF

John Golden
Boeing Defense & Space Group

LANL Results from Space-and Ground-based Atomic
Oxygen Exposures of Metals and Inorganic Materials

Jon Cross
Los Alamos National Laboratory (LANL)

AXAF Optical Materials and Issues

James Bilbro, NASA MSFC for Alan Shapiro
NASA Marshall Space Flight Center

Effects of Space Exposure on Pyroelectric
Infrared Detectors

James Robertson
NASA Langley Research Center

Status and Results of LDEF Optical Systems
SSIG Data Base

Gail Bohnhoff-Hlavacek
Boeing Defense & Space Group

5:00 p.m. **End Session**

Thursday, November 21, 1991

8:00 a.m.

Technical Session

• **Polymer-Matrix Composites (Concurrent Session)**

Cochairman: Rod Tennyson, University of Toronto
Cochairman: Gary Steckel, The Aerospace Corporation
Recorder: Pete George, Boeing Defense & Space Group

M0003 and Other Polymer-Matrix Composites

Gary Steckel
The Aerospace Corporation

A0134: Polymer Matrix Composites

Wayne Slemp
NASA Langley Research Center

Space Environmental Effects on LDEF Low-Earth
Orbit (LEO) Exposed Graphite-Reinforced
Polymer- Matrix Composites

Pete George
Boeing Defense & Space Group

Long-Term Environmental Effects on
Carbon-and Glass-Fiber Composites

Ann Whitaker
NASA Marshall Space Flight Center

Evaluation of Long-Duration Exposure to the
Natural Space Environment on Graphite-Polyimide
and Graphite-Epoxy Mechanical Properties

Richard VyhnaI
Rockwell International

Proposed Test Program and Data Base
for LDEF Polymer-Matrix Composites

Pete George
Boeing Defense & Space Group and
Rod Tennyson
University of Toronto

12:00 Noon **Lunch**

Thursday, November 21, 1991

8:00 a.m.

Technical Session

- **Lubricants, Adhesives, Seals, Fasteners, Solar Cells, and Batteries (Concurrent Session)**

Cochairman: James Mason, NASA Goddard Space Flight Center
Cochairman: Joel Edelman, LDEF Consultant
Recorder: Harry Dursch, Boeing Defense & Space Group

Identification and Evaluation of Lubricants,
Adhesives, and Seals Used on LDEF

Bruce Keough
Boeing Defense & Space Group

Results from the Testing and Analysis of
LDEF Batteries

Steve Spear
Boeing Defense & Space Group

Effects of Long-Term Exposure on Fastener Assemblies

Steve Spear
Boeing Defense & Space Group

Results from the Testing and Analysis of Solar Cells
Flown on LDEF

Harry Dursch
Boeing Defense & Space Group

System Related Testing and Analysis of FRECOPA

Christian Durin
Centre National D'etudes Spatiales

12:00 Noon Lunch

1:00 p.m.

- Working meetings of **Theme Panels** to prepare charts for Workshop Summary Session and begin draft of panel report. (**Concurrent Session**)

5:00 p.m. End Session

Friday, November 22, 1991

8:00 a.m.

Technical Session

- **LDEF Materials Workshop '91 - Summary (Plenary Session)**

- 20-minute presentations by panel chairmen followed by question/answer periods
- Final general discussion period moderated by workshop coordinators

12:00 Noon End Workshop

 **LDEF
MSIG
MATERIALS
SPECIAL INVESTIGATION GROUP**

ATTENDEE LIST

S. Carl Ahmed
POBox 03-4075
Technology Transfer Specialists, Inc.
Indialantic FL 32903-0975
407/777-0019

Ruth Amundsen
Mail Stop 431
NASA Langley Research Center
Hampton VA 23665-5225
804/864-7044
804/864-7202

J. I. Applin
Mail Stop 431
NASA Langley Research Center
Hampton VA 23665-5225
804/864-7082

D. F. Auvil
Mail Stop 424
NASA Langley Research Center
Hampton VA 23665-5225
804/864-5631

Robert D. Averill
Mail Stop 433
NASA Langley Research Ctr.
Hampton VA 23665-5225
804/864-7088
804/864-7009

C. D. Bailey
Mail Stop 424
NASA Langley Research Center
Hampton VA 23665-5225
804/864-5634

Bruce A. Banks
NASA LeRC M/S 302-1
21000 Brookpark Rd
Cleveland OH 44135
216/433-2308 (FTS 297-2308)
216/433-6106

W. M. Berrios
Mail Stop 434
NASA Langley Research Center
Hampton VA 23665-5225
804/864-7183

Charles F. Bersch
Institute for Defense Analyses
1801 N. Beauregard St.
Alexandria VA 22311
703/578-2863
703/578-2877

Anthony Beverina
Kaman Sciences Corp./Suite 200
2560 Huntington Ave.
Alexandria VA 22303
703/329-7167
703/329-7197

John Bianchi
202 Ross Hall/Dept. of Mech. Engrg
Auburn University
Auburn University AL 36899
205/844-3345
205/844-3307

James W. Bilbro
Mail Code EB23
NASA Marshall Space Flight Ctr.
Huntsville AL 35812
205/544-3467
205/544-2659

Brian Blakkolb
TRW Space & Defense
One Space Park M/S R4-2173
Redondo Beach CA 90278
213/813-8960
213/812-8768

Charles Blatchley
Spire Corporation
One Patriots Park
Bedford MA 01730
617/275-6000
617/275-7470

Dr. Jeffrey Blezius
MPB Technologies
151 Hymus Blvd.
Pointe-Claire, Quebec CANADA H9
91 514/694-8751
91 514/695-7492

M. D. Blue
GTRI/Baker Bldg. 323
Georgia Tech.
Atlanta GA 30332
404/894-3646
404/894-6285

Gail Bohnhoff-Hlavacek
Boeing M/S 8H-01
PO Box 3999
Seattle WA 98124
206/773-6892
206/773-4946

Roger J. Bourassa
Boeing Defense & Space Group-M/S
PO Box 3999
Seattle WA 98124-2499
206/773-8437
206/773-4946

David E. Bowles
Mail Stop 191
NASA Langley Research Ctr.
Hampton VA 23556-5225
804/864-3095
804/864-7729

F. L. Boyer
Mail Stop 424
NASA Langley Research Center
Hampton VA 23665-5225
804/864-5666

David Brinza
JPL Mail Stop 67-201
4800 Oak Grove Dr.
Pasadena CA 91109
818/354-6836
818/393-6869

W. Brower
Marquette University

Milwaukee WI 53233
414/288-7081
414/288-7082

Richard W. Cahill
Lockheed Missiles & Space Co. 0/77-60, B/
Box 3504
Sunnyvale CA 94088
408/743-2739
408/742-2423

George Caledonia
Physical Sciences, Inc.
20 New England Business Center
Andover MA 01810
508/689-0003

*** Where there are two phone numbers given, the second one is the **FAX** number.

Robert L. Calloway
LDEF Science Office M/S 404
NASA Langley Research Ctr.
Hampton VA 23665-5225
804/864-2960
804/864-8094

Mark A. Carlson
McDonnell Douglas Space Systems Co
5301 Bolsa Ave. M/S 15-1/103
Huntington Beach CA 92647
714/896-3311 x 70083
714/869-2937

Soo-Kong Chang
Spar Aerospace Ltd
1700 Ormond Dr.
Weston, Ontario CANADA M9L 2W
416/745-9696 X 4351
416/745-4172

Robert J Christie
Rockwell International
22021 Brookpark Rd
Cleveland OH 44126
216/734-2550
216/734-9129

Carroll H. Clatterbuck
Mail Code 313.2
NASA Goddard Space Flight Ctr.
Greenbelt MD 20771
301/286-67991
301/286-2717

Craig Cleckner
Mail Stop 431
NASA Langley Research Center
Hampton VA 23665-5225
804/864-7048
804/864-7202

Jean Clough
Mail Stop 115
NASA Langley Research Center
Hampton VA 23665-5225
804/864-6122

John M. Coggi
The Aerospace Corp.
PO Box 92957
Los Angeles CA 90009-2957
213/336-6922
213/336-1636

Capt. Cady Coleman
WL/MLBP
Wright Laboratory/USAF
Wright-Patterson AFB OH 45433-6
513/255-9163
513/255-9019

Thomas Cookson
General Dynamics Space Systems
POBox 85990
San Diego CA 92186-5990
619/547-5081
619/974-4000

John E. Cooney
Space Systems/Loral
3825 Fabian Way, M/S G-97
Palo Alto CA 94303
415/852-4703
415/852-4267

Jonathan D. Coopersmith
Mail Code 732.5; Bldg. 7, Rm. 011
NASA Goddard Space Flight Ctr.
Greenbelt MD 20771
301/286-7969
301/286-6916

Diane Cotten
Martin Marietta--M/S 8048
POBox 179
Denver CO 80227
303/977-8385
303/977-1907

Joan Cranmer
JHU/APL
Johns Hopkins Rd
Laurel MD 20833
301/953-5000 X3810
301/953-6119

Dr. Jon B. Cross
CLS-2/MS G738
Los Alamos National Laboratory
Los Alamos NM 87545
505/667-0511
505/665-4631

E. Russ Crutcher
Boeing Defense & Space Group-M/S 88-23
POBox 3999
Seattle WA 98124-2499
206/773-7002
206/773-4946

John M. Davis
NASA
Marshall Space Flight Ctr.
Huntsville AL 35812
205/544-2494
205/544-5786

Judith R. J. Davis
M/S 228
NASA Langley Research Ctr
Hampton VA 23665-5225
804/864-4255
804/864-8312

Dr. A. de Rooij
ESA/ESTEC
PO Box 299, 2200 AG
Noordwijk NETHERLANDS
9011 31 0 1719 83716
9011 31 0 2523 76722

Don D. Dees
Boeing Defense & Space Group-M/S JM-95
PO Box 240002,499 Boeing
Huntsville AL 35824
205/461-5839
205/461-2286

Linda L. DeHainaut
LITC
Phillips Laboratory (AFSC)
Kirtland AFB NM 87117-6008
505/846-9877
505/846-0473

Michael D. DePiero
C. S. Draper Lab, M/S 63
555 Technology Sq
Cambridge MA 02139
617/258-2775
617/258-1131

John M. Dispennette
202 Ross Hall/Dept. of Mech. Engrg
Auburn University
Auburn University AL 36899
205/844-3345
205/844-3307

Tom Dragone
Orbital Sciences Corp
14119-A Sullyfield Cr/POBox 10840
Chantilly VA 22021
703/802-8107
703/802-8245

Christian Durin
CNES-Space Center of Touloux
18 Avenue Edouard Belin
Toulouse Cedex FRANCE 31055
9011 33 61 28 14 39
9011 33 61 27 47 32

Harry W. Dursch
Boeing M/S 82-32
PO Box 3999
Seattle WA 98124
206/773-0527
206/773-4946

Capt. Deidra Dykeman
RL/OOCP
Griffiss AFB
Griffiss AFB NY 13441-5700
315/330-3145
315/330-7901

Joel Edelman
LDEF Corporation
14636 Silverstone Dr.
Silver Spring MD 20905
301/236-9311

Curt Eiche
Martin Marietta M/S B4383
PO Box 179
Denver CO 80201
303/971-1762
303/971-9768

Phyllis Ellingboe
Sheldahl, Inc.
1150 Sheldahl Rd, POBox 170
Northfield MN 55057
507/663-8000 x276
507/663-8470

John Emond
Ofc. of Commercial Programs Code CC
NASA Headquarters
Washington DC 20546
703/557-4599

W. W. Fernald
Mail Stop 433
NASA Langley Research Center
Hampton VA 23665-5225
804/864-7081

Robert H. Flowers
Martin Marietta M/S 8041
POBox 179
Denver CO 80201
303/977-6832
303/977-1907

Thad Frederickson
ILC Dover, Inc.
PO Box 266, Road 35
Frederica DE 19946
302/335-3911
302/335-0762

Al Freeland
Sheldahl, Inc.
1150 Sheldahl Rd., PO Box 170
Northfield MN 55057
507/663-8000 x502
507/663-8470

Joe Froeichtenigt
Martin Marietta Astronautics Group
PO Box 179
Denver CO 80201
303/971-9258
303/971-9141

Joan G. Funk
Mail Stop 188B
NASA Langley Research Center
Hampton VA 23665-5225
804/864-3092
804/864-7893

Carol R. Gautreaux
Mail Stop 226
NASA Langley Research Ctr
Hampton VA 23665-5225
804/864-4280
804/864-3800

Dr. Raymond B. Gavert
NASA Space Sta. Prgm MSS-2
10701 Parkridge Blvd., Rm. 2372
Reston VA 22091
703/487-7336
703/487-7994

Pete George
Boeing Defense & Space Group-M/S 73-09
POBox 3999
Seattle WA 98124-2499
206/234-2679
206/237-0052

Michael B. Glasgow
College of William & Mary/Chem. Dept.
PO Box 8795
Williamsburg VA 23787-8795
804/221-2540

Johnny L. Golden
Boeing Defense & Space Group-M/S
POBox 3999
Seattle WA 98124-2499
206/773-2055
206/773-4946

Tim Gordon
Applied Science Technologies
4801 S. Holland Way
Littleton CO
303/973-7708

Dana Gould
Mail Stop 431
NASA Langley Research Center
Hampton VA 23665-5225
804/864-7747
804/864-7202

Dr. Raj Gounder
Boeing Aerospace Operations, Inc.
2101 Executive Dr., Tower Bx 74
Hampton VA 23666
804/838-2741
804/838-2780

Brian Gries
McDonnell Douglas
16055 Space Center Blvd.
Houston TX 77062-6208

Doris K. Grigsby
NASA/AESP, Oklahoma State Univ
300 North Cordell
Stillwater OK 74078
405/744-7015
405/744-7785

Frederick C. Gross
Mail Code 313
NASA Goddard Space Flight Ctr.
Greenbelt MD 20771
301/286-8349
301/286-4661

Koorosh Guidanean
L'Garde Incorporated
15181 Woodlawn Ave.
Tustin CA 92680
714/259-0771
714/259-7822

Sandra R. Gyetvay
The Aerospace Corp. -M/S M2/241
PO Box 92957
Los Angeles CA 90009-2957
213/336-8339
213/336-1636

Yoshiro Harada
IIT Research Institute
10 West 35th St.
Chicago IL 60616
312/567-4432
312/567-4386

Gale Harvey
Mail Stop 401A
NASA Langley Research Ctr.
Hampton VA 23665-5225
804/864-6742
804/864-7790

Dr. James A. Harvey
Univ. of Dayton Research Inst.
OLAC PL/STSC Bldg. 8424
Edwards AFB CA 93523-5000
805/275-5976
805/275-5041

Yoshihiro Hashimoto
Thermal Control & Structure Group/Tech De
IHI 229, Tonogaya, Mizuho-Machi,
Nishitama-Gun, Tokyo JAPAN 190-
9011 81 0425-56-7184
9011 81 0425-56-7575

Dr. Carol Hemminger
The Aerospace Corp. M2/250
PO Box 92957
Los Angeles CA 90009-2957
213/336-7666
213/336-1636

Sylvester G. Hill
Boeing Defense & Space Group-M/S 82-32
PO Box 3999
Seattle WA 98124-2499
206/773-2767
206/773-4946

S. E. Holloway III
Mail Stop 433
NASA Langley Research Center
Hampton VA 23665-5225
804/864-7090

Jerry L. Hunter
Analytical Instrumentation Facility
North Carolina State Univ - Box 7916
Raleigh NC 27695
919/515-7659
919/515-2463

Charles Hurley
University of Dayton/Research Inst.
300 College Park
Dayton OH 45469-0137
513/255-3220
513/258-8075

Takashi Ishii
Nissan Research & Development Inc
750 17th St., NW #902
Washington DC 20006
202/466-5284
202/457-0851

C. E. Jenkins, Jr.
Mail Stop 433
NASA Langley Research Center
Hampton VA 23665-5225
804/864-7080

Roger N. Johnson
Westinghouse Hanford Co/LG-39
PO Box 1970
Richland WA 99352
509/376-3582 (FTS 444)
509/376-4945 (FTS 444)

James L. Jones
Mail Stop 404
NASA LaRC
Hampton VA 23665-5225
804/864-3795
804/864-8094

H. C. Jones
Mail Stop 424
NASA Langley Research Center
Hampton VA 23665-5225
804/864-5651

Michele D. Jones
MLBT
Wright Laboratory
Wright-Patterson AFB OH 45433-6533
513/255-8097
513/255-9019

Michael P. Joseph
7421 Orangewood Ave., PO Box 311
OCA Applied Optics
Garden Grove CA 92642
714/895-1667
714/4356

Lester Jung
G. E. Aerospace
PO Box 800 M/S 410-1D
Princeton NJ 08543
609/490-6321
609/490-3962 (63)

Rachel R. Kamenetzky
Mail Code EH12
NASA MSFC
MSFC AL 35812
205/544-2510
205/544-0212

Mike Kangilaski
G. E. Space Nuclear Engrg & Tech.
P. O. Box 530954/6835 Via Del Oro
San Jose CA 95153-5354
408/365-6351

Lonny Kauder
Mail Code 732.5
NASA Goddard Space Flight Ctr.
Greenbelt MD 20771
301/286-5309
301/286-6916

John M. Kazaroff
NASA-Lewis Research Ctr M/S SPTD-2
21000 Brookpark Rd
Cleveland OH 44135
216/977-7513
216/977-7500

William T. Kemp
PL/STET
Kirtland AFB
Albuquerque NM 87117-6008
505/846-4439
505/846-6098

Dr. John R. Kenemuth
LITC
Phillips Laboratory (AFSC)
Kirtland AFB NM 87117-6008
505/846-4270
505/846-0473

Hamed Khozaim
SSD/CNT
14800 Aviation Blvd.
Hawthorn CA 90250
213/363-8641
213/363-8725

Thomas D. Kim
OLAC PL/STSC
Phillips Laboratory
Edwards AFB CA 93523-5000
805/275-5304
805/275-5041

Thomas J. Kosic
Hughes Aircraft Co., EDSG
P O Box 902
El Segundo CA 90245
310/616-9819
310/616-5987

Dr. Kaplesh Kumar
C. S. Draper Laboratory, Inc. M/S 37
555 Technology Square
Cambridge MA 02139

617/258-1131

Chong Le
SSD/CNSE, Los Angeles AFB
PO Box 92960
Los Angeles CA 90009-2960
213/363-6867
213/363-6882

T. H. Leffel
Mail Stop 424
NASA Langley Research Center
Hampton VA 23665-5225
804/864-5647

François Levadou
ESA/ESTEC
POBox 299
2200 AG Noordwijk NETHERLANDS
31/1719-83915
31/1719-84992

James T. Kenny
Jet Propulsion Laboratory
4800 Oak Grove Dr. M/S 125-112
Pasadena CA 91109
818/354-3719
818/393-5011

Richard Kiefer
College of William & Mary/Chem. Dept.
PO Box 8795
Williamsburg VA 23787-8795
804/221-2553

Myung-Hee Kim
College of William & Mary/Chem. Dept.
PO Box 8795
Williamsburg VA 23787-8795
804/221-2540

James L. Koury
OLAC-PL/STSC
Phillips Lab
Edwards AFB CA 93523-5000
805/275-5646
805/275-5041

Richard Kutyn
Orbital Sciences Corp
PO Box 10840
Chantilly VA 22021
703/802-8098
704/802-8045

William T. Lee
Rocketdyne/Div of Rockwell Intl
6633 Canoga Ave LB25
Canoga Park CA 91303
818/700-3272
818/700-4313

Dr. William L. Lehn
Nichols Research Corp./Suite 157
4141 Col. Glenn Hwy
Dayton OH 45431
513/724-1173
513/427-1508

Arlene S. Levine
LDEF Science Ofc-M/S 404
NASA Langley Research Center
Hampton VA 23665-5225
804/864-3318
804/864-8094

Bruce Keough
Boeing Defense & Space Group-M/S
POBox 3999
Seattle WA 98124-2499
206/773-8438
206/773-4946

Brian Killough
Mail Stop 431
NASA Langley Research Center
Hampton VA 23665-5225
804/864-7047

William H. Kinard
LDEF Science Office M/S 404
NASA Langley Research Ctr.
Hampton VA 23665-5225
804/864-3796
804/864-8094

Thomas Kuelker
EDO Canada Ltd
1940 Centre Ave., NE
Calgary, Alberta CANADA 52E 0A7
91 403/569-5400
91 403 569-5499

T. J. Lash
Mail Stop 424
NASA Langley Research Center
Hampton VA 23665-5225
804/864-5644

Chia-Shih Lee
SSD/CNSE, Los Angeles AFB
PO Box 92960
Los Angeles CA 90009-2960
213/363-6867
213/363-6882

Dr. Alan Letton
Dept. of Mech Engrg/ M/S 3123
Texas A & M
College Station TX 77843-3123
409/845-1534
409/845-3081

Roger Linton
Mail Stop EH12
NASA Marshall Space Flight Ctr
Huntsville AL 35812
205/544-2526
205/544-0212

Scott Lissit
W. J. Schafer Associates, Inc./Suite 800
1901 N. Fort Myer Dr.
Arlington VA 22209
703/558-7900
703/525-2691

John Loria
CODE RX
NASA Headquarters
Washington DC 20546
FTS 453-2838
426-0608

M. H. Lucy
Mail Stop 433
NASA Langley Research Center
Hampton VA 23665-5225
804/864-7069

David H. Ma
Lockheed Missiles & Space Co
POBox 3504
Sunnyvale CA 94089-3504
408/742-1074
408/742-1071

Howard G. Maahs
Mail Stop 188B
NASA LaRC
Hampton VA 23665-5225
804/864-3498
804/864-7893

Diane J. Martin
W. J. Schafer Assoc, Inc./Suite 800
1901 N. Fort Myer Dr.
Arlington VA 22209
703/558-7900
703/525-2691

Glenna D. Martin
LDEF Science Project Ofc. M/S 404
NASA Langley Research Ctr.
Hampton VA 23665-5225
804/864-3773
804/864-8094

J. B. Mason
NASA
Goddard Space Flight Ctr.
Greenbelt MD 20771
301/286-6555
301/286-4653

Eugene McKannan
Boeing JR-03
499 Boeing Blvd. PO Box 240002
Huntsville AL 35824
205/461-3586
205/461-3800

Tom McKay
LORAL Infrared & Imaging Systems
2 Forbes Road M/S 345
Lexington MA 02173
617/863-4067
617/863-3496

Joe McKenzie
Grumman--SSEIC
12000 Aerospace Dr.
Houston TX 77546
713/929-7467
713/929-7333

Richard Mell
Mail Code EH-34, Bldg. 4612
NASA/MSFC
Huntsville AL 35812
205/544-7329

Bob Mercer
6337 N. Camino Los Mochis
Tucson AZ 85718-3528
602/293-1667 or 299-8530
602/293-7601

Celia Merzbacher
CODE 6505
Naval Research Lab
Washington DC 20375
202/404-7987
202/404-7085

Michael J. Meshishnek
The Aerospace Corp.
PO Box 92957
Los Angeles CA 90009-2957
213/336-8760
213/336-1636

Charles J. Miglionico
PL/WSMD
Kirtland AFB
Albuquerque NM 87117
505/846-4798
505/846-1724

Kristina M. Montt
MDSSC/Mail Code 732.5
NASA Goddard Space Flight Ctr.
Greenbelt MD 20771
301/286-4986
301/286-6916

Nigel Morris
Rutherford Appleton Laboratory
Chilton
Didcot, Oxon England OX11 0QX
9011 44 235 445210
9011 44 235 445848

W. H. Morrow
Resonance Ltd.
171 Dufferin St., So.; Unit # 7
Alliston, Ontario CANADA L0M 1A0
705/435-2577
705/435-2585

Thomas Morton
NASA Lewis Research Ctr.-M/S 301-3
21000 Brookpark Rd.
Cleveland OH 44135
216/433-6287
297-8311

James B. Moss
Martin Marietta M/S B4383
PO Box 179
Denver CO 80201
303/971-1554
303/971-9768

Henry Nahra
NASA Lewis Research Ctr
21000 Brookpark Rd
Cleveland OH 44135
216/433-5385 (FTS 297)
216/433-8050

Oscar Nespoli
Canadian Space Agency
POBox 11490, Station H
Ottawa, Ontario CANADA K2H 8S2
613/998-2187
613/998-2817

Walter F. Nicaise
L6-39
Westinghouse Hanford Co.
Richland WA 99352
509/376-0522
509/376-4945

Robert L. O'Neal
LDEF Science Ofc. M/S 404
NASA Langley Research Ctr.
Hampton VA 23665-5225
804/864-3792
804/864-8094

Richard Osiecki
Lockheed Research Lab/Orgn 92-40, B-205
3251 Hanover St.
Palo Alto CA 94304-1191
415/424-2389
415/354-5415

Norbert Pailer
Dornier GmbH/Space Division
PO Box 1420
D-7990 Friedrichshafen 1 GERMANY
9011 07545 83430
9011 07545/84411

Arthur T. Perry
American Space Technology, Inc. Suite 35
2800 28th St.
Santa Monica CA 90405
213/450-7515
213/450-7304

Brian C. Petrie
Lockheed Missiles & Space Co.
PO Box 3504, B-564, Dept. 78-30
Sunnyvale CA 94089-3504
408/742-8244
408/742-7743

H. Gary Pippin
Boeing Defense & Space Group-M/S 82-32
POBox 3999
Seattle WA 98124-2499
206/773-2846
206/773-4946

William H. Prosser
Mail Stop 231
NASA Langley Research Ctr.
Hampton VA 23665-5225
804/864-4960
804/864-4914

Douglas L. Reeder
General Research Corp.
5383 Hollister Ave.,
Santa Barbara CA 93111
805/964-7724
805/967-7094

Evelyne Orndoff
Johnson Space Center
NASA JSC
Houston TX 77058
713/483-9117
713/483-9167

V. A. Overbay
Mail Stop 424
NASA Langley Research Center
Hampton VA 23665-5225
804/864-5636

Alain Paillous
ONERA-CERT/DERTS
2 Ave. E. Belin
31055 Toulouse-Cedex FRANCE
9011 33 61 55 71 19
9011 33 61 55 71 72

Wanda C. Peters
McDonnell Douglas Space Systems Co.
7404 Executive Pl./Suite 200
Seabrook MD 20706
301/286-7969
301/464-7413

J. R. Phillips
Mail Stop 433
NASA Langley Research Center
Hampton VA 23665-5225
804/864-7075

Bob Poley
Ball Aerospace
PO Box 1062
Boulder CO 80306
303/939-4460
303/442-4812

J. R. Rawls
Mail Stop 424
NASA Langley Research Center
Hampton VA 23665-5225
804/864-4093

Brian Remington
ILC Dover, Inc.
PO Box 266, Road 35
Frederica DE 19946
302/335-3911
302/335-0762

Robert Orwoll
College of William & Mary/Chem. Dep
PO Box 8795
Williamsburg VA 23787-8795
804/221-2549

G. Owsley
Mail Stop 433
NASA Langley Research Center
Hampton VA 23665-5225
804/864-7070

George M. Parsons III
USArmy Strategic Defense Cmnd CS
POBox 1500
Huntsville AL 35807-3801
205/955-1667
205/955-5722

Ron Peterson
Hughes Aircraft

310/616-9048
310/616-5987

Ross Phillips
Mail Stop 433
NASA Langley Research Ctr.
Hampton VA 23665-5225
804/864-7075
804/864-7009

Professor R. Prabhakaran
Old Dominion University
Dept. of Mechanical Engineering
Norfolk VA 23529

Gary D. Rea
Martin Marietta M/S 8041
POBox 179
Denver CO 80201
303/977-6831
303/977-1907

G. Paul Richter
NASA-Lewis Research Ctr M/S SPT
21000 Brookpark Rd
Cleveland OH 44135
216/977-8538
216/977-7500

James B. Robertson
Mail Stop 152E
NASA Langley Research Ctr.
Hampton VA 23665-5225
804/864-6643
804/864-7793

William R. Robertson
Dynamics Research Corp.
1755 Jefferson Davis Hwy/ Suite 802
Arlington VA 22202
703/521-3812 X 6046
703/550-4123

Michael Rodriguez
MDSSC Mail Code 732.4
NASA Goddard Space Flight Ctr.
Greenbelt MD 20771
301/286-9296
888-6919

William A. Roettker
Mail Stop 431
NASA Langley Research Center
Hampton VA 23665-5225
804/864-7046
804/864-7202

Frank Rose
Auburn Univ/Space Power Inst.
231 Leach Ctr.
Auburn University AL 36849
205/844-5894
205/844-5900

Gilbert L. Roth
Code QP
NASA Headquarters
Washington DC 20546
202/453-1877
202/472-4841

Dr. H. R. Ruge
The Aerospace Corp. M2-264
PO Box 92957
Los Angeles CA 90009
213/336-7085
213/336-6136

T. S. Sampair
Mail Stop 904
Lockheed Engineering & Sciences Corp.
Hampton VA 23666
804/766-9600

Matthew Schor
W. J. Schafer Assoc., Inc/Suite 800
1901 N. Fort Myer Dr
Arlington VA 22209
703/558-7900
703/525-2691

John R. Schuster
General Dynamics Space Sys. M/Z C1-8900
POB 85990
San Diego CA 92186-5990
619-547-7120
619/547-7162

Dr. David Schwam
Case Western Reserve University

Cleveland OH 44106
216/368-3864
216/368-3209

Dr. Helmut Schulle
Dornier of North America, Inc.
1350 I Street, NW/Suite 800
Washington DC 20005
202/408-1110
202/408-4892

Martha Scott
Grumman Space Sta. Prgm
620 Discovery Dr.
Huntsville AL 35806
205/971-6012
205/971-6019

David Shular
Mail Code ED 64
NASA Marshall Space Flight Ctr.
Huntsville AL 35812
205/544-8734
205/544-5874

D. D. Shuster
Mail Stop 459
NASA Langley Research Center
Hampton VA 23665-5225
804/864-3336

Charles Simon
ISST/M&D SIG
1810 NW 6th St.
Gainesville FL 32609
904/371-4778
904/372-5042

Wayne S. Slemp
Mail Stop 183
NASA Langley Research Ctr.
Hampton VA 23665-5225
804/864-1334
804/864-3800

Fred A. Smidt
Code 4670
Naval Research Laboratory
Washington DC 20375-5000
202/767-4800
202/767-5301

Bryan K. Smith
NASA Lewis Research Ctr. M/S 500-222
21000 Brookpark Rd.
Cleveland OH 44135
216/433-6703 (FTS 297)
216/433-8050

Charles A. Smith
McDonnell Douglas
5201 Bolsa, M/S T-50
Huntington Beach CA 92647-2048
714/896-4015
714/896-3311 X 69339

Richard E. Snyder
Mail Stop 114
NASA Langley Research Ctr.
Hampton VA 23665-5225
804/864-6016

Steve Spear
Boeing M/S 73-09
PO Box 3999
Seattle WA 98124
206/234-2667
206/237-1750

Gary L. Steckel
The Aerospace Corp. M/S M2/321
PO Box 92957
Los Angeles CA 90009
310/336-7116
310/336-7055

Bland A. Stein
Mail Stop 188M
NASA Langley Research Ctr.
Hampton VA 23665-5225
804/864-3492
804/864-7729

Dr. Charles Stein
Phillips Lab/WSMD
Kirtland AFB
Albuquerque NM 87117
505/846-4822
505/846-1724

Dr. Thomas Strganac
Dept. of Aerospace Engrg M/S 3141
Texas A & M
College Station TX 77843-3123
409/845-1694
409/845-6051

John W. Strickland
BAMSI, Inc.
150 West Park Loop, Suite 107
Huntsville AL 35806
205/772-9072
205/722-9287

Dr. Wayne K. Stuckey
The Aerospace Corp. M2/250
PO Box 92957
Los Angeles CA 90009-2957
213/336-7389
213/336-1636

Dr. Richard D. Sudduth
Boeing Defense & Space Group-M/S JY-34
PO Box 240002,499 Boeing
Huntsville AL 35824

Louis A. Teichman
Mail Stop 191
NASA Langley Research Ctr.
Hampton VA 23665-5225
804/864-3510
804/864-7729

Stephen S. Tompkins
Materials Div. M/S 188B
NASA Langley Research Ctr.
Hampton VA 23665-5225
804/864-3096
804/864-7793

Bob Turner
W. J. Schafer
1901 N. Fort Myer Dr.
Arlington VA 22094
703/558-7900
703/525-2691

June Tveekrem
Mail Code 732
NASA Goddard Space Flight Ctr
Greenbelt MD 20771
301-286-2832
301/286-2477

Richard F. Vyhna
Rockwell International
POBox 582808
Tulsa OK 74158
918/835-3111 X2252
918/834-7722

Donald A. Wallace
QCM Research
2825 Laguna Canyon Rd/PO Box 277
Laguna Beach CA 92652
714/497-5748
714/497-7331

Scott A. Wallace
QCM Research
2825 Laguna Canyon Rd/PO Box 27
Laguna Beach CA 92652
714/497-5748
714/497-7331

Dr. Tom Ward
U.S. Dept. of Energy GA-155, SC-1
1000 Independence Ave., S. W.
Washington DC 20585
202/586-4612 FTS 896-4612
896-9386

Dr. Ann F. Whitaker
Mail Code EH, 11
NASA Marshall Space Flight Ctr.
MSFC AL 35812
205/544-2510
205/544-0212

Ken Whiteacre
Martin Marietta
PO Box 179, M/S 8048
Denver CO 80201
303/977-8373
303/977-1921

Dr. James B. Whiteside
Grumman Corporate Research Ctr.
Mail Stop A08-35
Bethpage NY 11714-3580
516/575-2354
516/575-7716

Donald R. Wilkes
AZ Technology
3322 Memorial Pky., SW Suite 93
Huntsville AL 35801
205/880-7481
205/880-7483

Kevin Duane Williams
Dept. of Mechanical Engrg. M/S 312
Texas A & M
College Station TX 77843-3123
409/847-9233
409/845-3081

Brenda K. Wilson
W. J. Schafer Associates
525 School St., SW/Suite 301
Washington DC 20024
202/863-9159
202/863-9292

B. B. Wolff
Mail Stop 424
Lockheed Engineering & Sciences Corp.
Hampton VA 23666
804/766-9604

Philip R. Young
Mail Stop 226
NASA Langley Research Ctr.
Hampton VA 23665-5225
804/864-4265 FTS 928-4265
804/864-8312

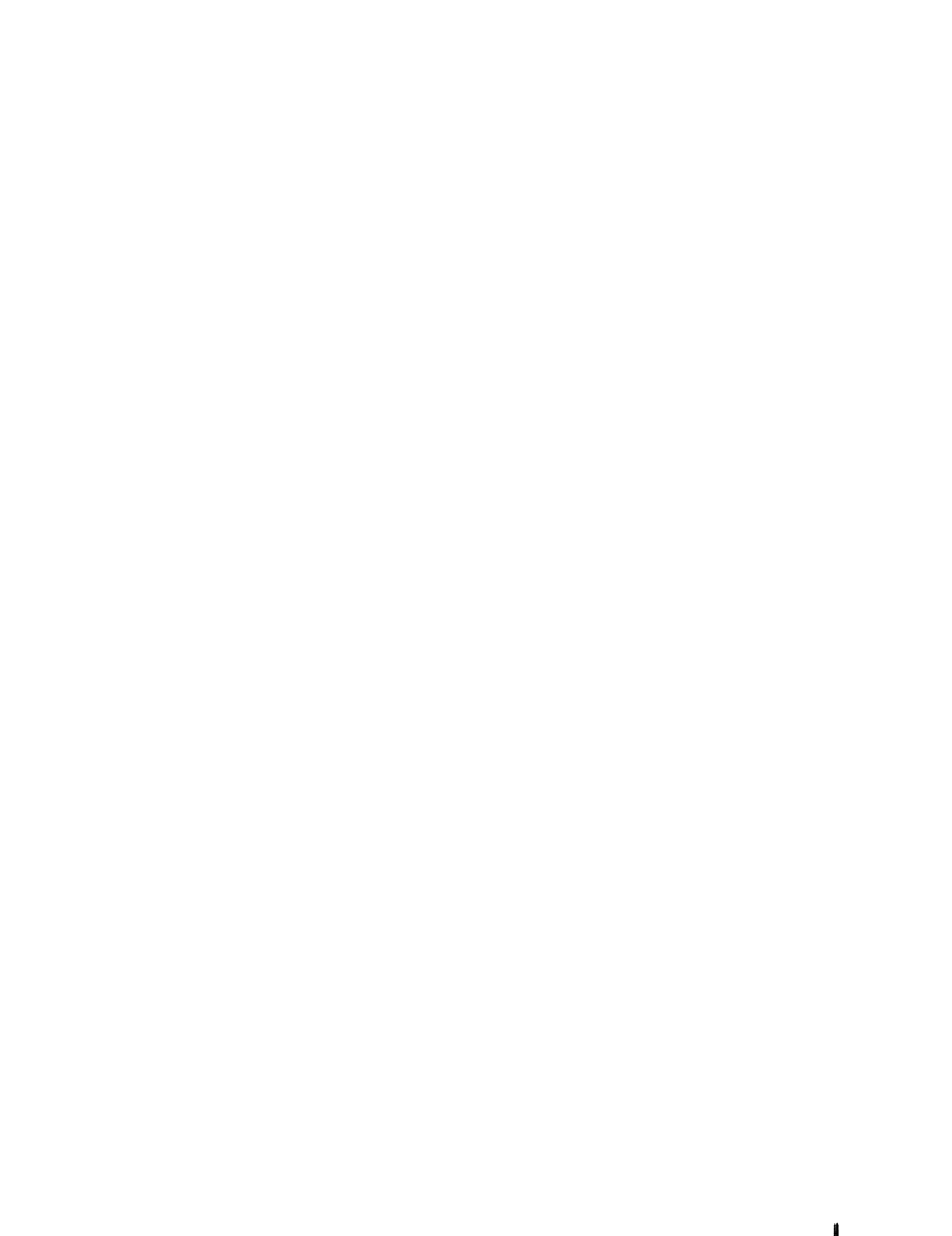
Ainslie T. Young, Jr.
Los Alamos National Lab/MST-DO, MS-G75
POBox 1663
Los Alamos NM 87545
505/667-4553 fts 843
505/665-3748

Naser Zargar
McDonnell Douglas Space Systems Co.
5301 Bolsa Ave. M/S 17-7
Huntington Beach CA 92647
714/896-3311 X70337
714/896-5034

Dr. D. G. Zircik
Canadian Space Agency
POBox 11490, Station H
Ottawa, Ontario CANADA K2H 8S2
613/998-2187
613/998-2817



REPORT DOCUMENTATION PAGE			Form Approved OMB No. 0704-0188	
Public reporting burden for this collection of information is estimated to average 1 hour per response, including the time for reviewing instructions, searching existing data sources, gathering and maintaining the data needed, and completing and reviewing the collection of information. Send comments regarding this burden estimate or any other aspect of this collection of information, including suggestions for reducing this burden, to Washington Headquarters Services, Directorate for Information Operations and Reports, 1215 Jefferson Davis Highway, Suite 1204, Arlington, VA 22202-4302, and to the Office of Management and Budget, Paperwork Reduction Project (0704-0188), Washington, DC 20503.				
1. AGENCY USE ONLY (Leave blank)	2. REPORT DATE September 1992	3. REPORT TYPE AND DATES COVERED Conference Publication		
4. TITLE AND SUBTITLE LDEF Materials Workshop '91			5. FUNDING NUMBERS 506-48-91-08	
6. AUTHOR(S) Bland A. Stein and Philip R. Young, Compilers				
7. PERFORMING ORGANIZATION NAME(S) AND ADDRESS(ES) NASA Langley Research Center Hampton, VA 23681-0001			8. PERFORMING ORGANIZATION REPORT NUMBER L-17135	
9. SPONSORING/MONITORING AGENCY NAME(S) AND ADDRESS(ES) National Aeronautics and Space Administration Washington, DC 20546-0001			10. SPONSORING/MONITORING AGENCY REPORT NUMBER NASA CP-3162, Part 2	
11. SUPPLEMENTARY NOTES				
12a. DISTRIBUTION/AVAILABILITY STATEMENT Unclassified-Unlimited Subject Category 27			12b. DISTRIBUTION CODE	
13. ABSTRACT (Maximum 200 words) The LDEF Materials Workshop '91 was a follow-on to the Materials Sessions at the First LDEF Post-Retrieval Symposium held in Kissimmee, Florida, June 1991. The workshop comprised a series of technical sessions on materials themes, followed by theme panel meetings. Themes included Materials, Environmental Parameters, and Data Bases; Contamination; Thermal Control and Protective Coatings and Surface Treatments; Polymers and Films; Polymer Matrix Composites; Metals, Ceramics, and Optical Materials; Lubricants Adhesives, Seals, Fasteners, Solar Cells, and Batteries. This report contains most of the papers presented at the Technical sessions. It also contains theme panel reports and visual aids. This document continues the LDEF Space Environmental Effects on Materials Special Investigation Group (MSIG) pursuit of its charter to investigate the effects of LEO exposure on materials which were not originally planned to be test specimens and to integrate this information with data generated by Principal Investigators into an LDEF Materials Data Base.				
14. SUBJECT TERMS Long Duration Exposure Facility (LDEF); Space environmental effects on materials; Space exposure of materials			15. NUMBER OF PAGES 308	
			16. PRICE CODE A14	
17. SECURITY CLASSIFICATION OF REPORT Unclassified	18. SECURITY CLASSIFICATION OF THIS PAGE Unclassified	19. SECURITY CLASSIFICATION OF ABSTRACT Unclassified	20. LIMITATION OF ABSTRACT	



National Aeronautics and
Space Administration
Code JTT
Washington, D.C.
20546-0001
Official Business
Penalty for Private Use, \$300

SPECIAL FOURTH-CLASS RATE
POSTAGE & FEES PAID
NASA
PERMIT No. G27



POSTMASTER: If Undeliverable (Section 158
Postal Manual) Do Not Return

